



**TECHNISCHE
UNIVERSITÄT
WIEN**
Vienna University of Technology

DISSERTATION

Structural Elucidation and Synthesis of Doping-Relevant SARM- and SERM-Metabolites

ausgeführt zum Zwecke der Erlangung des akademischen Grades eines Doktors der
technischen Wissenschaften unter der Leitung von

Ao. Univ.-Prof. Dipl.-Ing. Dr. techn. Peter **Gärtner**

Institut für Angewandte Synthesechemie

eingereicht an der **Technischen Universität Wien**

Chemische Fakultät

von

DI Katharina **Schragl**

Matr. Nr.: 0425304

Grünangergasse 12, A-3270 Scheibbs

Wien, im Juli 2014

*“I was not a doper, I told myself -
I just injected myself to recover
and needed pills to sleep.”*

(“Racing Through the Dark” by David Millar)

My heartfelt thanks to ...

- ... all those who have accompanied me during the past four years and have played a part in this Ph.D research, who have shown interest in my work and have supported me.
- ... *Prof. Dr. Peter Gärnter*, my Ph.D advisor, who has already been accompanying my studies and work at the Vienna UT since the beginning of my diploma research and who encouraged me to accomplish this Ph.D thesis in the first place. Thank you for arousing my interest in organic chemistry and scientific work, for giving me the opportunity to be part of your research group and for always being there to give valuable advice and motivation.
- ... *Dr. Valentin Enev*, who supervised my research and often put things on the right track. Thank you for your interest in my project and for teaching me so many things concerning synthetic work. Your knowledge and enthusiasm for chemistry is amazing!
- ... *Dr. Günter Gmeiner* and *Dr. Guro Forsdahl* from the doping control laboratory Seibersdorf, whose cooperation made it possible to conduct this Ph.D research on the subject of this interesting and fascinating topic of doping in sports. Thank you for giving me the possibility to work in your laboratory and to use all your facilities. It was a real pleasure to work with you.
- ... *Dr. Christian Hametner* for his assistance in performing the LC-NMR experiments and *Dr. Florian Rudroff* for providing me with helpful tips concerning LC-MS-MS.
- ... all my labmates and friends in the Gärtner group, who ensured every day in the lab to be absolutely unique, so that it was a pleasure to come to work. Thank you for sharing all ups and downs and for all the fun we had – those were good times: *Maria Vasiloiu, Anna Ressmann, Sonja Leder, Katharina Bica, Katharina Strassl, Philipp Gritsch, Sebastian Steiner* and *Max Kaiser*.
- ... all members of the other organic research groups (1st and 2nd floor), especially those of the “Fiaker”-group for all the enjoyable coffee breaks and “outdoor missions”, and those of our soccer circle for all the exciting matches and amusing evenings.
- ... *Florian Untersteiner*, for his support in so much more than just IT issues.
- ... my parents, *Marianne* and *Hans*, who have always supported and encouraged me throughout my studies. Better parents you could not ask for – my accomplishments are yours.
- ... my sister *Bettina*, for being the best sister in the world.
- ... *Florian*, for making up for everything I am not good at and bringing joy into my life.

PUBLICATIONS, POSTER AND ORAL PRESENTATIONS RESULTING FROM THIS THESIS

Publications

- “Novel Pathway for the Synthesis of Arylpropionamide-Derived Selective Androgen Receptor Modulator (SARM) Metabolites of Andarine and Ostarine” Schragl, K. M.; Forsdahl, G.; Gmeiner, G.; Enev, V. S.; Gaertner, P. *Tetrahedron Lett.* **2013**, *54* (18), 2239.

Participation at Symposia

- Poster Presentation at the “20th International Conference on Organic Synthesis (ICOS), **2014**”, entitled “Synthesis of Doping-Relevant Arylpropionamide-Derived SARM metabolites”, ELTE Convention Centre, Budapest, Hungary.
- Oral Presentation at the “15. Österreichische Chemietage, **2013**”, entitled “Novel Pathway for the Synthesis of Arylpropionamide-Derived Selective Androgen Receptor Modulator (SARM) Metabolites of Andarine and Ostarine”, TU Graz, Graz, Austria.
- Poster Presentation at the “14. Österreichische Chemietage, **2011**”, entitled “Mimicry of Drug Metabolism and Synthesis of Relevant Metabolites of the Doping Substance Clomiphene”, JKU Linz, Linz, Austria.

ABSTRACT

New achievements in pharmaceutical research constantly extend the range of doping-relevant substances. Efficient combating of illegal drug abuse in high-performance sports affords profound knowledge of drug metabolism. This is often aggravated by the fact that many substances, though already freely available on the black market, in fact are still objects of clinical trials and not even approved for the clinical administration on patients. The following research deals with the structural elucidation and synthesis of metabolites of different doping reagents, which are needed as reference substances for doping analysis. An efficient synthetic route was developed, that facilitates the synthesis of two important arylpropionamide-based SARM metabolites. Via epoxidation, amide bond formation and epoxide opening these metabolic products of andarine and ostarine can be obtained in their racemic forms and with slight modifications also in enantiopure form. Comparison to excretion studies confirmed their utility as reference substances for the detection of SARMS abuse. Different approaches for the synthesis of 4'-hydroxyclofiphenone, a potential metabolite of the SERM clomifene, are presented. Whereas the application of a McMurry coupling reaction and a Horner Wadsworth Emmons reaction turned out to be not expedient, stannyl lithiation of an acetylenic precursor compound followed by a Negishi coupling reaction finally gave the target metabolite. As this structure was shown not to be applicable for doping control purposes, a synthetic approach towards 3,4-di-hydroxy-di-hydroxyclofiphenone featuring two consecutive Pd-catalyzed α -arylation steps was compiled. Additionally a model system for the simulation of clomifene's metabolism applying human liver microsomes was developed. It facilitated the preparation of a larger quantity of major metabolic products that were analyzed by LC-SPE-NMR/MS. The obtained $^1\text{H-NMR}$ spectra have shown that 4-hydroxyclofiphenone is a useful reference substance for LC-MS-based doping tests.

KURZFASSUNG

Durch neue Errungenschaften der pharmazeutischen Forschung wird das Spektrum dopingrelevanter chemischer Verbindungen ständig erweitert. Um illegalem Medikamentenmissbrauch im Hochleistungssport effektiv entgegenwirken zu können, müssen die pharmakokinetischen Eigenschaften einer Substanz bekannt sein. Eine effiziente Abwicklung von Dopingtests basiert auf dem Wissen über metabolische Vorgänge, welchen ein Medikament im menschlichen Körper unterworfen wird. Dies wird oft dadurch erschwert, dass diverse sich noch in klinischer Untersuchung befindliche Präparate, welche demnach für die Anwendung am Patienten noch gar nicht zugelassen sind, trotzdem bereits am Schwarzmarkt erhältlich sind. Die vorliegende Arbeit beschäftigt sich mit der Strukturaufklärung und Synthese von Metaboliten verschiedener Dopingreagenzien, welche als Referenzsubstanzen für die Dopinganalytik benötigt werden. Für die Herstellung zweier SARM-Metaboliten mit Arylpropionamidstruktur wurde ein effizienter Syntheseweg entwickelt, welcher sowohl zu den racemischen Produkten als auch zu den entsprechenden enantiomerenreinen Verbindungen führt. Die Metaboliten von Andarine und Ostarine wurden schrittweise durch Epoxidierung, Amidbildung und Epoxidöffnung aufgebaut und ihre Nützlichkeit für die Dopinganalytik durch Vergleich mit einem Ausscheidungsversuch bestätigt. Für die Herstellung von 4'-Hydroxyclofifen, einem potenziellen Metaboliten des SERMs Clomifen, wurden verschiedene Ansätze getestet. Während sich die Wege über eine McMurry-Kupplung sowie über eine Horner-Wadsworth-Emmons Reaktion als nicht zielführend erwiesen haben, konnte die Zielstruktur letztendlich mittels Lithiumstannylierung eines Acetylens und einer anschließenden Negishi Kupplung erhalten werden. Da sich dieser Metabolit jedoch als unbrauchbar herausgestellt hat, wurde ein Ansatz zur Synthese von 3,4-Di-hydroxy-di-hydroclomifen, basierend auf zwei aufeinanderfolgenden Pd-katalysierten α -Arylierungen, entwickelt. Zusätzlich wurde ein Modellsystem zur Simulation des Clomifenmetabolismus erarbeitet. Durch Inkubation mit menschlichen Lebermikrosomen konnten die entsprechenden Metaboliten in größeren Mengen hergestellt und mittels LC-SPE-NMR/MS untersucht werden. Mit den erhaltenen ^1H -NMR-Spektren wurde gezeigt, dass es sich bei 4-Hydroxyclofifen um eine wertvolle Referenzsubstanz für den Nachweis von Clomifenmissbrauch handelt.

TABLE OF CONTENT

ACKNOWLEDGEMENTS	3
PUBLICATIONS, POSTER AND ORAL PRESENTATIONS RESULTING FROM THIS THESIS	4
ABSTRACT.....	5
KURZFASSUNG.....	6
1. INTRODUCTION	11
1.1. Doping – a survey	11
1.2. Doping – statutory regulations	14
1.3. Prohibited substances and methods.....	16
1.4. Doping analytics	17
1.4.1. Exogenous and endogenous doping agents	18
1.4.2. Analytical detection methods	19
1.4.3. LC-SPE-NMR/MS.....	21
1.5. Nonsteroidal selective androgen receptor modulators (SARMs)	23
1.5.1. SARMs – doping.....	25
1.5.2. SARMs – metabolism.....	25
1.5.3. Syntheses of andarine and ostarine metabolites	27
1.6. Selective estrogen receptor modulators (SERMs)	28
1.6.1. SERMs – doping	29
1.6.2. Clomiphene – metabolism	30
1.6.3. General approaches for the synthesis of 1,1,2-triphenylethylenes	32
1.7. Objective	35
2. RESULTS AND DISCUSSION - SYNTHESIS OF SARM METABOLITES	37
2.1. Retrosynthetic analysis for the andarine and ostarine metabolite	37
2.2. Synthesis of the racemic andarine and ostarine metabolite	37
2.2.1. Synthesis of epoxyamides <i>rac-7</i> and <i>rac-12</i>	38
2.2.1.1. Epoxyacid activation via mixed anhydrides	39
2.2.1.2. Epoxyacid activation via coupling reagents based on 1 <i>H</i> -benzotriazole	40
2.2.1.3. Amide bond formation via Crich procedure	42
2.2.2. Epoxide opening reaction.....	44
2.3. Enantioselective synthesis of the andarine and ostarine metabolite	45
2.3.1. Synthesis of (<i>R</i>)- 2 via Sharpless asymmetric epoxidation	46
2.3.2. Synthesis of (<i>S</i>)-2-methyloxirane-2-carboxylic acid ((<i>S</i>)- 3).....	49
2.3.3. Regioselective considerations regarding ring opening reactions in the course of the enantioselective synthesis of (<i>S</i>)- AM 1 and (<i>S</i>)- OM 1	51
2.4. Proofs of authenticity	53

3. RESULTS AND DISCUSSION - SYNTHESIS OF 4'-HYDROXYCLOMIPHENE	55
3.1. Retrosynthetic analysis.....	55
3.2. McMurry approach.....	55
3.3. Horner-Wadsworth-Emmons approach	61
3.4. Negishi approach.....	66
3.5. Proof of authenticity	71
4. RESULTS AND DISCUSSION - SYNTHESIS OF 3,4-DI-HYDROXY-DI-HYDROCLOMIPHENE	73
4.1. Retrosynthetic analysis.....	73
4.2. Approach 1	75
4.3. Approach 2	86
5. RESULTS AND DISCUSSION - SIMULATION OF DRUG METABOLISM VIA METABOLIC MODEL SYSTEMS	91
5.1. Nonenzymatic biomimetic model systems	92
5.1.1. Simulation of clomiphe metabolism via nonenzymatic model systems	95
5.2. <i>In vitro</i> model systems	97
5.2.1. Simulation of clomiphe metabolism via <i>in vitro</i> human liver microsomal incubation	98
5.2.2. LC-SPE-NMR/MS analysis of the enzyme extract	102
6. CONCLUSION AND OUTLOOK	108
6.1. SARM metabolites.....	108
6.1.1. Synthesis of racemic SARM metabolites	108
6.1.2. Synthesis of enantiopure SARM metabolites	109
6.2. SERM metabolites	109
6.2.1. Synthesis of 4'-hydroxyclo miphene	109
6.2.2. Synthesis of 3,4-di-hydroxy-di-hydroclomiphene	110
6.2.3. Simulation of clomiphe metabolism via metabolic model systems	111
7. EXPERIMENTAL SECTION	112
7.1. GENERAL METHODS	112
7.2. SYNTHESIS OF SARM METABOLITES	116
7.2.1. (2 <i>R</i>)-(-)-2-Methyl-2,3-epoxy-1-propanol (2).....	116
7.2.1.1. <i>rac</i> -2-Methyloxirane-2-carboxylic acid (<i>rac</i> - 3).....	117
7.2.2. (<i>S</i>)-2-Methyloxirane-2-carboxylic acid ((<i>S</i>)- 3).....	118
7.2.3. General method for the synthesis of epoxyamides <i>rac</i> - 7/12 and (<i>S</i>)- 7/12	118
7.2.3.1. <i>rac</i> -2-Methyl- <i>N</i> -(4-nitro-3-(trifluoromethyl)phenyl)oxirane-2-carbox-amide (<i>rac</i> - 7)	119
7.2.3.2. (<i>S</i>)-2-Methyl- <i>N</i> -(4-nitro-3-(trifluoromethyl)phenyl)oxirane-2-carbox-amide ((<i>S</i>)- 7)	120
7.2.3.3. <i>rac</i> - <i>N</i> -(4-Cyano-3-(trifluoromethyl)phenyl)-2-methyloxirane-2-carbox-amide (<i>rac</i> - 12)	120
7.2.3.4. (<i>S</i>)- <i>N</i> -(4-Cyano-3-(trifluoromethyl)phenyl)-2-methyloxirane-2-carbox-amide ((<i>S</i>)- 12)	121
7.2.4. General method for the preparation of diols <i>rac</i> - 8/13 and (<i>S</i>)- 8/13	121
7.2.4.1. <i>rac</i> -2,3-Dihydroxy-2-methyl- <i>N</i> -(4-nitro-3-(trifluoromethyl)phenyl)-propanamide (<i>rac</i> - 8)	121

7.2.4.2.	(<i>S</i>)-2,3-Dihydroxy-2-methyl- <i>N</i> -(4-nitro-3-(trifluoromethyl)phenyl)-propanamide (<i>S</i> - 8)	122
7.2.4.3.	<i>N</i> -(4-Cyano-3-(trifluoromethyl)phenyl)-2,3-dihydroxy-2-methyl-propanamide (<i>rac</i> - 13)	123
7.2.4.4.	(<i>S</i>)- <i>N</i> -(4-Cyano-3-(trifluoromethyl)phenyl)-2,3-dihydroxy-2-methyl-propanamide (<i>S</i> - 12)	123
7.2.5.	General procedure for the preparation of Mosher esters	124
7.2.5.1.	(2 <i>S</i>)-(2-Methyloxiran-2-yl)methyl 3,3,3-trifluoro-2-methoxy-2-phenyl-propanoate (15)	124
7.2.5.2.	(2 <i>S</i>)-2-Hydroxy-2-methyl-3-((4-nitro-3-(trifluoromethyl)phenyl)amino)-3-oxopropyl 3,3,3-trifluoro-2-methoxy-2-phenylpropanoate (16)	124
7.2.5.3.	(2 <i>S</i>)-3-((4-Cyano-3-(trifluoromethyl)phenyl)amino)-2-hydroxy-2-methyl-3-oxopropyl 3,3,3-trifluoro-2-methoxy-2-phenylpropanoate (17)	125
7.3.	SYNTHESIS OF CLOMIPHENE METABOLITES	125
7.3.1.	4'-Hydroxyclo MPHENE	125
7.3.1.1.	(4-(2-(Diethylamino)ethoxy)phenyl)(phenyl)methanone (19)	125
7.3.1.2.	4-(Benzyloxy)benzaldehyde (20)	126
7.3.1.3.	2-(4-(2-(4-(Benzyloxy)phenyl)-1-phenylvinyl)phenoxy)- <i>N,N</i> -diethyl-ethanamine (21)	127
7.3.1.4.	4-(2-(4-(2-(Diethylamino)ethoxy)phenyl)-2-phenylvinyl)phenol (22)	128
7.3.1.5.	2-((4-(Benzyloxy)phenyl)(hydroxy)methyl)-5,5-dimethyl-1,3,2-dioxaphos-phinane 2-oxide (27)	129
7.3.1.6.	2-((4-(Benzyloxy)phenyl)chloromethyl)-5,5-dimethyl-1,3,2-dioxaphos-phinane 2-oxide (28)	130
7.3.1.7.	4-Formylphenyl trifluoromethanesulfonate (30)	131
7.3.1.8.	4-((5,5-Dimethyl-2-oxido-1,3,2-dioxaphosphinan-2-yl)(hydroxy)methyl)-phenyl trifluoromethanesulfonate (31)	131
7.3.1.9.	4-(Chloro(5,5-dimethyl-2-oxido-1,3,2-dioxaphosphinan-2-yl)methyl)phenyl trifluoromethanesulfonate (32)	132
7.3.1.10.	<i>N,N</i> -Diethyl-2-(4-iodophenoxy)ethanamine (35)	133
7.3.1.11.	1-Iodo-4-(methoxymethoxy)benzene (37)	134
7.3.1.12.	1-(Methoxymethoxy)-4-(phenylethynyl)benzene (38)	134
7.3.1.13.	(<i>E</i>)- <i>N,N</i> -Diethyl-2-(4-(2-(4-(methoxymethoxy)phenyl)-1-phenyl-2-(trimethylstannyl)vinyl)phenoxy)ethanamine (39)	135
7.3.1.14.	(<i>E</i>)- <i>N,N</i> -Diethyl-2-(4-(2-iodo-2-(4-(methoxymethoxy)phenyl)-1-phenylvinyl)phenoxy)ethanamine (40)	136
7.3.1.15.	(<i>E</i>)-2-(4-(2-Chloro-2-(4-(methoxymethoxy)phenyl)-1-phenylvinyl)-phenoxy)- <i>N,N</i> -diethylethanamine (41)	137
7.3.1.16.	<i>tert</i> -Butyl(4-iodophenoxy)dimethylsilane (42)	137
7.3.1.17.	(<i>E</i>)-4-(1-chloro-2-(4-(2-(diethylamino)ethoxy)phenyl)-2-phenylvinyl)phenol (CM 2)	138
7.3.2.	3,4-Di-hydroxy-di-hydroclomiphene	139
7.3.2.1.	4-Bromobenzene-1,2-diol (45)	139
7.3.2.2.	4-Bromo-1,2-bis(methoxymethoxy)benzene (46)	140
7.3.2.3.	2-(4-Bromophenoxy)- <i>N,N</i> -diethylethanamine (49)	141
7.3.2.4.	(4-Bromophenoxy)triisopropylsilane (57)	142
7.3.2.5.	((4-Bromo-1,2-phenylene)bis(oxy))bis(methylene)dibenzene (62)	142
7.3.2.6.	Allyl[1,3-bis(2,6-diisopropylphenyl)imidazol-2-ylidene]chloropalladium(II) [(<i>IPr</i>)Pd(allyl)Cl] (51)	143
7.3.2.7.	General procedure for the preparation of deoxybenzoins 52 , 58 and 61	144
7.3.2.7.1.	2-(4-(2-(Diethylamino)ethoxy)phenyl)-1-phenylethanone (52)	144
7.3.2.7.2.	1-Phenyl-2-(4-((triisopropylsilyl)oxy)phenyl)ethanone (58)	145
7.3.2.7.3.	2-(4-Hydroxyphenyl)-1-phenylethanone (61)	146
7.3.2.8.	General procedure for the preparation of ketones 53 and 63	146
7.3.2.8.1.	2-(3,4-Bis(methoxymethoxy)phenyl)-2-(4-(2-(diethylamino)ethoxy)-phenyl)-1-phenylethanone (53)	147
7.3.2.8.2.	2-(3,4-Bis(benzyloxy)phenyl)-1-phenyl-2-(4-((triisopropylsilyl)oxy)-phenyl)-ethanone (63)	148
7.3.2.9.	General procedure for the preparation of alcohols 54 and 64	149
7.3.2.9.1.	2-(3,4-Bis(methoxymethoxy)phenyl)-2-(4-(2-(diethylamino)ethoxy)-phenyl)-1-phenylethanol (54)	149
7.3.2.9.2.	2-(3,4-Bis(benzyloxy)phenyl)-1-phenyl-2-(4-((triisopropylsilyl)oxy)phenyl)-ethanol (64)	151

7.4. Metabolic model reactions	152
7.4.1. Chemical oxidation of clomiphene.....	152
7.4.2. Incubation of clomiphene with human liver microsomes.....	153
7.4.2.1. Experiments for the optimization of incubation parameters.....	153
7.4.2.2. Identification of the unknown clomiphene metabolites.....	154
8. APPENDICES	156
8.1. LIST OF ABBREVIATIONS	156
8.2. SELECTED SPECTRA	159
8.2.1. <i>rac</i> -2,3-Dihydroxy-2-methyl- <i>N</i> -(4-nitro-3-(trifluoromethyl)phenyl)-propanamide (<i>rac</i> - 8 , AM 1) ..	159
8.2.1.1. Comparison of synthetic AM 1 with excretion sample.....	160
8.2.2. <i>rac</i> - <i>N</i> -(4-Cyano-3-(trifluoromethyl)phenyl)-2,3-dihydroxy-2-methyl-propanamide (<i>rac</i> - 13 , OM 1).....	161
8.2.2.1. Comparison of synthetic OM 1 with excretion sample.....	162
8.2.3. (2 <i>S</i>)-2-Hydroxy-2-methyl-3-((4-nitro-3-(trifluoromethyl)phenyl)amino)-3-oxopropyl 3,3,3-trifluoro-2-methoxy-2-phenylpropanoate (16).....	163
8.2.4. (2 <i>S</i>)-3-((4-Cyano-3-(trifluoromethyl)phenyl)amino)-2-hydroxy-2-methyl-3-oxopropyl 3,3,3-trifluoro-2-methoxy-2-phenylpropanoate (17).....	164
8.2.5. (<i>E</i>)-4-(1-chloro-2-(4-(2-(diethylamino)ethoxy)phenyl)-2-phenylvinyl)-phenol (CM 2).....	165
8.2.6. 2-(3,4-Bis(methoxymethoxy)phenyl)-2-(4-(2-(diethylamino)ethoxy)-phenyl)-1-phenylethanone (53).....	166
8.2.7. 2-(3,4-Bis(benzyloxy)phenyl)-1-phenyl-2-(4-((triisopropylsilyl)oxy)-phenyl)ethanone (63).....	167
8.2.8. 4-Hydroxyclophene (CM 1).....	168
9. REFERENCES	170
10. CURRICULUM VITAE	177

1. INTRODUCTION

1.1. Doping – a survey

The World Anti-Doping Agency (WADA) defines doping as “*the occurrence of one or more of the anti-doping rule violations set forth in Article 2.1 through Article 2.10 of the World Anti-Doping code*”.¹ The presence of a prohibited substance or its metabolites or markers in an athlete’s sample is thereby assessed as the most important rule violation. Further regulations cover the use, the possession, the trafficking and the administration of prohibited substances and methods, as well as prescriptions concerning doping control procedures.

The fact that the etymological origin of the term *doping* is to be found in Afrikaans, shows that doping is definitely not a fashion trend of modern times. It can be traced back to the term *dop*, which was used by the indigenous people of southeast Africa and meant a special spirit that was drunk during rituals for stimulation purposes. The Boers adopted it and used it as a general term for stimulating beverages. Since the first doping incidents go back to the Ancient Olympic Games, its connection to drug misuse and cheating in sports was drawn long time ago. The ancient Greeks have already made use of various performance-enhancing substances to gain advantages in competition. It was for example common to extract the tryptamine alkaloid bufotenin from fly agarics, because owing to its hallucinogenic effect it was assumed to provide superhuman strength. The Incas on the other hand mixed caffeine with different alcoholic beverages and chewed coca leaves to prevent physical fatigue during sporting events.²

In modern times doping came up again in the second half of the 18th century, when among cyclists the use of caffeine- and alcohol-containing beverages as well as of nitroglycerine and cocaine grew in popularity.³ In 1896 the first documented doping incident was reported, when the British cyclist Arthur Linton died during a race due to the abuse of ephedrine. Also the death of Tom Simpson at the Tour de France 1967 caused uproar in the media. Despite immediate medical attendance, he died after having administered amphetamines.

One of the last decades’ most popular doping incidents occurred at the Olympic Games 1988 in Seoul, where Ben Johnson, winner of the 100-metre dash, was found guilty of having administered the anabolic steroide stanozolol. This conviction can also be regarded as the

first major breakthrough of doping analytics, a to this point emerging field of analytic chemistry, devoted to the development of techniques for the proof of doping violations. In parallel with the increasing drug abuse in sports, doping analysis rapidly made progress. In the 1980s compact GC-MS devices for in-competition testings were available for the first time. They allowed for routine screenings of a variety of doping substances. Further efforts were focused on the study of metabolic pathways of doping reagents. As the majority of drugs are subjected to enzymatic transformations in human metabolism, a detection of the original molecule in the urine is often not possible any more. The chemical structures of the most abundant metabolites have to be elucidated, otherwise an abuse by athletes often cannot be verified. Stanozolol was found to be converted into different hydroxy-metabolites, which were detected in Johnson's urine sample and convicted him of illicit steroid abuse.⁴

Another big doping scandal is linked with the Tour de France 1998. The finding of a vast amount of doping substances in the quarters of the *Festina* cycling team entailed severe investigations, which unveiled a widespread network of systematic doping leading to the disqualification of many racing teams and even to the arrest of team personnel. Among other substances mainly erythropoietin (EPO) was confiscated. EPO is a non-species-specific glycoprotein hormone that controls erythropoiesis (the production of red blood cells). Athletes use it to increase the capacity of oxygen transport for a markedly higher oxygen supply of strained muscles, which directly leads to an enhancement of physical endurance. Besides anabolic steroids, EPO and its analogs belong to the publicly best known doping substances. Though EPO was known to be widely used for doping purposes in the 1990s, its direct detection from urine has only been possible since 2001.⁵ Until then it had not been feasible to distinguish the synthetic EPO from the nearly identical endogenous hormone.

The last decade's doping scandals involve the so-called *BALCO* affair (2003), in the course of which the American company *Bay Area Laboratory Co-Operative* was accused of supplying American and European top-class athletes with the designer steroid tetrahydrogestrinone (THG), and the affair around the Spanish doctor Fuentes (2006), who was alleged to have provided hundreds of cyclists and other athletes with blood doping, among them the famous German racer Jan Ullrich.

More recent incidents concern the Austrian racer cyclist Bernhard Kohl, who was convicted of doping with the EPO-analogue CERA (continuous erythropoietin receptor activator) after his sensational performance at the Tour de France 2008, and of course the affair around

Lance Armstrong. The former cycling luminary, who had vehemently demented all accusations for years, in January 2013 finally admitted to doping within a 3-hour interview on television in the famous US talk show of Oprah Winfrey. This big confession has received a great deal of attention from the international press and once again has provoked thought about the problem of ever-present drug abuse in sports.

An alarming fact in this connection is that illicit drug abuse is definitely not a phenomenon just to be found in high-performance sports. Whereas in former times the use of anabolic steroids and hormone preparations was mainly common among bodybuilders and strength athletes, nowadays more and more recreational athletes administer performance enhancing substances to gain advantages in various types of sport events.

Most substances misused for doping purposes are valuable therapeutics. They were originally developed for the treatment of various diseases and their performance-enhancing impacts on the body are primarily just side-effects in their activity spectra. Therefore administration of these substances without any medical indication, in defiance of contraindications, interactions and dosage prescriptions is a highly risky business. Thus, doping is not merely forbidden because of ethical reasons, but rather because it severely endangers athletes' health. Compounds traded on the black market represent an additional source of danger, because they are often not intended for an application in human medicine and cannot be compared to legally commercially available drugs regarding their potency of active ingredients or level of purity.

New achievements in pharmaceutical research constantly extend the range of doping-relevant substances. Unlike any other field of analytical chemistry, doping-analytics is one with a constantly moving target. Novel doping methods instantaneously require new analytic detection methods. The challenges of anti-doping analysis are growing ever more complex, as more and more compounds become available, which not only mimic the function of endogenous compounds, but also become almost indistinguishable in their chemistry. Additionally, there is the continuous challenge of identifying the next potential doping reagents and providing a method for their detection before they become widely used. This is aggravated by the fact that many substances, though already freely available on the black market, in fact are still objects of clinical trials and not even approved for the clinical administration on patients. This is why the WADA aims for an intensified cooperation with

leading drug makers, so that in future potential doping substances, although not clinically approved, nevertheless can be included into routine doping analyses.⁶

Apart from all the health risks, doping brings along, also its ethical aspect should be mentioned. Doping ruins equal opportunities and disagrees with all basic ideas of sports. After all it should be the athletes who fight for winning a contest and not people who produce, administer or deal with performance-enhancing substances.

1.2. Doping – statutory regulations

In earlier times anti-doping measures were mainly realized by national initiatives. In Austria the *IMSB-Austria (Institute for Sports Medicine and Science)*⁷ was commissioned to develop and implement a nationwide anti-doping strategy by the former federal minister Dr. H. Moritz in 1986. This involved the first itemization of doping regulations and in further consequence the implementation of the first controls on prohibited substances during sport competitions.

In the mid-eighties the Council of Europe launched an initiative and installed a task force devoted to the elaboration of a *European anti-doping convention*. Besides Austria, Switzerland, Germany, France, Belgium, Denmark and Luxembourg were the participating countries. The leadership was held by the *International Olympic Committee (IOC)*⁸. All member states committed themselves to take measures against doping in sports, which should be facilitated by transnational cooperation and the linkage of national anti-doping facilities. This worldwide first doping convention was signed by Austria in 1991.

In 1995 the first *Austrian Anti-Doping-Committee (Österreichisches Anti-Doping-Komitee ÖDAC)* was found. It took over the tasks of the *IMSB-Austria* and was in principle a predecessor institution of today's *National Anti-Doping Agency (NADA)*. Additionally to the already established in-competition controls, the ÖDAC also started to conduct out-of-competition controls during the phases of training.

The doping scandal at the Tour de France 1998 produced new efforts in the fight against doping and entailed the first *World Conference on Doping in Sport*, which took place in Lausanne in February 1999. Its main achievement was the foundation of the *World Anti-Doping Agency (WADA)*⁹, which has been controlling anti-doping policies since that time. In 2003 the first *World Anti-Doping-Code* was published, to which all international associations

and Olympic committees had to commit themselves. This set of anti-doping rules is the core document that provides the framework for harmonized anti-doping policies, rules and regulations within sport organizations and among public authorities. A revised version of this first code has been in force since 2009. In the course of the *World Conference on Doping in Sport 2013* the *World Anti-Doping-Code* was adapted again and the new version¹ will become effective on January 1st, 2015.

In 2008 the NADA Austria was established as independent anti-doping organization, whose purpose is to implement the *Anti-Doping Federal Act 2007* (Anti-Doping Bundesgesetz, ADBG). Its key mission is to fight illegal drug abuse in sports by providing an efficient, state-of-the-art doping control system and the prevention of doping via education, information and awareness-raising programs.¹⁰

Table 1 depicts an extract from the official WADA statistics published for the year 2012.¹¹ It shows that from a total of 267 645 analyzed A-samples 1.2% of the results were adverse analytical findings (AAFs). This means that the presence of a prohibited substance or its metabolites or markers, respectively the use of a prohibited method, was verified for these samples. 0.8% of the results are referred to as atypical findings (ATFs), which means that these samples provided atypical values and had to be analyzed in more detail. It has to be pointed out that the number of AAFs and ATFs does not necessarily reflect the number of sanctioned anti-doping rule violations, because these findings also include cases where banned substances were approved by an anti-doping organization for legitimate medical reasons. Non-ADAMS data refers to figures that cannot be reported via the Anti-Doping Administration and Management System (ADAMS), because they comprise professional and university testing programs. Over the past five years the number of analyzed A-samples as well as the number of findings has remained fairly constant.

Table 1 Extract from the official WADA statistics for the year 2012¹¹.

Sport	A-Samples analyzed	Adverse Analytical Findings	Atypical Findings	Total Findings
Olympic Sports	184 955	1 831 (0.99%)	1 063 (0.58%)	2 894 (1.56%)
Non-Olympic Sports	21 436	718 (3.35%)	147 (0.69%)	865 (4.03%)
Non-ADAMS Data	61 254	641 (1.05%)	323 (0.53%)	964 (1.57%)
Total	267 645	3 190 (1.19%)	1 533 (0.57%)	4 723 (1.76%)

1.3. Prohibited substances and methods

The *Prohibited List* is a summary of all prohibited substances and methods. According to Article 4 of the *World Anti-Doping-Code* it should be published as often as necessary and no less often than annually as an international standard. The version of 2014¹² categorizes as follows:

- Substances and methods prohibited at all times (in- and out of competition)
 - Prohibited substances
 - S0. Non-approved substances
 - S1. Anabolic agents
 - S2. Peptide hormones, growth factors and related substances
 - S3. Beta-2 agonists
 - S4. Hormone and metabolic modulators
 - S5. Diuretics and other masking agents
 - Prohibited methods
 - M1. Manipulation of blood and blood components
 - M2. Chemical and physical manipulation
 - M3. Gene doping
- Substances and methods prohibited in-competition
 - Prohibited substances
 - S6. Stimulants
 - S7. Narcotics
 - S8. Cannabinoids
 - S9. Glucocorticosteroids
- Substances prohibited in particular sports
 - P1. Alcohol
 - P2. Beta-blockers

The prohibited agents are listed in terms of selected examples, so that basically not all prohibited substances are mentioned. This gap is bridged by the phrase “*and other substances with a similar chemical structure or similar biological effect(s)*”, which terminates

each list. This comprehensive inclusion of all similar agents is primarily related to designer substances and drugs with unknown chemical structures at the time of list publishing. Since 2011 also an introductory sentence, emphasizing the status of drugs with no official approval and not covered by other sections of the *Prohibited List*, has been added (S0. section) to ensure the clear prohibition of all substances that are currently not approved for human therapeutic use (e.g. therapeutics under clinical or preclinical development or substances only approved for veterinary use).

Figure 1 summarizes the amounts of worldwide identified substances for the year 2012¹¹, divided into the particular drug classes. As half of all positive A-samples (50.6%) indicated illicit administration of anabolic agents, they can be regarded as currently prevailing doping substances.

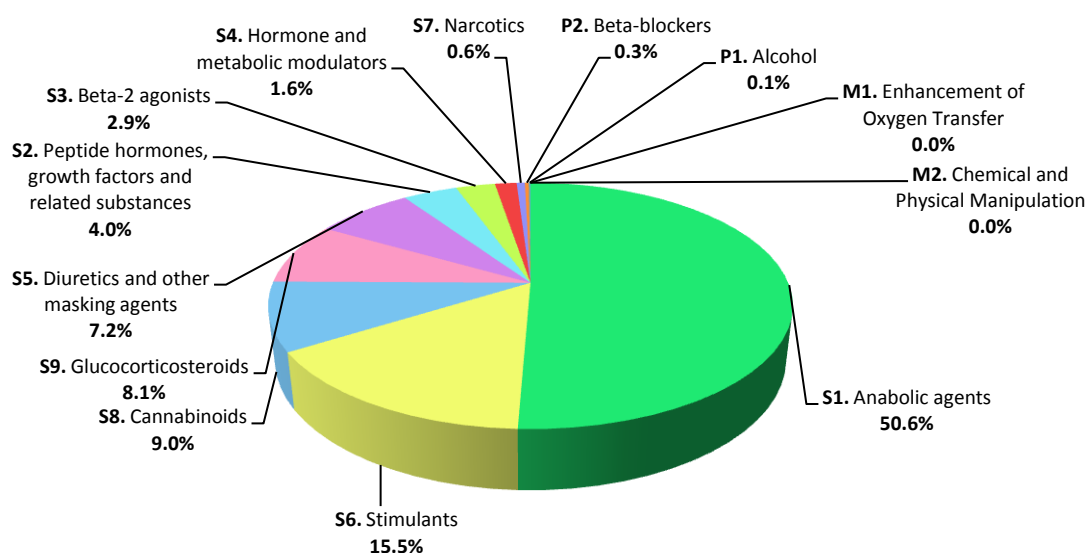


Figure 1 Summary of substances identified in each drug class in ADAMS for the year 2012¹¹.

1.4. Doping analytics

The development of new anti-doping analyses for the detection and quantification of prohibited substances presents a great challenge to analytical chemists. A wide range of chemically entirely different compounds shall be detected simultaneously, applying robust procedures that feature high sample throughputs combined with high sensitivities and specificities for the targets in question. Until the end of the last century gas chromatography with or without mass spectrometry (GC-MS) was the prevailing standard procedure in

routine doping controls. The limitations of GC concerning e.g. high molecular weight analytes or highly polar compounds, which need to be converted into less polar derivatives prior to analysis, more and more led to a switch to liquid chromatography (LC) based methods during the past decade. Nowadays mass spectrometry coupled with chromatographic separation is still an essential analytical method in anti-doping laboratories, but new generations of doping substances also require the additional use of various bioanalytical approaches like isoelectric focusing (IEF), gel electrophoresis or immunological methods.

1.4.1. Exogenous and endogenous doping agents

The first important question in the course of method development in anti-doping analysis is whether the substance in question is an exogenous xenobiotic or an analog or recombinant form of an endogenous compound. In the case of xenobiotic substances, their physical and chemical properties as well as their metabolic fate in human metabolism have to be examined first. While some drugs are excreted mainly unchanged, others are subjected to complicated metabolic processes so that the parent compound cannot be traced to significant amounts in the urine any more. In these cases the detection method has to target the main metabolite(s) of the doping agent in question. These metabolites need to be available as reference substances, because the unequivocal proof of an illicit xenobiotic substance in a urine sample requires its comparison to a standard. Important criteria that have to be identical are the retention time, the fragmentation pattern and the fragments' relative abundances. If these reference compounds are not available as synthetic standards, human excretion samples have to be utilized. As the latter method is ethically rather questionable and most of the metabolites are not commercially available, they have to be synthesized especially for this purpose.

Recombinant forms or analogs of endogenous compounds represent the second big class of doping agents. As these agents are chemically nearly indistinguishable from the endogenous forms, the challenge in this case consists in the development of special techniques that allow the direct or indirect proof that these substances have been exogenously administered. The first endogenously occurring substance that had been abused in that way was testosterone. In contrast to xenobiotic substances, where a detection at any concentration results in an adverse analytical finding, testosterone is always present in doping control samples.

Therefore thresholds for urinary concentrations or concentration ratios such as the testosterone/epitestosterone quotient¹³ were developed. Due to large biological variations in these parameters, indirect methods are often inconclusive. These uncertainties were overcome in the mid-1990s by the development of gas chromatography/combustion/isotope ratio mass spectrometry (GC/C/IRMS), the state-of-the-art-method for the direct detection of endogenous steroids. After the online combustion of organic compounds eluting from the GC, the formed CO₂ is transferred into the mass spectrometer, where the ¹³C/¹²C ratios are analyzed. As steroids produced inside the body exhibit a different ratio than synthetic steroids, the proof of their illicit administration is feasible. Due to promising results in the research of approaches based on ²H/¹H ratios, this method might complement the ¹³C/¹²C method in doping controls in the near future.¹⁴

Another popular example for endogenous doping agents are erythropoiesis stimulating agents (ESAs) like EPO and its analogs (e.g. epoetin delta – *Dynepo* or continuous erythropoietin receptor activator – *CERA*). Their direct detection affords diverse bioanalytical methods such as isoelectric focusing in polyacrylamide slab gels (IEF-PAGE), sodium dodecylsulfate polyacrylamide gel electrophoresis (SDS-PAGE), enzyme-linked immunoassays (ELISA) or membrane assisted isoform immunoassays (MAIIA). Additionally in 2010 the concept of the *Haematological Module* in the *Athlete Biological passport* was launched, an indirect method that monitors changes of haematological data for each athlete individually.¹⁵ Since the beginning of 2014 it has been complemented by the *Steroid Module* and most likely the inclusion of other endogenous drug profiles will follow.¹⁶

1.4.2. Analytical detection methods

In the course of a doping control athletes have to provide a urine sample. As some agents such as many peptide hormones are better detectable from a blood matrix, also blood samples are common. The first blood samples were taken at the Olympic Games in Sydney in the year 2000. The athlete's sample is divided into an A-sample to two-thirds and into a B-sample to one-third. The A-sample subsequently gets analyzed in a WADA-accredited laboratory according to the specified guidelines. In the case of an adverse analytical finding, the B-sample may be opened upon the athlete's request.

The first step in the doping analysis process is the sample preparation, which aims for the isolation of the target analytes from the urine. Many compounds are excreted as

glucuronides or sulfates and have to be hydrolyzed therefore prior to analysis. In special cases also different derivatization techniques are required, e.g. for the GC-MS analysis of polar compounds.

With regard to detection methods, a general distinction is made between screening- and confirmation methods. The screening aims for the parallel detection of a vast number of substances in a short time, conducting little efforts and costs. Whereas in previous times it was common to have different assays for each group of substances, nowadays the trend is towards multi-analyte screening procedures independently from substance classes. As LC-MS(-MS) is the predominant method for analysis, sophisticated derivatization methods or structure-specific pre-concentration and purification are often not mandatory anymore and screening procedures have become mostly independent of substance groupings. If the screening provides an indication for the presence of a prohibited substance, the analyte is isolated once again applying a substance specific isolation procedure and identified within a confirmation method with utmost sensitivity and specificity.¹⁷

There are two different approaches concerning detection methods in LC-MS(-MS) analysis. One possibility is to use low resolution mass spectrometers and focus on preselected target analytes using diagnostic precursor-product ion pairs (multiple or selected reaction monitoring, MRM/SRM). The other common approach uses high resolution/high accuracy mass spectrometry and records accurate masses of intact molecules or their product ions in full scan measurements. The major advantage of this untargeted approach is that it does not just focus on fixed ion transitions, but rather collects the complete raw data, which provides the retrospective opportunity of analyzing old data for formerly unknown compounds or new drugs when they become relevant for doping controls. This was for example the case with the stimulant 4-methyl-2-hexanamine, which was retrospectively detected in 11 urine samples that were initially tested negative.¹⁸

Figure 2 gives a general overview on all analytical detection methods that are currently in use for the analysis of doping control samples in WADA-accredited laboratories.¹⁹

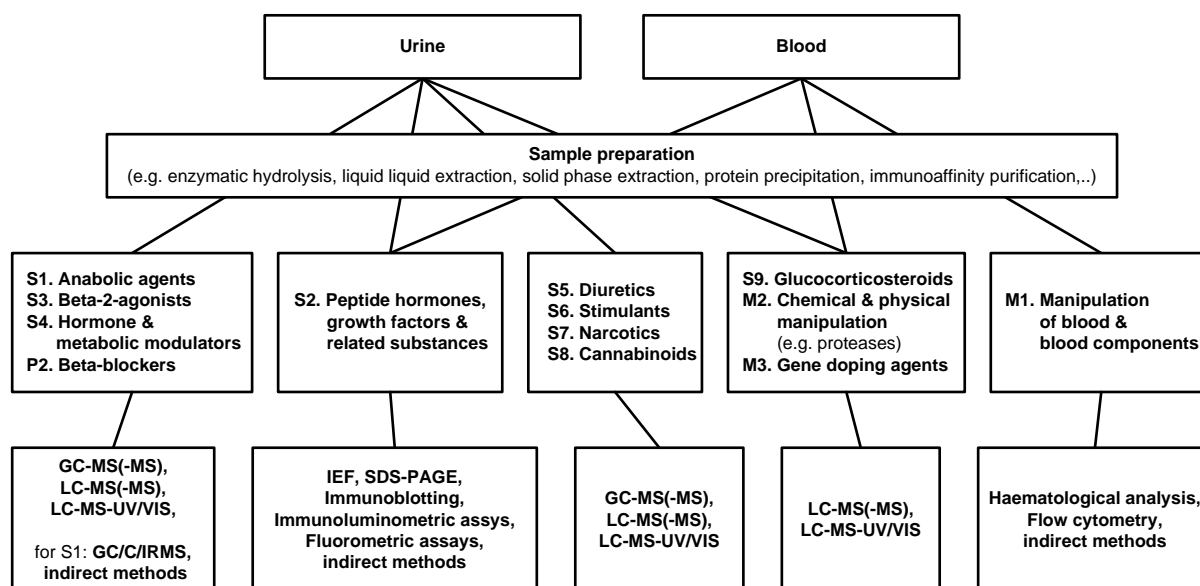


Figure 2 Analytical detection methods used in WADA-accredited laboratories¹⁹.

1.4.3. LC-SPE-NMR/MS

The demand for reference materials for doping-control analysis requires extensive studies of human drug metabolism. In cases when human excretion studies are not feasible (e.g. in preclinical research), metabolic pathways can be mimicked by *in vitro*- or *in vivo* models. The resulting drug metabolites have to be evaluated with regard to their relative abundance and long-term traceability to identify potential markers that can be used for doping-control purposes. A prerequisite for the target-oriented synthesis of these marker substances is their unequivocal structural characterization. This is often achieved by LC-MS(-MS) analysis of the corresponding urinary or microsomal extracts. MS spectral data provides information on the elemental formulae and secondary fragmentation allows deeper insights into molecular structures. However, in cases of partially or completely unknown metabolites when no reference MS data is available, MS alone is usually not enough for unequivocally ascertaining molecular scaffolds, thus requiring the application of NMR spectroscopy as complementary method. Due to its relatively poor sensitivity and technical complexity, its hyphenation with LC has not been realized for a long time. The classical method for obtaining NMR data for major compounds of a mixture was to use a (semi-)preparative scale separation, to evaporate the mobile phase and to dissolve the residues in a deuterated solvent followed by classical NMR tube analysis.²⁰ As the evaporation step bears the risk of unwanted chemical reactions (e.g. oxidation or degradation of analytes) and the whole

approach is rather time-consuming, it was sought for technical solutions for the realization of practical LC-NMR coupling. The first on-line LC-NMR experiments were conducted in the late 1970s by Watanabe and coworkers, who performed stopped-flow measurements of a mixture of known compounds.²¹ From thereon, NMR spectrometer field strength gradually increased, methods for solvent suppression became available, special flow-through probe heads were developed and technical progress was made concerning the physical connection of LC and NMR. Experimental setups improved from on-flow operation modes to stopped-flow settings and further to loop-storage modes, meaning the temporary storage of each analyte peak in individual capillary loops for NMR data acquisition at a later stage without interrupting the chromatographic run. With the development of peak storage by solid-phase extraction (SPE), the sensitivity of LC-NMR again has increased significantly.²² In the course of LC-SPE-NMR the separated peaks are diluted postcolumn with water and get trapped automatically on SPE cartridges. The solvents used for chromatographic separation are removed by drying the cartridges under a stream of nitrogen gas. Afterwards the analytes are transferred with a deuterated solvent of choice to the NMR flow-cell probe, where NMR data acquisition is performed. Thus, LC separations may be conducted under optimized conditions and non-deuterated solvents get removed completely prior to NMR analysis. This not only represents a significant cost reduction compared to conventional LC-NMR, but also reduces the need for solvent suppression which always leads to a loss of spectral information in the vicinity of attenuated signals. Another advantage of LC-SPE-NMR is the option of multiple peak trapping, which means the concentration of the analyte of interest on the cartridge by repeated trappings in the course of up to ten chromatographic runs resulting in highly concentrated re-elution bands. Thus, NMR analysis gets feasible even in cases of very low analyte concentrations and it is possible to obtain in reasonable experimental time not only high quality one-dimensional spectra, but also two-dimensional spectra. Considering the complementary structure information obtained by NMR and MS, the logical consequence was the extension of LC-SPE-NMR to LC-SPE-NMR/MS, which is at the moment the most powerful analytical tool for structure elucidation in natural product chemistry and pharmaceutical industry.²³

A general scheme for LC-SPE-NMR/MS coupling is depicted in Figure 3. After chromatographic separation the flow is split in two parts. Whereas the minor part is directed into the MS, the major part is guided through the UV/VIS-detector to the SPE device where

analytes of interest can be trapped manually or automatically on different cartridges. Their retention on the cartridge packing material is facilitated by a make-up pump that delivers water to the chromatographic flow. After the removal of the mobile phase by nitrogen gas subsequent NMR analysis can be performed on-line or off-line.

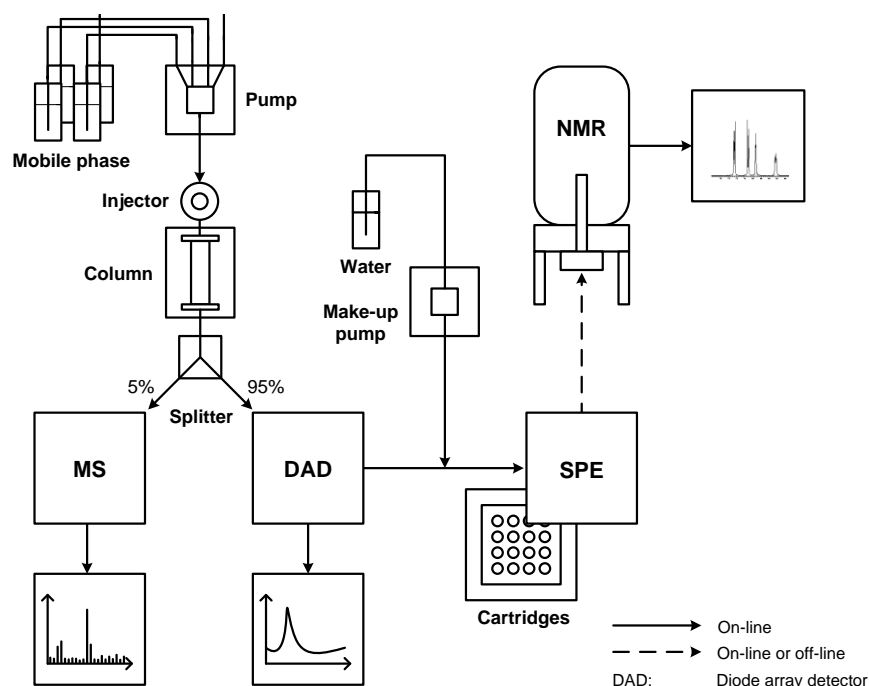


Figure 3 General Scheme for LC-SPE-NMR/MS.

1.5. Nonsteroidal selective androgen receptor modulators (SARMs)

Nonsteroidal selective androgen receptor modulators are a quite new class of androgen receptor ligands. They have been intensively investigated during the last decade, because of their potential ability to replace anabolic-androgenic steroids in the treatment of benign prostatic hyperplasia, hypogonadism, androgen deficiency in the aging male, muscle wasting and osteoporosis.²⁴ Also their eventual application for hormonal male contraception has been discussed.²⁵ Like anabolic-androgenic steroids, SARMs promote cellular protein synthesis resulting in an amplified buildup of cellular tissue, especially in muscles.

While showing the same effectiveness in the activation of the androgen receptor, unlike androgenic steroids, SARMs are not substrates for 5α -reductases and aromatases. Thus, metabolic amplification of androgenic effects in non-target tissues such as the prostate are eliminated and due to the resulting markedly high selectivity to muscle and bone tissue,

SARMs seem to be much more tolerable concerning undesirable side effects.²⁶ Results of preclinical and clinical studies also indicate better pharmacokinetic properties compared to steroidal compounds, including a higher oral bioavailability and a longer half-life.²⁷

In the last few years efforts have been made in identifying new pharmacophores of nonsteroidal SARMs. The first substances to show tissue-selective actions were structurally derived from the anti-androgens flutamide and bicalutamide, building the class of arylpropionamides. They are currently the best investigated SARM-subgroup and comprise the two important lead candidates andarine ((*S*)-3-(4-acetylphenoxy)-2-hydroxy-2-methyl-*N*-(4-nitro-3-trifluoromethylphenyl)-propionamide, also referred to as *S-4* or *GTx-007*) and ostarine ((*S*)-3-(4-cyano-phenoxy)-*N*-(4-cyano-3-trifluoromethylphenyl)-2-hydroxy-2-methyl-propionamide, also *Enobosarm*, *S-22* or *GTx-024*), two investigational drugs developed by *GTx, Inc.* (Figure 4). Whereas andarine is no longer being developed, ostarine is at the advanced clinical phase III.²⁸

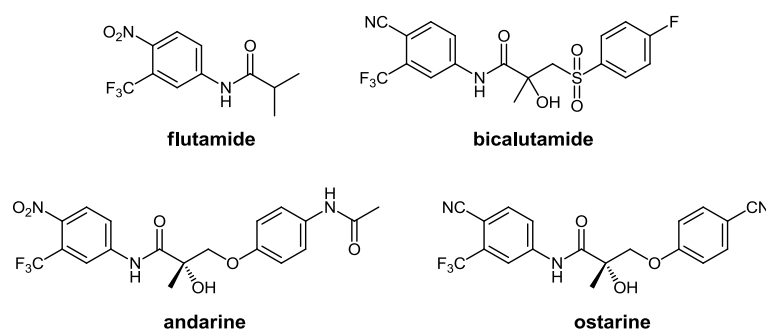


Figure 4 Chemical structures of arylpropionamide-derived SARMs.

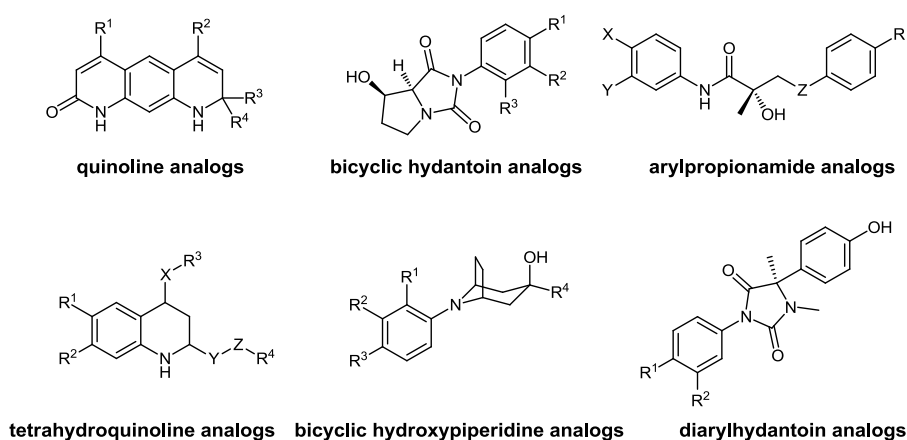


Figure 5 Pharmacophores of SARMs.

Further important pharmacophores include bicyclic hydantoin, quinolines and tetrahydroquinolinones.²⁶ Recently also diarylhydantoin²⁹ and bicyclic hydroxypiperidine derivatives³⁰ were reported to exhibit tissue-selective effects on muscle and bone, while sparing the prostate (Figure 5).

1.5.1. SARMs – doping

As is the case with anabolic steroids, also SARMs have a very high potential for misuse in sports due to their beneficial effects on muscle growth and strength. Accordingly, the whole class has been included in the list of prohibited substances by the WADA since 2008. They are listed in subgroup “2. Other Anabolic Agents” of group “S1. Anabolic Androgenic Steroids”.¹² This step proved correct with the first finding of the arylpropionamide-derived substance andarine in a black market product in 2009.³¹ Although by now none of the lead candidates has received clinical approval, various substances are already freely available on the internet.³² In 2010, the Swiss laboratory for doping analyses reported the first case of SARMs abuse during an in-competition testing resulting in an adverse analytical finding. It was again andarine, which an athlete’s urine sample was tested positive for.³³ The first doping breach involving ostarine was reported in 2013, when the Russian cyclist Nikita Novikov delivered a positive A-sample during an out-of-competition testing.³⁴

1.5.2. SARMs – metabolism

SARM lead candidates are under current clinical investigation, so pharmacokinetic and pharmacodynamic studies have not been completed yet. Hence, a lot of data concerning metabolism and potential adverse drug reactions is still pending. But their use as doping substances pushes anti-doping research in getting profound insight into the metabolic pathways of SARMs.

In the case of andarine numerous *in vitro* simulations³⁵ as well as animal administration studies³⁶ have been published to indicate potential targets for doping analysis. The first mass spectrometric characterization of urinary metabolites, obtained from an authentic human urine specimen, was performed by Thevis and coworkers in 2010. They identified various phase I and II metabolites, including glucuronic acid and sulfate conjugates of the active drug and of hydroxylated and/or deacetylated products (see Figure 6). One of the most

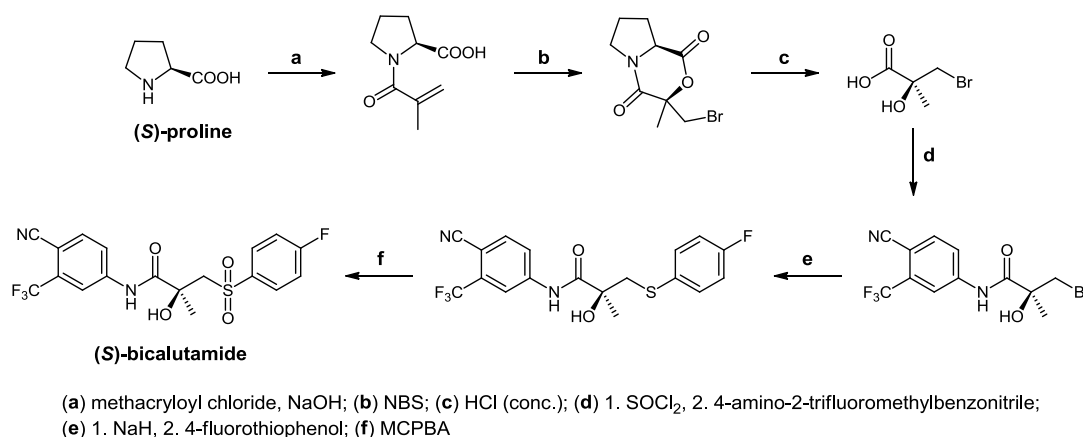


Figure 8 Synthesis of (*S*)-bicalutamide.

The first SARM metabolite that was prepared as reference compound for doping control purposes was **AM 1**. It was obtained by Thevis *et al.* via electrochemical oxidation of andarine in sufficient amounts for LC/NMR-analyses and inclusion in routine doping control procedures.⁴⁵

1.6. Selective estrogen receptor modulators (SERMs)

Estrogens play an essential role in reproductive physiology. Their binding to the estrogen receptors activates transcription of genes involved in cellular growth control. Estrogenic unbalances can be a causative factor in the pathogenesis of various diseases, so is estrogen deficiency the main cause of postmenopausal osteoporosis, whereas excess estrogen can stimulate the proliferation of breast epithelial cells and thus promote breast cancer.

Unlike estrogens, which act solely as agonists, and antiestrogens, which act solely as antagonists, selective estrogen receptor modulators (SERMs) can selectively exert both effects on different tissues. Thus, beneficial effects of estrogenic or antiestrogenic activity are focused on the target tissue, while adverse effects on other tissues are diminished or even eliminated.⁴⁶ Examples for SERMs in clinical use are tamoxifene and toremifene for the treatment of breast cancer or raloxifene for the treatment of postmenopausal osteoporosis (Figure 9).

Clomiphene was one of the first described SERMs. It was shown to suppress the proliferation of cultured human breast cells and to inhibit the growth of chemically induced breast cancer in the rat, but toxicological issues prevented further drug development for this indication.⁴⁷ Clomiphene was also found to induce ovulation in subfertile women⁴⁸ and is

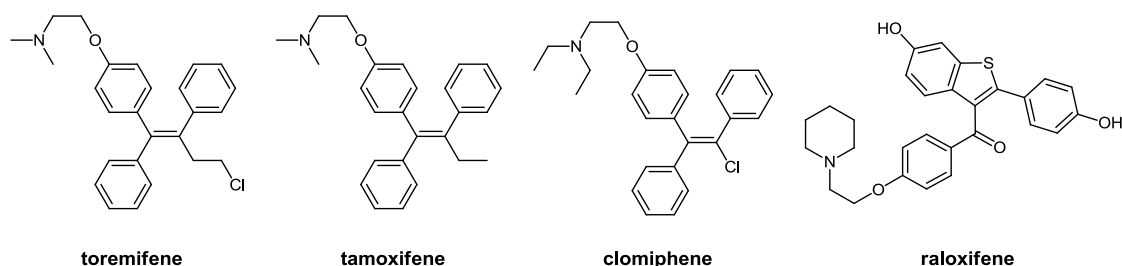


Figure 9 Pharmacophores of SERMs.

now in use as therapeutic agent for the induction of ovulation. Acting as estrogenic antagonist in the hypophysis, it simulates an estrogen deficiency and thus amplifies the release of follicle stimulating hormone (FSH) and luteinizing hormone (LH), which in further consequence promotes ovulation. Clomiphene is sold as a mixture of (*E*)- and (*Z*)-stereoisomers, the percentage of the (*Z*)-isomer varying between 30 and 50%, depending on the brand. Whereas (*Z*)-clomiphene is an estrogenic agonist, (*E*)-clomiphene acts as estrogenic antagonist.

1.6.1. SERMs – doping

Anti-estrogenic substances prevent the conversion of the male sexual hormone testosterone into the female hormone estrogen in different ways. By stimulating gonadotropine-release, the endogenous production of androgens also may be increased.⁴⁹ Athletes benefit from this direct effect and misuse this class of drugs primarily to compensate for the adverse effects of an extensive abuse of anabolic androgenic steroids, which often entails a decrease in endogenous androgens production or gynaecomastia. On that account these substances have been prohibited in- and out-of-competiton by the WADA since 2000.

Considering the anti-estrogenic action of its (*E*)-isomer, Clomiphene is listed in subgroup “3. Other anti-estrogenic substances” of group “S4. Hormone and Metabolic Modulators”. The other subgroups are “1. Aromatase inhibitors”, “2. SERMs”, “4. Agents modifying myostatin function(s)” and “5. Metabolic modulators”.¹² In the beginnings aromatase inhibitors, anti-estrogens and SERMs were listed as “Substances with anti-estrogenic activity” and their prohibition only applied for men. Since 2005 they have also been banned for women. In 2008 the group was extended by myostatin inhibitors and since 2012 metabolic modulators have been included.

Two famous doping breaches involving SERMs were reported in 2003. In the course of the handball world championships a player of the Egyptian national team was tested positive for tamoxifene, as was the Swiss Rene Zimmermann, Mr. Universe in bodybuilding, in the same year.⁵⁰

1.6.2. Clomiphene – metabolism

Considering its clinical application for decades, unlike as it is the case with SARMs, a lot of data dealing with clomiphene's metabolism is available nowadays. Early *in vitro*- and *in vivo* experiments⁵¹ were later extended by studies of metabolites occurring in humane urine. The first analysis of urinary metabolites was performed by GC-MS and identified a hydroxy derivative as main metabolite. The exact position of hydroxylation could not be determined to that point.⁵² A few years later Vitoriano and coworkers as well as Oueslati *et al.* asserted this result and designated 4-hydroxyclophene as predominantly occurring metabolic product beside numerous others.⁵³ Further metabolites were also described by Mazzarino and coworkers.⁵⁴ In 2012 the group of Lu reported a new metabolic pathway of hydrogenation at the double bond and designated 3,4-di-hydroxy-di-hydroclomiphene and 3,4-di-hydroxy-di-hydro-*N*-desethylclomiphene as potential biomarkers for monitoring oral administration of clomiphene in urine for doping control purposes. According to them, these two metabolites' abundances are much higher than that of 4-hydroxyclophene. They also described the formation of tri- and tetrahydroxylated metabolic products for the first time.⁵⁵ In 2013 further new structures of metabolites were reported by Mazzarino *et al.* and the group of Lu.⁵⁶ Figure 10 summarizes all described metabolite structures of clomiphene with the most important ones highlighted.

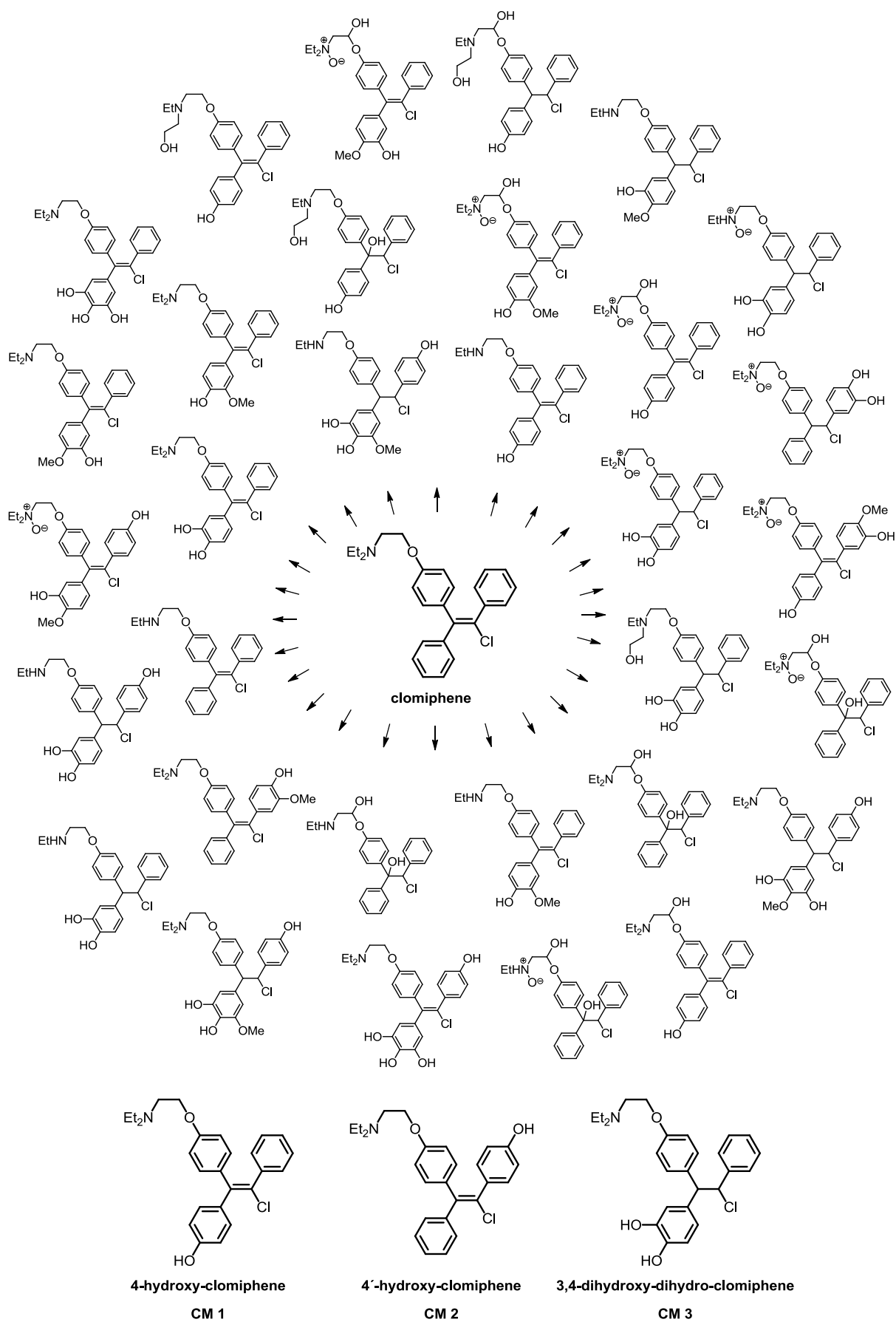


Figure 10 Summary of all described urinary clomiphen metabolites.

1.6.3. General approaches for the synthesis of 1,1,2-triphenylethylenes

Regarding their chemical structure, a large part of SERMs can be described as derivatives of 1,1,2-triphenylethylene (TPE) (see Figure 11). Apart from clomiphene also tamoxifene and toremifene are based on this structural element (see Figure 9). Considering the general structural formula of TPE-based clinically applied SERM-reagents, substitution is mostly found on the free double bond position (R^1) as well as on the α' -phenyl moiety in *para*-position (R^2). *Para*- and *meta*-substitution of the α - and β -ring (R^3 , R^4 , R^5 , R^6) are common modifications reported for the corresponding metabolites, which are often hydroxylated or methoxylated at these positions.

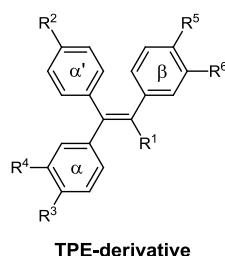


Figure 11 General structure of a TPE-derivative.

The key step in the synthesis of TPEs is the setup of the alkene backbone. In general this can be achieved via four different approaches. The addition of organometallic compounds to a deoxybenzoin- or benzophenone derivative followed by acid catalyzed dehydration is a well established approach in the synthesis of SERM metabolites (see Figure 12). Additionally to Grignard reagents⁵⁷ also organolithium compounds are used for this purpose. The corresponding reagents are obtained via metal halogen exchange reactions⁵⁸ or metalation of alkylbenzenes using strong bases⁵⁹.

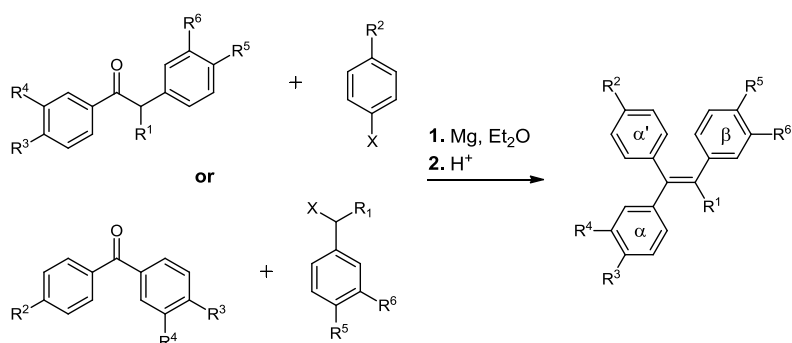


Figure 12 TPE-synthesis via Grignard reaction ($X = \text{halogene}$).

A second common method for the synthesis of TPE-derivatives is the McMurry cross coupling reaction, which is defined as reductive dimerization of ketones or aldehydes in the presence of low-valent titanium reagents to yield alkenes. Via coupling of substituted benzophenones with benzaldehyde- or propiophenone derivatives, TPEs can be obtained as mixtures of their (*E*)- and (*Z*)-isomers (see Figure 13).⁶⁰ In 1989 Ruenitz *et al.* described the first synthesis of phenolic clomiphene metabolites using this reaction type.⁵¹ The separation of these diastereomers can generally be achieved chromatographically or by fractionated crystallization, but often proves to be difficult or even not feasible. Nevertheless, in the following years a lot of methods for the stereoselective preparation of different isomers of SERM metabolites via McMurry coupling reaction were reported. These strategies involve methods to directly improve the (*E*)/(*Z*)-ratio of the coupling⁶¹ as well as rather time-consuming derivatization-, separation- and isomerization techniques⁶² of the crude reaction mixture. By this means, different metabolites of tamoxifene and toremifene were obtained in high isomeric purity.

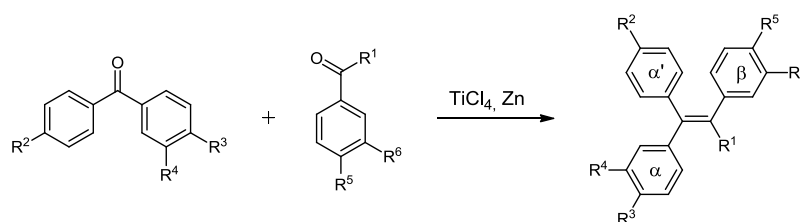


Figure 13 TPE-synthesis via McMurry reaction.

Also Wittig-type reactions have been described in literature for the construction of the TPE-carbon skeleton. They start from an aldehyde or ketone, which is reacted with the ylide obtained from a phosphonium salt. In this manner using a strong base, benzhydryl(triphenyl)phosphonium bromide can be converted into the corresponding ylide, which gives the TPE upon reaction with an arylcarbonyl compound (see Figure 14).⁶³ However, due to the lower reactivity of ketones and difficulties caused by steric hindrances, this route has been barely applied for the synthesis of TPE-based SERM metabolites. Marques *et al.* succeeded in the synthesis of 4-hydroxy-3-methoxy-*N*-desethyl-clomiphene via a Horner Wadsworth Emmons reaction. They obtained the target structure as (*E*)/(*Z*)-mixture after the reaction of the appropriate benzophenone derivative with a cyclic α -chlorophosphonate (see Figure 14).⁶⁴

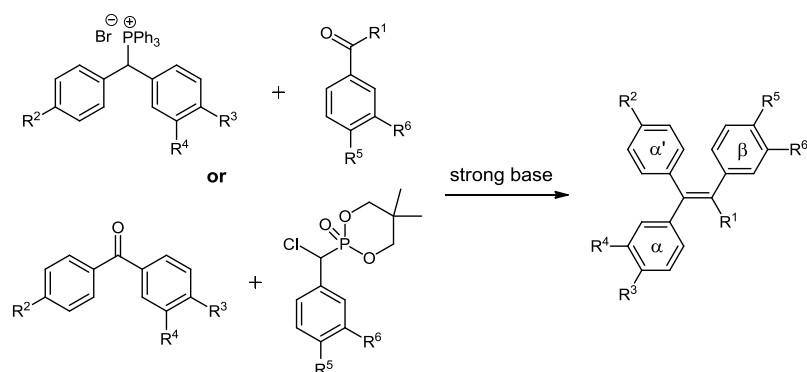


Figure 14 TPE-synthesis via Wittig-type reactions.

The major drawback of all by now discussed procedures for the synthesis of TPEs is their lack of control over stereoselectivity. A comparatively new approach enabling the selective synthesis of tetrasubstituted olefins consists in palladium-catalyzed reactions. Their generality and ability to tolerate a wide range of functional groups make them a promising alternative pathway for the preparation of tetrasubstituted alkenes. Starting from an alkyne the vinylic palladium intermediate generated by carbopalladation can be trapped by various reagents, thus facilitating the regio- and stereoselective synthesis of highly substituted olefins (see Figure 15).

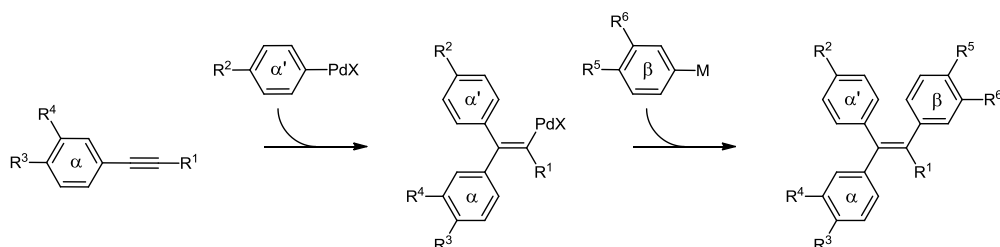


Figure 15 TPE-synthesis via palladium-catalyzed reactions.

Al-Hassan *et al.* reported early on the stereoselective synthesis of (*Z*)-tamoxifene via a multistep procedure starting from an alkynylsilane. Via directed carbometalations, halogenations and arylations both tamoxifene isomers were prepared in a stereoselective manner.⁶⁵ Larock and coworkers later presented a more convenient method for the selective synthesis of tetrasubstituted olefins. They developed a three-component coupling of an aryl iodide, an internal alkyne and an arylboronic acid, enabling the regio- and stereoselective preparation of tamoxifene and some of its derivatives in a one-step reaction.⁶⁶ In 2010 Tsuji *et al.* demonstrated the highly regioselective synthesis of 4-hydroxytamoxifene and its

isomer 4'-hydroxytamoxifene via stannyl lithiation of a diarylacetylene followed by sequential palladium-catalyzed arylation- and ethylation reactions.⁶⁷

1.7. Objective

Human metabolism studies conducted for the SARMs andarine and ostarine indicate hydrolysis of the ether linkage as predominant metabolic transformation yielding the molecules *O*-dephenylandarine **AM 1** and *O*-dephenylostarine **OM 1** (see Figure 16).^{37,38} One of this thesis' targets was to develop a convenient synthetic route towards **AM 1** and **OM 1** and to examine whether these molecules are indeed the main metabolites occurring in human urine. If so, larger quantities should be provided for the application as reference materials in doping control analysis.

There is a lot of literature dealing with the human metabolism of the antiestrogenic drug clomiphene. Whereas it has been assumed for a long time that clomiphene's main metabolite occurring in human urine is a hydroxy-derivative^{52,53}, more recent publications describe various double bond-hydrogenated compounds as predominant metabolic products. Especially 3,4-di-hydroxy-di-hydroclomiphene and 3,4-di-hydroxy-di-hydro-*N*-desethyl-clomiphene were presented as potential biomarkers for the monitoring of clomiphene administration.⁵⁵ The total synthesis of 4-hydroxyclophene **CM 1** has already shown that **CM 1** is in fact a detectable urinary metabolite, but not the predominant one.⁶⁸ For elucidating the chemical structure of clomiphene's main metabolite, 4'-hydroxy-clomiphene **CM 2** and 3,4-di-hydroxy-di-hydroclomiphene **CM 3** (see Figure 16) should be synthesized and compared to the compounds present in an excretion sample after the oral administration of clomiphene.

In parallel to these synthetic tasks, a convenient model system for the simulation of clomiphene's metabolic fate should be developed. It is known that the Cytochromes P450 are the predominant enzymes in drug metabolism. Among others, they mediate oxidation reactions, resulting in a higher hydrophilicity of drugs. The task was to develop an appropriate chemical or enzymatic model system to mimic these reactions. By these means, it should be accomplished to prepare the target metabolite in a larger amount, so that its unequivocal structure elucidation by LC-SPE-NMR/MS would get feasible.

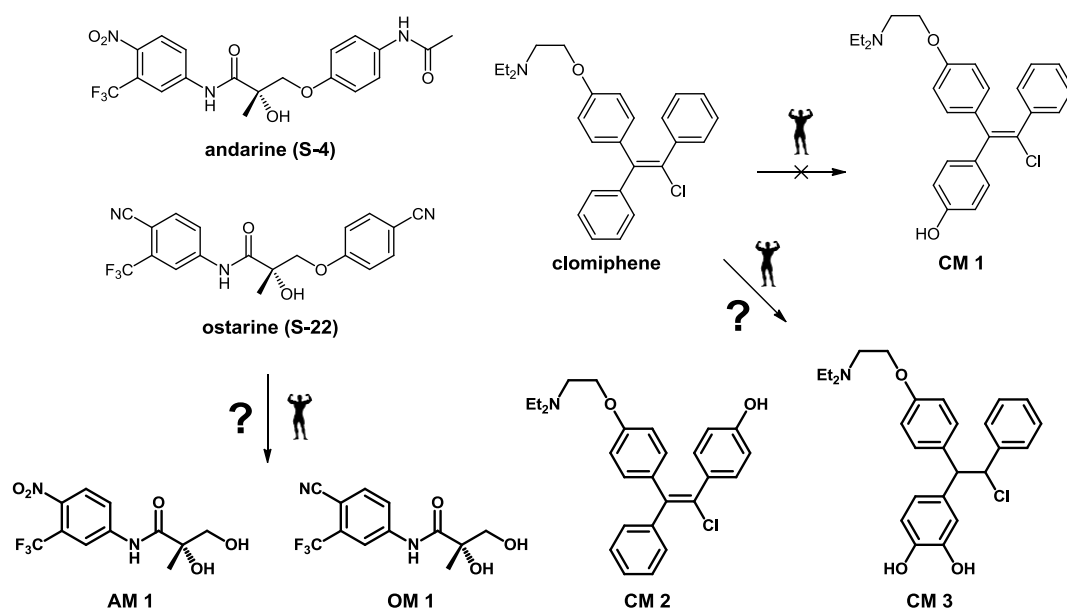


Figure 16 Target molecules for synthesis.

2. RESULTS AND DISCUSSION - Synthesis of SARM metabolites

2.1. Retrosynthetic analysis for the andarine and ostarine metabolite

Considering the cleavage of the ether linkage as major metabolic pathway, the resulting metabolite structures of andarine and ostarine just differ in one aromatic substituent. Accordingly, we envisioned a synthetic route capable of providing both target molecules just by the use of different aromatic starting materials. Enzymatic *O*-dephenylation of the drugs gives the vicinal diols **AM 1** and **OM 1**. Figure 17 shows our retrosynthetic analysis for the corresponding target structure. As illustrated, the diol can be ascribed to the epoxyamide, which in turn can be disconnected into the corresponding aniline and the epoxyacid. The racemic epoxyacid can be obtained straightforward via epoxidation of methacrylic acid. Considering the exclusive occurrence of **AM 1** and **OM 1** as enantiopure compounds in urine specimens, we also wanted to provide a synthetic route for the preparation of the enantiopure metabolites. In line with this, we considered Sharpless asymmetric epoxidation of allylic alcohol 2-methyl-prop-2-en-1-ol followed by oxidation as reasonable approach to obtain the (*S*)-epoxyacid.

2.2. Synthesis of the racemic andarine and ostarine metabolite

Due to the fact that reference substances for doping control purposes do not have to fulfill the criterion of enantiopurity, we first concentrated on the synthesis of the racemic forms of **AM 1** and **OM 1**. According to the reaction scheme illustrated in Figure 18, we planned the selective epoxidation of methacrylic acid (**14**) by using *m*-CPBA to give the corresponding epoxyacid *rac*-**3**. Via the reaction with isobutyl chloroformate, *rac*-**3** should be converted into the corresponding mixed anhydride and by this means activated for the reaction with anilines **4/9** to give the epoxyamides *rac*-**7/12**. Epoxide opening under basic conditions should finally give the target structures *rac*-**8** (**AM 1**) and *rac*-**13** (**OM 1**), respectively.

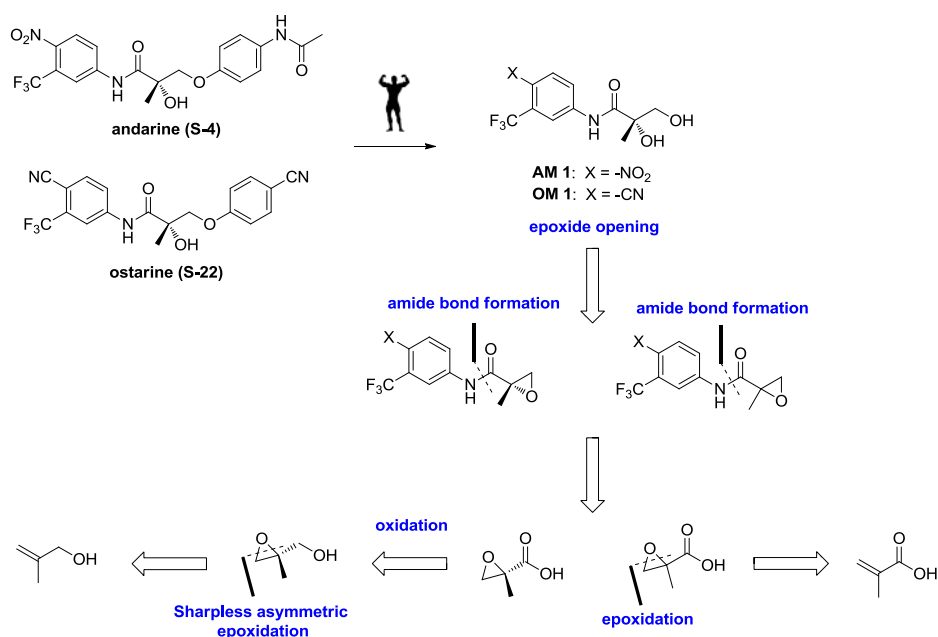


Figure 17 Retrosynthetic analysis for *O*-dephenyl-target structure considering racemic and enantioselective approach.

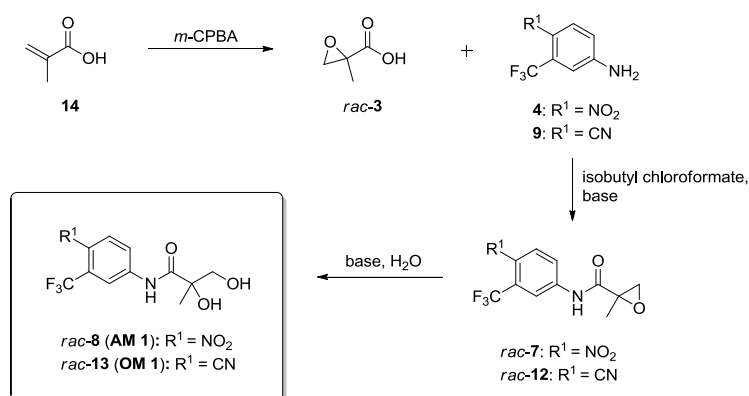


Figure 18 Envisioned pathway for the synthesis of AM 1 and OM 1.

2.2.1. Synthesis of epoxyamides *rac*-7 and *rac*-12

According to Figure 18, the first step in the synthesis of SARM metabolites **AM 1** and **OM 1** was the epoxidation of methacrylic acid (**14**) to obtain the corresponding epoxyacid *rac*-3. This was readily achieved by the use of *m*-CPBA following a literature procedure.⁶⁹ *Rac*-3 was obtained in 70% yield to serve as starting material for the subsequent amide bond formation, which represents the key step in the construction of the arylpropionamide core structure. As illustrated in Figure 19, the reaction of a carboxylic acid and an amine to form an amide bond usually affords the initial activation of the acid by conversion of its hydroxy group into a good leaving group prior to treatment with the amine. For this purpose a large

variety of so-called coupling reagents has been developed, facilitating the conversion of carboxylic acids into its activated counterparts, such as acid chlorides, (mixed) anhydrides, carbonic anhydrides or active esters.

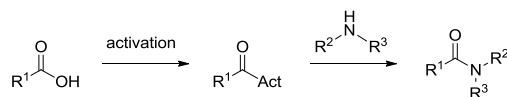


Figure 19 General principle of the activation process for amide-bond formation.⁷⁰

2.2.1.1. Epoxyacid activation via mixed anhydrides

The mixed anhydride method is a classic method of amide bond formation. It was first reported by Vaughan *et al.*, who showed in 1951 that in the presence of base, the reaction between a carboxylate and a chloroformate yields a mixed carbonic anhydride, which readily reacts with amines to form amides.⁷¹ A few years later, Anderson and coworkers investigated this method with regard to its applicability for peptide synthesis and suggested isobutyl chloroformate as most efficient reagent.⁷² In accordance with this, Vince *et al.* successfully applied isobutyl chloroformate for the coupling reaction of glycidic acid and adamantamine in the course of their synthesis of glutathione peptidomimetics. Starting from glycidol, they obtained the corresponding amide in 52% yield over two steps (Figure 20).⁷³

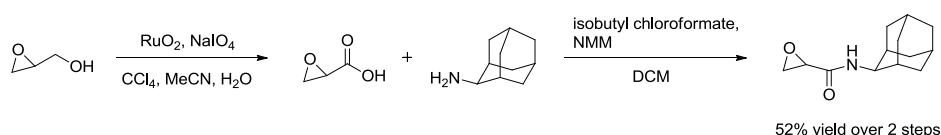


Figure 20 Literature example for the use of isobutyl chloroformate for the generation of an amide bond.⁷³

Considering the close resemblance of glycidic acid to compound **3**, we tried to adapt the described procedure for the amide bond formation between carboxylic acid *rac*-**3** and aniline **4** to yield the target epoxyamide *rac*-**7**. However, despite the conduction of numerous experiments, we did not succeed in the preparation of *rac*-**7** via the described method. Due to the high instability and susceptibility for polymerization of *rac*-**3**, most experiments resulted in a total loss of carboxylic acid, whereas the remaining isobutyl chloroformate reacted with the aromatic amine to give the corresponding carbamate. Our attempt to increase the stability of *rac*-**3** via its application as preformed *N*-methylmorpholine (NMM)-salt failed, because like the free acid also its salt showed a very

high tendency for degradation under the applied reaction conditions, as well as just in the course of storage. Considering its higher reactivity in comparison to isobutyl chloroformate, we also conducted experiments using Yamaguchi's reagent (2,4,5-trichlorobenzoyl chloride)⁷⁴ instead of isobutyl chloroformate. Nevertheless, we did not achieve the formation of the desired epoxyamide. To test the reaction outcome for the application of aliphatic amines instead of anilines, we reacted epoxyacid *rac-3* with *n*-butylamine under the same conditions as used for previous experiments. The corresponding amine **67** was obtained in 29% yield (see Figure 21). Due to this result, we ascribed the failure of our initial approaches of amide bond formation between *rac-3* and aniline **4** to the rather poor nucleophilicity of the aromatic amino group, which was additionally deactivated by the electron-withdrawing nitro substituent.

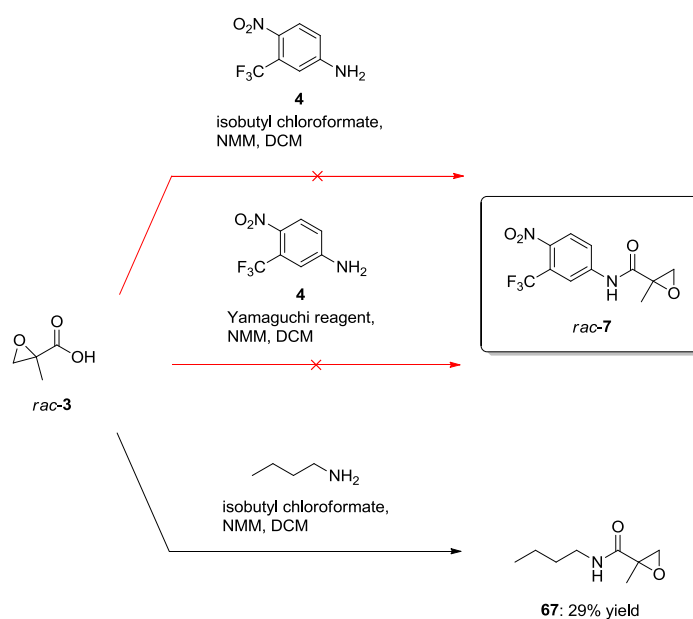


Figure 21 Attempts for the preparation of *rac-7* via the mixed anhydride method.

2.2.1.2. Epoxyacid activation via coupling reagents based on 1*H*-benzotriazole

Another common method for the activation of carboxylic acids in order to obtain amide bonds, is the application of coupling reagents based on the hydroxybenzotriazole (HOBt)/1-hydroxy-7-azabenzotriazole (HOAt) system. Among them, the uronium/aminium salts are the most widely described ones. Figure 22 illustrates some important representatives in their active isomer forms. Whereas for TATU/TBTU it is not clear which isomer form is the active one, HATU/HBTU was shown to be present as the aminium isomer.

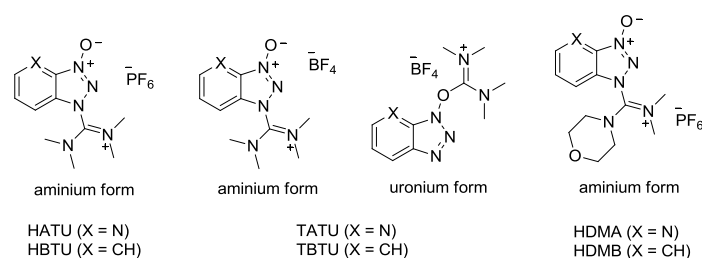


Figure 22 Examples for uronium/aminium-based coupling reagents.

As illustrated in Figure 23 these reagents react with carboxylic acids to form OAt/OBt active esters, which then react with amines to give the corresponding amides.

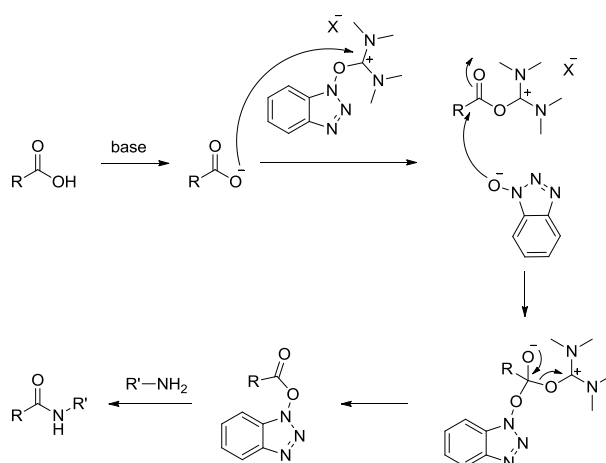


Figure 23 Activation process using uronium/aminium-type reagents.⁷⁰

Much work has been carried out with variation of the counter anions and the substituents leading to a huge variety of coupling reagents available nowadays. Additionally to the uronium/aminium salts also phosphonium, immonium and carbonium salts are associated with HOBT/HOAt reagents. Nevertheless, they all can be considered rather similar concerning their activation mechanism and their impact on the outcome of couplings. Overall it can be said that coupling reagents based on HOAt generally give faster, more efficient couplings with less epimerization compared to HOBT-based reagents.⁷⁵

We found some literature exemplifying the activation of glycidic acid derivatives via HOBT/HOAt systems, but none of them used amines featuring a comparably low nucleophilicity as aniline **4**.⁷⁶ Nevertheless, we gave it a try and conducted some reactions applying TBTU for the coupling of *rac*-**3** and amine **4**, but we did not achieve a reaction (see Figure 24). As it was the case with acid chlorides, our attempts resulted in a complete loss of starting material. Based on the detection of tetramethylurea via GC-MS, we assumed the

occurrence of acid activation to some extent, but obviously the reactivity of the aniline was too low for attacking the activated ester.

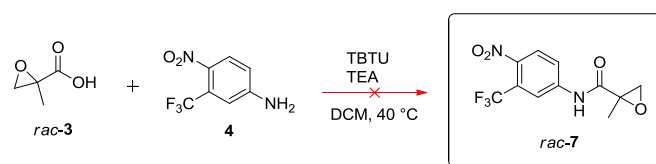


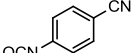
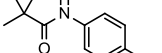
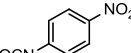
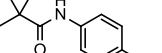
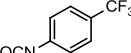
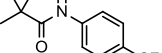
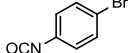
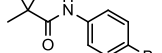
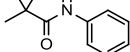
Figure 24 Attempted amide coupling reaction using TBTU.

2.2.1.3. Amide bond formation via Crich procedure

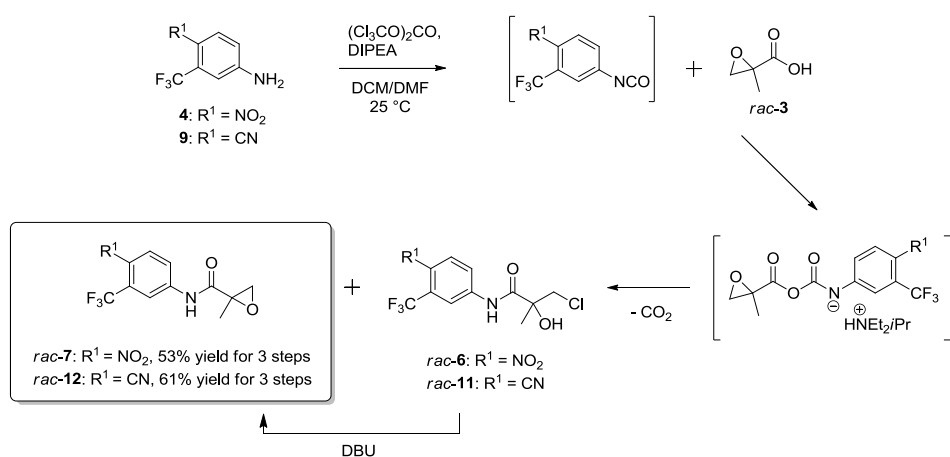
Ascribing the failure of all experiments that had been conducted so far to the poor nucleophilicity of the aromatic amino group, we were looking for alternative methods that could enable the amide bond formation between epoxyacid *rac-3* and anilines **4/9**. Moving away from the idea of acid activation, we shifted our focus towards possibilities for the conversion of anilines **4/9** into more reactive compounds. By doing this, a procedure of Crich *et al.*, describing the amide bond formation from carboxylic acids and isocyanates, caught our attention. By simple stirring different carboxylic acids with aryl and other electron-deficient isocyanates in the presence of a hindered amine at room temperature, they succeeded in preparing a huge variety of anilides and other substituted amides in good to excellent yields.⁷⁷ The reaction scope reaches from aliphatic to aromatic acids and comprises a wide range of electron-deficient isocyanates. Table 2 gives an overview of the results obtained by the use of pivalic acid. Considering this procedure as a very promising option for the solution of our synthetic problem, we adapted it for the reaction of epoxyacid *rac-3* and anilines **4/9**. According to a modified procedure of Glorius⁷⁸ we converted anilines **4/9** into the corresponding isocyanates by the usage of triphosgene in the presence of DIPEA. We monitored the conversion via GC-MS and due to their rather unstable character then reacted these *in situ* generated isocyanates right away with epoxyacid *rac-3*. As shown in Figure 25, an intermediate adduct was formed, which readily extruded carbon dioxide to give the corresponding amide. Additionally to the target epoxyamides *rac-7/12*, also the corresponding chlorohydrines *rac-6/11* were formed. This was ascribed to the presence of chloride ions in the reaction mixture due to the initial application of triphosgene. Nucleophilic attack of the target epoxyamide by chloride ions gave the corresponding chlorohydrines, resulting in a 1:1 product mixture after work up. By treating these crude

Table 2 Literature results for amide bond formation from carboxylate salts and isocyanates.⁷⁷

$$\text{R}^1\text{COOH} + \text{R}^2\text{NCO} \xrightarrow[\text{DMF, 25 }^\circ\text{C}]{\text{DIPEA}} \text{R}^1\text{CONHR}^2$$

entry	R ¹ COOH	R ¹ NCO	product	yield [%]
1				90
2				93
3				82
4				85
5				77

product mixtures with DBU, we achieved the reconversion of the side products *rac-6/11* into the desired epoxyamides via ring closure reaction and finally obtained *rac-7* in 53% and *rac-12* in 61% yield over three steps. As critical factor in our developed three-step procedure, we consider the used amount of triphosgene. Whereas insufficient amounts resulted in incomplete conversions of anilines, amounts of more than 0.5 equivalents related to the amine entailed a strong drop in yields due to the inactivation of epoxyacid *rac-3*. Based on our optimization studies, we consider the use of 0.4 equivalents triphosgene as optimum amount.

**Figure 25** Synthesis of epoxyamides *rac-7* and *rac-12* via the Crich procedure.

2.2.2. Epoxide opening reaction

The last step in the synthesis of SARM metabolites **AM 1** and **OM 1** was the epoxide opening reaction to give the vicinal diols. Epoxide hydrolysis is known to proceed either under acidic or under basic conditions. Accordingly we screened several reagents for their applicability as catalysts for the ring opening of *rac-7/12* in aqueous media. Aspects of regioselectivity shall be discussed later in the course of enantioselective synthesis of SARM metabolites (see 2.3.3). Table 3 summarizes the results, obtained for the ring opening of epoxyamide *rac-7* using different catalysts. Whereas the reaction of *rac-7* with 2N NaOH led to amide cleavage, various acidic reagents proved to be efficient. Among them, only the acidic resin Amberlyst-15⁷⁹ was shown to give no conversion at all. The use of *p*-toluenesulfonic acid as well as of phosphoric acid resulted in moderate yields of diols. We ascribed this drop in yields to partially occurring polymerization according to the mechanism proposed in Figure 26. The best result was obtained by refluxing *rac-7* in a DMF/water mixture.

Table 3 Reagents tested for the epoxide opening reaction of epoxyamide *rac-7*.

entry	reagent	T [° C]	t [h]	yield [%]
1	H ₂ O	100	5	no conv.
2	NaOH (2N)	r.t.	15	no conv.
		60	2	amide cleavage
3	Amberlyst-15	r.t.	15	no conv.
		60	15	no conv.
4	<i>p</i> -TsOH	r.t.	15	no conv.
		100	5	53%
5	H ₃ PO ₄	100	5	47%
6	DMF/H ₂ O	100	5	75%

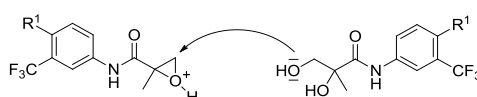


Figure 26 Partial polymerization under acidic conditions.

As it was shown by Jiang *et al.*, DMF is a very useful reagent affording the mild and efficient hydrolysis of epoxides in the absence of acids or bases.⁸⁰ According to their proposed

mechanism (see Figure 27), upon reaction of DMF with the epoxide an *N,N*-dimethylformamide ethylene acetal derivative **A** is formed. In the presence of H₂O, **A** is converted into species **B**, featuring a nucleophilic oxygen ion and carbon cation. Reaction with H₂O gives intermediate **C**, which in further consequence undergoes C-O bond cleavage to afford the corresponding vicinal diol and regenerate DMF. By refluxing *rac*-7/12 in a 1:1 mixture of DMF and water for 5 hours, we obtained the target metabolites *rac*-8 (**AM 1**) and *rac*-13 (**OM 1**) in yields of 75% and 72%, respectively. The same results were obtained by subjecting the reaction mixtures to microwave irradiation for three hours.

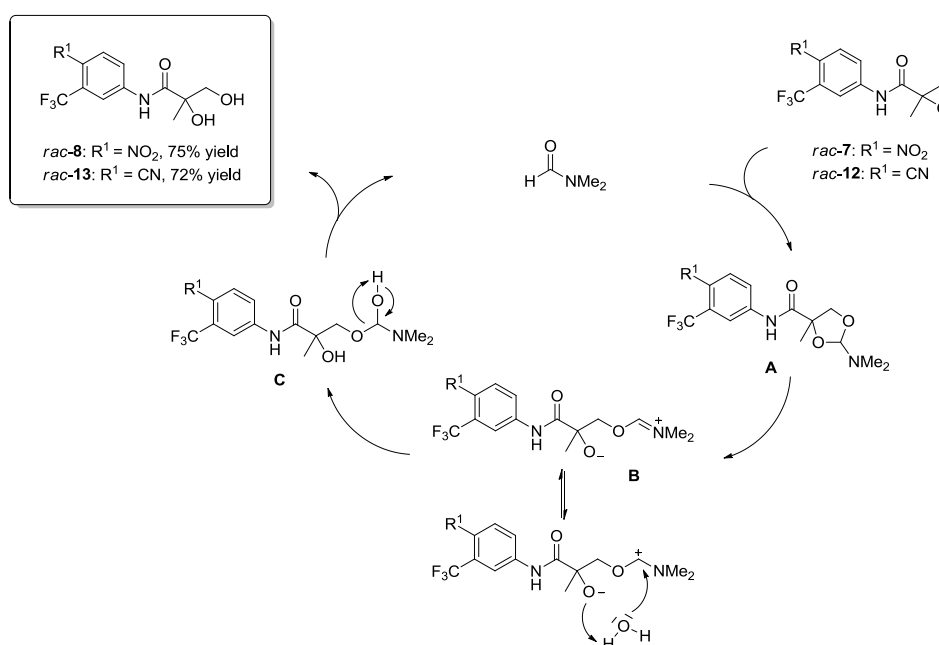


Figure 27 Proposed mechanism of DMF-promoted hydrolysis of epoxides.⁸⁰

2.3. Enantioselective synthesis of the andarine and ostarine metabolite

Considering the medical application of andarine and ostarine in the form of their (*S*)-isomers, entailing the exclusive occurrence of (*S*)-metabolites in urine specimens, we also wanted to provide an enantioselective version of the previously described pathway. This should be accomplished by asymmetric synthesis of epoxyacid (*S*)-**3**, which could be subjected to amide bond formation and epoxide opening according to the same procedure that was developed for the preparation of racemic metabolites. As outlined in Figure 28, we envisioned the preparation of (*S*)-**3** starting from allylic alcohol 2-methyl-prop-2-en-1-ol (**1**),

which after Sharpless asymmetric epoxidation should give epoxyalcohol (*R*)-**2**. Via Ru-mediated oxidation the (*S*)-isomer of epoxyacid **3** should be obtained, which in further consequence should finally afford (*S*)-**8** (**AM 1**) and (*S*)-**13** (**OM 1**).

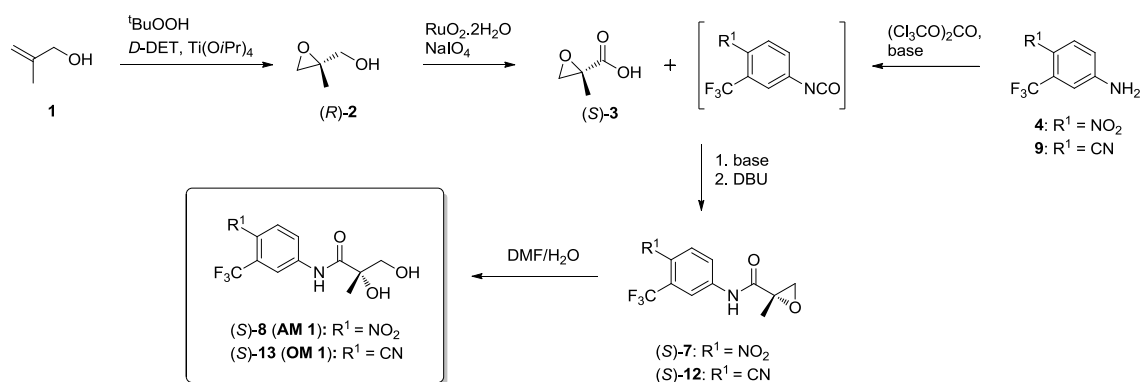


Figure 28 Envisioned pathway for the enantioselective synthesis of (*S*)-**8** (**AM 1**) and (*S*)-**13** (**OM 1**).

2.3.1. Synthesis of (*R*)-**2** via Sharpless asymmetric epoxidation

The Sharpless asymmetric epoxidation (SAE) represents a reaction of immense significance for asymmetric synthesis. It was introduced in 1980 by Sharpless *et al.*, who discovered that the reaction of a prochiral allylic alcohol with *tert*-butyl hydroperoxide (*t*-BuOOH) in the presence of $\text{Ti}(\text{O}i\text{Pr})_4$ and diethyl tartrate (DET) gives the corresponding epoxy alcohol in high enantiomeric purity.⁸¹ The asymmetric induction is thereby exerted by the tartrate derivative, which has to be added in enantiopure form to give a chiral catalyst complex upon reaction with the titanium tetraalkoxide. Whereas the initially described procedure employed a stoichiometric amount of catalyst, some years later a much more convenient method was reported allowing the reaction to be carried out with just 5 – 10% catalyst in the presence of molecular sieves.⁸² Both (+)- and (-)-DET are readily available, so either enantiomer of the product can be prepared. The method has been successful for a wide range of primary allylic alcohols, including substrates where the double bond is mono-, di-, tri- and tetrasubstituted, and is highly useful in natural product synthesis. The only limitation concerns the presence of an allylic hydroxy group, which is essential for the binding to the catalyst. By using a slightly modified procedure, also the kinetic resolution of secondary allylic alcohols can be effected.⁸³

In view of its convenience and excellent results regarding enantioselectivity, we chose SAE for the preparation of chiral building block (*R*)-**2**, which in further consequence should give

the enantiopure SARM metabolites (*S*)-**AM 1** and (*S*)-**OM 1**. Thus, (*R*)-epoxide **2** was synthesized in 86% yield, using 4.8 mol% of $\text{Ti}(\text{O}i\text{Pr})_4$ and 6.1 mol% of (-)-DET (see Figure 29). The slightly different molar amounts of $\text{Ti}(\text{O}i\text{Pr})_4$ and (-)-DET are due to the finding that the formation of the dimeric catalyst complex occurs most efficiently, when at least a 20% excess of tartrate ester is applied.⁸⁴

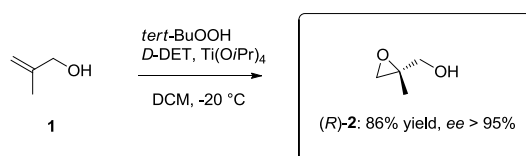


Figure 29 Sharpless asymmetric epoxidation of 2-methyl-prop-2-en-1-ol (**1**) to give (*R*)-**2**.

Figure 30 shows the putative active titanium complex, as it was proposed by Sharpless *et al.* (**A**).⁸⁵ Addition of the oxidizing agent causes displacement of one isopropoxide ligand and one tartrate carbonyl group (**B**). Coordination of 2-methyl-prop-2-en-1-ol (**1**) to the metal center again causes the displacement of one isopropoxide ligand leading to intermediate **C**, which brings the two reactants into immediate proximity. Due to the usage of *D*-(-)-tartrate and the respective shape of the complex, the reactive oxygen atom of the bound hydroperoxide gets delivered to the upper face of the allylic alcohol (intermediate **D**) resulting in the enantioselective formation of epoxyalcohol (*R*)-**2**. Figure 31 illustrates a general model system for the prediction of the reaction outcome. By arranging the allylic alcohol in a rectangle with the hydroxy group top left, the *si* side is usually facing upwards, whereas the *re* side is facing downwards. The use of *D*-(-)-diethyl tartrate delivers oxygen to the top face of the alkene, which is equivalent to a *si* side attack leading to (*R*)-**2**, whereas *L*-(+)-tartrate causes a *re* side attack of the oxidizing agent giving (*S*)-**2**.⁸⁶

Based on the fact that epoxyalcohol **2** exhibits a rather modest UV/VIS absorbance, which would complicate the determination of the enantiomeric excess (*ee*) via HPLC analysis, we decided to determine the enantiomeric composition of the obtained alcohol via ^{19}F -NMR spectroscopy according to the Mosher ester method⁸⁷. We therefore also prepared a racemic sample of **2** by conducting epoxidation with *t*-BuOOH and $\text{Ti}(\text{O}i\text{Pr})_4$ in the absence of any tartrate ester. Both epoxyalcohol samples were then subjected to Steglich esterification with (*S*)-(-)-MTPA assisted by the DCC/DMAP system (see Figure 32).⁸⁸ Whereas the racemic

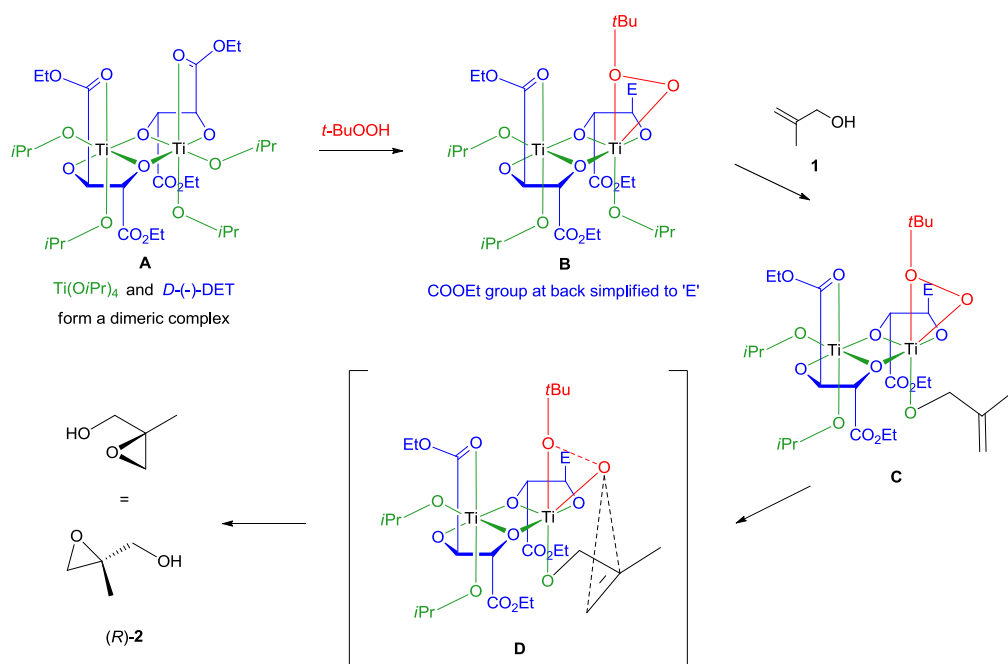


Figure 30 Mechanism for asymmetric epoxidation of allylic alcohol **1** via dimeric titanium complex.

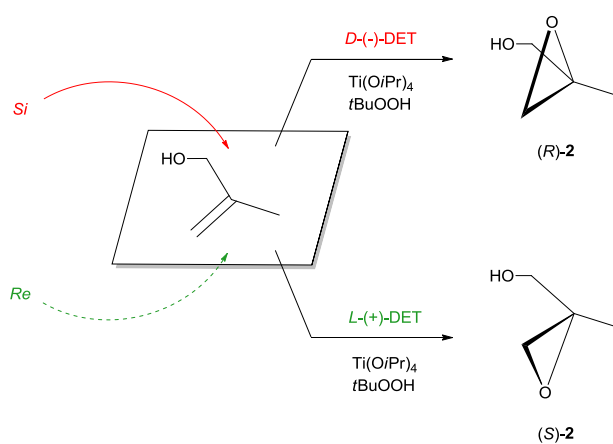


Figure 31 Enantioselectivity in the Sharpless asymmetric epoxidation.⁸⁶

sample gave two diastereomeric esters resulting in two different signals in the ^{19}F -NMR spectrum, **(R)-2** was exclusively transformed into the **(R,S)**-diastereomer. Via the quantitative analysis of the obtained ^{19}F -NMR spectra (see Figure 33), we could determine an *ee* value of > 95% for epoxyalcohol **(R)-2**.

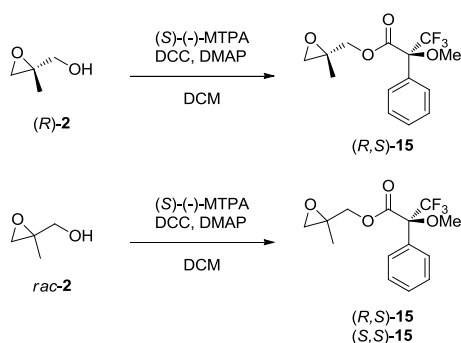


Figure 32 Conversion of (R)-2 and rac-2 into their Mosher esters.

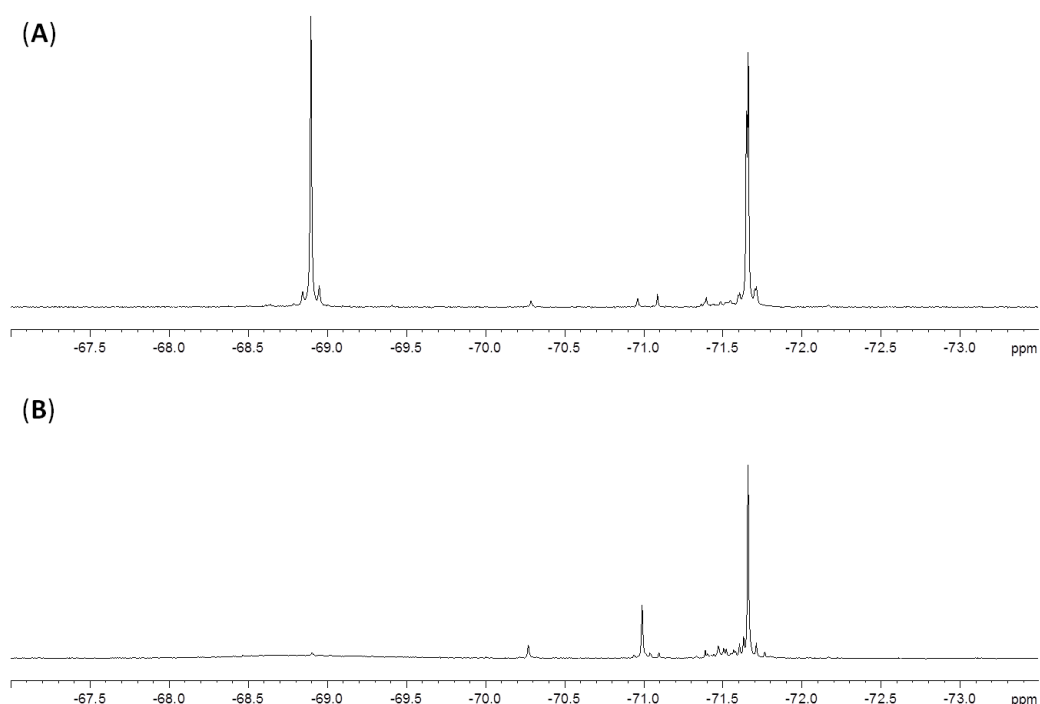


Figure 33 *ee*-determination of epoxyalcohol via ^{19}F -NMR of Mosher esters **15**: (A) Mosher esters of rac-2, (B) Mosher ester of (R)-2.

2.3.2. Synthesis of (S)-2-methyloxirane-2-carboxylic acid ((S)-3)

The transformation of primary alcohols to carboxylic acids belongs to the most fundamental reactions in organic chemistry. Thus, a lot of reagents and procedures for the direct conversion are nowadays available, including the use of $\text{CrO}_3/\text{H}_2\text{SO}_4$ ⁸⁹, TEMPO/ NaClO or TEMPO/ NaClO_2 ⁹⁰, PCC/periodic acid⁹¹ or TPAP/NMO⁹². Among them, $\text{RuO}_2/\text{NaIO}_4$ is a very well established oxidant/cooxidant system, enabling the formation of a huge variety of carboxylic acids starting from the corresponding primary alcohols. The active oxidant, RuO_4 , was very early introduced by Djerassi and coworkers⁹³ and since that its utility for a variety of oxidative transformations has been recognized. The expense of Ru-metal prompted the

development of catalytic processes, the most popular of which involve the use of periodate or hypochlorite as stoichiometric cooxidants.⁹⁴ Thus, RuO_4 is usually *in situ* generated from catalytic amounts of RuCl_3 or RuO_2 and due to its low solubility in water, the reaction is conducted in a two-phase system with the cooxidant in the aqueous phase and reoxidation of Ru occurring at the phase boundary interface. The relatively high oxidizing power of Ru-reagents enables the conduction of transformations under very mild conditions, which is why we envisioned Ru-mediated oxidation as reasonable method for the preparation of epoxyacid (*S*)-**3**. By comparing $\text{RuCl}_3 \cdot \text{H}_2\text{O}$ and $\text{RuO}_2 \cdot 2\text{H}_2\text{O}$ in combination with NaIO_4 , we observed faster and cleaner conversions upon the usage of $\text{RuO}_2 \cdot 2\text{H}_2\text{O}$, which we ascribed to the absence of oxidized chlorine contaminations. The prevention of any side product formation turned out to be of utmost importance in this reaction step, because the instability of epoxyacid **3**, as it was already encountered in the preparation of *rac*-**3**, rendered any purification of the crude product impossible. Also aqueous reaction workup had to be circumvented, due to the high water solubility of epoxyacid **3**. By conducting the oxidation in a 1:1 mixture of MeCN/ CCl_4 , we experienced some problems due to epoxide opening and partially occurring polymerization. Ascribing this to an unfavourably acidic reaction medium, we added a buffer solution (pH 6.88, 7.5 vol%) and thereby accomplished the complete suppression of unwanted ring opening and polymerization reactions. In the end, we succeeded in the transformation of (*R*)-**2** into carboxylic acid (*S*)-**3** with 79% yield and high purity, enabling the direct subjection of (*S*)-**3** to the next reaction step without further purification (see Figure 34).

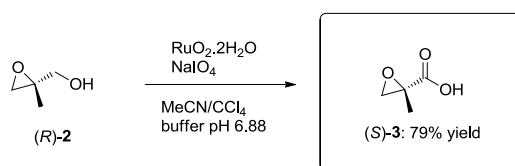


Figure 34 Ru-mediated oxidation of (*R*)-**2** to (*S*)-**3**.

2.3.3. Regioselective considerations regarding ring opening reactions in the course of the enantioselective synthesis of (S)-AM 1 and (S)-OM 1

Considering the installation of the asymmetric center already in the course of the first step, it had to be ensured that the following reactions would not provide the risk of racemization. Steps that could affect the chiral center included all ring opening reactions involving a potential nucleophilic attack at the asymmetric carbon atom. As illustrated in Figure 35, the regioselectivity of epoxide opening depends on the reaction media. Whereas under acidic conditions the nucleophilic attack on a 1,1-dialkyl epoxide generally occurs at the more substituted end, basic conditions promote the reaction on the sterically less hindered C2 carbon atom. Protonation in acidic media produces a positive charge, which gets optimally stabilized at the more substituted end due to the $+I$ -effects exerted by the two alkyl groups. Accordingly the nucleophile exclusively attacks at carbon C1. In contrast to that, there is no build-up of positive charge under basic conditions, so that the epoxide oxygen as poor leaving group needs a strong nucleophile to be pushed away. In consequence, the reaction becomes pure S_N2 with steric hindrance as controlling factor, resulting in the exclusive attack at the less hindered C2 carbon atom.

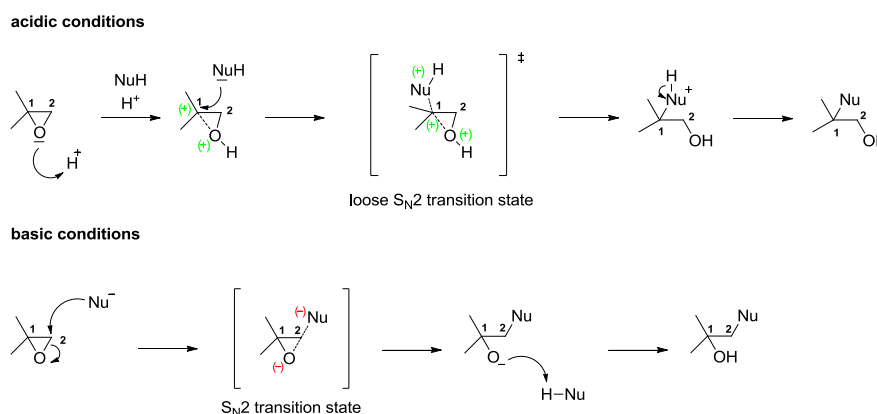


Figure 35 General mechanism of epoxide opening under acidic and under basic conditions.

Reaction steps that could potentially bear the risk of racemization were the formation of the chlorohydrine in the course of amide bond formation and, of course, the epoxide opening at the end of the sequence. Considering the strongly basic reaction conditions, under which amide bond formation according to Crich's procedure was conducted, we could largely exclude the possibility of racemization due to chlorohydrine formation. As exemplified by

Figure 35, in the basic reaction media, steric hindrance would become the controlling factor leading to the exclusive attack on the less hindered C2 carbon atom by chloride ions. As additional factor that would definitely favor the C2 attack of epoxyamides (*S*)-**7/12**, we rated the carbonyl group next to carbon C1. Contrarily to the two alkyl substituents in Figure 35, the carbonyl group would exert a strongly destabilizing effect on any positive charge on C1, certainly rendering a C1 attack even under acidic conditions impossible. The same considerations applied for the DMF-promoted ring opening reaction. The positive partial charge at the carbonyl carbon would prevent the formation of a second positive charge in the course of a nucleophilic attack on adjacent C1. We therefore assessed the formation of transition state **TS 2** (see Figure 36) upon reaction of epoxyamides (*S*)-**7/12** with DMF as a rather implausible event. Much more likely, transition state **TS 1** would be formed, in the course of which the chiral center at C1 would not be affected.

Our considerations regarding the regioselectivity of ring opening reactions in the course of the enantioselective synthesis of SARM metabolites indeed proved to be true, since we obtained (*S*)-**AM 1** and (*S*)-**OM 1** in 90% and 86% *ee*, respectively. The enantiomeric excess values for the diols were again determined by the Mosher ester method. It has to be admitted that we lost about 5% of enantiopurity in the course of four reaction steps, but we rate this as tolerable and do not ascribe this to one special step, but rather to the whole sequence.

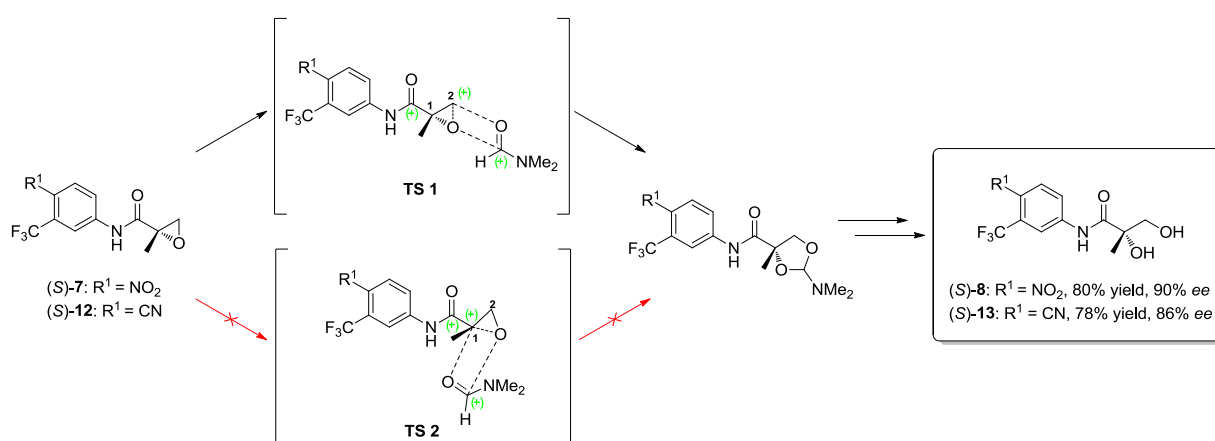


Figure 36 Regioselective DMF-promoted epoxide opening reaction.

2.4. Proofs of authenticity

With our synthetic metabolites in hand, we turned our attention to their potential practical application as reference materials for doping analysis. Therefore both racemic metabolites **AM 1** and **OM 1** were compared to urine samples that were taken after the oral administration of andarine and ostarine, respectively. Based on the official WADA guidelines for the mass spectrometric detection and identification of molecules with masses less than 800 Da^{95} , product ion scans were conducted for each synthesized drug metabolite and the relative abundances of five diagnostic ions were compared to the corresponding abundances of urinary metabolites (**AM 1**: $205 m/z$, $175 m/z$, $159 m/z$, $155 m/z$, $107 m/z$; **OM 1**: $185 m/z$, $158 m/z$, $145 m/z$, $138 m/z$, $115 m/z$). Abundance values were determined from the peak areas of integrated selected ion chromatograms. As illustrated in Figure 37 and Figure 38 for **AM 1** as well as for **OM 1**, the calculated percentages were identical to the values obtained from urinary metabolites. Accordingly, both synthesized substances proved to be applicable as reference standards for the detection of SARMs abuse.

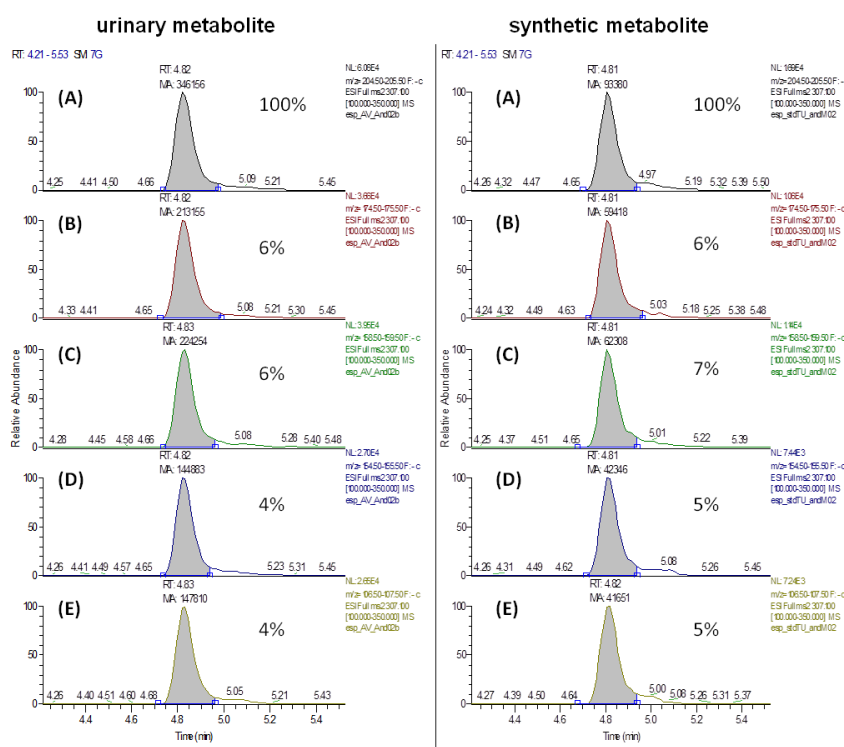


Figure 37 Extracted ion chromatograms of a urine sample positive for andarine and of the synthetic *O*-dephenylandarine (**AM 1**): (A) $205 m/z$ extracted, (B) $175 m/z$ extracted, (C) $159 m/z$ extracted, (D) $155 m/z$ extracted, (E) $107 m/z$ extracted.

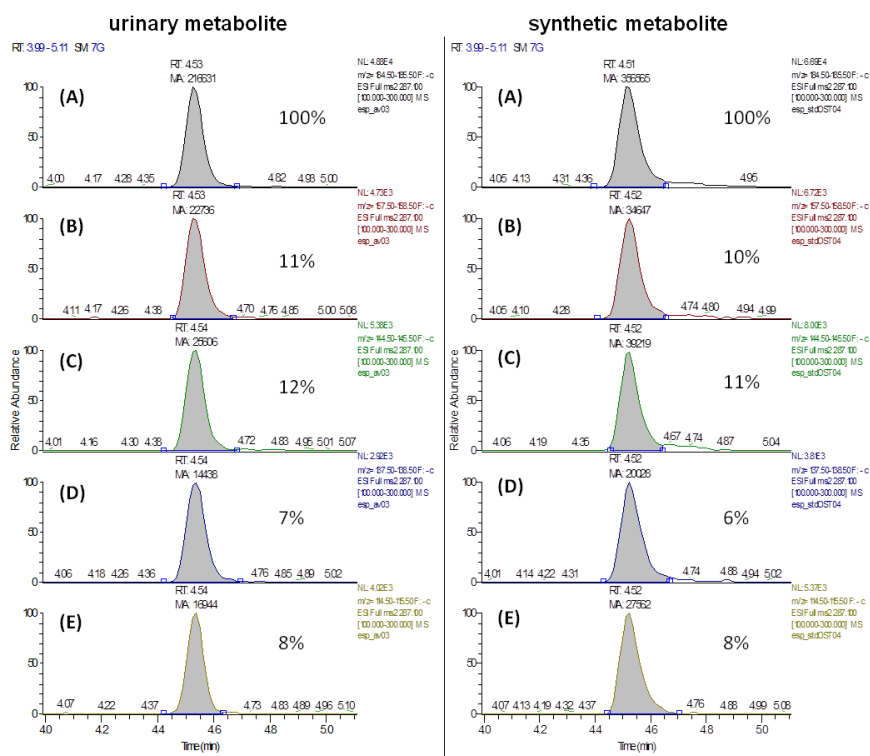


Figure 38 Extracted ion chromatograms of a urine sample positive for ostarine and of the synthetic *O*-dephenylostarine (**OM 1**): (A) 185 *m/z* extracted, (B) 158 *m/z* extracted, (C) 145 *m/z* extracted, (D) 138 *m/z* extracted, (E) 115 *m/z* extracted.

3. Results and Discussion - Synthesis of 4'-hydroxyclophene

3.1. Retrosynthetic analysis

The key step in the synthesis of the alkene backbone of 4'-hydroxyclophene (**CM 2**) is the formation of the double bond. Considering all general methods for the synthesis of TPE derivatives (see chapter 1.6.3), we regarded the three approaches outlined in Figure 39 as most promising ones to achieve structure **CM 2**. The McMurry coupling of appropriate benzophenone and benzaldehyde derivatives, followed by chlorination of the resulting triphenylethylene seemed to be a very convenient method for the preparation of **CM 2**. Alternatively, the double bond could also be established via a Horner-Wadsworth-Emmons reaction between a ketone and an appropriate α -chlorophosphonate. As third option we envisioned the regioselective lithium trimethylstannylation of a diarylacetylene followed by a Negishi coupling reaction to obtain a TPE stannyl compound, which could be converted into the corresponding chloride. Although this last approach would probably become more demanding than the two previously described ones, it would offer the great advantage of stereoselective synthesis of (*E*)-**CM 2**.

3.2. McMurry approach

The McMurry coupling reaction is defined as reductive dimerization between two carbonyl compounds to yield alkenes on treatment with low valent titanium reagents. Providing access to sterically hindered or macrocyclic alkenes, it represents an important key step of many natural product syntheses.

The ability to couple different ketones and aldehydes to provide olefins is unique to titanium. Common reagent systems that are applied nowadays are combinations of TiCl_4 or TiCl_3 with Zn, Zn-Cu, Li, LiAlH_4 , K and Mg-amalgam. In former times the active titanium species was believed to be metallic titanium, resulting from reduction of titanium halogenide in solution. In the course of more detailed investigations of the inorganic aspects of McMurry coupling, this prevailing opinion had to be revised due to the finding that depending on the preparation method, the presence of several low valent titanium

Depending on the applied reagent system and thus on the active titanium complex, different mechanisms may be relevant, which until now have not been completely elucidated. The stable Ti-O bond can be regarded by all means as driving force for the deoxygenation process. Under normal circumstances, coupling reactions between two different carbonyl compounds lead to a roughly statistical mixture of the possible alkene products. For synthetic purposes, such mixed couplings are therefore only useful, if one component is applied in excess and if the products are easily separable. However, this is not the case when one of the carbonyl partners is a diaryl ketone. Coupling of a diaryl ketone with an equimolar amount of any ketone or aldehyde selectively provides the mixed coupled product.⁹⁸ This exception can be ascribed to the relatively large differences in the reduction potentials of the participating carbonyl compounds.

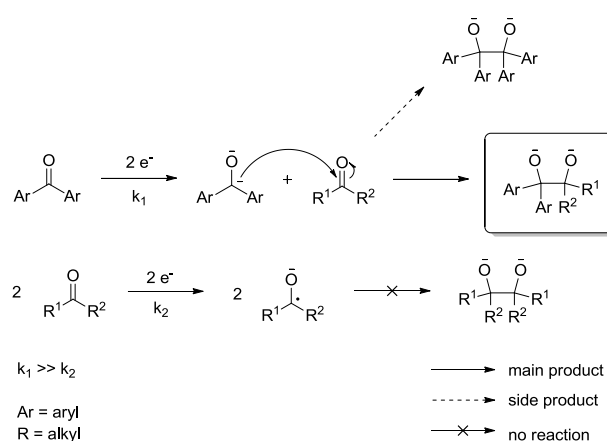


Figure 41 Reaction mechanism upon involvement of a diarylketone.

Due to the fact that the second reduction potential of diaryl ketones is less negative than the first reduction potential of normal saturated ketones, the formation of the diarylketone dianion (taking place with rate constant k_1) occurs more easily than an electron uptake by the second coupling partner (taking place with rate constant k_2 , see Figure 41). This allows the nucleophilic attack of the dianion on the other carbonyl compound, resulting in the selective formation of the mixed pinacol product and shifting the reaction mechanism from radical to polar.

Considering previous successful applications of the McMurry mixed coupling for the synthesis of different SERMs and corresponding metabolites^{51,61,62}, we assessed it as useful method for the construction of the clomiphene alkene backbone. In line with this, we

planned our synthesis of metabolite **CM 2** according to the reaction sequence outlined in Figure 42. The cross coupling reaction between diarylketone **19** and aldehyde **20** should provide access to the TPE derivative **21**. After deprotection of the phenolic hydroxy group, chlorination should yield the target structure **CM 2**. Previous attempts in preparing **CM 2** had shown that cleavage of the benzylic protecting group via catalytic hydrogenation also affected the double bond.⁹⁹ For this reason we planned to apply lithium naphthalenide (LiN) for deprotection and therefore scheduled the deprotection step prior to chlorination.

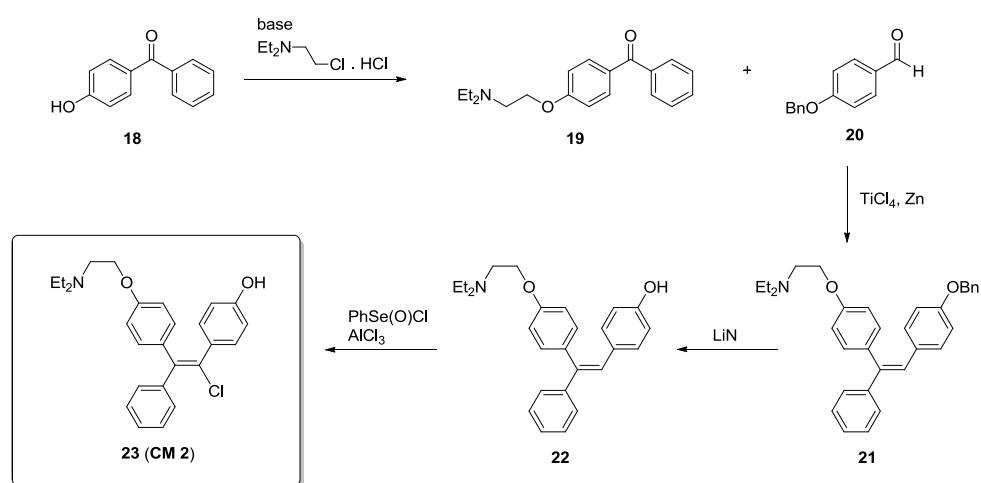


Figure 42 Envisioned pathway for the synthesis of 4'-hydroxyclophene (**23, CM 2**) via McMurry approach.

The afforded coupling partners, diarylketone **19** and benzaldehyde **20**, were prepared via simple ether syntheses as depicted in Figure 43. Starting from 4-hydroxybenzophenone (**18**) and 4-hydroxybenzaldehyde (**24**), compounds **19** and **20** were obtained in almost quantitative yields.

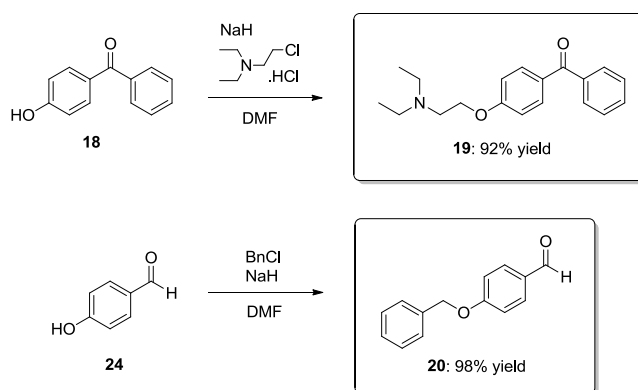


Figure 43 Synthesis of coupling compounds **19** and **20** for the McMurry reaction.

The coupling reaction was conducted with TiCl_4/Zn in anhydrous THF. Figure 44 shows our proposed mechanism. Upon coordination of TiCl_4 to the benzophenone derivative and Zn-mediated reduction thereof, the nucleophilic species **A** is formed, which readily adds to benzaldehyde **20** to give dititanium(III) glycolate **B**. Further reduction leads to dititanium(II) glycolate **C**, which undergoes stepwise homolytic cleavage under release of TiOCl to yield the TPE derivative **21** in the end.

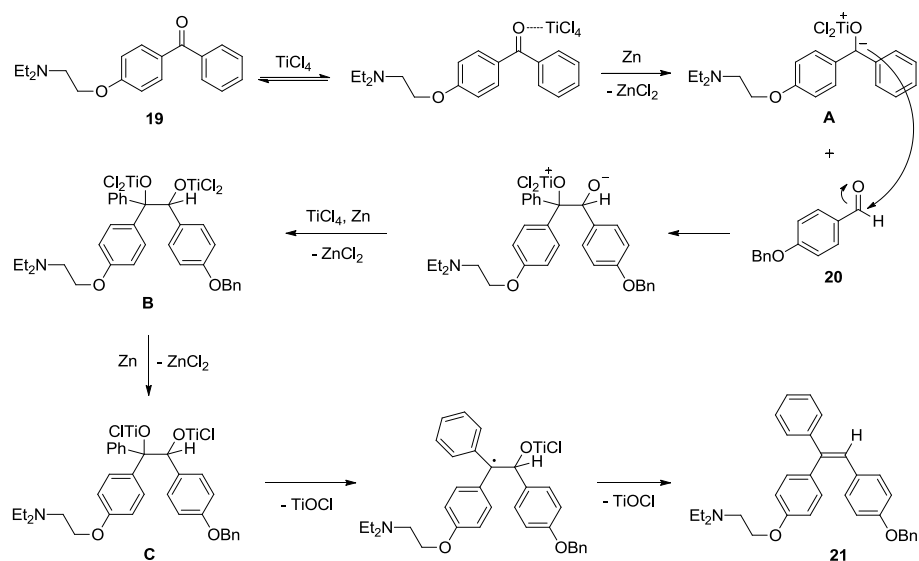


Figure 44 Proposed mechanism for the McMurry cross coupling between compounds **19** and **20**.

We isolated the target cross coupling product as a mixture of its (*E*)- and (*Z*)-isomer in 51% yield (see Figure 45). Homocoupling of the benzophenone compound was observed to take place as side reaction. The formation of the benzaldehyde homoproduct did not occur, which was in accordance with the general reaction mechanism upon the participation of diarylketones (see Figure 41). In the course of our attempts to optimize the yield, we experienced the order of reagent addition as a very important factor. Apparently, the formation of the nucleophilic intermediate **A** (see Figure 44) needed some time and got negatively influenced by the presence of the benzaldehyde coupling compound. We therefore obtained best results by stirring the mixture of TiCl_4/Zn and compound **19** for 30 minutes at room temperature, before benzaldehyde **20** was finally added. The ratio of products resulting from cross coupling/homo coupling (**21** : **68**) was optimized to 2.2 : 1.0. Separation was accomplished via silica gel chromatography.

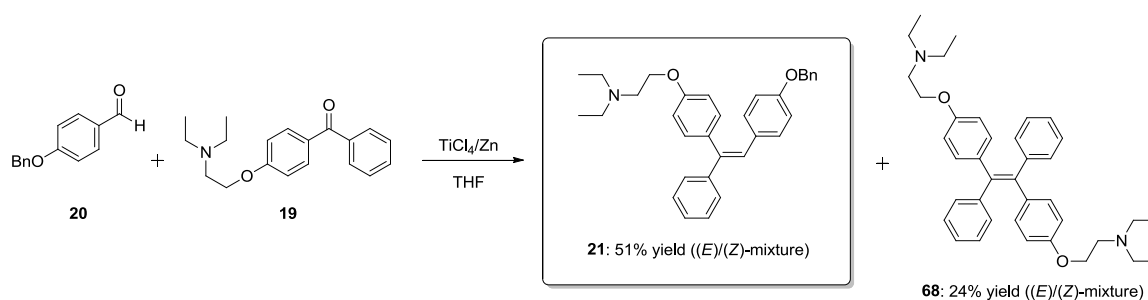
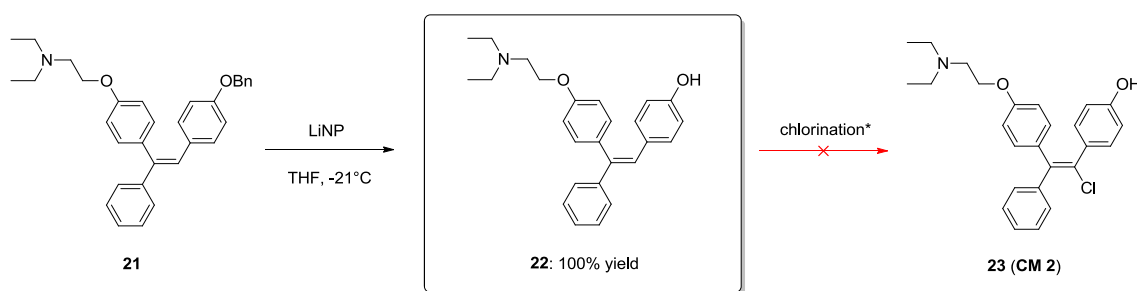


Figure 45 Synthesis of TPE derivative **21** via McMurry coupling reaction.

Following our synthetic plan, reductive cleavage of the benzylic protecting group was accomplished by LiN. The reagent was prepared via the reaction of elemental lithium with naphthalene and its usage provided the deprotected phenolic alcohol **22** in quantitative yield (see Figure 46).

As last step of our synthetic route, we envisioned the chlorination of **22** to yield target structure **CM 2**. Previous attempts of our group to incorporate chlorine atoms into very similar systems, had already shown that selective chlorination of the vinylic position is very difficult to accomplish. Due to the *ortho*-directing effect exerted by the phenolic hydroxy group, the aromatic ring was also very prone to chlorination, leading to the formation of the dichloro side product. Attempts to weaken this directing effect by the use of different protecting groups had failed.^{68,99} We therefore planned the selective formation of the monochloro product via optimization of the reaction time and screened a variety of chlorination reagents for this purpose. Unfortunately, none of the tested reagent systems was capable of exclusively providing compound **23**. We either ended up with no conversion or with inseparable mixtures of compounds **22**, **23** and dichloro product. Table 4 summarizes the corresponding results. Despite a lot of efforts in optimizing reaction times and separating obtained product mixtures, we finally came to the conclusion that our McMurry approach, involving chlorination as last step, was not the appropriate method for the preparation of clomiphene metabolite **CM 2**.



*reagents: PhSe(O)Cl/AlCl₃, NCS, SO₂Cl₂/AcOH, NCS/HMPA, NCS/PhSeCl

Figure 46 Deprotection of compound **21** and failed attempts of chlorination.

Table 4 Conducted experiments for the chlorination of compound **22** (listed are all products that had been identified in the course of the reaction; their relative ratios varied in dependence of reaction times).

entry	ref	reagent	product(s)
1	51d	NCS	22
2	100	NCS/HMPA	22
3	101	SOCl ₂	22
4	102	SO ₂ Cl ₂ /AcOH	-
5	103	NCS/PhSeCl	22 , 23 , dichloro product
6	104	PhSe(O)Cl/AlCl ₃	22 , 23 , dichloro product

3.3. Horner-Wadsworth-Emmons approach

The Horner-Wadsworth-Emmons (HWE) reaction is a Wittig-type condensation between carbonyl compounds and phosphonates yielding alkenes. It was first introduced in 1961 by Wadsworth and Emmons¹⁰⁵, who had modified an already existing approach by Horner¹⁰⁶. Since that time it has evolved to one of the most powerful and reliable methods for stereocontrolled olefin synthesis.¹⁰⁷ The classical HWE reaction is predominantly an (*E*)-alkene formation tool. Nevertheless, it has been demonstrated that the stereochemical outcome can be influenced by the structure of the reaction partners as well as by the reaction medium. Thus, the use of bis(2,2,2-trifluoroethyl)phosphonoacetates or bis(*O*-aryl)phosphonates induces (*Z*)-selectivity, known as Still-Gennari-version¹⁰⁸ and Ando-version¹⁰⁹, respectively. Whereas the HWE olefination of aldehydes for the preparation of di- and trisubstituted alkenes has been extensively studied, only few accounts have appeared in the literature describing the convenient preparation of tetrasubstituted alkenes by the use of ketones.¹¹⁰ This scarceness can largely be ascribed to practical difficulties such as steric

bulk and lower reactivity of ketones. A method to overcome this lack of reactivity was published by Kumara Swamy *et al.*, who succeeded in the preparation of trisubstituted vinyl chlorides from cyclic α -chlorophosphonates and ketones.¹¹¹ Compared to acyclic phosphonates, cyclic phosphonates were shown to exhibit enhanced reactivity and thus enable the HWE reaction of sterically simple ketones. As a great advantage of the HWE approach, we regarded the simultaneous formation of the double bond and incorporation of the chlorine atom. In this manner we could circumvent the troublesome step of vinylic chlorination. Accordingly, we developed a synthetic plan based on a HWE reaction between α -chlorophosphonate **32** and ketone **19** (see Figure 47). While ketone **19** had already been synthesized in the course of the McMurry approach, we had to prepare an appropriate chlorophosphonate that would in the end bear the β -aryl ring of target structure **CM 2**. By masking the *p*-hydroxy group as triflate, we planned to maximize the electrophilicity of the carbonyl C-atom of benzaldehyde **29** to favor the nucleophilic attack of phosphonate **21**. Chlorination with SOCl_2 should convert α -hydroxyphosphonate **31** into chlorophosphonate **32**, which then could be subjected to a HWE reaction with ketone **19**. Hydrolysis of the triflate group should finally provide the target molecule **CM 2** (**23**).

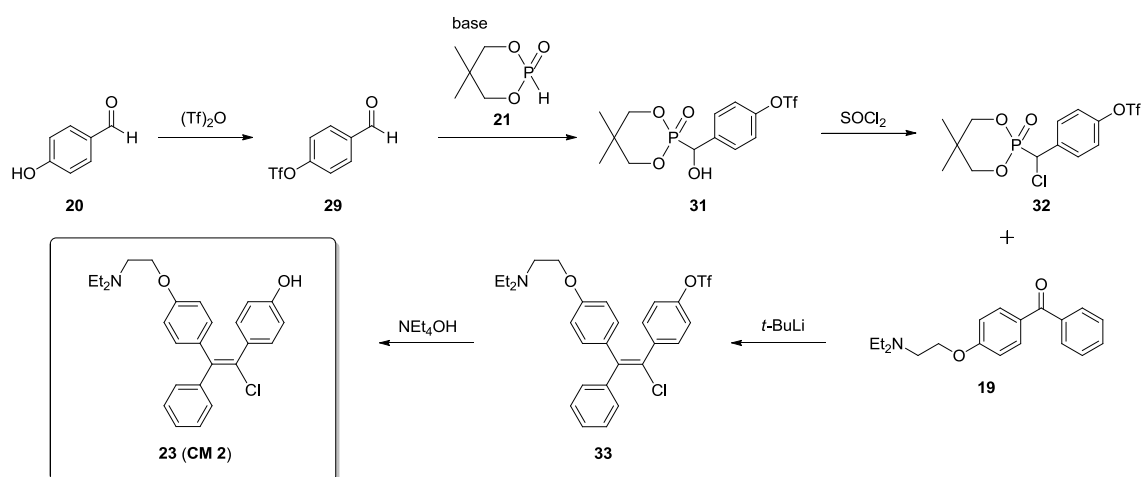


Figure 47 Envisioned pathway for the preparation of clomiprene metabolite **CM 2** (**23**) via HWE approach.

We started with the conversion of 4-hydroxybenzaldehyde (**20**) into triflate ester **29**, which was accomplished by the usage of triflic anhydride providing compound **29** in 76% yield. The following step represented the addition of cyclic phosphite **21** (5,5-dimethyl-1,3,2-dioxaphosphinan-2-one) to the carbonyl group of aldehyde **29**. This was achieved in the presence of TEA and is generally known as Pudovik reaction.¹¹² To assess the influence of

different aromatic substituents on the reaction outcome, we conducted the reaction besides using triflic ester **29**, also with benzaldehyde (see Table 5, entry 1), unprotected 4-hydroxybenzaldehyde (**24**, entry 2) and benzylprotected 4-hydroxybenzaldehyde (**20**, entry 3). As expected, the electron donating effect exerted by an -OH or -OR group in *para*-position decreased the electrophilicity of the carbonyl C-atom resulting in lower yields of the respective α -hydroxyphosphonates, when compared to the application of unsubstituted benzaldehyde. Whereas the usage of unprotected hydroxybenzaldehyde resulted in no conversion at all, its strong +*M*-effect could be weakened by the use of a benzylic protecting group leading to a yield of 36% of desired product **27**. A further increase in yield was obtained by installing an electron-withdrawing triflate group and so getting very close to the reactivity of unsubstituted benzaldehyde. These observations extended the results of Kumara Swamy *et al.*, who tested the reactivity of different aldehydes in the Pudovik reaction and came to the conclusion that aromatic aldehydes afforded better yields than aliphatic aldehydes.^{112b}

Table 5 Influence of substituent effects on formation of α -hydroxyphosphonate. ^aReaction was conducted in toluene/*n*-hexane (1:1).

entry	-R	product	yield [%]
1	-H		80
2	-OH		no conv.
3 ^a	-OBn		36
4	-OTf		72

Chlorination of the α -hydroxyphosphonates was accomplished by the usage of thionyl chloride according to literature procedures for the halogenations of similar compounds.^{112b} Whereas the benzylprotected phosphonate **27** was very smoothly converted into the chloride just by stirring it with SOCl₂ in DCM at ambient temperature overnight, the

conversion of triflate ester **31** afforded harsher conditions. Apparently the presence of the electron-poor aromatic substituent impeded the nucleophilic substitution, prompting us to use chloroform as solvent, so that the application of higher reaction temperatures would be possible. In the end, we managed to obtain α -chlorophosphonate **32** in 76% yield by stirring compound **31** and SOCl_2 in chloroform at 60 °C for three days (see Figure 48).

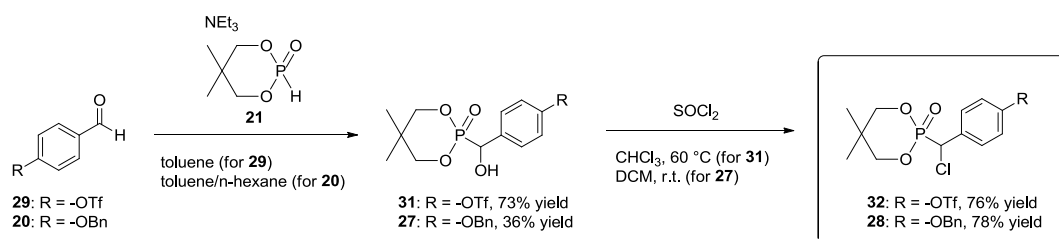


Figure 48 Synthesis of α -chlorophosphonates **28** and **32**.

Having the α -chlorophosphonates in hand, we turned our attention towards the envisioned HWE reaction for the construction of the TPE alkene backbone. In our first attempts to achieve a coupling reaction, we applied common HWE conditions using THF as solvent and *t*-BuLi as base for the generation of the phosphonate carbanion. Via quenching the carbanion with D_2O and subsequent NMR analysis, we could prove the complete deprotonation of chlorophosphonates **32** and **28** after 30 minutes. However, the condensation of ketone **19** could not be accomplished with neither of the phosphonates. After three days reaction time the corresponding alkene products were present only in traces.

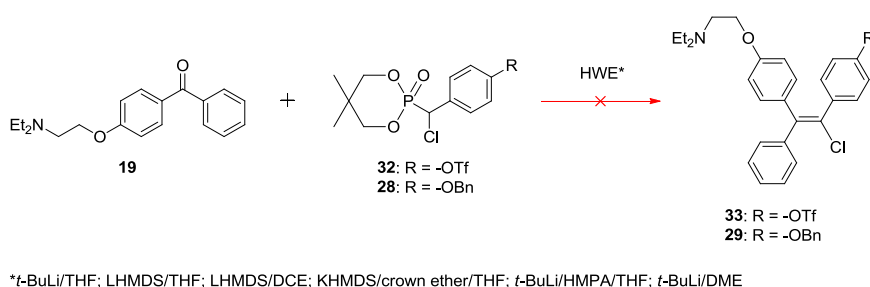


Figure 49 Failed attempts to accomplish a HWE reaction between ketone **19** and chlorophosphonates **32/28**.

We tried to improve our results by changing the reaction conditions. Instead of *t*-BuLi we also tested LHMDS and KHMDS, and THF was substituted by 1,2-dichloroethane (DCE) and 1,2-dimethoxyethane (DME). Also HMPA and crown ether 18-crown-6 were applied as

additives that should enable a better complexation and stabilization of the HWE reagent as well as of occurring intermediates. Nevertheless, all these attempts did not improve our preliminary results, prompting us to the conclusion that ketone **19** was simply too unreactive for this kind of condensation. To prove this assumption, we conducted a cross experiment applying a 1:1 mixture of ketone **19** and benzaldehyde. As expected, the deprotonated phosphonate readily reacted with benzaldehyde to give the corresponding trisubstituted olefin **34** in 70% yield, whereas ketone **19** could be fully recovered (see Figure 50).

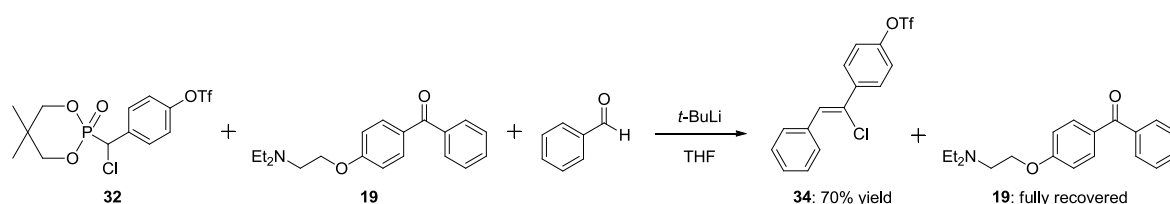


Figure 50 Cross experiment applying a 1:1 mixture of benzaldehyde and ketone **19**.

In light of these results, we considered the HWE reaction between compounds **19** and **32/30** as unfeasible. Either ketone **19** is too stable, so that it did not get to a nucleophilic attack in the first place, or the alcoholate formed by this attack could not be converted into the oxaphosphetane. Figure 51 illustrates the assumed reaction steps of the present HWE condensation. The deprotonated phosphonate **A** represents the starting point of the reaction. Its reaction with ketone **19** to yield alcoholate **B** affords energy input E_{A1} . Alcoholate **B** can then either be transformed to the heterocyclic oxaphosphetane **C** by bringing up E_{A3} , or it can again decompose into the starting materials via affording E_{A2} . A possible explanation for the lack of reactivity in the present HWE reaction could be the high energy barrier between alcoholate **B** and oxaphosphetane **C** leading rather to a back reaction than to cyclization. This theory is also in accordance with mechanistic insights into the HWE reaction provided by the literature. Although the exact mechanism is still unknown, many evidences indicate a two-stage formation of the oxaphosphetane via the alcoholate as well as the reversibility of alcoholate formation.¹¹³ In view of our conducted investigations into the HWE reaction of compounds **19** and **28/32**, we came to the conclusion that our envisioned HWE approach neither was the appropriate method for the preparation of clomiphene metabolite **CM 2**.

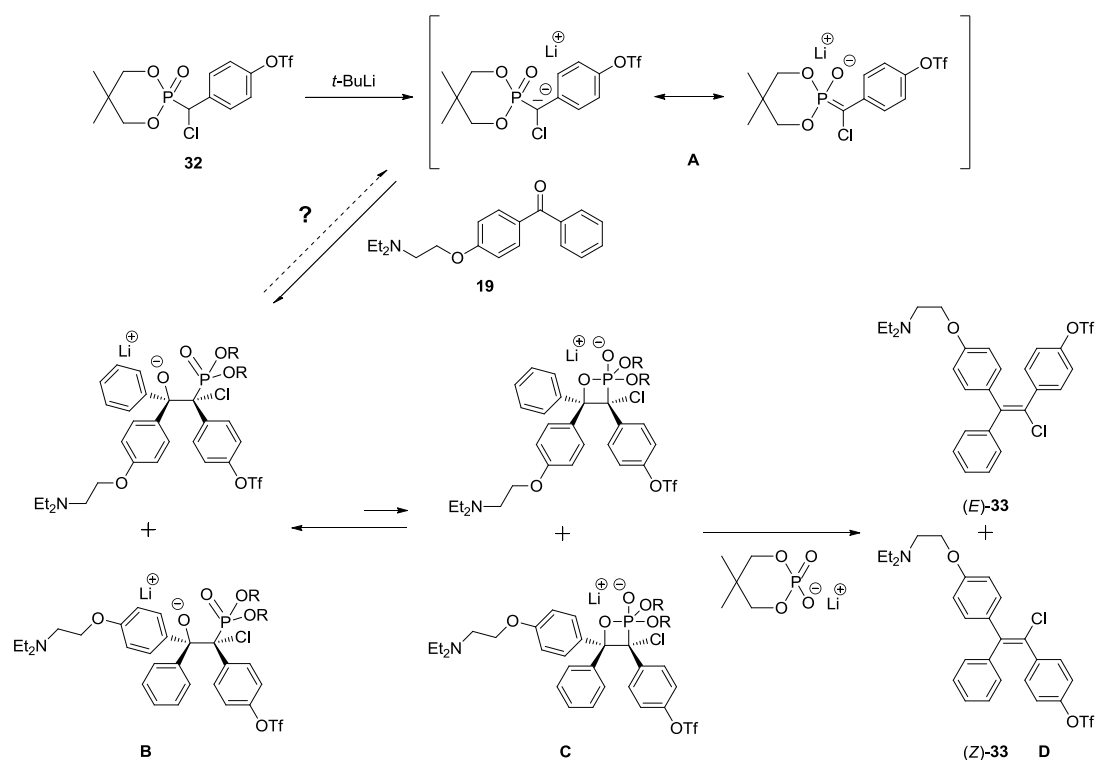


Figure 51 Proposed mechanism for conducted HWE reaction between compounds **19** and **32**.

3.4. Negishi approach

In view of the fact that both McMurry and HWE approach had turned out as dead ends, we turned our attention to the next possible synthetic route, which should be based on an adapted procedure by Tsuji *et al.*⁶⁷ Given their successful preparation of two different hydroxytamoxifene isomers, we considered this method as potentially equally useful for the construction of the very similar clomiphene TPE backbone. As illustrated in Figure 52, it should be set up via lithium stannylation of diarylacetylene **38**, followed by a Pd-catalyzed Negishi coupling to install the α' -aromatic ring, bearing the amino group. Considering the high regioselectivity, which had been reported for the stannylation step, we envisioned the synthesis of **CM 2** to take place in a regio- and stereoselective manner. After conversion of vinyl stannane **39** into the corresponding chloride, cleavage of the MOM-ether should finally afford target compound **CM 2** (**23**).

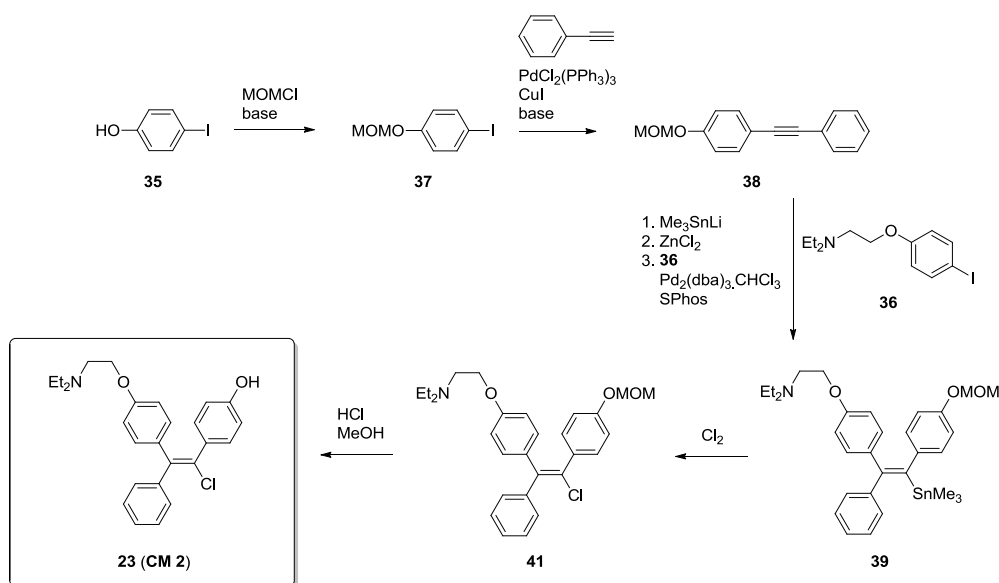


Figure 52 Envisioned synthetic route for the preparation of **CM 2 (23)** via Negishi approach.

The conduction of the three-step key reaction required diarylacetylene **38** and *N,N*-diethyl-2-(4-iodophenoxy)ethanamine (**36**) as starting materials. Aryl iodide **36** was provided by ether synthesis between 4-iodophenol (**35**) and 2-chloro-*N,N*-diethylethanamine in 70% yield. In the same manner, MOM-ether **37** was obtained quantitatively from the reaction between **35** and chloromethyl methyl ether (MOMCl). By subjecting the MOM-protected aryl iodide to a Pd-assisted Sonogashira coupling reaction with phenylacetylene following a literature procedure¹¹⁴, we obtained diarylacetylene **38** in 78% yield (see Figure 53).

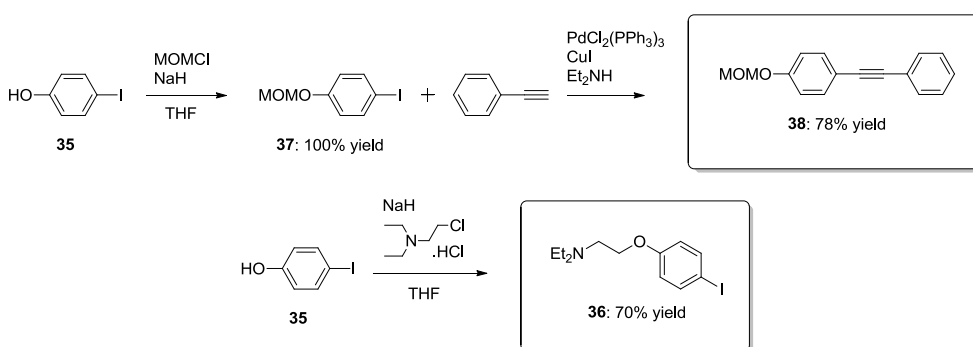


Figure 53 Synthesis of coupling components **36** and **38**.

As reported by Tsuji *et al.*, stannyl lithiation of a diarylacetylene proceeds with 100% *anti*-selectivity affording a lithio vinyl stannane intermediate, which can be reacted to a tetrasubstituted alkene by sequential conversion of the C-Li and C-Sn bond into C-C bonds. In the course of their investigations, the authors reached regioselectivities from 60 – 99% by

reacting different acetylenes with Me_3SnLi and could finally determine the steric and electronic effects exerted by the two aryl groups as major controlling factors.⁶⁷

Employing their results on our planned synthesis of **CM 2**, the electron-rich aryl group, bearing the *para*-MOM group, should direct the stannyl group onto the same carbon to which it was attached itself. As exemplified in Figure 54, this could be ascribed to the stabilizing effect on the lithium atom by a negative charge on the vinylic carbon atom that developed during the course of the reaction. As it was also shown earlier for the carbolithiation of substituted acetylenes, the addition is dominantly controlled by electrostatic interactions between the organolithium reagent and the acetylene.¹¹⁵ Accordingly, we prepared Me_3SnLi from metallic lithium and hexamethyl distannane and reacted it with the MOM-protected diarylacetylene **38** to achieve an addition to the triple bond. The addition of ZnCl_2 solution afforded transmetalation from lithium to zinc and the resulting *in situ* generated organozinc compound was then subjected to a Negishi coupling reaction with aryl iodide **36**. As catalyst for this last arylation step $\text{Pd}_2(\text{dba})_3 \cdot \text{CHCl}_3$ in combination with SPhos was applied (see Figure 54).

Having conducted this three-step procedure quite a lot of times to optimize the preparation process of vinyl stannane **39**, we experienced this reaction sequence as highly non-reproducible. Additionally to the product regioisomers **39** and **69**, several side products were formed in varying amounts (see Figure 55), leading in most cases to inseparable product mixtures. Via GC-MS analysis of the obtained crude mixtures, we could identify compound **70** and its corresponding regioisomer resulting from destannylation of **39** and **69**. Failure of transmetalation or of the Negishi coupling gave the trisubstituted alkene **71** plus its isomer, and an excess of Me_3SnLi apparently entailed a metal halogen exchange on iodide **36** providing compound **72** and leading in further consequence to the formation of the Stille coupling product **73**. Also transmetalation of the vinyl lithium intermediates **A** and **B** to the distannane **74** was observed.

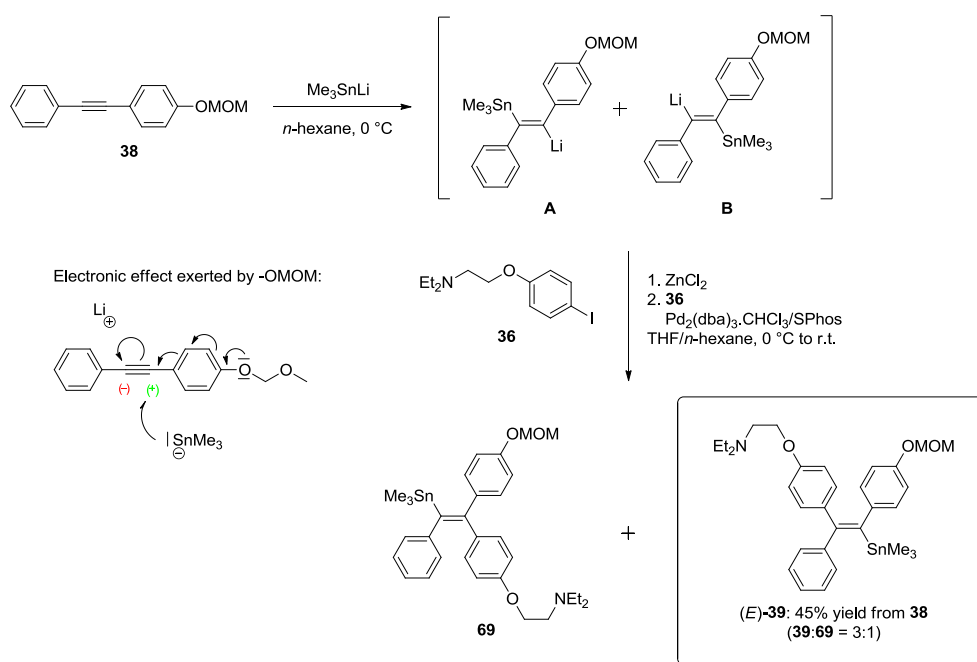


Figure 54 Synthesis of vinyl stannane (*E*)-**39** via regioselective lithium stannylation of **38** followed by transmetalation and Negishi arylation.

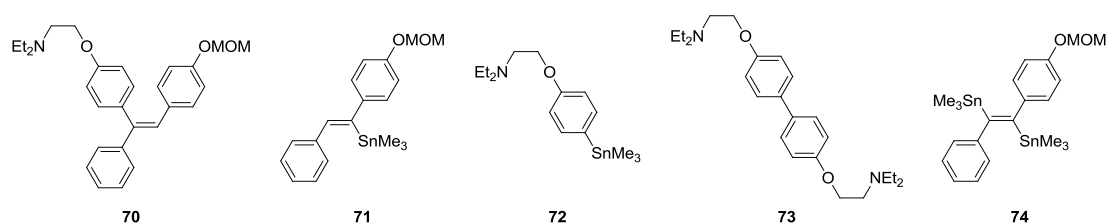


Figure 55 Side products formed in the course of three-step procedure for preparation of compound **39**.

In our attempts to gain control of the reactions going on during the course of this three-step procedure, we first developed a method for monitoring the formation of the active intermediates **A** and **B** (see Figure 54). Via quenching a reaction sample with D_2O and subsequent GC-MS analysis, we could assess the amount of active addition product that was actually present in the mixture due to Li-deuterium exchange. After having checked the proper formation of addition products **A** and **B**, we continued with the transmetalation step. For this purpose, we ensured the ZnCl_2 solution and all other applied reagents and solvents to be absolutely free of water traces, so that the risk of hydrolysis of the active intermediate was minimized. Considering all the side products that apparently had been formed due to an excess of Me_3SnLi (which applies to products **72** - **74**), we tested three different methods for the preparation of the bimetallic species. Additionally to $\text{Me}_6\text{Sn}_2/\text{Li}$ also $\text{Me}_6\text{Sn}_2/n\text{-BuLi}$ and $\text{Me}_3\text{SnCl}/\text{Li}$ were used for the generation of Me_3SnLi , with $\text{Me}_6\text{Sn}_2/\text{Li}$ proving to be the most

reliable procedure due to the absence of lithium halide, which was shown to cause complications. To exclude a negative influence of THF on the stannyl lithiation process, we planned to conduct one experiment with solid Me_3SnLi , which should be obtained after evaporation of THF. To our surprise the achieved loss of weight after solvent removal was lower than expected, which prompted us to take a sample for NMR measurement. We found different signals for the methyl groups referring to an at least partially occurred decomposition and we still detected signals of THF indicating a possible incorporation of the solvent due to complex formation. This assumption was confirmed by a publication of Wells and coworkers¹¹⁶, who had investigated the preparation and properties of methyltin-lithium compounds and had found that Me_3SnLi was exclusively stable in THF and that solvent removal immediately lead to decomposition with $[(\text{CH}_3)_3\text{Sn}]_3\text{SnLi} \cdot (\text{OC}_4\text{H}_8)_3$ being the major identified product. In view of these findings we retained the usage of THF. Also the exchange of *n*-hexane by Et_2O did not result in any improvements. Considering the preparation of diarylacetylene **38** via a Sonogashira coupling reaction, we thought that possibly residual varying copper contaminations might be accounted for the non-reproducibility of the reaction. We therefore conducted a series of reactions in pairs and added copper in form of CuI in varying amounts from 0.1 w% - 6.4 w%. However, we could not detect any significant differences concerning reactivity to the corresponding blind experiments without copper. As last attempt in attaining reproducible reaction conditions, we exchanged aryl iodide **36** with the TBS-protected iodophenol **42** to rule out any disturbing effect exerted by the amino group (see Figure 56). But also this approach provided the target molecule **43** only in low yields and attended by corresponding side products.

Summing up all the conducted experiments of *in situ* stannyl lithiation and Negishi coupling, our best result was the isolation of target vinyl stannane **39** in form of a mixture with regioisomer **69** (isomer ratio 3:1 in favor of the target structure **39**) in 45% yield. According to GC-MS analysis, this mixture also contained residues from the destannyl side product **70**, which we were not able to separate from.

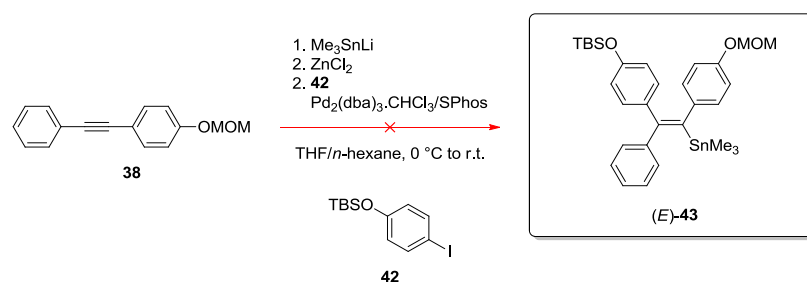


Figure 56 Failed attempt to prepare TBS-protected compound **43** via three-step procedure.

To obtain a sample that could be compared to a urine specimen, we subjected the product mixture containing vinyl stannane **39** to chloro destannylation. Our first attempts to achieve chlorination by the use of chlorine gas failed, which prompted us to reproduce the literature results for the iodination of compound **39**. The vinyl iodide was smoothly obtained in 91% yield, which encouraged us to search for other possible reagents capable of chloro destannylation and in the end lead us to CuCl_2 ¹¹⁷, which enabled a quantitative conversion into vinyl chloride **41**. Acidic cleavage of the MOM-ether by using HCl/MeOH finally gave the target metabolite **CM 2** (see Figure 57).

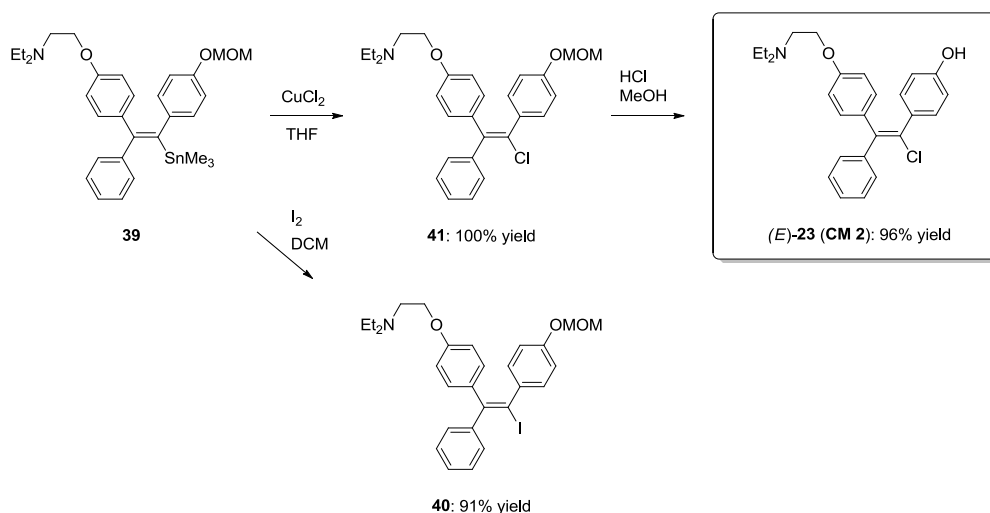


Figure 57 Preparation of target metabolite **CM 2** from **39** via chlorination and MOM-cleavage.

3.5. Proof of authenticity

To clarify whether **CM 2** was the major metabolite of clomiphen present in human urine, we compared the product mixture containing compound **23 (CM 2)** with a urine sample taken after the oral administration of clomiphen. For this purpose, both samples were treated with MSTFA to convert phenolic groups into less polar TMS-ethers and afterwards

both specimens were subjected to GC-MS analysis. The TMS-ether of (*E*)-4'-OH-clomiphene (**75**, **(B)**) could be identified by its mass spectrum and by comparison to previously obtained product mixtures from other approaches. As depicted by the TIC-comparison in Figure 58, it was shown that compound **75** (**(B)**) exhibited another retention time than the TMS-ether of the urinary metabolite (**(A)**), clearly indicating that 4'-OH-clomiphene (**CM 2**) could not be clomiphene's metabolite predominant in GC-MS measurements. The additional signals of the product mixture could be assigned to the TMS-ether of the corresponding regioisomer 4-OH-clomiphene (**76**, **(C)**), to the deschloro regioisomers **77** and **78** and to the regioisomers resulting from methanolysis in the course of our purification attempts (see Figure 59). The separation of clomiphene-like compounds was shown to work best by using DCM/MeOH with TEA (1%) as mobile phase, but unfortunately all compounds bearing the 4'-OH-moiety turned out to be very prone to nucleophilic substitution under these conditions and target compound **75** was so partially converted into the corresponding methoxy derivative **79**. Unlike a *para*-hydroxy group located at the α -ring, a *para*-hydroxy group at the β -ring perfectly stabilizes the positive charge, which is formed in the course of chloride substitution and so makes this group of clomiphene metabolites very susceptible for solvolysis (see Figure 60).

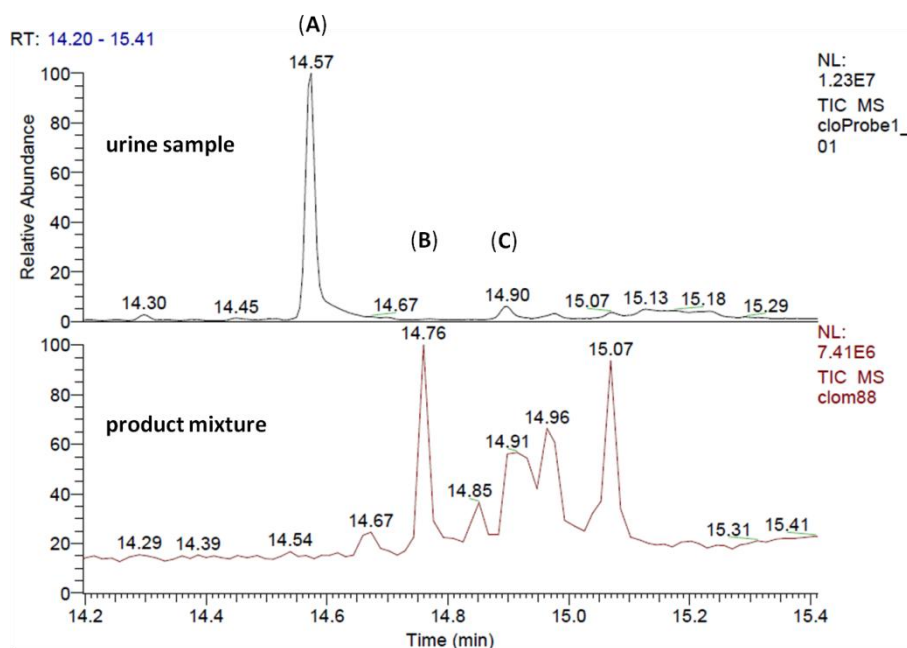


Figure 58 TIC-comparison of urine sample and product mixture obtained from Negishi approach: (A) urinary metabolite, (B) TMS-ether of (*E*)-4'-OH-clomiphene (**75**), (C) TMS-ether of regioisomer (*E*)-4-OH-clomiphene (**76**).

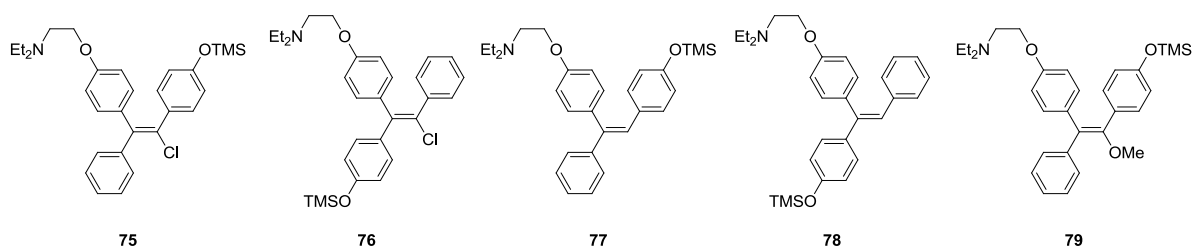


Figure 59 Compounds identified in product mixture resulting from Negishi approach after derivatization.

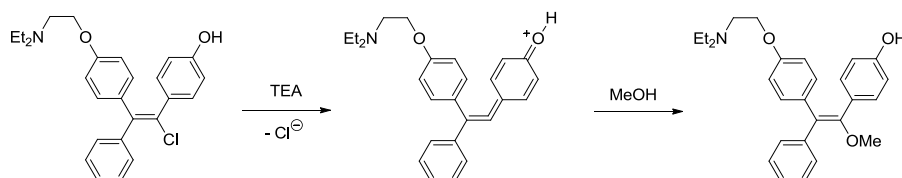


Figure 60 Formation of methoxylated side product via methanolysis in the course of purification.

In view of the fact that 4'-OH-clomiphene (**CM 2**) definitely had turned out not to be clomiphene's main metabolite and with regard to all difficulties encountered in the course of its preparation so far, we decided to leave it at that and to turn our attention towards the next possible target structure 3,4-di-hydroxy-di-hydroclomiphene (**CM 3**).

4. Results and Discussion - Synthesis of 3,4-di-hydroxy-di-hydroclomiphene

4.1. Retrosynthetic analysis

Considering the metabolic transformation of clomiphene into 3,4-di-hydroxy-dihydro-clomiphene (**CM 3**) via enzymatic hydroxylation and double bond hydrogenation⁵⁵, it seems obvious to synthesize this structure via the corresponding TPE derivative followed by double bond hydrogenation. But due to the failure of the McMurry and the HWE approach in preparing target structure **CM 2**, we also considered them as unrewarding options for the synthesis of **CM 3**, as we would encounter the same problems. On closer examination also the Negishi approach turned out to be not suitable for the preparation of **CM 3**, because due to the electronic effects exerted by the aryl groups of the applied diarylacetylenes, in either possible case the wrong regioisomer would be formed. Accordingly it was not possible to prepare **CM 3** via the stannyl lithiation method, which had been applied for the synthesis of

the other clomiphen metabolite **CM 2**. We therefore decided against the route via the unsaturated TPE derivative and planned the direct construction of the hydrogenated TPE core structure in the course of two consecutive α -arylation steps.

According to our retrosynthetic analysis (see Figure 61), we envisioned to obtain the chloride by substitution of the corresponding alcohol, which in turn could be delivered by reduction of an appropriate 1,2,2-triphenylethanone derivative. Applying the concept of Pd-catalyzed α -arylation, the triphenylethanone was ascribed to the deoxybenzoin, which again could be obtained by α -arylation, ending up with acetophenone and 2-(4-bromophenoxy)-*N,N*-diethylethanamine (approach 1 in Figure 61). Alternatively, the amino group could be installed at last, which would lead to acetophenone and 4-bromophenol as starting materials (approach 2 in Figure 61).

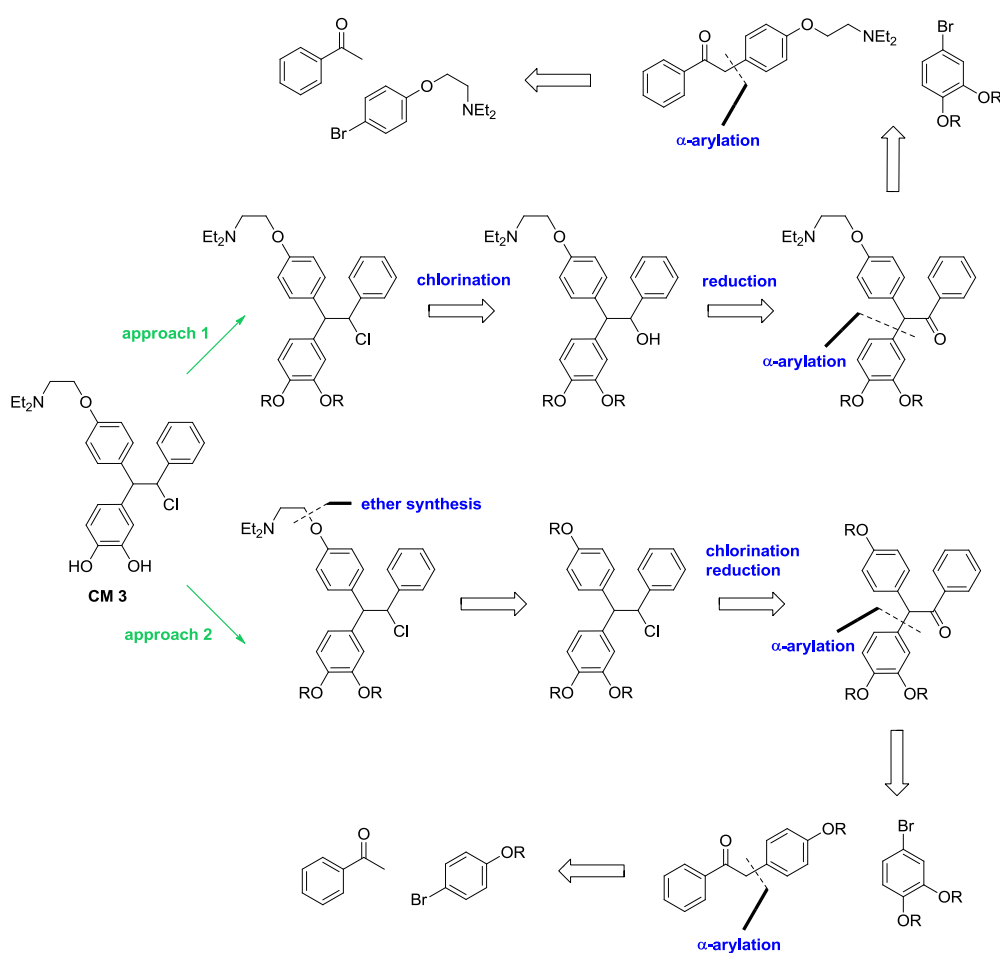


Figure 61 Retrosynthetic analysis of 3,4-dihydroxy-dihydroclomiphen (**CM 3**).

4.2. Approach 1

Finding a convenient and efficient way to prepare α -aryl ketones via direct arylation in α -position of the carbonyl group has been a challenging problem in organic synthesis for many years. A method for the formation of α -aryl ketones that has been known for a very long time is the nucleophilic aromatic substitution (S_NAR) of a stabilized enolate with an aryl halide or a benzyne derivative, but due to severe limitations concerning the reaction scope and regioselectivity, these methods cannot be regarded as very general approaches for the α -arylation of carbonyl compounds (see Figure 62).¹¹⁸

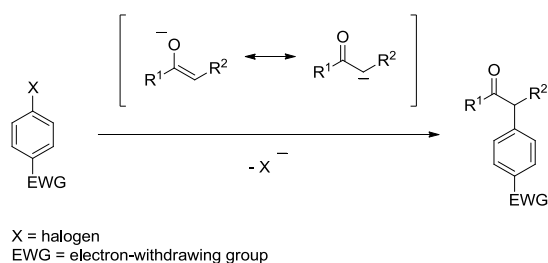


Figure 62 Arylation of ketones via nucleophilic aromatic substitution.

Also the more recently discovered radical-nucleophilic aromatic substitution ($S_{RN}1$) mechanism would offer a general opportunity of generating a C_{α} - C_{aryl} bond.¹¹⁹ Via reaction of an aryl halide with an electron donor, an aryl radical is formed, which subsequently reacts with a nucleophile. If this nucleophile is an enolate, an α -aryl ketone is formed (see Figure 63).¹²⁰

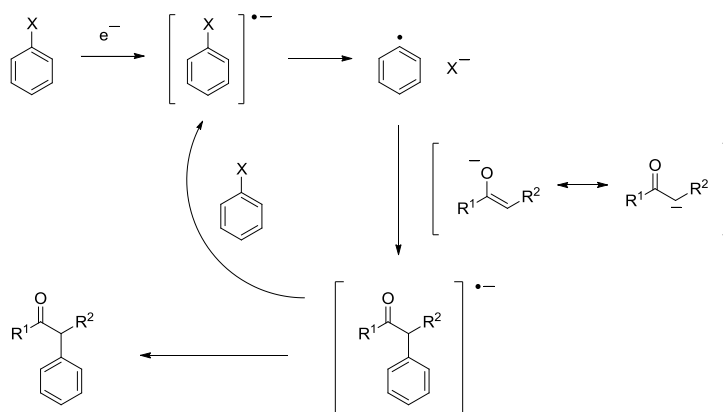


Figure 63 General mechanism of a $S_{RN}1$ reaction with an enolate as nucleophile.¹²⁰

The main advantage over the before mentioned methods is that there are no limitations concerning the nature of the aryl halide – the use of electron-rich as well as of electron-deficient or -neutral aryl halides is possible. Nevertheless, also this approach suffers from problems concerning regioselectivity. Additionally only a limited number of solvents can be applied and radical side reactions considerably lower the yields.¹²¹ This obvious lack of general methods for α -arylations prompted the development of various reagents for that purpose, most of them involving toxic main group elements such as tin, lead or bismuth.¹²² While many of them showed to be quite effective, their major drawback consists in their stoichiometric application. Furthermore many of these procedures cannot be regarded as direct arylation methods, because instead of carbonyl compounds very often less readily available carbonyl derivatives like silyl enol ethers or α -halo carbonyl compounds are applied.

The discovery of Pd-catalyzed direct coupling between ketones and aryl halides without the use of any intermediates was regarded as a major breakthrough in the synthesis of α -aryl ketones. The groups of Hartwig, Buchwald and Satoh showed that the *in situ* generated enolate of a ketone can efficiently react as transmetalating agent in a catalytic transformation leading to the formation of new sp^2 - sp^3 bonds.¹²³ The conversion of ketones with two enolizable positions was reported to take place with high regioselectivities. By the use of enantiopure ligands also asymmetric conversions were achieved.¹²⁴ The first catalyst systems, enabling these conversions, were based on ligands bearing tertiary phosphines, like PPh_3 , $PtBu_3$, PCy_3 or more advanced bisphosphines, such as BINAP (2,2'-bis(diphenylphosphino)-1,1'-binaphthyl), Xantphos (4,5-bis(diphenylphosphino)-9,9-dimethylxanthene) or DtBPF (1,1'-bis-(di-*tert*-butylphosphino)ferrocene) (see Figure 64).

In 2002, Nolan and coworkers described a new class of palladium catalysts bearing an *N*-heterocyclic carbene (NHC) ligand to be effective for the α -arylation of ketones.¹²⁵ SIPr [*N,N'*-bis(2,6-diisopropylphenyl)-4,5-dihydroimidazol-2-ylidene], IPr [*N,N'*-bis(2,6-diisopropylphenyl)imidazol-2-ylidene], IMes [*N,N'*-bis(2,4,6-trimethylphenyl)imidazole-2-ylidene] and ItBu [*N,N'*-bis-*tert*-butylimidazol-2-ylidene] were shown to be capable of mediating the direct coupling of ketones with a variety of aryl chlorides, bromides and triflates. The catalyst with the general formula (NHC)Pd(allyl)Cl was obtained by the reaction of $[(\eta^3\text{-allyl})Pd(Cl)]_2$ with the free carbene and is believed to be activated via nucleophilic attack on the allyl moiety by a base. This active NHC-Pd species would then be able to

oxidatively add aryl halides or pseudohalides. The bulky substituents on the imidazole nitrogens and the important σ -donating properties of the NHC exert a beneficial effect on the oxidative addition and reductive elimination steps of the cross coupling catalytic cycle. Figure 64 depicts some of the most common catalysts used for the Pd-catalyzed α -arylation process. A limited number of substrate combinations was even reported to react without any ligands to give the corresponding α -aryl ketones in good yields.¹²⁶

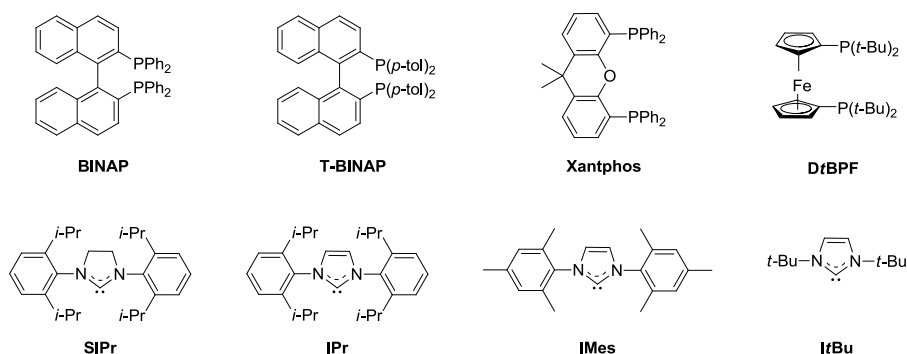


Figure 64 Common ligands used for the Pd-catalyzed α -arylation of ketones.

Figure 65 shows a proposed catalytic cycle for the Pd-catalyzed cross coupling reaction of aryl halides and ketones.¹²⁷ Whereas for bulky monophosphines, it is believed that only one phosphine binds to the metal center of aryl palladium enolate intermediates **D1** - **D3**, the ligand binding of biphosphines to Pd is assumed to be chelating. This mechanism was supported by high selectivities obtained with bidentate ligands in reactions of relatively unhindered aliphatic ketones, whereas the use of monodentate ligands resulted only in low selectivities. Most probably the increased steric congestion around the metal center when biphosphines are used, could be accounted for this rise in selectivity.¹²⁶

Considering the successful preparation of a variety of differently methoxy substituted 1,2,2-triarylethanones via Pd-catalyzed α -arylation by Domínguez *et al.*¹²⁷, we chose this method for the preparation of triarylketone **53**. The deoxybenzoin **52** was envisioned to be prepared in the same manner, preferably via a ligandless arylation reaction. Reduction of compound **53** should give the corresponding alcohol, which could subsequently be subjected to chlorination using SOCl_2 . Cleavage of the MOM-ethers should finally afford the target structure **CM 3** (see Figure 66).

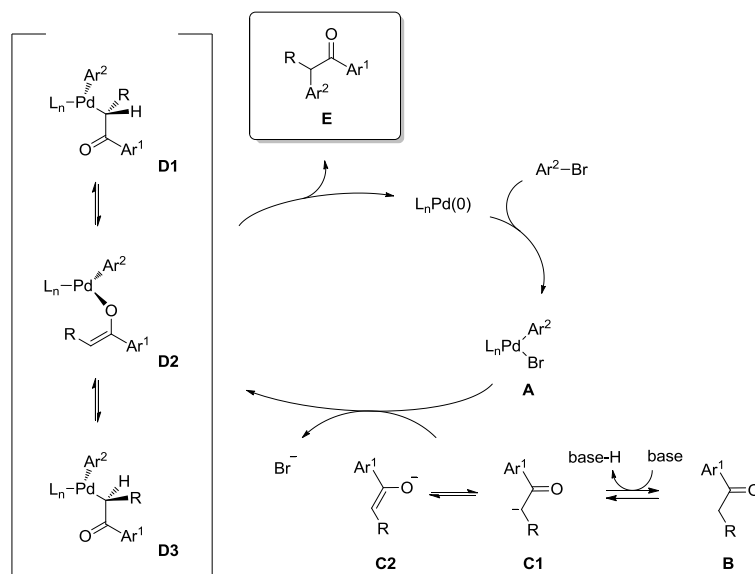


Figure 65 Proposed catalytic cycle for Pd-catalyzed α -arylation of ketones.¹²⁷

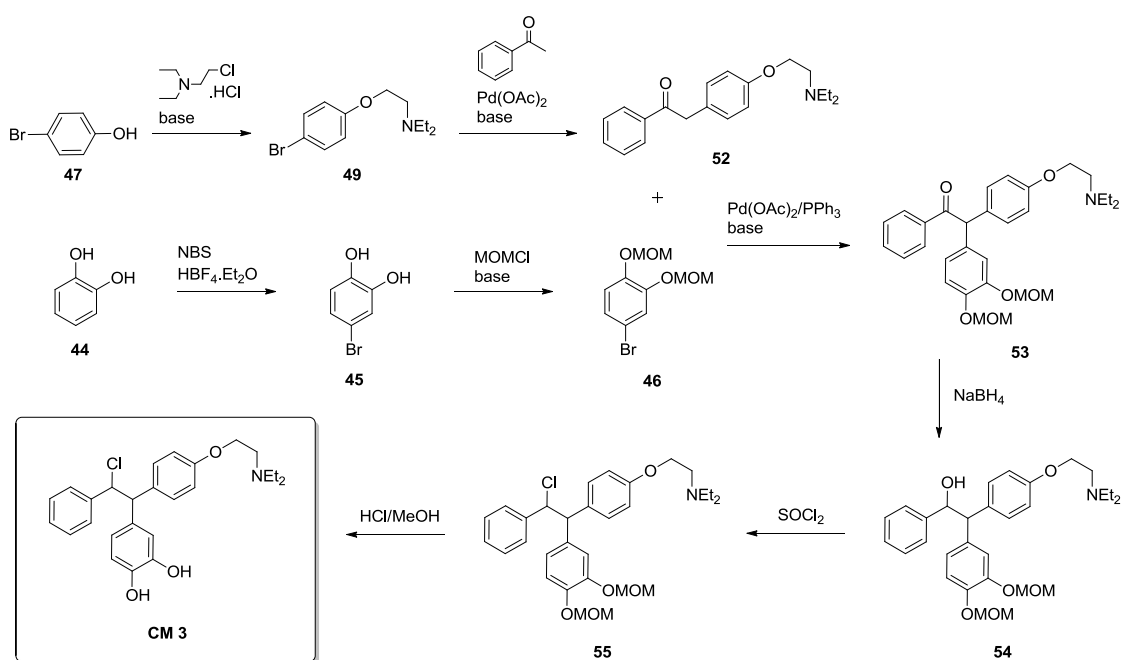


Figure 66 Envisioned pathway for the preparation of 3,4-di-hydroxy-di-hydroclomiphene (**CM 3**).

The syntheses of the aryl bromides **46** and **49**, which were required as starting materials for the two cross coupling reactions, were straightforward. Compound **49** was obtained from the reaction of 4-bromophenol and 2-chloro-*N,N*-diethylethanamine hydrochloride in 88% yield and bromide **46** was prepared via MOM-protection of 4-bromocatechol, which in turn was produced by bromination of catechol using NBS¹²⁸ (see Figure 67).

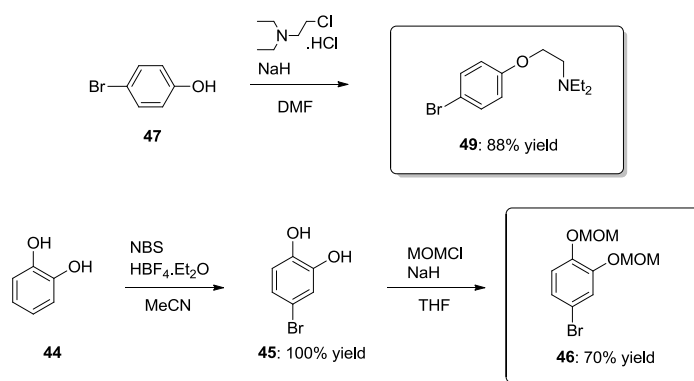


Figure 67 Synthesis of starting materials for Pd-catalyzed α -arylations.

The first C _{α} -C_{aryl}-bond had to be formed between aryl bromide **49** and acetophenone. In our first attempt to accomplish that, we used Pd(OAc)₂ in the absence of any ligands according to a procedure by Buchwald *et al.*, who had successfully arylated propiophenone with 1-bromo-4-methoxybenzene in this manner.¹²⁶ The reaction proceeded very slowly and gave the desired deoxybenzoin in moderate yield. As side products, we detected the products resulting from diarylation (**81**) and *ortho*-arylation (**83**). An increase in the reaction temperature lead to an enhanced side product formation and lowered the yield of the target product. Also the application of PPh₃ and the direct use of Pd(PPh₃)₄ did not entail any improvement, even on the contrary facilitated the formation of side product **82** via phenyl migration from the phosphine ligand. The occurrence of this palladium-mediated P-C bond cleavage upon the use of PPh₃ was also reported in literature and is most likely to happen when electron-rich arenes or aryl halides are employed¹²⁷. We therefore ceased from using catalyst systems based on phosphines and tested the NHC-Pd-catalyst (IPr)Pd(allyl)Cl for its ability to mediate the cross coupling reaction between aryl bromide **49** and acetophenone. Although the reaction proceeded very slowly, our first attempt resulted in a yield of 62% of desired product and totally lacked the formation of any side products. By using a larger excess of ketone and conducting the reaction in a microwave reactor at 100 °C, we were able to reduce the time needed for total conversion to one hour and in this manner obtained the target deoxybenzoin **52** in an excellent yield of 96%. All results are summarized in Table 6.

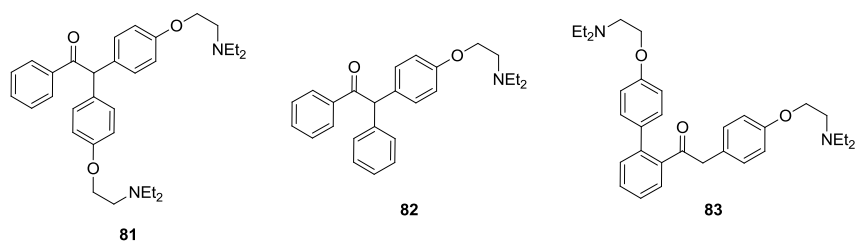


Figure 68 Side products in the synthesis of deoxybenzoin **52** via Pd-catalyzed α -arylation.

Table 6 Synthesis of deoxybenzoin **52** via Pd-catalyzed α -arylation. Except otherwise noted, reactions were conducted using 1.0 equiv **49** and 1.2 equiv acetophenone. ^aReaction was conducted in the microwave using 2.5 equiv acetophenone and 2.5 equiv NaOtBu.

entry	catalyst	T [° C]	solvent	time [h]	yield [%]
1	Pd(OAc) ₂ (1 mol%)	80	toluene	16	38
2	Pd(OAc) ₂ (1 mol%)	100	toluene	16	28
3	Pd(OAc) ₂ /PPh ₃ (1 mol%)	80	toluene	16	27
4	Pd(PPh ₃) ₄ (1 mol%)	80	toluene	16	31
5	(IPr)Pd(allyl)Cl (2 mol%)	60	THF	48	62
6 ^a	(IPr)Pd(allyl)Cl (2 mol%)	100	THF	1	96

The second α -arylation step, which should afford triarylketone **53**, was envisioned to be conducted under similar conditions like the first cross coupling reaction. Following a literature procedure¹²⁷, we first tested the catalyst system Pd(OAc)₂/PPh₃ for its ability to mediate the arylation. The target ketone was indeed formed, but as it was also the case in the first arylation step upon usage of PPh₃, phenyl migration and *ortho*-arylation were observed as concomitant side-processes resulting in the corresponding by-products **84** and **85** (see Figure 69). Whereas the use of AsPh₃ instead of PPh₃ just deteriorated the situation, conduction of the reaction in a microwave reactor was shown to exert a positive impact on the reaction time as well as on the yield of target product. Nevertheless, the obtained crude mixture still contained undesired side products and proved to be rather difficult to purify. Our attempt to prevent phenyl migration by the application of PCy₃ instead of PPh₃ did not work out, as it resulted in no conversion at all. Considering the good results of our first arylation step upon the usage of (IPr)Pd(allyl)Cl, we tested the NHC-ligand also for the

preparation of triarylketone **53**, but applying the same reaction conditions as for the previous coupling step, afforded **53** only in very low yields. Upon the use of Cs_2CO_3 in combination with $(\text{IPr})\text{Pd}(\text{allyl})\text{Cl}$, we interestingly observed the predominant formation of α -diketone **86**, obviously resulting from oxidation. α -Oxidation of ketones affected by molecular oxygen under basic conditions had also been described in literature, but could be prevented by the use of degassed solvents.^{127,129} In view of the fact that we applied for all experiments the same solvents and that we solely used degassed ones, we ascribed this outcome to the catalyst/base system.

Considering the failure of monophosphines and $(\text{IPr})\text{Pd}(\text{allyl})\text{Cl}$, we continued by employing biphosphines in the hope that their chelating effect would positively influence product formation. While (*R*)-T-BINAP resulted in no conversion at all, DtBPF appeared to be the perfect ligand, as concomitant side processes were completely averted and the desired product was cleanly formed and could be isolated in 79% yield.

Table 7 gives an overview of all conducted experiments for the synthesis of 1,2,2-triarylethanone **53**.

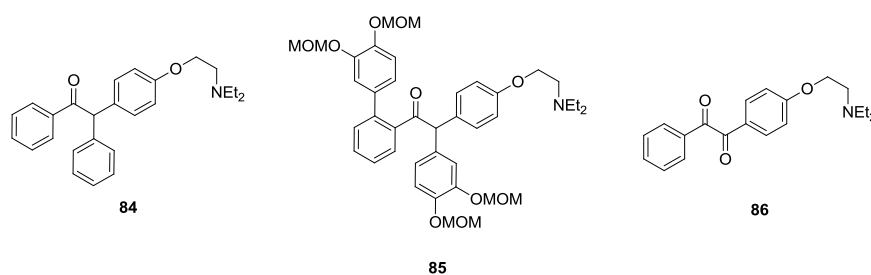
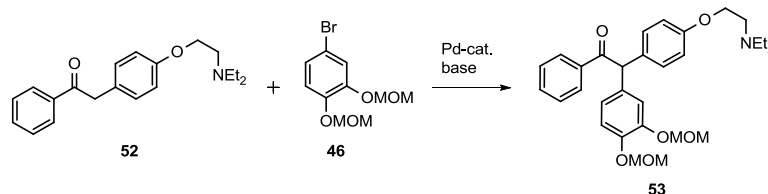


Figure 69 Side products in the synthesis of 1,2,2-triarylethanone **53** via Pd-catalyzed α -arylation.

In light of our results, obtained in the course of optimizing the two α -arylation steps, we consider the optimization of two factors as key prerequisite for a successful cross coupling. The proper choice of the catalyst system, especially of the ligand, ensures the perfect electronic and steric influences on oxidative addition and reductive elimination to achieve high yields of target product while avoiding concomitant side reactions. Whereas $(\text{IPr})\text{Pd}(\text{allyl})\text{Cl}$ was shown to efficiently catalyze the conversion of acetophenone and arylbromide **49** to deoxybenzoin **52**, the combination of $\text{Pd}_2(\text{dba})_3 \cdot \text{CHCl}_3/\text{DtBPF}$ turned out to be the right choice for the preparation of triarylketone **53**. As second important factor, we

Table 7 Synthesis of triarylethanone **53** via Pd-catalyzed α -arylation. *Conducted in the microwave. ^aConducted with 2 mol% Pd-cat., 8 mol% ligand and 2.5 equiv base. ^b2 mol% Pd-cat., 8 mol% ligand, 2 equiv base and 5 equiv LiCl. ^c4 mol% Pd-cat. and 4 mol% ligand. ^d2 mol% Pd-cat. and 2.5 equiv base. ^e2 mol% Pd-cat. and 3 equiv base. ^f6 mol% Pd-cat., 7 mol% ligand and 3 equiv base. ^g6 mol% Pd-cat., 7.5 mol% ligand and 2.5 equiv base.



entry	46 [equiv]	catalyst	base	solvent	time [h]	T [° C]	yield [%]
1 ^a	1.0	Pd(OAc) ₂ /PPh ₃	Cs ₂ CO ₃	DMF	4.0	140	53 (47%), 84/85 (27%), 52 (8%)
2 ^a	1.2	Pd(OAc) ₂ /AsPh ₃	Cs ₂ CO ₃	DMF	24.0	140	53 (25%), 84/85 (45%), 52 (26%)
3 ^{*a}	1.3	Pd(OAc) ₂ /PPh ₃	Cs ₂ CO ₃	DMF	1.0	140	53 (75%), 84/85 (20%)
4 ^{*b}	1.5	Pd(OAc) ₂ /PPh ₃	LiOH	THF	2.0	130	no conv.
5 ^{*b}	1.5	Pd(OAc) ₂ /PPh ₃	LiOH	DMF	1.0	150	53 (17%), 84/85 (68%), 52 (15%)
6 ^{*c}	1.3	Pd(OAc) ₂ /P(Cy) ₃	NaOtBu	THF	4.0	70	no conv.
7 ^{*d}	1.5	(IPr)Pd(allyl)Cl	Cs ₂ CO ₃	THF	5.0	130	86 (49%), 52 (26%)
8 ^{*d}	1.5	(IPr)Pd(allyl)Cl	Cs ₂ CO ₃	DMF	5.0	130	86 (90%)
9 ^{*e}	0.66	(IPr)Pd(allyl)Cl	NaOtBu	THF	4.0	140	53 (7%), 84/85 (38%), 52 (54%)
10 ^{*f}	1.3	Pd ₂ (dba) ₃ .CHCl ₃ / (R)-T-BINAP	NaOtBu	THF	3.0	70	no conv.
11 ^{*g}	1.3	Pd ₂ (dba) ₃ .CHCl ₃ / DtBPF	NaOtBu	THF	3.5	70	53 (79%)

consider the amount of base present in the reaction mixture. To ensure the presence of the ketone in its enolate form and to avoid eventual homo condensation reactions, at least one equivalent base should be added. However, at the same time it should be settled whether an eventual excess of base could negatively affect the reaction outcome. Considering the arylation of acetophenone, an excess of base has to be clearly avoided, because the deoxybenzoin can easily be subject of a second deprotonation leading to the diarylproduct **81**. In contrast to that, the application of 2.5 equivalents base in the formation of triarylketone **53** seemed to have no negative impacts. We ascribe this to the two electron-rich aromatic substituents, which reduce the acidity of the benzylic position, as well as to the sterically rather crowded vicinity, rendering a second arylation a rather improbable event to take place.

Having developed a very efficient method for the preparation of triarylketone **53**, we focused on the next reaction steps leading to target structure **CM 3**. We first converted the ketone into the corresponding alcohol diastereomers, which was easily achieved by the use of LiAlH_4 . The reduction was also conducted with NaBH_4 , but we experienced the reaction to take place more smoothly upon the usage of LiAlH_4 . Following our envisioned synthetic route, chlorination of alcohol **54** was supposed to be the next step. In our first attempt to achieve the nucleophilic substitution of the hydroxy group by a chloride, we reacted compound **54** with SOCl_2 . These rather harsh reaction conditions resulted in elimination as well as in the cleavage of one or both MOM-ethers, giving a refractory mixture of products with chloride **55** only in traces present. Considering the formation of the extensive conjugated double bond system upon elimination of H_2O or HCl , we had compounds **53** and **54** already expected to be very susceptible for elimination processes and turned our attention towards milder chlorination methods. The use of diethyl azodicarboxylate (DEAD), PPh_3 and zinc halide was reported as very convenient method to convert primary, secondary and allylic alcohols into halides, while being sufficiently mild for acid- and base-sensitive molecules.¹³⁰ According to Figure 70, the reaction of alcohol with DEAD and PPh_3 gives the ionic species **A**, which in further consequence is assumed to react with the zinc halide to give the reactive alkoxyphosphonium halide **B**. $\text{S}_{\text{N}}2$ -type displacement of the resulting alkoxyphosphonium species by the halide anion completes the reaction.

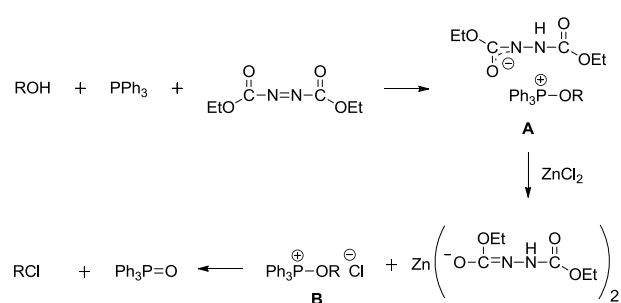


Figure 70 Possible reaction mechanism for the chlorination of alcohols upon usage of DEAD/ PPh_3 / ZnCl_2 .¹³⁰

Accordingly, we applied the DEAD/ PPh_3 / ZnCl_2 system on alcohol **54**, but were only able to isolate a mixture of starting material and elimination product in the end. The same results were obtained by the application of LiCl ¹³¹ instead of ZnCl_2 and also the use of $\text{PPh}_3\text{-CCl}_4$ complex¹³² was not successful (see Figure 71).

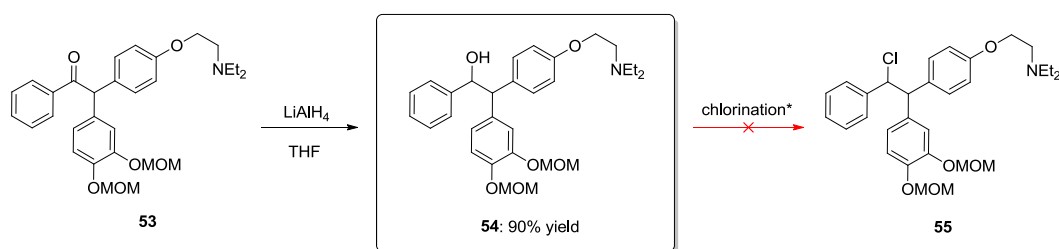


Figure 71 Synthesis of alcohol **54** via reduction of compound **53** and attempted chlorination.

In light of these findings, we came to the conclusion that due to the apparently very high stability of the conjugated system featured by the elimination product, compound **54** was simply too sensitive for being subjected to chlorination as it had been originally envisioned. We therefore put our backup plan into effect, according to which ketone **53** should be converted into its triflate, which in further consequence again could be subjected to Pd- or Ru-assisted chlorination¹³³. Hydrogenation of the double bond and cleavage of the two MOM-ethers would finally give target structure **CM 3** (see Figure 72).

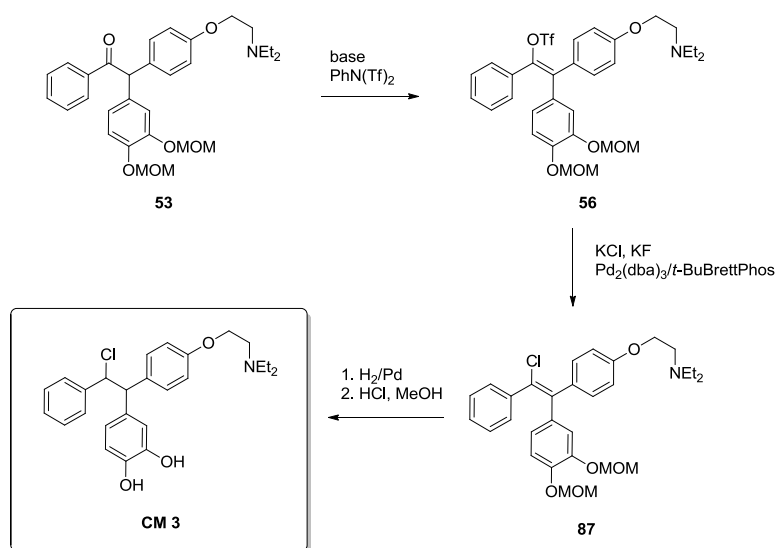


Figure 72 Envisioned synthesis of clomiphene metabolite **CM 3** via triflate **56**.

To ensure the complete conversion of **53** into its enolate form, we first conducted a series of deprotonation experiments applying different bases. By quenching the enolates with D₂O and subsequent NMR analysis, we were able to determine the degree of conversion. Whereas NaHMDS, LDA and NaOtBu did not enable a deprotonation, NaH and KH facilitated the complete transformation into the enolate within one hour. Apparently the place

surrounding the α -H atom was sterically rather congested, leaving enough space for proton abstraction only for very small bases, whereas NaHMDS, LDA and NaOtBu were simply too space-filling. In our first attempts to achieve a conversion of the enolate into vinyl triflate **56** we applied the pyridine-derived triflating reagents phenyl triflimide PhN(Tf)₂ and Comins' reagent (2-[N,N-bis(trifluoromethylsulfonyl)amino]-5-chloropyridine), which are generally known to mediate the triflation of metallo enolates under very mild conditions.¹³⁴ We conducted lots of experiments, using varying base/reagent combinations in different solvents (DMF, THF and DME), but were not able to isolate enol triflate **56**. So we also applied triflic anhydride (Tf)₂O in combination with KH, pyridine and 2,6-di-*tert*-butylpyridine, but were just as unsuccessful as we had been in our previous attempts. We indeed detected small amounts of triflate by taking LC-MS samples directly from the reaction mixture, but these traces used to disappear in the course of work up and we always ended up with refractory mixtures of starting material and several indefinable products. Suggesting that enolate triflate **56** was simply too unstable, we conducted some *in situ* chlorinations by adding the chlorination reagents directly to the reaction mixture after triflation, but also this approach did not afford the desired chloride **87** (see Figure 73).

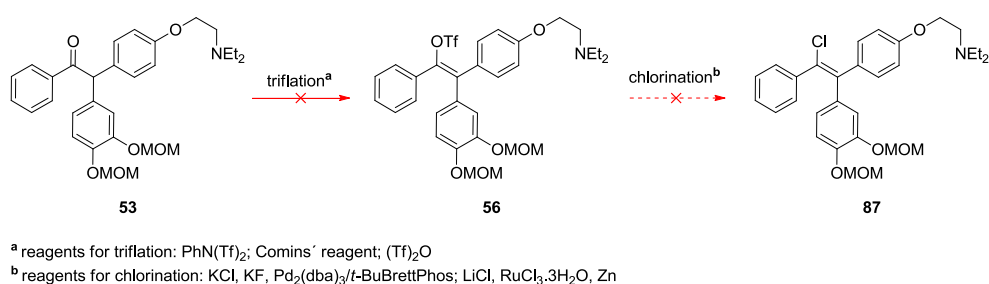


Figure 73 Failed attempts of triflation and chlorination to obtain compound **87**.

According to NMR and LC-MS analyses of the crude mixtures, the triflating reagents reacted with different sites of the ketone. We found products resulting from cleavage of the MOM-ethers as well as different amino salts. The high susceptibility of all the ether moieties and the nitrogen atom for an electrophilic attack by the triflating reagents apparently rather lead to a degradation of starting material instead of giving a clean triflation. We therefore condemned triarylketone **53** as educt for triflation and sought for other possibilities to obtain target structure **CM 3**.

4.3. Approach 2

Given the formation of ammonium salts upon treatment of ketone **53** with triflating reagents and also in consideration of general problems arising from the zwitterionic character of **CM 3** and its precursor compounds, we modified the previously discussed synthetic route, so that the installation of the diethylaminoethyl group would occur at the end of the sequence. We therefore envisioned triarylketone **63**, which could be analogously converted to ketone **53**, as starting point for two alternative pathways leading to **CM 3** (see Figure 74). Similarly to approach 1, chlorination could either occur via the corresponding triflate **66** or via alcohol **64**. The use of orthogonal protecting groups should then facilitate the installation of the amino group without affecting the dihydroxy moiety. To reduce the number of atoms bearing free electron pairs that could interfere with triflating reagents, we planned to protect the catechol moiety as benzyl ethers, whereas the phenol site was envisioned to be masked as silyl ether. Pd-catalyzed hydrogenation as last step in either pathway should finally afford 3,4-di-hydroxy-di-hydroclomiphene (**CM 3**).

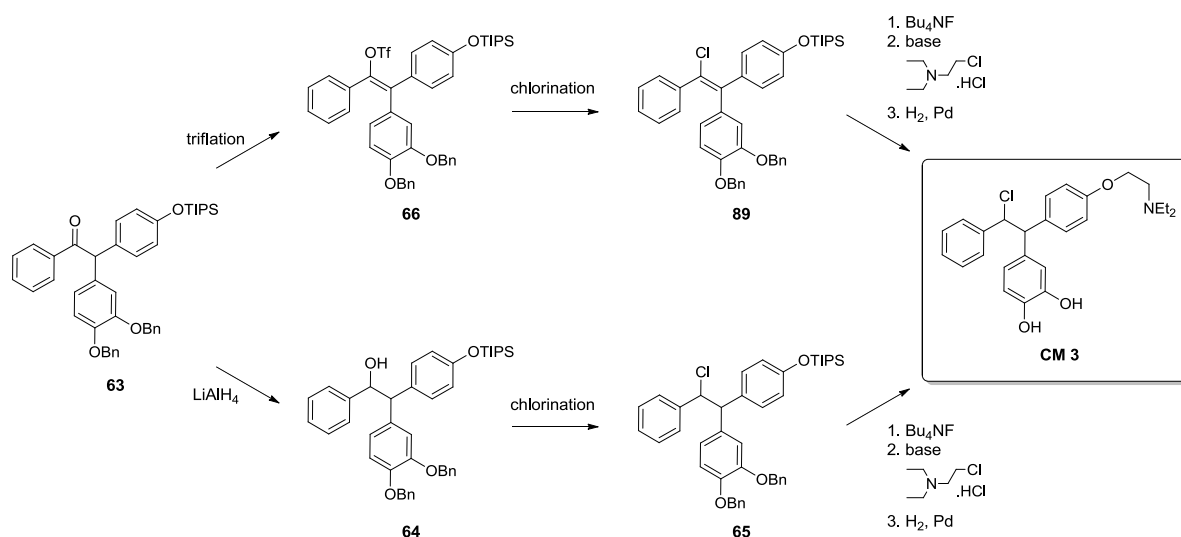


Figure 74 Envisioned alternative synthetic routes towards clomiphene metabolite **CM 3**.

The installation of the two different protecting groups gave the precursor compounds for the α -arylation steps. The benzyl-protected bromocatechol **62** was obtained in 85% yield and the TIPS-protected bromophenol **57** could be isolated quantitatively after ether synthesis with the corresponding silyl chloride (see Figure 75).

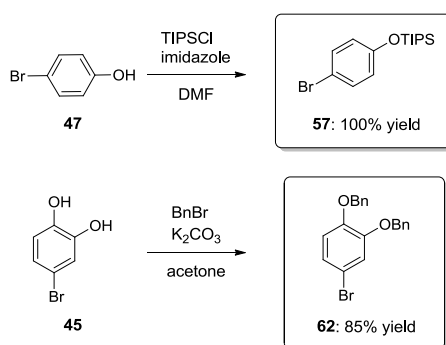


Figure 75 Synthesis of starting materials for Pd-catalyzed α -arylations.

The construction of the 1,2,2-triarylethanone core structure of ketone **63** was achieved according to the two-step α -arylation process, which had already been optimized in the course of approach 1. To determine the nature of the silyl protecting group that should finally be installed, we tested the arylation of acetophenone with two different substrates. Additionally to the TIPS-protected bromophenol **47** also the TBS-protected iodophenol **42** was subjected to microwave-assisted cross coupling. Whereas we did not observe any differences in the reactivity of bromide and iodide – both couplings smoothly occurred within one hour providing the deoxybenzoins in equal yields – the behaviour of the protecting groups was shown to be completely contrary to each other. Whereas we observed the complete cleavage of the TBS group resulting in the deprotected deoxybenzoins **61**, the TIPS group proved to be robust enough for the applied reaction conditions. Accordingly, compound **61** was isolated in 67% yield and subjected to the second arylation step yielding the key structure, triarylethanone **63**, in 57% (see Figure 76).

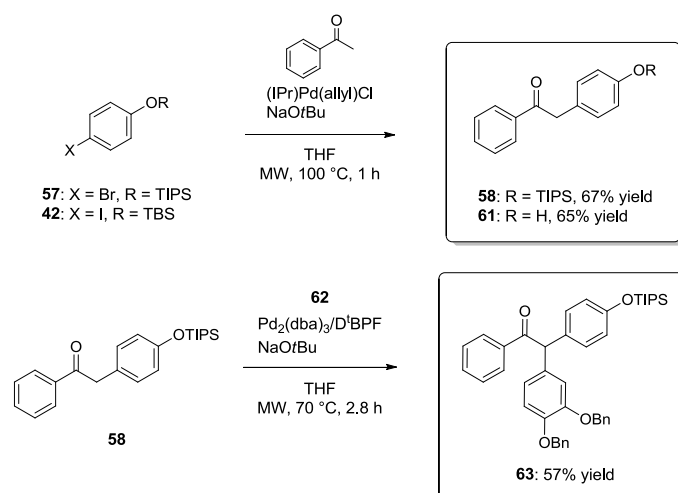
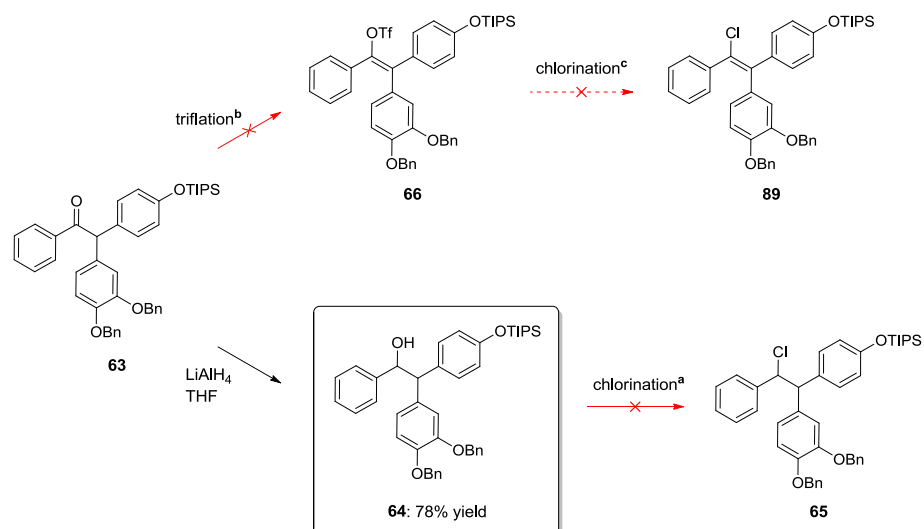


Figure 76 Synthesis of triarylethanone **63** via two consecutive Pd-catalyzed α -arylations.

Having compound **63** in hand, we focused on the incorporation of the chlorine atom. We basically applied the same strategies as we did in the course of approach 1, but hoped that the absence of the amino group as well as of the MOM-ethers would enhance the chance of a selective transformation. Via LiAlH₄-induced reduction of ketone **63**, we obtained the corresponding alcohol **64** as a mixture of two diastereomers. We again applied CCl₄/PPh₃ and DEAD/PPh₃ in combination with ZnCl₂ and LiCl, but as it had been the case with alcohol **54**, we ended up with either no conversion or elimination. Considering the presumably pretty same susceptibility to the formation of an extended conjugated double bond system as it was encountered for compound **54**, we had somehow expected this outcome and turned our attention towards the alternative pathway of chlorination via the vinyl triflate **66**. Much to our regret, also in this attempt we found ourselves confronted with the same problems as we had experienced previously. Instead of affording the triflate, all applied reagents first attacked the silyl ether and in further consequence also the benzylic ethers, resulting in unusable varying product mixtures. Also in this case, an attempted *in situ* chlorination failed (see Figure 77).

Apparently, ketone **63** still offers too many concurring reaction sites for triflating reagents, rendering a selective conversion into vinyl triflate **66** virtually impossible. We therefore assess the two different pathways that were described within the last sections, as rather unrewarding options to achieve the preparation of clomiphen metabolite **CM 3**. Our developed strategy of two-step α -arylation starting from acetophenone was indeed proven to be an excellent way for the preparation of different triarylketones, but the difficulties, encountered in the course of subsequent transformations, lead us to the conclusion that these compounds most likely are not the appropriate key structures in the process of synthesizing **CM 3**.

The development of a new synthetic pathway for the preparation of target structure **CM 3** would have exceeded the scope of this Ph.D-thesis, but to assess whether it would principally be worth it, we compared the crude mixture, provided by SOCl₂ treatment of alcohol **54**, with an excretion sample obtained after the oral administration of clomiphen. As already explained in section 4.2, subsection of alcohol **54** to SOCl₂-mediated chlorination entailed a number of different reactions. Via LC-MS analysis of the crude mixture we also detected traces of a product exhibiting *m/z* 440, most probably resulting from concomitant chlorination and cleavage of both MOM-ethers resulting in our target metabolite **CM 3**.



^a chlorination reagents: CCl₄/PPh₃, LiCl/PPh₃/DEAD, ZnCl₂/PPh₃/DEAD

^b reagents for triflation: PhN(Tf)₂; Comins' reagent; (Tf)₂O

^c reagents for chlorination: KCl, KF, Pd₂(dba)₃/*t*-BuBrettPhos; LiCl, RuCl₃·3H₂O, Zn

Figure 77 Synthesis of alcohol **64** and attempts to obtain chlorides **89** and **65**.

Accordingly, we compared the product ion scan performed on m/z 440 for the urinary metabolite with that of our crude mixture and indeed found a match. As depicted in Figure 78, the retention times as well as the abundant product ions were nearly the same, indicating very clearly that **CM 3** most likely indeed represents the major metabolite of clomiphen, predominant in urine specimens.

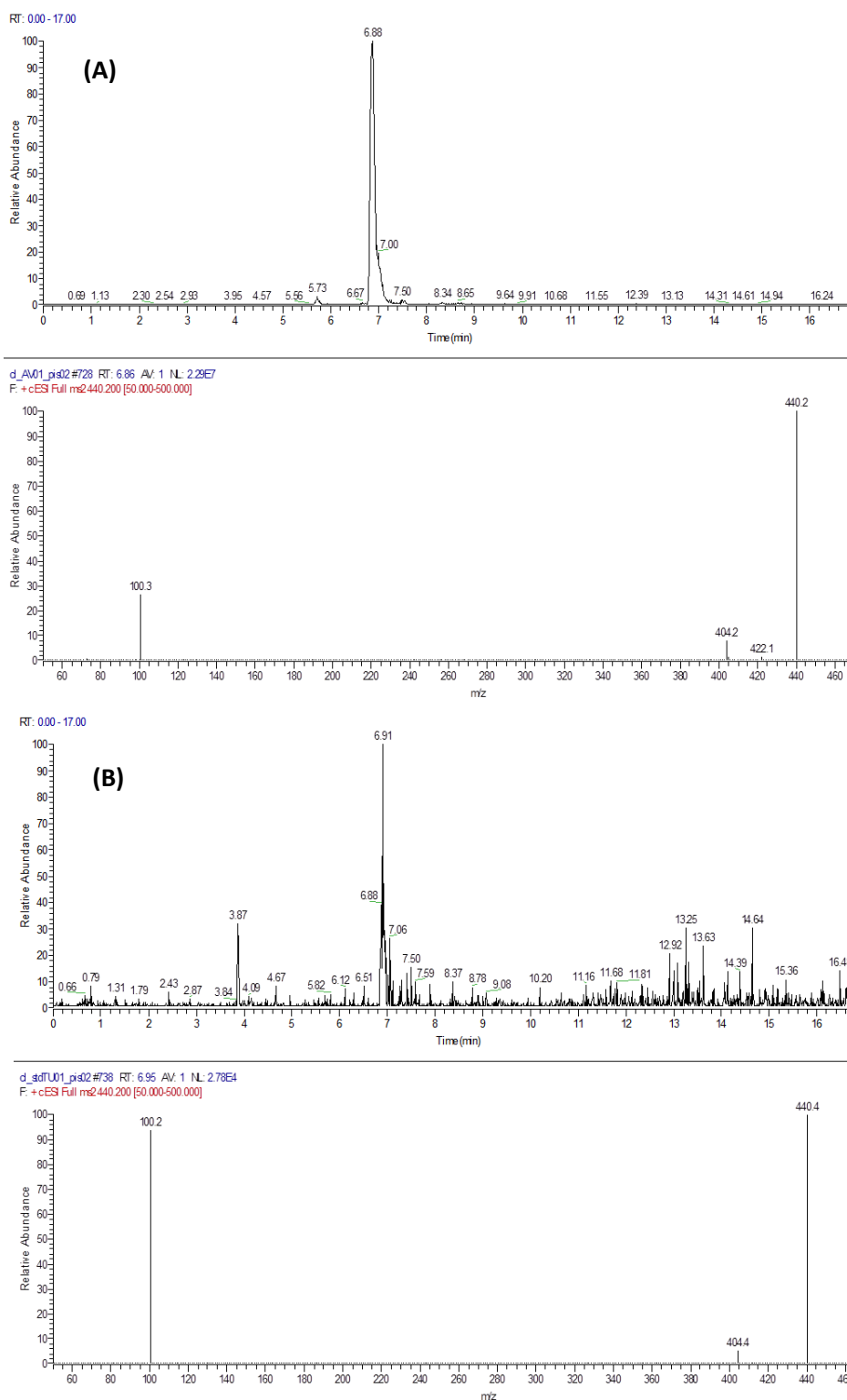


Figure 78 Comparison of product ion scans performed on m/z 440 for urinary metabolite (A) and the crude mixture obtained from SOCl_2 treatment of triarylketone **53** (B).

5. Results and Discussion - Simulation of drug metabolism via metabolic model systems

Drug metabolism is categorized into phase I and phase II metabolism. Whereas phase I metabolism primarily involves functionalization of nonpolar molecules providing them with higher hydrophilicities (oxidation, reduction, hydrolysis), phase II metabolism mainly consists in conjugation reactions (glucuronidation, sulfation, glutathione conjugation, acetylation and methylation). Due to the fact that phase I metabolites may also carry pharmacological or toxicological activities, their formation in the course of enzymatic biotransformations after drug administration is of great interest during the development of new pharmaceuticals. For this reason a variety of different model systems has been developed, capable of predicting the metabolic fate of drug candidates in the human body to variable extents.

The predominant phase I reactions in drug metabolism are oxidations, mediated by enzymes of the cytochrome P450 (CYP450) superfamily. These are membrane-bound heme-containing monooxygenases, which catalyze the incorporation of one oxygen atom from molecular oxygen into a substrate, while the other oxygen atom is reduced by two electrons (usually provided by the coenzyme NADPH) to give water. The active site of CYP450 enzymes contains an iron protoporphyrin IX with cysteine as fifth ligand and a sixth coordination site that is available for the binding and activation of molecular oxygen. Figure 79 illustrates the overall oxidation process taking place at the active site of CYP450. In the resting state of the enzyme (**A**) the sixth coordination site is occupied by water. Substrate binding and uptake of one electron leads to Fe(II) intermediate **C**, which consecutively binds molecular oxygen. After the uptake of one further electron, a nucleophilic Fe(III) peroxo complex (**E**) is formed that is converted into the hydroperoxide intermediate **F** by protonation. A second protonation step leads to the electrophilic Fe(IV) oxo species **G** that is considered to be the active oxidant. Release of the oxidized substrate causes reformation of the resting state (**A**). In the case of single electron donors instead of molecular oxygen, the intermediates **C – F** are bypassed by the so-called “peroxide shunt”.¹³⁵

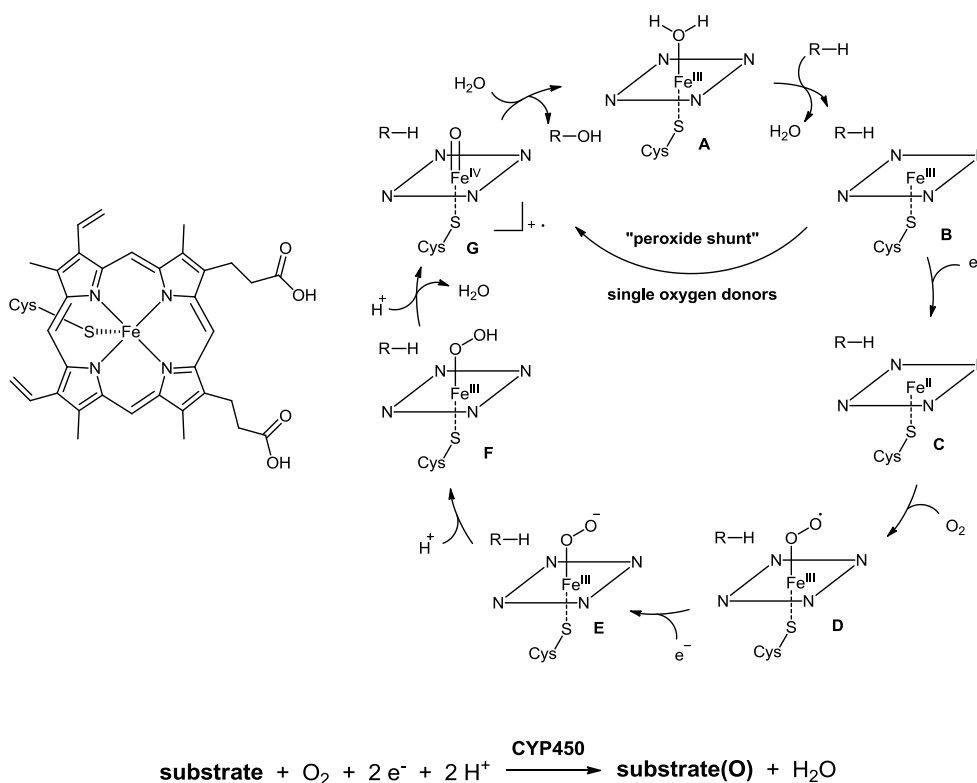


Figure 79 Catalytic cycle of oxidation at the active site of CYP450 (protoporphyrin IX).¹³⁵

Methods for the simulation of these metabolic reactions reach from relatively simple nonenzymatic model systems via more complicated *in vitro* models through to *in vivo* studies on animals. A rough rule that applies to all systems is that, whereas the complexity is directly related, the practicability is inversely related to the transferability to the *in vivo* situation in the human body. Thus, the treatment of drugs with common chemical oxidants is easy practicable, but the *in vitro-in vivo* correlation is rather low. On the other side, *in vivo* studies on animals are extremely labour-intensive, but exhibit the highest transferability to the human metabolism.

5.1. Nonenzymatic biomimetic model systems

Very common metabolic model systems that are often described in literature are chemical Fenton systems, based on the Fenton oxidation. According to Fenton's discovery in 1894, that tartaric acid in the presence of ferrous salts and H_2O_2 is oxidized to dihydroxy maleic acid, "Fenton's reagent" is nowadays defined as mixture of H_2O_2 and a ferrous salt, capable of oxidizing a variety of organic substrates.¹³⁶ Although Fenton chemistry has been known for over a century by now, the complete mechanism of the Fenton reaction and the identity

of the oxidizing intermediates are still under discussion.¹³⁷ Figure 80 illustrates a simplified reaction principle. Due to a single electron transfer from Fe^{2+} to H_2O_2 , Fe^{2+} is oxidized to Fe^{3+} , whereas one oxygen atom is reduced to one hydroxyl ion. In the course of this redox process one hydroxyl radical is released. This highly electrophilic species is capable of initiating various reactions with organic substrates, such as addition to unsaturated systems or hydrogen atom abstraction.

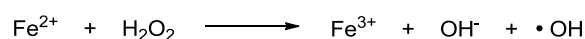


Figure 80 Principle of the Fenton reaction.

Especially the kinetics and reaction dynamics of aromatic hydroxylations are subject of many publications. In the course of their investigations on hydroxylations of benzenoid compounds by Fenton's reagent, in 1969, Norman and coworkers discovered that the addition of copper(II) ions markedly increases the yield of oxidation products.¹³⁸ This positive effect was explained by the effective oxidation of the hydroxyl radical **A** to give phenol (**B**), as it is illustrated in Figure 81. Furthermore it was found that higher yields are obtained when conducting the experiments under inert gas atmosphere. Contrary to what was assumed before, the presence of oxygen decreases the yields of hydroxylation products by promoting the formation of polyoxygenated byproducts (**C**).¹³⁹ Instead of H_2O_2 also other oxidants can be used for aromatic hydroxylation. Peroxydisulfate was found to form $\text{SO}_4^{\cdot-}$ radicals upon the reaction with Fe^{2+} . These radicals oxidize aromatic substrates to radical cations, which can undergo hydration to hydroxycyclohexadienyl radicals (**A**). In the presence of Cu^{2+} further oxidation occurs to give the same phenolic products (**B**) as obtained by the usage of H_2O_2 .¹⁴⁰

Early works in the field of drug metabolism simulation via Fenton systems were presented by the groups of Van der Steen¹⁴¹ and Zbaida¹⁴². They showed that Fenton's reagent is capable of mimicking hydroxylation, *N*-dealkylation and *S*-oxidation of drugs, similar to enzymatic conversions. More recent publications in this field showed that Fe^{2+} ions can be generated *in situ* by the application of an Fe(III) salt and a reductive agent, such as ascorbic acid or *N,N,N',N'*-tetramethylphenylenediamine (TMPD). This approach enables the permanent regeneration of Fe^{2+} , so that only catalytic amounts of iron are needed.¹⁴³ This effect may

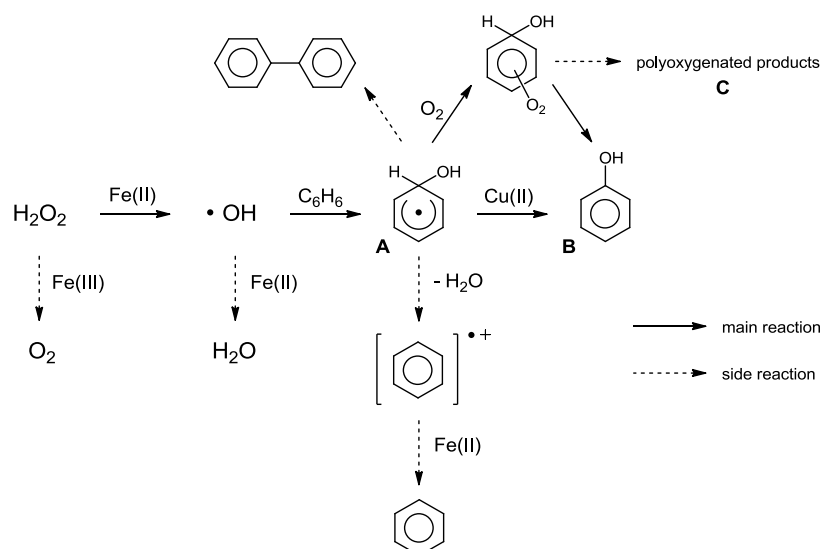


Figure 81 Possible side reactions in the Fenton hydroxylation of benzene.¹³⁹

also be obtained electrochemically by the reduction of Fe^{3+} at a working electrode. The corresponding field of electrochemical assisted Fenton reactions is often referred to as “EC-Fenton chemistry”. State of the art are on-line EC-Fenton-LC-MS systems that facilitate the direct on-line analysis of oxidation products subsequently to their formation in a flow reactor.^{143b,144}

Apart from EC-Fenton systems, there are also electrochemical (EC) systems in use as simulation techniques in drug metabolism studies. Whereas the first anodic oxidations of drugs were performed in off-line EC batch reactors, nowadays on-line EC-(LC)-MS devices are the systems of choice. The major advantage of electrochemical generation of metabolites over other methods is the rather simple integration of the oxidation reaction into the instrumental device that is required for analysis. Although this method is not capable of simulating the complete spectrum of CYP450-mediated metabolic reactions adequately, its instrumental simplicity makes it to an interesting option for future high-throughput screenings in pharmaceutical industry.¹³⁵

A third option for the nonenzymatic simulation of drug metabolism is represented by metalloporphyrin systems. These are metalloorganic complexes that mimic the active site of CYP450 enzymes (see Figure 79). By the addition of single oxygen donors, a reactive species similar to the radical Fe(IV) oxo species **7** is formed that can insert oxygen into substrates. Typical systems consist of porphyrin or porphine complexes with iron, manganese or chromium ions, together with oxygen donors such as H_2O_2 , NaClO , periodates or amine-*N*-oxides.¹⁴⁴

5.1.1. Simulation of clomiphene metabolism via nonenzymatic model systems

Considering all the synthetic efforts that had been made for the preparation of clomiphene's major metabolite, just to come to the conclusion that the synthesized target structures did not coincide with the corresponding urinary product, we decided to approach this project from another side. By the application of a metabolic model system, we envisioned the preparation of the relevant metabolites in amounts that would be sufficient for LC-SPE-NMR/MS analysis. Although we were aware of the already mentioned inverse practicability - transferability relation regarding metabolic model systems, we thought that it would be worth a try to start with the simple treatment of clomiphene citrate with common oxidants. Beside H_2O_2 and *t*-BuOOH, we also applied trifluoroacetic peracid, which was *in situ* generated by the reaction of trifluoroacetic acid with H_2O_2 or *m*-CPBA. As these reagents had been successfully applied for the aromatic hydroxylation of thiophenes¹⁴⁵, we thought that they might also be applicable for the hydroxylation of clomiphene. All experiments were monitored via TLC and in the case of conversion, the formed products were analyzed via LC-MS. Whereas treatment with $\text{CF}_3\text{COOH}/\text{H}_2\text{O}_2$ yielded no products, the application of $\text{CF}_3\text{COOH}/m\text{-CPBA}$ as well as of H_2O_2 and *t*-BuOOH gave the clomiphene-*N*-oxide **CM 4** (as a mixture of (*E*)- and (*Z*)-isomer) and the deschloro-hydroxyclophiphen **CM 5** (see Figure 82). The retention times of both substances did not coincide with the target urinary metabolite's.

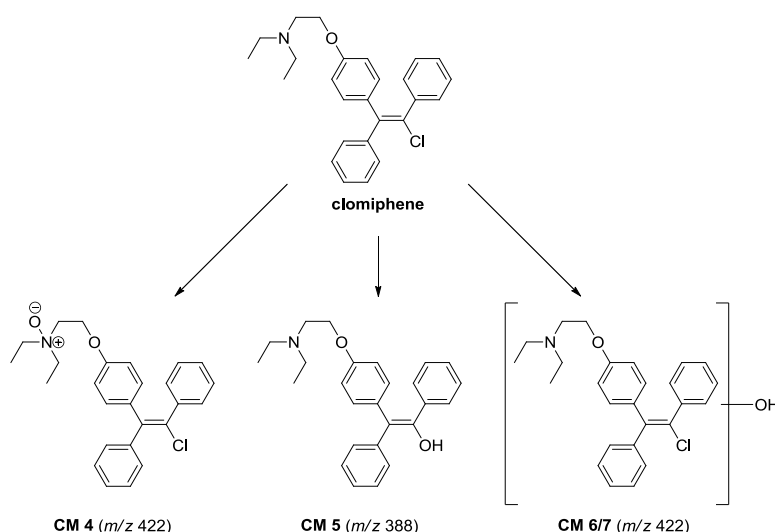


Figure 82 Oxidation products obtained via chemical model reactions.

Additionally to common oxidants, we also screened various Fenton systems for their potential applicability as metabolic model reactions. According to a procedure of Zbaida *et al.* we tested different combinations of $\text{FeCl}_2 \times 4\text{H}_2\text{O}/\text{FeSO}_4 \times 7\text{H}_2\text{O}$ and $\text{H}_2\text{O}_2/t\text{-BuOOH}$ in aqueous reaction media.¹⁴² To assess the reactivity in organic solvents, one reaction was performed in DCM using anhydrous FeSO_4 .¹⁴¹ Since all these experiments failed in terms of no conversion, we tested various additives for their potential to enhance aromatic hydroxylation. Whereas the extension of the original Fenton system by EDTA showed to have no effect on yields, the addition of ascorbic acid, CuSO_4 and TMPD efficiently promoted the formation of products.^{139,140,143} Additionally to the already detected deschloro-hydroxy-clomiphene **CM 5**, two different hydroxy-metabolites **CM 6** and **CM 7** were formed in all conducted experiments. Due to four different peaks with 422 *m/z*, we assume the formation

Table 8 Results of clomiphene oxidation via nonenzymatic biomimetic model reactions.

entry	oxidant	Fe-salt	additives	products
1	H_2O_2 (6 equiv)	-	-	CM 4, CM5
2	<i>t</i> -BuOOH (6 equiv)	-	-	CM 4, CM5
3	H_2O_2 (0.2 equiv)	-	CF_3COOH (3 equiv)	no conv.
4	<i>m</i> -CPBA (0.2 equiv)	-	CF_3COOH (3 equiv)	CM 4, CM5
5	H_2O_2 (4 equiv)	$\text{FeCl}_2 \times 4\text{H}_2\text{O}$ (2 equiv)	-	no conv.
6	H_2O_2 (4 equiv)	$\text{FeSO}_4 \times 7\text{H}_2\text{O}$ (2 equiv)	-	no conv.
7	<i>t</i> -BuOOH (4 equiv)	$\text{FeCl}_2 \times 4\text{H}_2\text{O}$ (2 equiv)	-	no conv.
8	H_2O_2 (2 equiv)	$\text{FeSO}_4 \times 7\text{H}_2\text{O}$ (1 equiv)	-	no conv.
9	H_2O_2 (2 equiv)	$\text{FeCl}_2 \times 4\text{H}_2\text{O}$ (1 equiv)	-	no conv.
10	H_2O_2 (2 equiv)	FeSO_4 (anhydrous) (2 equiv)	-	no conv.
11	H_2O_2 (5 equiv)	$\text{FeCl}_2 \times 4\text{H}_2\text{O}$ (5 equiv)	EDTA (5 equiv)	no conv.
12	H_2O_2 (2 equiv)	$\text{FeCl}_2 \times 4\text{H}_2\text{O}$ (1 equiv)	EDTA (1 equiv)	no conv.
13	H_2O_2 (10 equiv)	FeCl_3 (1 equiv)	EDTA (1 equiv), <i>L</i> -(+)-ascorbic acid (5 equiv)	CM 4, CM5, CM6, CM7
14	H_2O_2 (2 equiv)	$\text{FeSO}_4 \times 7\text{H}_2\text{O}$ (1 equiv)	CuSO_4 (3 equiv), H_2SO_4 (5 equiv)	CM 4, CM5
15	H_2O_2 (10 equiv)	FeCl_3 (1 equiv)	TMPD (1 equiv), H_2SO_4	CM 4, CM5, CM6, CM7
16	$\text{K}_2\text{S}_2\text{O}_8$ (2 equiv)	$\text{FeSO}_4 \times 7\text{H}_2\text{O}$ (1 equiv)	CuSO_4 (3 equiv), H_2SO_4 (5 equiv)	CM 4, CM5, CM6, CM7

of two different hydroxylated products, each present as a mixture of (*E*)- and (*Z*)-isomer. Nevertheless, none of them had the same retention time as the target urinary metabolite, so we did not investigate the precise structures of the generated oxidation products in further detail. Table 8 summarizes the results of all nonenzymatic biomimetic model reactions.

5.2. *In vitro* model systems

Considering the liver's predominant role in the biotransformation of xenobiotics, *in vitro* model systems for the evaluation of drug metabolites are commonly based on CYP450 enzymes originating from the liver. Studies on isolated perfused animal liver in this regard exhibit the best *in vitro-in vivo* correlations, however, this method is characterized by some significant disadvantages, such as extremely high labor intensity and poor reproducibilities due to the relatively short functional integrity of the abstracted organ. Liver slices for the most part still exhibit the intact cellular system, but their handling also requires specific techniques and expensive equipment. The use of primary hepatocytes (liver epithelial cells) for the simulation of drug metabolism is very well established. They are commercially available in cryopreserved form, retaining the activities of most phase I and phase II enzymes. However, they are very sensitive to cell damage and therefore rather difficult to handle. A good compromise between labor intensity and transferability to the human metabolism can be attained by the application of liver homogenates. Although the liver architecture gets destroyed by the homogenization process, they are still a rich source for all drug metabolizing hepatic enzymes. Differential centrifugation of liver homogenate gives cytosol, S9-fractions and microsomes. Among them, liver microsomes are the most popular source for drug metabolizing enzymes used for *in vitro* models. Compared to the previously described methods, they are rather easy in handling and relatively inexpensive. There are inter-individual variations in their activity, but this can be easily compensated by the use of pooled human liver microsomes. Although they are not able to simulate the full spectrum of CYP450-catalyzed reactions, they provide a fast survey over possible metabolic products and represent one of the best characterized *in vitro* models for the research of drug biotransformations.^{135,146}

5.2.1. Simulation of clomiphenes metabolism via *in vitro* human liver microsomal incubation

Since our attempts to generate clomiphenes predominant metabolite in the course of biomimetic model reactions so far had not been successful, we turned away from nonenzymatic systems and focused our attention on *in vitro* methods. Considering all the advantages of human liver microsomal incubation over other enzymatic systems, we regarded this method as reasonable starting point. As already mentioned above, HLMs account for the most popular *in vitro* model, accordingly there is a vast amount of literature dealing with HLM-induced drug biotransformations. Applications include metabolite identification, comparison of metabolism by different species, prediction of *in vivo* clearance and reaction phenotyping. For the characterization of drug metabolites obtained via HLM-incubation, LC-MS(-MS) is usually the method of choice¹⁴⁷, but due to its deficiencies with regard to the unequivocal assignment of molecular scaffolds (see 1.4.3), the use of off-line and on-line NMR analysis is on the rise.^{20,22b,148}

To check whether clomiphenes metabolite predominant in GC-MS measurements is formed in the course of microsomal incubation, we set up an initial experiment using 10 μ M clomiphenes citrate and 0.5 mg/mL HLM protein. Figure 83 illustrates the total ion currents (TICs) of the corresponding time-dependent GC-MS spectra in comparison to the TIC of a urine sample taken after the oral administration of clomiphenes citrate. After an incubation time of 23 hours, we observed an almost complete conversion of (*E*)-clomiphenes (**A**), whereas (*Z*)-clomiphenes (**B**) was not transformed. We indeed observed the formation of a metabolic product **MM 1** exhibiting the same retention time (t_R 14.57 min) as the urinary metabolite (**D**). Two additional metabolites were detected at t_R 14.90 min (**MM 2**, (**E**)) and t_R 15.21 min (**MM 3**, (**F**)). **MM 2**, which is even more abundant than the target compound, featured the same retention time as the already synthesized 4-hydroxy-derivative **CM 1** (see Figure 10), which was shown to be present in a urine sample, but only to a very small amount compared to the major metabolite.⁶⁸ From this observation the quantitative metabolite ratios seem to be sort of reverse to the *in vivo* situation.

With increasing incubation time a decrease in the concentration of the target metabolite was detected through to its complete disappearance after 23 hours. We ascribed this to further metabolic conversions, to which our target compound got subjected in the course of

progressing incubation time. According to this observation further optimization studies were required to find the optimum parameters for scale-up synthesis.

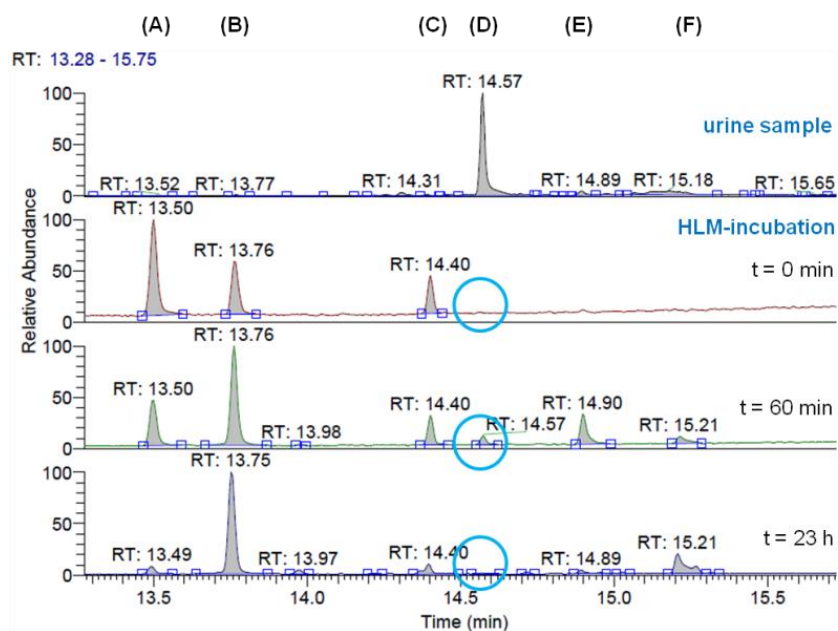


Figure 83 TIC comparison of a urine sample positive for clomiphene and HLM incubation after 0 min, 60 min and 23 h: (A) (E)-clomiphene, (B) (Z)-clomiphene, (C) compound originating from microsomal solution, (D) target microsomal metabolite **MM 1**, (E) microsomal metabolite **MM 2**, (F) microsomal metabolite **MM 3**.

Before we concentrated on the set-up of new experiments, it had to be clarified whether the *in vitro* generated metabolite and the observed urinary metabolite were the same. Based on the official WADA guidelines for the mass spectrometric detection and identification of molecules with masses less than 800 Da⁹⁵, the relative abundances of four diagnostic ions were compared (Figure 84, 86 *m/z* (A), 100 *m/z* (B), 478 *m/z* (C), 493 *m/z* (D)). Abundance values were determined from the peak areas of integrated selected ion chromatograms. Although the signal-to-noise ratios of the two least intense diagnostic ions are rather low ((C) and (D)), which is due to their natural low abundances and the relatively low metabolite concentration in the sample, the obtained almost identical values are a good index of the *in vitro* metabolite's authenticity.

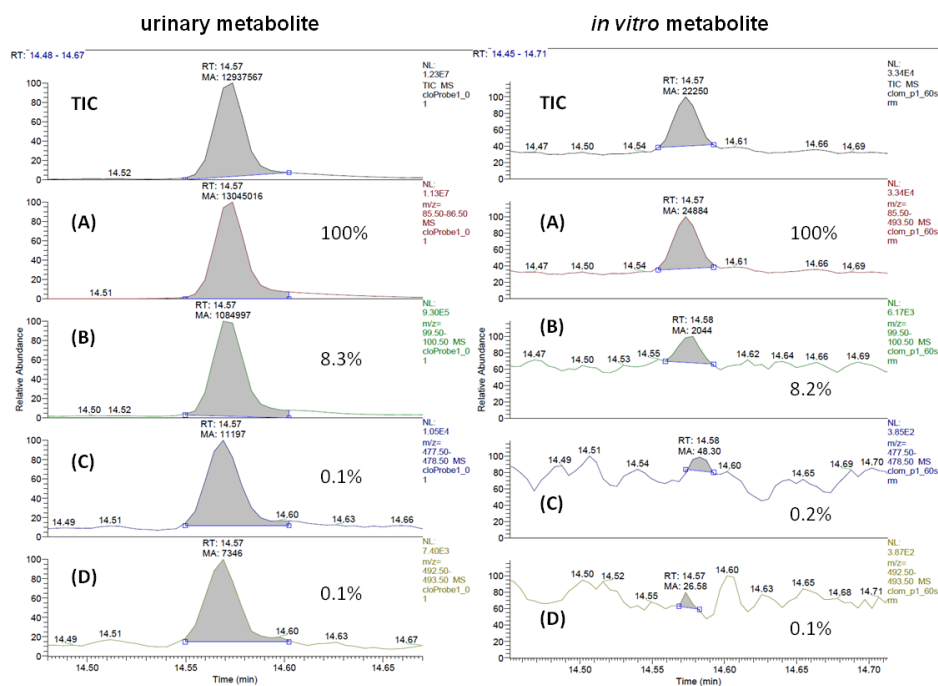


Figure 84 Extracted ion chromatograms of a urine sample positive for clomiphene and of the *in vitro* metabolite: (A) m/z 86 extracted, (B) m/z 100 extracted, (C) m/z 478 extracted, (D) m/z 493 extracted.

Having proven its identity to the urinary metabolite, we turned our attention towards the optimization of relevant incubation parameters to target the maximum possible concentration of **MM 1**. For this purpose we conducted a series of 1 mL – scale experiments and varied the substrate concentration $c_{\text{clomiphene}}$ over a broad range of values at two fixed HLM concentrations c_{protein} (0.25 mg/mL and 0.5 mg/mL, see Table 9). We monitored the formation of **MM 1** via withdrawal of GC-MS samples at regular time intervals and determined for each experiment the time when the maximum concentration of **MM 1** was reached (t_{max}). Metabolite yields were estimated from integrated areas of corresponding peaks in the total ion currents. In view of the fact that (*Z*)-clomiphene had not been metabolized in preceding experiments – at least not to a substantial extent – we used it as reference for our calculations to estimate the yield of **MM 1** after the envisioned scale-up by the factor of 20. As illustrated in Table 9, we observed an increase in **MM 1** yield with increasing substrate concentrations $c_{\text{clomiphene}}$ at a fixed c_{protein} value. From a $c_{\text{clomiphene}}$ value of 100 μM on, the estimated yields remained quite constant and even the application of 8-fold $c_{\text{clomiphene}}$ had no more effect. With increasing $c_{\text{clomiphene}}$ we also observed a shift in the time of maximum **MM 1** concentration towards higher values.

Table 9 Optimization of reaction conditions for the *in vitro* - preparation of metabolite **MM 1**.

$C_{\text{protein}}/C_{\text{clomiphene}}$ [mg/ μ g]	C_{protein} [mg/mL]	$C_{\text{clomiphene}}$ [μ M]	t_{max} [h]	estimated yield after scale-up [μ g]
1:8	0.50	7	1.0	2
1:12	0.50	10	1.0	4
1:24	0.25	10	3.0	2
	0.50	20	1.5	4
1:36	0.25	15	3.5	4
	0.50	30	4.5	6
1:48	0.25	20	3.0	4
	0.50	40	4.5	8
1:120	0.25	50	15.0	13
	0.50	100	23.0	21
1:240	0.50	200	23.0	20
1:960	0.50	800	23.0	22

Figure 85 shows the isomer ratio of the parent compound as a function of incubation time for different concentrations of clomiphene. Due to the exclusive transformation of the (*E*)-isomer, we observed a rise in the (*Z*)/(*E*)-ratio followed by a flattening of the curve, indicating the end of the reaction. Whereas (*E*)-clomiphene was almost completely metabolized at 7 μ M clomiphene (signified by a high (*Z*)/(*E*) value after 23 hours), at 200 μ M the experiment ended with a 1:1 ratio. Applying 800 μ M clomiphene the (*Z*)/(*E*) ratio hardly changed, indicating a substrate overload of the protein.

Based on the results of this optimization study, the following conditions were selected for scale-up synthesis of metabolite **MM 1**: 167 μ M clomiphene and 0.5 mg/mL HLM protein. The selected substrate concentration should assure the maximum possible yield of target metabolite. A higher concentration would probably yield the same amount of **MM 1**, but would also give an unnecessarily higher amount of non-metabolized parent compound, which would hamper the separation process. The partial substrate overload of protein would repress further metabolic transformations of **MM 1**. For the preparation of **MM 1** in amounts sufficient for characterization, the optimized HLM-incubation was scaled up to a final volume of 5 mL and four of these 5 mL-scale experiments were conducted in parallel.

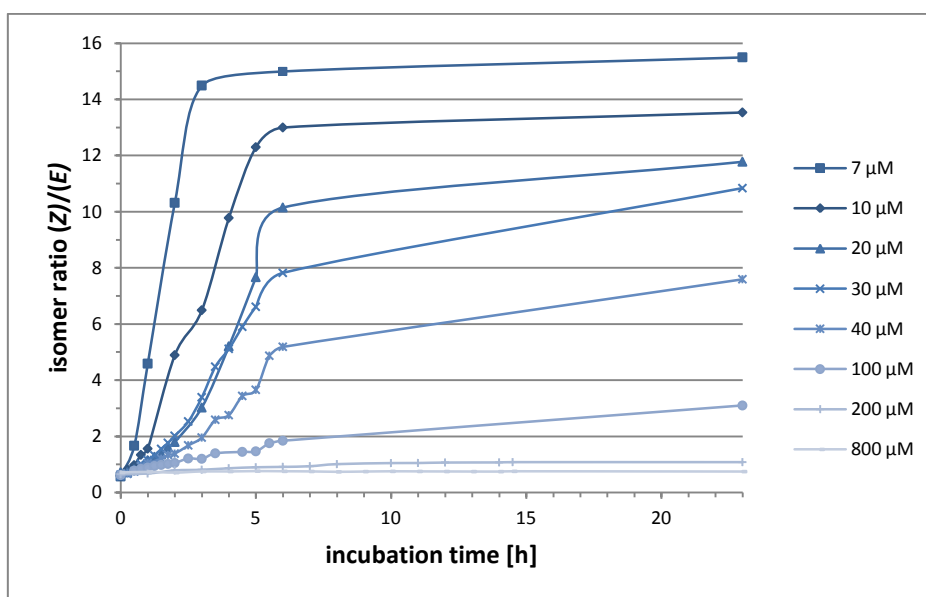


Figure 85 (Z)-/(E)-ratio of parent compound as a function of incubation time for different concentrations of clomiphe c_{clomiphe} at a fixed protein concentration c_{protein} of 0.5 mg/mL.

The total substrate amount of all conducted experiments was 2.0 mg. Based on the results of the prior optimization studies, we expected **MM 1** to be formed to a total amount of about 29 μg and **MM 2** (the most abundant microsomal metabolite) to about 135 μg .

5.2.2. LC-SPE-NMR/MS analysis of the enzyme extract

For the optimization of the envisioned on-line-separation-trapping process via LC-SPE-NMR/MS, an analytic sample of the enzyme extract was analyzed and compared to a urine sample. Figure 86 shows the corresponding extracted ion chromatograms. Different from the GC-MS chromatogram of the urine sample, which showed just one major metabolite (**A**) (see Figure 83), the LC-MS chromatogram indicated a second metabolite (**B**) that was even more abundant. This discrepancy between GC-MS and LC-MS is not unusual and can be ascribed to the different ionization techniques that were applied. Whereas GC-MS uses EI (electron ionization) featuring a very high degree of fragmentation, LC-MS applies ESI (electrospray ionization), which is regarded as a “soft” ionization technique leading to very little fragmentation. The relative abundances of ions depend on the ionization probabilities of the corresponding molecules, which in turn can be ascribed to the ionization method and the molecular structure. Thus, GC-MS- and LC-MS-profiles can sometimes differ to a large extent with regard to quantitative relations. Since **MM 2 (B)** featured the same retention time as the already synthesized 4-OH-clomiphe **CM 1** and

considering its mass spectrum, indicating a monohydroxy metabolite (see Figure 88), we expected that **MM 2** and **CM 1** were identical. If this assumption would prove to be true, then the previously synthesized hydroxy metabolite **CM 1** – contrarily to what had been assumed before – would be very well applicable as reference substance, if doping tests were conducted via LC-MS instead of GC-MS. To prove this theory, we planned to trap **MM 2** (**B**) additionally to our original target **MM 1** (**A**) for structure elucidation via NMR spectroscopy. Whereas **MM 2** was already detectable in the normal scanning mode, we had to enhance the sensitivity for the detection of **MM 1** by isolation of the molecular ion (440 m/z , see Figure 87) in the ion trap. This method allows for the exclusive detection of specific ions instead of scanning a whole mass range resulting in a significant enhancement of sensitivity.

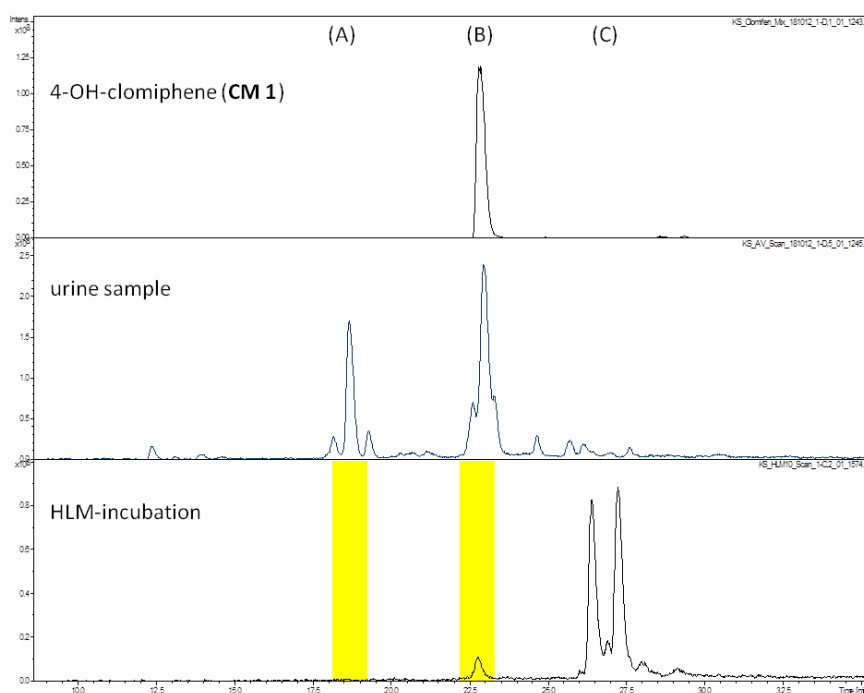


Figure 86 LC-MS chromatograms of 4-OH-clomiphene, urinary sample and enzyme extract: (A) target metabolite **MM 1** (**CM 3?**), 440 m/z ; (B) **MM 2** (4-OH-clomiphene **CM 1?**), 422 m/z ; (C) clomiphene isomers.

The enzyme extract from the scale-up experiment was dissolved in the mobile phase to obtain 475 μL of sample solution that was consecutively injected in five 95 μL -portions into the LC-device. The trapping process of **MM 1** and **MM 2** was controlled manually via monitoring the corresponding isolated molecular ions (440 m/z and 422 m/z) and for each metabolite five cumulative trappings on C18 HD cartridges were performed.

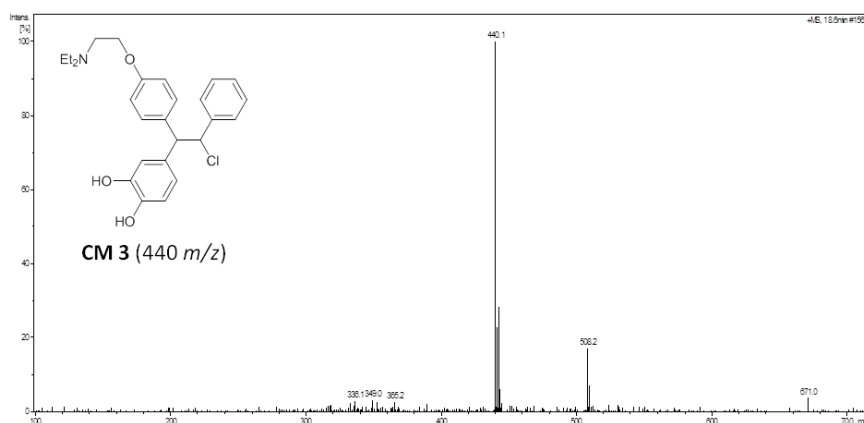


Figure 87 Mass spectrum of target metabolite **MM 1 (A)** and assumed structure **CM 3**.

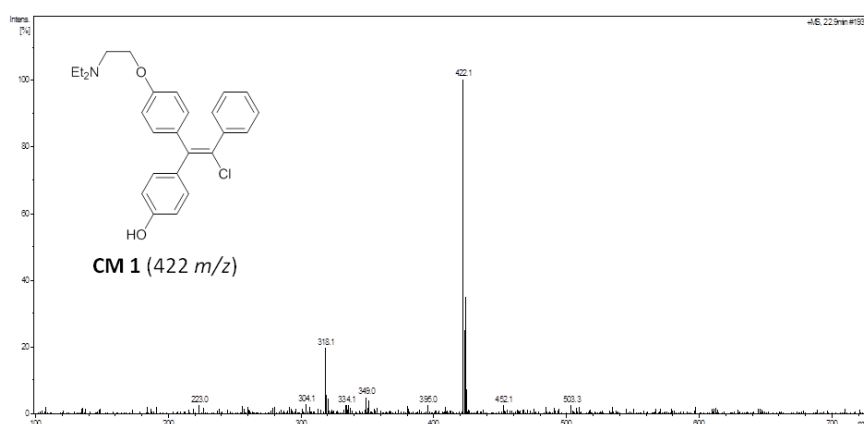


Figure 88 Mass spectrum of **MM 2 (B)** and assumed structure **CM 1**.

Despite all our efforts, the isolated amount of **MM 1** was in the end too low for $^1\text{H-NMR}$ analysis. We had hoped to prove hydrogenation of the double bond via the corresponding characteristic proton signals that should be clearly visible as two doublets, but unfortunately we could not manage to get significant spectra with our current equipment. Nevertheless, **MM 2** could be isolated in amounts sufficient for $^1\text{H-NMR}$ analysis. Additionally to an ^1H -spectrum, an $^1\text{H}, ^1\text{H-COSY}$ spectrum was recorded and all collected data was compared to NMR data of the synthetic hydroxy metabolite **CM 1**. Figure 89 shows the ^1H -spectra of the isolated metabolite **MM 2 (A)** in comparison to **CM 1** measured under normal conditions (**C**) and **CM 1** measured under the same conditions as were applied for the SPE measurement of **MM 2 (B)**. NMR acquisition of compounds from SPE cartridges requires suppression of residual solvent signals arising from the mobile phase used for LC separation. This solvent suppression can also affect signals with resonance frequencies in the immediate vicinity of the solvent signals. We could observe this impact for the methylene protons next to the resonance frequency of MeOH. To enable a direct comparison between **MM 2** and **CM 1**, it

was necessary to measure **CM 1** under the same conditions as were applied for **MM 2**. Accordingly spectrum **B** was obtained from a very low concentrated sample of **CM 1** using MeOH- and water suppression. As expected, we could observe a diminution of the methylene protons close to the methanol signal to a significant degree.

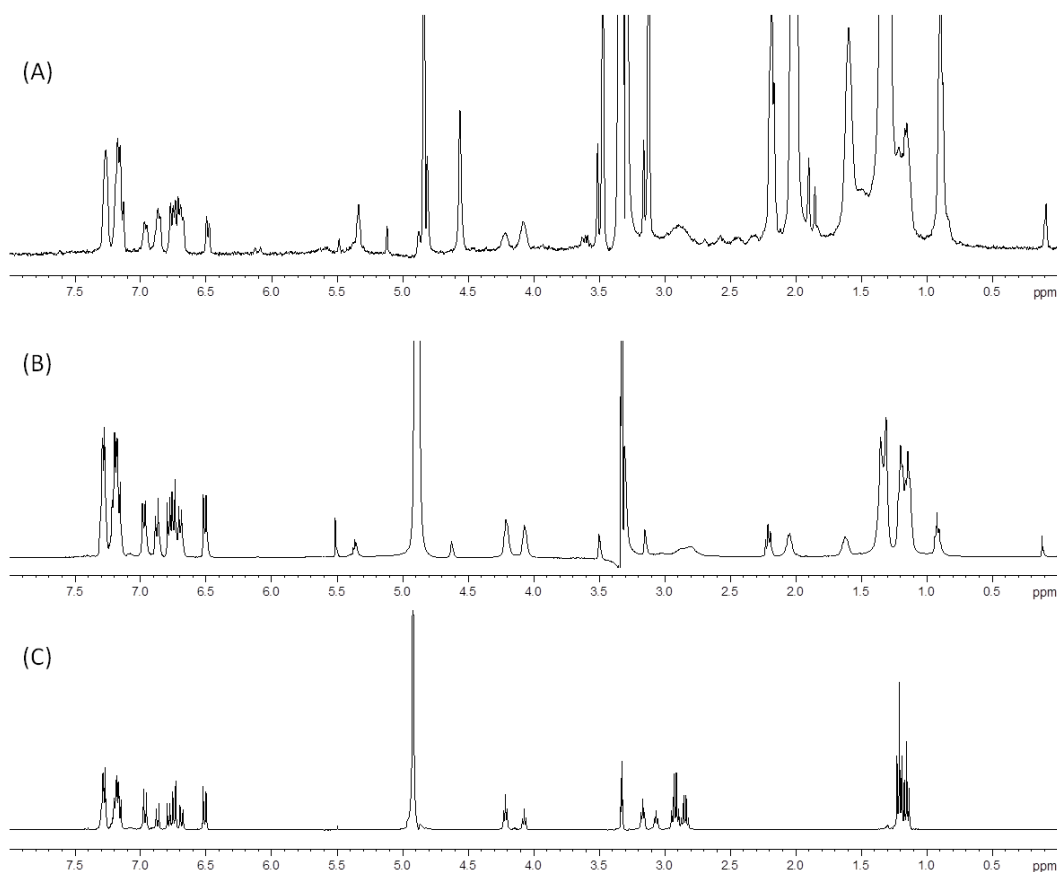


Figure 89 Comparison of ¹H-NMR spectra: (A) **MM 2** isolated from enzyme extract, (B) 4-OH-clomiphene (**CM 1**) measured under SPE conditions, (C) 4-OH-clomiphene (**CM 1**) measured under normal conditions.

Additionally to ¹H spectra also ¹H,¹H-COSY spectra of **MM 2** were recorded. Figure 90 shows the aromatic region of **MM 2** (A) in comparison to that of the already synthesized reference substance **CM 1** (B). Like the 1D spectra, also the cross peak patterns of the 2D spectra were shown to be identical, leaving no doubt that the isolated metabolite, generated by microsomal incubation, was 4-OH-clomiphene (**CM 1**). Interestingly, **MM 2** was shown to be present as a mixture of its (*E*)- and (*Z*)-isomer, just like the reference substance **CM 1**. Apparently also the (*Z*)-isomer of clomiphene got hydroxylated to some extent in the course of microsomal incubation.

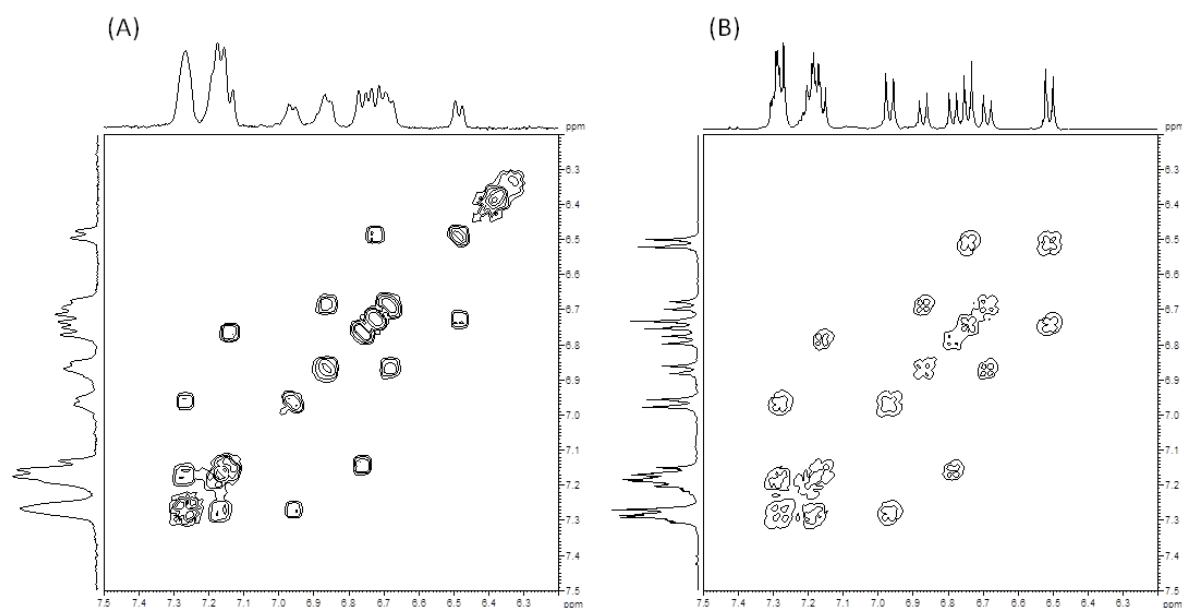


Figure 90 Comparison of $^1\text{H},^1\text{H}$ -COSY spectra: (A) **MM 2** isolated from enzyme extract, (B) 4-OH-clomiphene (**CM 1**).

Considering the more or less unproblematic structural elucidation of **MM 2**, whereas it had not been possible to obtain significant spectra of **MM 1**, we were interested in the total amounts of metabolites that were finally transferred into the probehead of the NMR spectrometer. We therefore recorded reference spectra of **CM 1** using different dilution factors and compared them to the spectra that were obtained by SPE measurement. Based on these results we estimate the final amount of **MM 2** in the probehead to be about 50 μg , whereas **MM 1** had to be present to an amount of less than 10 μg . With regard to the estimated amounts of initially generated metabolites, this means a substance loss of about two thirds due to metabolite extraction, preparation of injection solution, separation process, trapping and elution from the cartridges into the NMR probehead. As most critical steps, we consider the separation process and the multitrapping procedure. Due to the higher amounts of substance that are needed for SPE-NMR analysis, the LC column needs to be overloaded, resulting in peak broadening and deterioration of separation performance compared to analytical runs. To exclude broad peak overlapping, the separation process therefore has to be carefully optimized prior to the conduction of semi-quantitative runs. The multitrapping procedure represents the second bottleneck of the process. To ensure efficient analyte retention on the cartridges, the nature of the solid phase material has to be chosen carefully, the flow rate of water added during trapping to the mobile phase has to be adjusted and the nature of the eluting deuterated solvent has to be defined. Also the

number of repeated trappings is important. At some point a steady-state is reached, when the cartridge is saturated with analyte and already trapped material gets washed away in the course of the next trapping cycle. Although we had initially optimized the multitraping and elution steps with small and defined quantities of **CM 1** to facilitate $^1\text{H-NMR}$ spectra with sufficient signal-to-noise ratio, a certain degree of material loss throughout the overall process had to be accepted.

In view of the above discussed results regarding the structure elucidation of clomiphene metabolites, it seems that we were operating quite at the limits of our LC-SPE-NMR/MS system. Whereas we succeeded in identifying **MM 2**, our equipment apparently was not powerful enough for generating significant $^1\text{H-NMR}$ spectra of **MM 1**. Due to the fact that energy differences between nuclear spin states and consequently the population differences are proportional to the applied magnetic field, the use of a stronger NMR magnet would be an obvious option to enhance the sensitivity of NMR experiments. In fact, our hyphenated device is limited to the magnetic field strength of the NMR spectrometer. Considering field strengths of modern state-of-the-art NMR magnets of 500 to 750 MHz, it is clearly visible that our 400 MHz magnet can be considered as the bottleneck of the system. A further option that is in use for the enhancement of signal output of NMR measurements is the application of cryogenic probeheads. By cooling the signal sender and receiver units with liquid helium down to 20 – 30 K, the signal loss between spectrometer and data processing unit is minimized. This leads to an improvement of the signal to noise ratio by the factor of four, which means a shortening of acquisition time by the factor sixteen. Of course, it shall not be overlooked that the suggested methods for performance enhancement are related to an instrumental and costly very high level of maintenance, but in return efforts are rewarded with sensationally low detection limits.^{22c}

6. CONCLUSION AND OUTLOOK

6.1. SARM metabolites

One of the aims of this Ph.D research was the synthesis of *O*-dephenylandarine (**8**, **AM 1**) and *O*-dephenylostarine (**13**, **OM 1**), two SARM metabolites relevant for doping control analysis. The approach, which was established to be the most efficient for the construction of the arylpropionamide core, was amide bond formation between epoxyacid **2** and the corresponding isocyanate, which had been *in situ* generated from anilines **4** and **9**. Based on this key step, two different synthetic routes were developed, enabling the synthesis of the two metabolites in their racemic forms as well as in their naturally occurring (*S*)-forms. The racemic metabolites have already proven to be valuable reference substances of utmost importance for the unequivocal proof of illicit andarine and ostarine administration by athletes.

6.1.1. Synthesis of racemic SARM metabolites

The racemic metabolites *rac*-**8** (**AM 1**) and *rac*-**13** (**OM 1**) were obtained after five reaction steps in overall yields of 28 and 31%, respectively (see Figure 91).

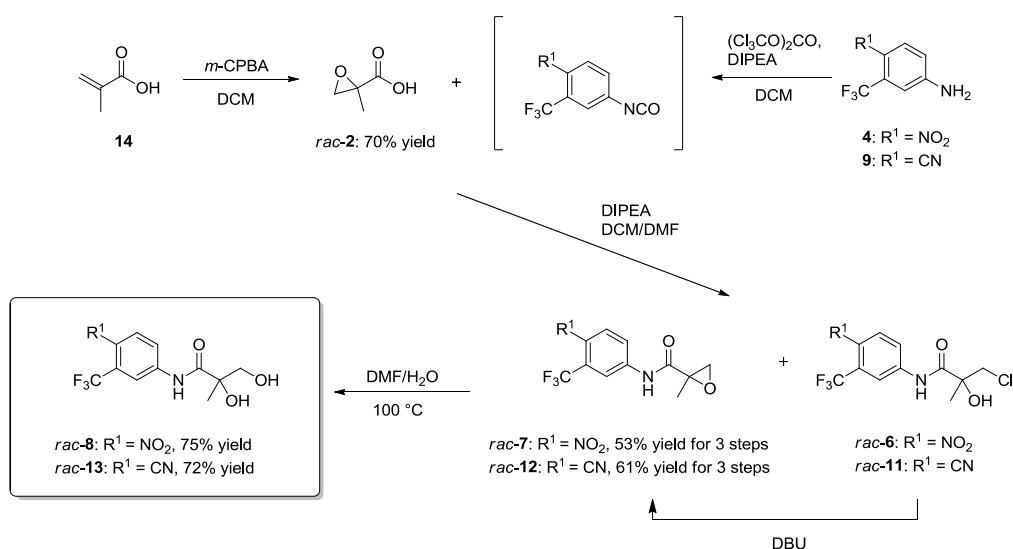


Figure 91 Synthesis of racemic *O*-dephenylandarine (*rac*-**8**, *rac*-**AM 1**) and *O*-dephenylostarine (*rac*-**13**, *rac*-**OM 1**).

6.1.2. Synthesis of enantiopure SARM metabolites

Slight modifications of the racemic procedure provided the enantiopure metabolites (*S*)-**8** (**AM 1**) and (*S*)-**13** (**OM 1**) after six reaction steps in 20 and 23% overall yield, respectively (see Figure 92).

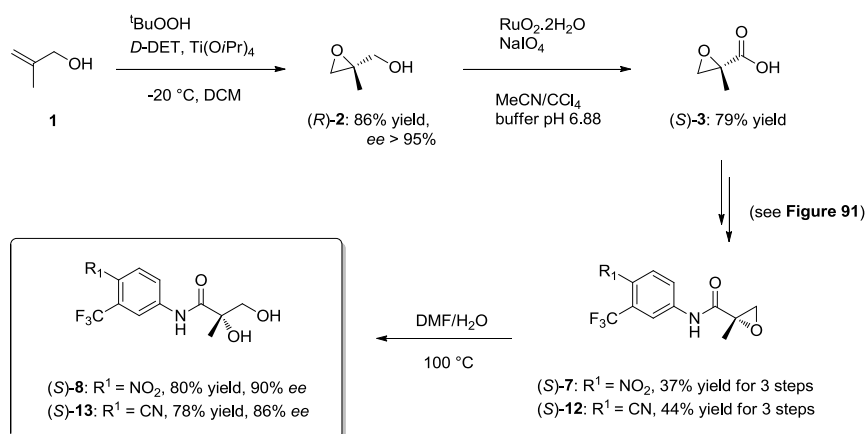


Figure 92 Synthesis of (*S*)-*O*-dephenylandarine ((*S*)-**8**, (*S*)-**AM 1**) and (*S*)-*O*-dephenylostarine ((*S*)-**13**, (*S*)-**OM 1**).

6.2. SERM metabolites

The second aim of this research was the synthesis of different clomiphene metabolites involving an evaluation of all synthesized compounds with regard to their applicability as reference substances for doping analysis. Whereas the actual structure of clomiphene's main metabolite, predominant in urine specimens, is not known, 4'-hydroxyclophene (**CM 2**) and 3,4-di-hydroxy-di-hydroclomiphene (**CM 3**) were chosen as possible target structures.

6.2.1. Synthesis of 4'-hydroxyclophene

For the synthesis of 4'-hydroxyclophene (**CM 2**), three different approaches were tested with regard to their usefulness. Whereas a McMurry coupling reaction and a Horner-Wadsworth-Emmons reaction proved to be rather unrewarding key steps to provide **CM 2**, the target compound was finally obtained via a regioselective trimethylstannyl lithiation of a diarylacetylene followed by a Negishi coupling and subsequent chlorination. According to the reaction scheme illustrated by Figure 93, **CM 2** was obtained in form of a product mixture in an overall yield of 34% and featuring a ratio between

(*E*)-4'-hydroxyclo MPHene (**CM 2**) and its regioisomer (*E*)-4-hydroxyclo MPHene (**CM 1**) of 3:1. Via comparison of this product mixture with an excretion sample, taken after the oral administration of clomiphene, it was clearly shown that **CM 2** was not the predominant metabolite and therefore is not applicable for doping control purposes.

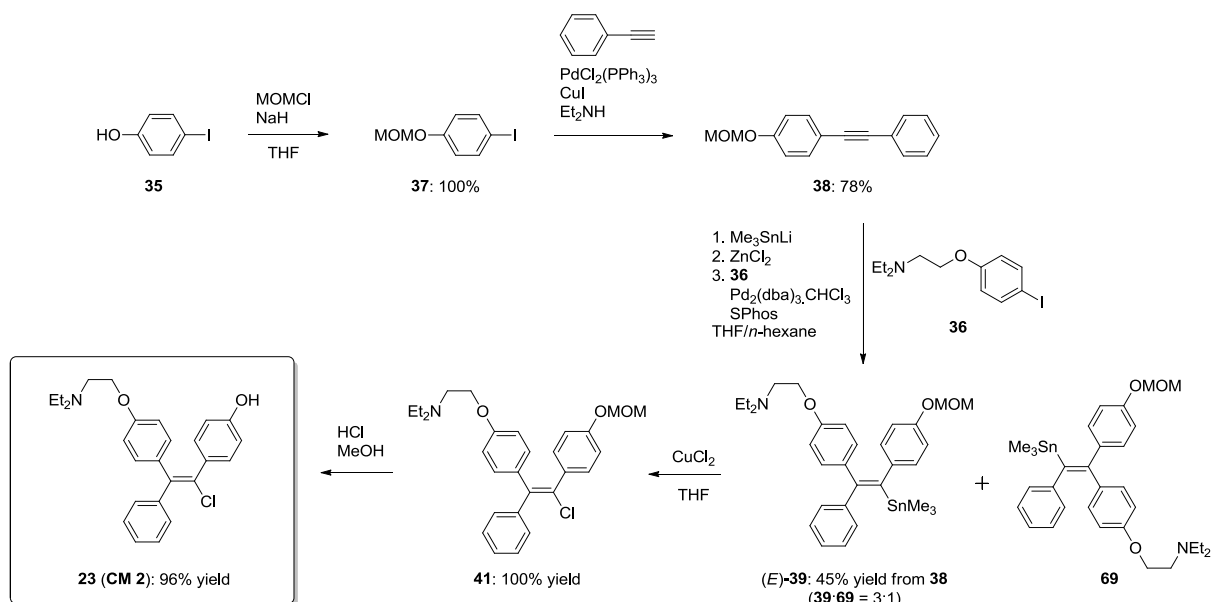


Figure 93 Synthesis of 4'-hydroxyclo MPHene (**23, CM 2**).

6.2.2. Synthesis of 3,4-di-hydroxy-di-hydroclomiphene

For the construction of the 1,2,2-triarylethane core structure of 3,4-di-hydroxy-di-hydroclomiphene (**CM 3**), a very efficient strategy based on two consecutive Pd-catalyzed α -arylation steps was developed, which enabled the preparation of compounds **53** and **63** in overall yields of 73% and 38%, respectively (see Figure 94). Unfortunately, these structures were shown to be not appropriate precursor substances leading to **CM 3**, because all attempts of triflation as well as of chlorination of the corresponding alcohols failed. Nevertheless, via comparison of a urine extract to a crude mixture containing traces of **CM 3**, it was shown that **CM 3** most probably represents the main metabolite of clomiphene, which is most abundant in GC-MS measurements and therefore is applicable as reference standard for doping analysis.

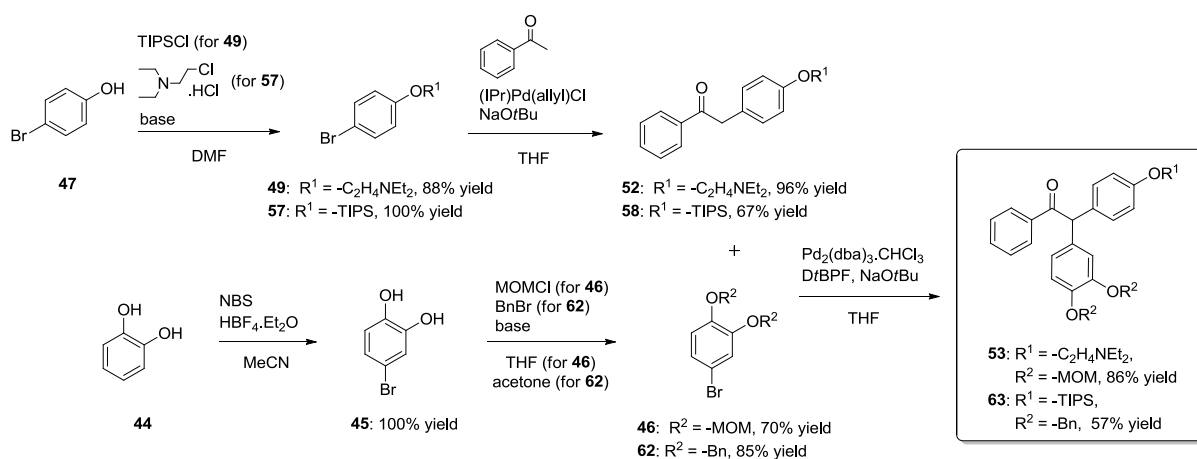


Figure 94 Synthesis of 1,2,2-triarylethanones **53** and **63**.

6.2.3. Simulation of clomiphen metabolism via metabolic model systems

Three different metabolic model systems were assessed regarding their ability to produce clomiphen's main metabolite in amounts sufficient for structure elucidation via LC-SPE-NMR/MS analysis. Whereas the application of common chemical oxidants and various Fenton systems was shown to be not useful in respect thereof, incubation of the drug with pooled human liver microsomes resulted in the formation of the desired target metabolite. Reaction scale-up resulted in the production of target compound **MM 1** in an amount of about 30 μg and in 140 μg of a second metabolite **MM 2**. Whereas the isolated amount of **MM 1** was in the end too low for NMR structure elucidation, **MM 2** was identified as 4-hydroxyclophen (CM 1) and was shown to be a useful reference substance for the detection of clomiphen abuse via LC-MS-based doping analysis.

7. EXPERIMENTAL SECTION

7.1. GENERAL METHODS

Chemicals and solvents

All purchased reagents and solvents were used without further purification unless otherwise specified. Dichloromethane, petroleum ether and ethyl acetate were distilled prior to use. Chloroform and carbon tetrachloride were passed through a column filled with basic aluminium oxide. Anhydrous toluene, methanol, diethyl ether and dichloromethane were purified in a *PureSolv*-solvent purification system from *Innovative Technology, Incorporation*. Anhydrous THF was distilled from sodium/benzophenone and degassed via the freeze-pump-thaw method. Triethylamine and *N,N*-diisopropylethylamine were stored over KOH and distilled from calcium hydride. Zinc chloride was flame-dried prior to use. 1,3-bis(2,6-diisopropylphenyl)imidazolium chloride (IPr.HCl) was prepared according to the literature¹⁴⁹. NADPH generating system for microsomal incubations was prepared by mixing *NADPH regenerating system solution A (BD Biosciences)* and *NADPH regenerating system solution B (BD Biosciences)* in a ratio of 5:1. Pooled human liver microsomes were also supplied by *BD Biosciences*.

Synthetic Methods

Oxygen- and moisture sensitive reactions were run in flame-dried reaction vessels under an argon atmosphere using standard Schlenk techniques. All reactions were stirred magnetically unless otherwise stated.

Thin-layer chromatography

All reactions were monitored using TLC silica gel 60 F₂₅₄ plates (*Merck*). UV active compounds were detected at longwave UV (254 nm). For visualization the following reagents were used: *Ceric(IV)sulfate* [0.1 g Ce(SO₄)₂, 4.5 g phosphormolybdic acid, 100 mL H₂SO₄ (10%)], *Potassium permanganate* [2 g KMnO₄, 40 g K₂CO₃, 1 g NaOH, 320 mL H₂O], *Anisaldehyde* [6 g anisaldehyde, 250 ml ethanol, 25 ml H₂SO₄ (conc.)] and *Sulfuric acid* (conc.).

Preparative column chromatography

Preparative flash chromatography was done manually using glass columns and compressed air or with an automated *Büchi Sepacore* flash chromatography system. In either case silica gel 60 (0.040 – 0.063 mm, 230 – 400 mesh, *Merck*) was used.

LC-MS(-MS)

Characterization of synthetic and urinary SARM metabolites was conducted on a LC-TSQ *Vantage* triple stage quadrupole mass spectrometer, equipped with an electrospray-interface. Product ion scans were performed on precursor ions m/z 307 (for compound **AM 1**) and m/z 287 (for compound **OM 1**). Chromatography was performed on a *Zorbax Eclipse XDB-C18* column (2.1 x 50 mm, particle size 3.5 μm) at a flow rate of 0.4 mL/min and as solvents 0.2% formic acid (A) and methanol, containing 0.1% formic acid, (B) were used (0 min, 100% A; 6.5 min, 0% A; 7.0 min, 0% A; 7.1 min, 100% A; 12 min, 100% A).

The characterization of clomiphene related compounds was performed on two different devices:

Method A: measurements were performed on an *Esquire/HCT* ion trap mass spectrometer from *Bruker Daltonics*, coupled to an *Agilent 1100 series* LC system via an electrospray interface. The separations were conducted at 25 °C on an *Agilent ZORBAX Eclipse XDB-C18* (150 x 4.6 mm, particle size 5 μm) LC column with a flow rate of 0.8 mL/min. The mobile phase consisted of 30% MeOH (A) in water (B) with 0.1% acetic acid added (0 min, 30% A; 25 min, 70% A; 38 min, 70% A; 40 min, 30% A; 45 min, 30% A).

Method B: measurements were conducted on a LC-TSQ *Vantage* triple stage quadrupole mass spectrometer, equipped with an electrospray-interface. The separations were performed at 25 °C at a flow rate of 0.2 mL/min on an *Agilent ZORBAX Eclipse XDB-C18* (50 x 2.1 mm, particle size 3.5 μm) LC column, using an *Agilent ZORBAX Eclipse XDB-C8* (2.5 x 2.1 mm, particle size 5 μm) precolumn. The mobile phase consisted of 30% MeOH (A) in water (B) with 0.1% formic acid added (0 min, 30% A; 10 min, 100% A; 15 min, 100% A; 15.1 min, 30% A; 20 min, 30% A).

GC-MS

GC-MS analysis was conducted on a *Thermo Finnigan DSQ II* quadrupole mass spectrometer directly interfaced to a *Trace GC Ultra 2000* gas chromatograph using a *Restek RTX - 1 ms*

(15 m x 0.25 mm i.d., 0.1 μm film thickness) capillary column. The oven program temperature was 174 $^{\circ}\text{C}$ //3 $^{\circ}\text{C}/\text{min}$ //209 $^{\circ}\text{C}$ //25 $^{\circ}\text{C}/\text{min}$ //304 $^{\circ}\text{C}$ (2 min).

NMR-Spectroscopy

NMR spectra were recorded on a *Bruker AC 200* at 200 MHz (50 MHz) or on a *Bruker AC 400* at 400 MHz (100 MHz, 377MHz). Chemical shifts are given in ppm and were referenced to the solvent residual peak(s)¹⁵⁰. Multiplicities are referred to as s (singlet), d (doublet), t (triplet), q (quartet), quin (quintet), sext (sextet), sept (septet), m (multiplet) and bs (broad singlet). Coupling constants are given in Hz.

Infrared-Spectroscopy

IR-spectra were recorded on a *Perkin Elmer Spectrum 65 FT-IR* spectrometer, equipped with a *MK II Golden Gate Single Reflection ATR* system.

Polarimetry

Optical rotations were measured on a *MCP 500* polarimeter (*Anton Paar*) in a 10 cm cell at 20 $^{\circ}\text{C}$ with 589 nm wavelength. The concentration *c* is given in g/100 ml.

Melting points

Melting points were determined on a *Kofler* hot-stage apparatus *MPA100* or on an automated melting point apparatus (*Stanford Research Systems*) and are uncorrected.

Microwave Synthesis

Microwave assisted reactions were run in a *Biotage Initiator* microwave synthesizer. For this purpose the reaction mixtures were transferred into a glass pressure microwave tube equipped with a magnetic stirring bar, sealed with a Teflon septum and exposed to microwave irradiation at the required temperature. The absorption mode was set to "Normal" for water/DMF mixtures and "Low" for THF.

High-resolution mass spectrometry

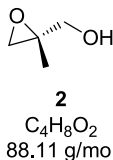
HRMS was performed on a *Shimadzu LC-IT-TOF-MS* system with ESI-interface.

HPLC-SPE-NMR/MS

The LC-SPE-NMR/MS system used was a completely hyphenated on-line system. The LC separations were performed on an *Agilent 1100 series* LC system equipped with a quaternary pump, a column oven, an autosampler and a diode array detector. The separations were conducted at 25 °C on an *Agilent ZORBAX Eclipse XDB-C18* (5 µm, 150 x 4.6 mm) LC column with a flow rate of 0.8 ml/min. The mobile phase consisted of 30% MeOH (A) in water (B) with 0.1% acetic acid added (0 min, 30% A; 25 min, 70% A; 38 min, 70% A; 40 min, 30% A; 45 min, 30% A). The post-column diluent (pure water, flow rate 3 mL/min) was delivered by a *Knauer K120* (isocratic pump). Injection volume was 100 µl. The eluate followed the flow path via a *BNMI Bruker Interface* to a *Prospekt II* automated SPE unit (*Bruker/Spark Holland*) under the control of *Bruker Hystar 3.2* software. Analyte trapping was done manually via an *Esquire/HCT* from *Bruker Daltonics*. Five cumulative trappings on *HySphere C18 HD* cartridges were performed. The *Esquire/HCT* was equipped with an electrospray interface as ion source and was operated with the following conditions: dry temperature 365 °C; nebulizer gas 30 psi; drying gas 11.0 L/min; capillary voltage -4000 V (pos), scan range 100 – 1000 *m/z* or isolation of relevant masses (440 or 422 *m/z*) via manual MS/MS. Compounds were eluted from the SPE cartridges with CD₃OD. The ¹H-NMR spectra were recorded on a *Bruker Avance Ultrashield 400* MHz NMR spectrometer equipped with a 60 µl TXI (¹H/¹³C/¹⁵N) flow probe. The spectra were calibrated to the residual solvent signal of CD₃OD at 3.31 ppm.

7.2. SYNTHESIS OF SARM METABOLITES

7.2.1. (2*R*)-(-)-2-Methyl-2,3-epoxy-1-propanol (**2**)



A suspension of 3 Å activated powder molecular sieves in anhydrous DCM (24 mL) was cooled to -35 °C, titanium tetraisopropoxide (0.098 mL, 0.33 mmol) and (-)-diethyl *D*-tartrate (0.072 μL, 0.42 mmol) were added and the resulting mixture was stirred for 30 min at -35 °C. After the dropwise addition of 2-methyl-prop-2-en-1-ol (**1**, 0.588 mL, 6.93 mmol) and a solution of 5.5 M *tert*-butyl hydroperoxide (1.90 mL, 10.45 mmol) via syringe, the mixture was stirred at -35 °C for 1 h and then at -20 °C for 27 h. A solution of potassium sodium tartrate, saturated with sodium chloride, was added (1 mL). After the mixture was stirred at ambient temperature for 3 h, excess *tert*-butyl hydroperoxide was destroyed by adding sodium peroxodisulfate (0.548 g, 2.30 mmol) and continuing stirring for 30 min. The resulting slurry was filtered over a pad of Celite and the filtrate was concentrated by evaporation. Chromatography on silica gel impregnated with TEA using pentane/Et₂O (1:1) → Et₂O provided **2** as a colourless oil (0.526 g, 86%, *ee* > 95%). The enantiomeric excess was determined by the Mosher ester method (see 7.2.5).

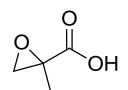
$[\alpha]_D^{20} = 8.7$ (*c* 0.460, DCM).

R_f (DCM/MeOH, 10:1) = 0.54.

¹H-NMR (200 MHz, CDCl₃): $\delta_H = 3.72$ (1H, d, *J* = 12.3 Hz, HO-CH₂), 3.59 (1H, d, *J* = 12.3 Hz, HO-CH₂), 2.91 (1H, d, *J* = 4.8 Hz, O-CH₂), 2.64 (1H, d, *J* = 4.8 Hz, O-CH₂), 1.93 (1H, bs, -OH), 1.35 (3H, s, Me).

¹³C-NMR (50 MHz, CDCl₃): $\delta_C = 64.4$ (d, HO-CH₂), 57.5 (q), 51.2 (d, O-CH₂), 18.1 (s, Me).

Analytical data were in accordance with literature values¹⁵¹.

7.2.1.1. *rac*-2-Methyloxirane-2-carboxylic acid (*rac*-3)

rac-**3**
C₄H₆O₃
102.09 g/mol

To a solution of freshly distilled 2-methylpropenoic acid (**14**, 3.0 g, 34.8 mmol) in anhydrous DCM (110 mL) *m*-CPBA (77% maximum peroxide content, 16.31 g, 94.5 mmol) was added. The reaction mixture was heated to reflux and stirred for 24 h. Then it was cooled down to room temperature and filtered through a pad of Celite. Solids were discarded and the filtrate was concentrated *in vacuo* giving a yellow residue. Ultrasound-assisted extraction of this residue with water was performed and the resulting aqueous phase was again filtered through Celite. After the removal of water by rotary evaporation, the residue was dissolved in Et₂O and dried by stirring the solution with Na₂SO₄ for 1 h. Filtration and concentration under reduced pressure yielded *rac*-**3** as light yellow oil (2.50 g, 70%), which was subjected to the next reaction step without further purification.

Spectroscopically pure material can be obtained by sublimation into a liquid-nitrogen cooled trap under high vacuum, but due to the rather high thermal instability of **3**, losses concerning yield have to be taken into account.

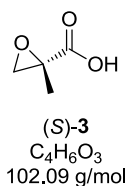
R_f (DCM/MeOH, 10:1) = 0.44.

¹H-NMR (200 MHz, CDCl₃): δ_H = 10.34 (1H, bs, -COOH), 3.13 (1H, d, *J* = 5.9 Hz, O-CH₂), 2.82 (1H, d, *J* = 5.9 Hz, O-CH₂), 1.58 (3H, s, Me).

¹³C-NMR (50 MHz, CDCl₃): δ_C = 176.4 (q, -COOH), 53.7 (q, H₃C-C), 53.3 (d), 17.0 (s).

Analytical data were in accordance with literature values⁶⁹.

7.2.2. (S)-2-Methyloxirane-2-carboxylic acid ((S)-3)



Epoxyalcohol (*R*)-2 (0.120 g, 1.36 mmol) was dissolved in a CCl₄/MeCN mixture (1 mL/1 mL) and pH 6.88 buffer solution (*Baker*, 0.15 mL) was added. After the addition of ruthenium dioxide dihydrate (6 mg, 2.6 mol%), the resulting suspension was stirred for 5 min at ambient temperature. Sodium metaperiodate (1.194 g, 5.58 mmol) was added in small portions over a period of 10 min, before the mixture was allowed to stir for another 2 h. The reaction media was diluted with Et₂O (10 mL) and dried over Na₂SO₄. Filtration through a pad of Celite provided a clear solution, which was concentrated *in vacuo* yielding (S)-3 as colourless oil (0.109 g, 79%).

$[\alpha]_D^{20} = -17.5$ (*c* 0.690, DCM).

Further analytical data were in accordance with the racemic epoxyacid *rac*-3 (see 7.2.1.1).

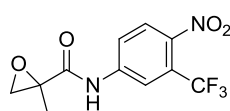
7.2.3. General method for the synthesis of epoxyamides *rac*-7/12 and (S)-7/12

The appropriately substituted aniline (1 equiv) is dissolved in anhydrous DCM (20 mL/g **7**, 27 mL/g **12**) and DIPEA (2.2 equiv) is added. This mixture is slowly added via canula to a previously prepared solution of triphosgene (0.4 equiv) in DCM (22 mL/g triphosgene) at 0 °C. After stirring the resulting solution for 15 min under cooling, the icebath is removed and stirring continued for another 3.5 h at room temperature. After complete conversion to the corresponding isocyanate has been indicated by GC-MS analysis, the reaction mixture is again cooled to 0 °C. In a separate flask, a solution of epoxyacid (1.1 equiv) in DMF (37 mL/g acid) and DIPEA (1.4 equiv) is prepared and then slowly added to the isocyanate solution via canula at 0 °C. The reaction mixture is allowed to warm up to ambient temperature and is stirred for 42 h. It is diluted with DCM and washed consecutively with small amounts of water and saturated NaHCO₃ solution. The aqueous phases are back extracted with EtOAc and the combined organic phases dried with Na₂SO₄ and concentrated

in vacuum. Vacuum flash filtration through a pad of silica with toluene → toluene/EtOAc (1:3) yields a mixture of epoxyamide and the corresponding chlorohydrine.

For converting the chlorohydrine (1 equiv) into the epoxyamide, DBU (1.1 equiv) is added to a solution of the obtained residue in DCM (74 mL/g mixture). After stirring at room temperature for 2.5 h, the solution is washed with small amounts of water and NaHCO₃, dried over Na₂SO₄ and filtered through a short pad of silica. Evaporation of the solvent yields the epoxyamide.

7.2.3.1. *rac*-2-Methyl-*N*-(4-nitro-3-(trifluoromethyl)phenyl)oxirane-2-carbox-amide (*rac*-7)



rac-7
C₁₁H₉F₃N₂O₄
290.20 g/mol

5-Amino-2-nitrobenzotrifluoride (**4**, 0.050 g, 0.24 mmol) and epoxyacid *rac*-**3** (0.027 g, 0.26 mmol) were reacted to a 1:1-mixture of product *rac*-**7** and chlorohydrine *rac*-**6** according to 7.2.3. Ring closure reaction with DBU yielded *rac*-**7** as yellow solid (0.037 g, 53% yield).

R_f (toluene/EtOAc, 1:2) = 0.66.

M_p = 117 – 119 °C.

GC/EI-MS: t_R = 9.50 min, m/z = 290 (M^+ , 6), 231 (6), 173 (9), 132 (6), 85 (13), 63 (10), 58 (47), 57 (100).

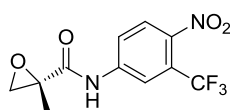
¹H-NMR (400 MHz, CD₃OD): δ_H = 8.28 (1H, d, J = 2.2 Hz, H_{Ar}), 8.12 (1H, dd, J = 9.0 and 2.2 Hz, H_{Ar}), 8.01 (1H, d, J = 9.0 Hz, H_{Ar}), 3.04 (1H, d, 2J = 5.0 Hz, OCH₂), 2.96 (1H, d, 2J = 5.0 Hz, OCH₂), 1.61 (3H, s, Me).

¹³C-NMR (100 MHz, CD₃OD): δ_C = 172.3 (q, C=O), 144.3 (q, C_{Ar}), 143.8 (q, C_{Ar}), 127.9 (t, C_{Ar}), 125.2 (q, $^2J_{CF}$ = 33.8 Hz), 124.4 (t, C_{Ar}), 123.5 (q, $^1J_{CF}$ = 272.5 Hz), 119.8 (t, $^3J_{CF}$ = 5.9 Hz), 57.1 (q, C(Me)), 54.3 (t, O-CH₂), 17.2 (s, Me).

IR (neat): ν = 3337 (NH), 1706 (CO), 1517 (NO), 1342 (NO), 1129, 852, 707.

HRMS (ESI): m/z [M-H]⁻ calcd. for C₁₁H₉F₃N₂O₄: 289.0442; found: 289.0444.

7.2.3.2. (S)-2-Methyl-N-(4-nitro-3-(trifluoromethyl)phenyl)oxirane-2-carbox-amide ((S)-7)

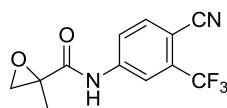


(S)-7
C₁₁H₉F₃N₂O₄
290.20 g/mol

Starting from 5-amino-2-nitrobenzotrifluoride (**9**, 0.116 g, 0.56 mmol) and epoxyacid (S)-**3** (0.063 g, 0.62 mmol), preparation of epoxyamide (S)-**7** yielded the compound as yellow solid (0.060 g, 37% yield).

Analytical data were in accordance with the racemic epoxyamide *rac*-**7** (see 7.2.3.1).

7.2.3.3. *rac*-N-(4-Cyano-3-(trifluoromethyl)phenyl)-2-methyloxirane-2-carbox-amide (*rac*-12)



rac-12
C₁₂H₉F₃N₂O₂
270.21 g/mol

Reaction of 4-amino-2-(trifluoromethyl)benzonitril (**9**, 0.052 g, 0.28 mmol) and epoxyacid *rac*-**3** (0.031 g, 0.31 mmol) provided a 1:1-mixture of epoxyamide *rac*-**12** and chlorohydrine *rac*-**11**. Ring closure reaction of *rac*-**11** yielded epoxyamide *rac*-**12** as white crystals (0.046 g, 61% yield).

R_f (toluene/EtOAc, 1:2) = 0.60.

M_p = 146 – 147 °C.

GC/EI-MS: t_R = 9.05 min, m/z = 270 (M⁺, 27), 211 (15), 199 (15), 186 (17), 58 (48), 57 (100).

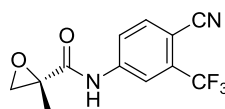
¹H-NMR (400 MHz, CD₃OD): δ_H = 8.28 (1H, d, J = 1.8 Hz, H_{Ar}), 8.09 (1H, dd, J = 8.5 and 1.8 Hz, H_{Ar}), 7.90 (1H, d, J = 8.5 Hz, H_{Ar}), 3.03 (1H, d, ²J = 5.0 Hz, OCH₂), 2.96 (1H, d, ²J = 5.0 Hz, OCH₂), 1.60 (3H, s, Me).

¹³C-NMR (100 MHz, CD₃OD): δ_C = 172.3 (q, C=O), 144.0 (q, C_{Ar}), 137.1 (t, C_{Ar}), 134.2 (q, ²J_{CF} = 32.4 Hz, C_{Ar}), 124.0 (t, C_{Ar}), 123.9 (q, ¹J_{CF} = 273.0 Hz), 119.0 (t, ³J_{CF} = 5.1 Hz), 116.6 (q, CN), 104.8 (q, C_{Ar}), 57.1 (q, C(Me)), 54.3 (t, O-CH₂), 17.2 (s, Me).

IR (neat): ν = 3347 (NH), 2228 (CN), 1704 (CO), 1526, 1325, 1130, 848.

HRMS (ESI): m/z [M-H]⁻ calcd. for C₁₂H₉F₃N₂O₂: 269.0543; found: 269.0547.

7.2.3.4. (S)-N-(4-Cyano-3-(trifluoromethyl)phenyl)-2-methyloxirane-2-carbox-amide ((S)-12)



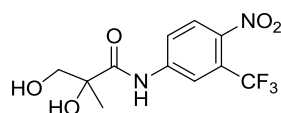
(S)-12
C₁₂H₉F₃N₂O₂
270.21 g/mol

4-Amino-2-(trifluoromethyl)benzonitrile (**9**, 0.105 g, 0.56 mmol) and epoxyacid (S)-**3** (0.063 g, 0.62 mmol) yielded epoxyamide (S)-**12** as white crystals (0.066 g, 44%) according to 7.2.3. Analytical data were in accordance with the racemic epoxamide *rac*-**12** (see 7.2.3.3).

7.2.4. General method for the preparation of diols *rac*-**8/13** and (S)-**8/13**

A solution of epoxyamide (1 equiv) in a mixture of water (100 mL/g epoxyamide) and DMF (125 mL/g epoxyamide) is prepared, heated to reflux and stirred for 5.5 h. Alternatively the reaction mixture can be exposed to microwave irradiation at 100 °C for 3.0 h. Concentration by rotary evaporation gives a viscous residue, which is dissolved in EtOAc. The solution is stirred with Na₂SO₄ for 1 h, filtered through a pad of Celite and concentrated under reduced pressure. Purification is performed by silica gel chromatography using toluene/EtOAc (10:1 → 1:3) and remaining volatiles are removed under high vacuum to yield the pure diol.

7.2.4.1. *rac*-2,3-Dihydroxy-2-methyl-N-(4-nitro-3-(trifluoromethyl)phenyl)-propanamide (*rac*-**8**)



rac-**8**
C₁₁H₁₁F₃N₂O₅
308.21 g/mol

Epoxyamide *rac*-**7** (1.268 g, 4.37 mmol) was subjected to epoxide opening reaction according to 7.2.4, yielding diol *rac*-**8** as yellow crystals (1.010 g, 75% yield).

R_f (EtOAc, 100%) = 0.39.

M_p = 119 – 120 °C.

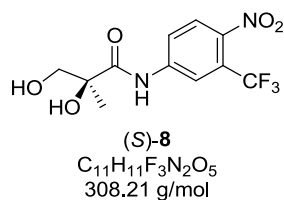
$^1\text{H-NMR}$ (400 MHz, CD_3OD): δ_{H} = 8.37 (1H, d, J = 2.2 Hz, H_{Ar}), 8.14 (1H, dd, J = 8.9 and 2.2 Hz, H_{Ar}), 8.03 (1H, d, J = 8.9 Hz, H_{Ar}), 3.85 (1H, d, 2J = 11.1 Hz, HO- CH_2), 3.53 (1H, d, 2J = 11.1 Hz, HO- CH_2), 1.39 (3H, s, Me).

$^{13}\text{C-NMR}$ (100 MHz, CD_3OD): δ_{C} = 177.0 (q, C=O), 144.2 (q, C_{Ar}), 143.9 (q, C_{Ar}), 127.9 (t, C_{Ar}), 125.3 (q, $^2J_{\text{CF}}$ = 33.7 Hz), 124.1 (t, C_{Ar}), 123.5 (q, $^1J_{\text{CF}}$ = 271.7 Hz), 119.6 (t, $^3J_{\text{CF}}$ = 5.9 Hz), 77.6 (q, C(Me)), 69.4 (t, HO- CH_2), 22.6 (s, Me).

IR (neat): ν = 3448 (NH, OH), 3305 (OH), 1686 (CO), 1527 (NO), 1320 (NO), 1141, 1044, 901, 759.

HRMS (ESI): m/z $[\text{M-H}]^-$ calcd. for $\text{C}_{11}\text{H}_{11}\text{F}_3\text{N}_2\text{O}_5$: 307.0547; found: 307.0554.

7.2.4.2. (*S*)-2,3-Dihydroxy-2-methyl-*N*-(4-nitro-3-(trifluoromethyl)phenyl)-propanamide (**(S)-8**)

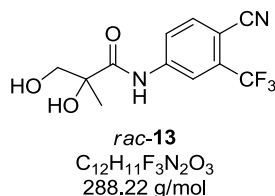


(*S*)-**8** was isolated as yellow crystals (0.046 g, 80% yield, 90% *ee*) after the exposure of (*S*)-**7** (0.054 g, 0.19 mmol) to microwave irradiation according to above mentioned procedure (see 7.2.4). Enantiomeric excess was determined by the Mosher ester method (see 7.2.5).

$[\alpha]_{\text{D}}^{20}$ = -21.2 (c 0.480, MeOH)

Further analytical data were in accordance with the racemic diol *rac*-**8** (see 7.2.4.1).

7.2.4.3. *N*-(4-Cyano-3-(trifluoromethyl)phenyl)-2,3-dihydroxy-2-methylpropanamide (*rac*-**13**)



Starting from epoxyamide *rac*-**12** (1.132 g, 4.19 mmol), diol *rac*-**13** was obtained as white crystals (0.869 g, 72% yield), following the procedure described in 7.2.4.

R_f (EtOAc, 100%) = 0.35.

M_p = 113 – 115 °C.

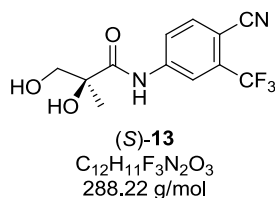
¹H-NMR (400 MHz, CD₃OD): δ_H = 8.37 (1H, s, H_{Ar}), 8.10 (1H, d, *J* = 8.5 Hz, H_{Ar}), 7.91 (1H, d, *J* = 8.5 Hz, H_{Ar}), 3.85 (1H, d, ²*J* = 11.1 Hz, HO-CH₂), 3.52 (1H, d, ²*J* = 11.1 Hz, HO-CH₂), 1.38 (3H, s, Me).

¹³C-NMR (100 MHz, CD₃OD): δ_C = 177.0 (q, C=O), 144.1 (q, C_{Ar}), 137.1 (t, C_{Ar}), 134.2 (q, ²*J*_{CF} = 32.4 Hz, C_{Ar}), 123.9 (q, ¹*J*_{CF} = 272.9 Hz), 123.7 (t, C_{Ar}), 118.7 (t, ³*J*_{CF} = 5.1 Hz), 116.7 (q, CN), 104.6 (q, C_{Ar}), 77.6 (q, C(Me)), 69.4 (t, HO-CH₂), 22.6 (s, Me).

IR (neat): ν = 3447 (NH, OH), 3298 (OH), 2226 (CN), 1688 (CO), 1504, 1325, 1124, 1049, 620.

HRMS (ESI): *m/z* [M-H]⁻ calcd. for C₁₂H₁₁F₃N₂O₃: 287.0649; found: 287.0652.

7.2.4.4. (*S*)-*N*-(4-Cyano-3-(trifluoromethyl)phenyl)-2,3-dihydroxy-2-methylpropanamide ((*S*)-**12**)



(*S*)-**13** was isolated as white crystals (0.047 g, 78% yield, 86% *ee*) after the exposure of (*S*)-**12** (0.057 g, 0.21 mmol) to microwave irradiation according to above mentioned procedure (see 7.2.4). Enantiomeric excess was determined by the Mosher ester method (see 7.2.5).

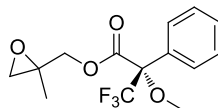
[α]_D²⁰ = -28.1 (*c* 0.585, MeOH).

Further analytical data were in accordance with the racemic diol *rac*-**13** (see 7.2.4.3).

7.2.5. General procedure for the preparation of Mosher esters

A solution of (*S*)-(-)-MTPA (for esterification of monoalcohols: 0.07 mmol, for diols: 0.14 mmol) in DCM (3.0 mL) was added to DCC (0.08 mmol/0.17 mmol). The resulting mixture was cooled to 0 °C and stirred. After 15 min a DCM (4.5 mL) solution containing the alcohol (0.07 mmol) and DMAP (0.07 mmol/0.14 mmol) was added and stirring continued for 3 h. Then the ice bath was removed and the reaction solution allowed to stir overnight at ambient temperature. The resulting suspension was filtered through a pad of Celite and the filtrate washed with saturated NaHCO₃ solution and water. After drying over Na₂SO₄, the solvent was removed by rotary evaporation. Purification by silica gel chromatography yielded the respective Mosher ester. Enantiomeric excess values for the alcohols (*R*)-**2**, (*S*)-**8** and (*S*)-**13** were determined from ¹⁹F-NMR spectra, recorded of enantiopure and racemic Mosher esters **15**, **16** and **17**.⁸⁷

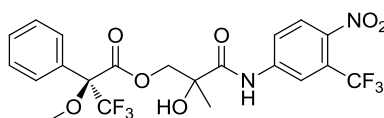
7.2.5.1. (*2S*)-(2-Methyloxiran-2-yl)methyl 3,3,3-trifluoro-2-methoxy-2-phenylpropanoate (**15**)



15
C₁₄H₁₅F₃O₄
304.26 g/mol

¹⁹F-NMR (376.5 MHz, CDCl₃): δ_F = -68.9 (s, -CF₃ (*S,R*)), -71.7 (s, -CF₃ (*S,S*)).

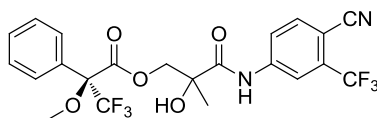
7.2.5.2. (*2S*)-2-Hydroxy-2-methyl-3-((4-nitro-3-(trifluoromethyl)phenyl)amino)-3-oxopropyl 3,3,3-trifluoro-2-methoxy-2-phenylpropanoate (**16**)



16
C₂₁H₁₈F₆N₂O₇
524.37 g/mol

¹⁹F-NMR (376.5 MHz, CD₂Cl₂): δ_F = -60.1 (2s, -CF_{3,Ar} (*S,R*)/(*S,S*)), -71.4 (s, -CF₃ (*S,R*)), -71.6 (s, -CF₃ (*S,S*)).

7.2.5.3. (2S)-3-((4-Cyano-3-(trifluoromethyl)phenyl)amino)-2-hydroxy-2-methyl-3-oxopropyl 3,3,3-trifluoro-2-methoxy-2-phenylpropanoate (17)



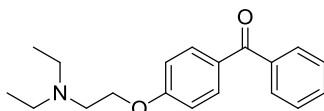
17
C₂₂H₁₈F₆N₂O₅
504.38 g/mol

¹⁹F-NMR (376.5 MHz, CD₂Cl₂): δ_F = -62.2 (2s, -CF_{3,Ar} (S,R)/(S,S)), -71.5 (s, -CF₃ (S,R)), -71.7 (s, -CF₃ (S,S)).

7.3. SYNTHESIS OF CLOMIPHENE METABOLITES

7.3.1. 4'-Hydroxyclofomiphene

7.3.1.1. (4-(2-(Diethylamino)ethoxy)phenyl)(phenyl)methanone (19)



19
C₁₉H₂₃NO₂
297.39

Sodium hydride (as 60% dispersion in mineral oil, 11.46 g, 477.5 mmol) was washed with anhydrous THF and suspended in anhydrous DMF (200 mL). A solution of 4-hydroxybenzophenone (**18**, 14.20 g, 71.6 mmol) in anhydrous DMF (100 mL) was slowly added via a dropping funnel. After the gas formation had ceased, 2-chloro-*N,N*-diethylethanamine hydrochloride (30.80 g, 179.0 mmol) was added and the reaction mixture was stirred at 100 °C for 17 hours. It was cooled down to room temperature and poured into 500 mL of ice water. This mixture was extracted with Et₂O (4 x 200 mL) and the combined organic phases again were extracted with 2N HCl (3 x 200 mL). The resulting aqueous phase was adjusted to an alkaline pH by the addition of 2N NaOH and extracted with Et₂O (3 x 200 mL). The combined organic phases were consecutively washed with saturated

NaHCO₃ solution, water and brine. After drying over Na₂SO₄, the solvent was removed by rotary evaporation to give compound **19** as brown oil (19.59 g, 92% yield).

R_f (DCM/MeOH, 10:1) = 0.49.

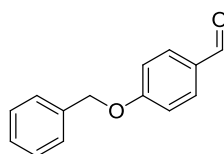
¹H-NMR (400 MHz, CDCl₃): δ_H = 7.81 (2H, d, *J* = 8.7 Hz, H_{Ar}), 7.74 (2H, d, *J* = 7.1 Hz, H_{Ar}), 7.50 (3H, m, H_{Ar}), 6.95 (2H, d, *J* = 8.8 Hz, H_{Ar}), 4.12 (2H, t, *J* = 6.3 Hz, O-CH₂), 2.90 (2H, t, *J* = 6.3 Hz, CH₂N), 2.64 (4H, q, *J* = 7.1 Hz, Me-CH₂), 1.07 (6H, t, *J* = 7.2 Hz, Me).

¹³C-NMR (100 MHz, CDCl₃): δ_C = 195.7 (s, CO), 162.7 (s, O-C_{Ar}), 138.4 (s, C_{Ar}), 132.6 (d, C_{Ar}), 132.0 (d, C_{Ar}), 130.2 (s, C_{Ar}), 129.8 (d, C_{Ar}), 128.3 (d, C_{Ar}), 114.2 (d, C_{Ar}), 67.1 (t, O-CH₂), 51.7 (t, N-CH₂), 48.0 (t, Me-CH₂), 12.0 (q, Me).

HRMS (ESI): *m/z* [M+H]⁺ calcd. for C₁₉H₂₃NO₂: 298.1802; found: 298.1793.

Analytical data were in accordance with literature values¹⁵².

7.3.1.2. 4-(Benzyloxy)benzaldehyde (**20**)



20
C₁₄H₁₂O₂
212.24

Sodium hydride (as 60% dispersion in mineral oil, 2.74 g, 114.0 mmol) was washed with anhydrous THF and suspended in anhydrous DMF (100 mL). A solution of 4-hydroxybenzaldehyde (**24**, 6.94 g, 56.8 mmol) in anhydrous DMF (60 mL) was slowly added via a dropping funnel. After the gas formation had ceased, benzylchloride (17.35 g, 137.1 mmol) was added and the reaction mixture was stirred at 100 °C for 20 hours. It was cooled down to room temperature and poured into 500 mL of ice water. This mixture was extracted with EtOAc (four 200 mL-portions) and the combined organic phases were consecutively washed with saturated NaHCO₃ solution, water and brine. After drying over Na₂SO₄, the solvent was removed by rotary evaporation. The crude product was recrystallized from ethanol to give **20** as beige-colored crystals (11.76 g, 98% yield).

R_f (PE/EtOAc, 15:1) = 0.3.

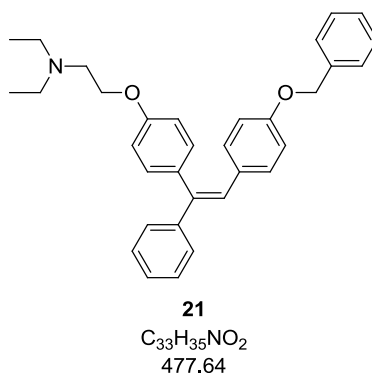
M_p = 70 – 71 °C.

¹H-NMR (400 MHz, CDCl₃): δ_{H} = 9.89 (1H, s, CHO), 7.84 (2H, d, J = 8.7 Hz, H_{Ar}), 7.40 (5H, m, H_{Ar}), 7.09 (2H, d, J = 8.7 Hz, H_{Ar}), 5.15 (2H, s, CH₂).

¹³C-NMR (100 MHz, CDCl₃): δ_{C} = 190.9 (d, CHO), 163.8 (s, O-C_{Ar}), 136.0 (s, C_{Ar}-CH₂), 132.1 (d, C_{Ar}), 130.2 (s, CHO-C_{Ar}), 128.8 (d, C_{Ar}), 128.4 (d, C_{Ar}), 127.6 (d, C_{Ar}), 70.4 (t, CH₂).

Analytical data were in accordance with literature values¹⁵³.

7.3.1.3. 2-(4-(2-(4-(Benzyloxy)phenyl)-1-phenylvinyl)phenoxy)-*N,N*-diethylethanamine (**21**)



A suspension of zinc (1.964 g, 30.0 mmol) in anhydrous THF (25 mL) was cooled to -10 °C and titanium tetrachloride (2.846 g, 15.0 mmol) was slowly added. The reaction mixture was allowed to warm up to ambient temperature and was then refluxed for two hours. After cooling down to room temperature, a solution of ketone **19** in THF (14 mL) was added. The reaction mixture was stirred for 30 minutes, before a solution of aldehyde **20** in THF (14 mL) was added and the mixture was again refluxed. The conversion was completed after three hours. After cooling down to room temperature, the reaction mixture was hydrolyzed with K₂CO₃ solution (10%, 330 mL) and afterwards extracted with Et₂O (4 x 200 mL). The combined organic phases were washed with water (2 x 300 mL) and dried over Na₂SO₄. Evaporation of the solvent gave the crude product, which was purified by silica gel chromatography using chloroform/MeOH (20:1 → 5:1) to yield the triphenylethylene **21** as light-yellow oil (0.611 g, 51% yield).

R_f (chloroform/MeOH, 20:1) = 0.39/0.45.

¹H-NMR (400 MHz, CDCl₃): δ_{H} = 7.48 – 7.15/7.06 – 6.74 (38H, 2m, H_{Ar} + H_{vinyllic}), 5.05/5.03 (4H, 2s, H_{benzylic}), 4.38/4.35 (4H, 2t, J = 5.5/5.2 Hz, O-CH₂), 3.26/3.23 (4H, 2t, J = 5.0/4.9 Hz,

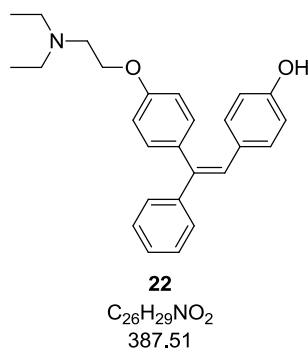
N-CH₂-CH₂), 3.05/3.02 (8H, 2q, $J = 7.3/7.2$ Hz, Me-CH₂), 1.35/1.32 (12H, 2t, $J = 7.8/7.2$ Hz, Me).

¹³C-NMR (100 MHz, CDCl₃): $\delta_C = 157.7/157.5$ (2s, O-C_{Ar}), 157.6/157.4 (2s, O-C_{Ar}), 143.9 (2s, C), 140.7 (2s, C), 140.2/140.1 (2s, C), 137.1/137.0 (2s, C), 131.9 (2d, CH), 130.9/130.8 (2d, CH), 130.5 (2s, C), 130.5 (2d, CH), 128.8 (2d, CH), 128.6 (2d, CH), 128.2/128.0 (2d, CH), 127.6/127.5 (2d, CH), 127.4/127.3 (2d, CH), 126.4 (2d, CH), 114.7/114.4 (2d, CH), 114.5/114.3 (2d, CH), 70.0 (2t, C_{benzylic}), 64.5 (2t, O-CH₂-CH₂), 51.2 (2t, N-CH₂-CH₂), 47.6/47.5 (2t, Me-CH₂), 10.2 (q, Me).

IR (neat): $\nu = 1604$ (conjugated double bond system), 1509 (conjugated double bond system), 1232, 1176, 1013, 826, 739, 697.

HRMS (ESI): m/z [M+H]⁺ calcd. for C₃₃H₃₅NO₂: 478.2741; found: 478.2744.

7.3.1.4. 4-(2-(4-(2-(Diethylamino)ethoxy)phenyl)-2-phenylvinyl)phenol (**22**)



Naphthalene (0.317 g, 2.5 mmol) was dissolved in anhydrous THF (9 mL) and small pieces of lithium (0.041 g, 5.9 mmol) were added. The resulting suspension was treated for two hours with ultrasound, giving a dark green solution. After cooling it down to -21 °C, a solution of compound **21** in THF (2 mL) was slowly added. The color first changed from green to brown and then to yellow. After two more hours of stirring at -21° C it darkened again. The solution was allowed to warm up to room temperature and residual pieces of lithium were taken out with the aid of tweezers. After hydrolysis with saturated NH₄Cl-solution, EtOAc (40 mL) was added and the resulting mixture was consecutively washed with water and brine. It was dried by the addition of Na₂SO₄ and evaporated. Purification was performed by silica gel chromatography using chloroform/MeOH (20:1 → 5:1) to give the pure alcohol **22** as light brown crystals (0.779 g, 100% yield).

M_p = 49 – 51 °C.

R_f (chloroform/MeOH, 10:1) = 0.27/0.36.

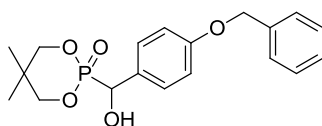
$^1\text{H-NMR}$ (400 MHz, CDCl_3): δ_{H} = 7.37 – 7.03/6.97 – 6.70/6.67 – 6.51 (28H, 3m, H_{Ar} + H_{vinyl}), 5.92 (2H, bs, OH), 4.10 (2H, t, J = 5.8 Hz, O- CH_2), 4.07 (2H, t, J = 5.8 Hz, O- CH_2), 2.96 (2H, t, J = 5.7 Hz, N- CH_2 - CH_2), 2.93 (2H, t, J = 5.5 Hz, N- CH_2 - CH_2), 2.74 (4H, q, J = 7.7 Hz, Me- CH_2), 2.72 (4H, q, J = 7.8 Hz, Me- CH_2), 1.12 (6H, t, J = 6.3 Hz, Me), 1.10 (6H, t, J = 6.0 Hz, Me).

$^{13}\text{C-NMR}$ (100 MHz, CDCl_3): δ_{C} = 158.0 (2s, O- C_{Ar}), 155.5/155.2 (2s, O- C_{Ar}), 144.2/141.0 (2s, C), 139.8 (2s, C), 136.6/133.2 (2s, C), 131.7/130.9 (2d, CH), 131.0/130.5 (2d, CH), 129.7 (2s, C), 128.7/128.6 (2d, CH), 128.2/127.7 (2d, CH), 127.6/127.3 (2d, CH), 127.2/126.4 (2d, CH), 115.4 (2d, CH), 114.7/114.2 (2d, CH), 65.9/65.6 (2t, O- CH_2), 51.5 (2t, N- CH_2 - CH_2), 47.4 (2t, Me- CH_2), 11.1/11.0 (2q, Me).

IR (neat): ν = 1606 (conjugated double bond system), 1508 (conjugated double bond system), 1237, 1171, 1013, 829, 698.

HRMS (ESI): m/z $[\text{M}+\text{H}]^+$ calcd. for $\text{C}_{26}\text{H}_{29}\text{NO}_2$: 388.2271; found: 388.2261.

7.3.1.5. 2-((4-(Benzyloxy)phenyl)(hydroxy)methyl)-5,5-dimethyl-1,3,2-dioxaphosphinane 2-oxide (27)



27
 $\text{C}_{19}\text{H}_{23}\text{O}_5\text{P}$
362.36

4-(Benzyloxy)benzaldehyde (**20**, 0.127 g, 0.6 mmol) and 5,5-dimethyl-2-oxo-1,3,2-dioxaphosphorinane (**25**, 0.090 g, 0.6 mmol) were dissolved in a 1:1-mixture of *n*-hexane and toluene (1.4 mL). TEA was added and the resulting reaction mixture was stirred for four days. The precipitated product was isolated by centrifugation and purified by recrystallization in DCM/toluene. α -Hydroxyphosphonate **27** was obtained as white crystals (0.095 g, 44% yield).

M_p = 167 – 169 °C.

R_f (DCM/MeOH, 20:1) = 0.21.

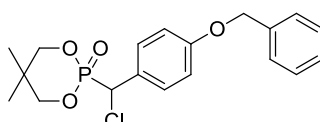
$^1\text{H-NMR}$ (200 MHz, CDCl_3): δ_{H} = 7.47 – 7.30 (7H, m, H_{Ar}), 6.98 (2H, d, J = 8.6 Hz, H_{Ar}), 5.11 (1H, d, 2J = 10.3 Hz, HO- CH), 5.06 (2H, s, $\text{H}_{\text{benzylic}}$), 4.10-3.93 (4H, m, $2\times\text{CH}_2$), 2.72 (1H, bs, OH), 1.11/0.84 (6H, 2s, $2\times\text{Me}$).

$^{13}\text{C-NMR}$ (50 MHz, CDCl_3): $\delta_{\text{C}} = 158.9$ (s, C_{Ar}), 137.0 (s, C_{Ar}), 128.8 (C_{Ar}), 128.7 (C_{Ar}), 128.5 (C_{Ar}), 128.1 (C_{Ar}), 127.5 (C_{Ar}), 115.0 (C_{Ar}), 77.4 (t, $^2J_{\text{CP}} = 10.3$ Hz, O- CH_2), 71.5 (d, $^1J_{\text{CP}} = 159.6$ Hz, HO- CH), 70.1 (t, $\text{C}_{\text{benzylic}}$), 32.5 (s, $^3J_{\text{CP}} = 7.7$ Hz, CMe_2), 21.9/21.0 (2q, Me).

IR (neat): $\nu = 1609, 1508, 1230, 1200, 1167, 1047, 990, 834, 753, 616$.

HRMS (ESI): m/z $[\text{M}+\text{H}]^+$ calcd. for $\text{C}_{19}\text{H}_{23}\text{O}_5\text{P}$: 363.1356; found: 363.1354.

7.3.1.6. 2-((4-(Benzyloxy)phenyl)chloromethyl)-5,5-dimethyl-1,3,2-dioxaphosphinane 2-oxide (**28**)



28
 $\text{C}_{19}\text{H}_{22}\text{ClO}_4\text{P}$
380.80

To a solution of α -hydroxyphosphonate (**27**, 0.234 g, 0.65 mmol) in DCM, freshly distilled thionylchloride (0.208 g, 1.75 mmol) was added. The resulting reaction mixture was stirred overnight at ambient temperature. After hydrolysis with water, the phases were separated and the DCM-phase once again washed with water. It was dried with Na_2SO_4 and removal of the solvent by rotary evaporation gave the crude product, which was recrystallized in DCM/heptane to give α -chlorophosphonate **28** as white crystals (0.193 g, 78% yield).

R_f (DCM/MeOH, 20:1) = 0.36.

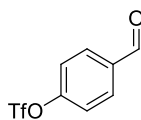
$M_p = 146 - 148$ °C.

$^1\text{H-NMR}$ (200 MHz, CDCl_3): $\delta_{\text{H}} = 7.55 - 7.29$ (7H, m, H_{Ar}), 6.97 (2H, d, $J = 8.6$ Hz, H_{Ar}), 5.09 (1H, d, $^2J = 10.1$ Hz, Cl- CH), 5.06 (2H, s, $\text{H}_{\text{benzylic}}$), 4.20 - 4.09 (4H, m, $2\times\text{CH}_2$), 2.72 (1H, bs, OH), 1.17/0.95 (6H, 2s, $2\times\text{Me}$).

$^{13}\text{C-NMR}$ (50 MHz, CDCl_3): $\delta_{\text{C}} = 159.5$ (s, C_{Ar}), 136.7 (s, C_{Ar}), 130.3 (C_{Ar}), 128.7 (C_{Ar}), 128.1 (C_{Ar}), 127.5 (C_{Ar}), 126.0 (C_{Ar}), 115.2 (C_{Ar}), 78.2/78.1 (2t, $^2J_{\text{CP}} = 7.4/7.3$ Hz, O- CH_2), 70.1 (t, $\text{C}_{\text{benzylic}}$), 53.7 (d, $^1J_{\text{CP}} = 158.4$ Hz, Cl- CH), 32.8 (s, $^3J_{\text{CP}} = 8.0$ Hz, CMe_2), 21.9/21.1 (2q, Me).

IR (neat): $\nu = 1610, 1511, 1251, 1176, 1156, 1009, 983, 830, 741, 697, 545$.

HRMS (ESI): m/z $[\text{M}+\text{H}]^+$ calcd. for $\text{C}_{19}\text{H}_{22}\text{O}_4\text{PCl}$: 381.1017; found: 381.1014.

7.3.1.7. 4-Formylphenyl trifluoromethanesulfonate (30)¹⁵⁴

30
C₈H₅F₃O₄S
254.18

4-Hydroxybenzaldehyde (**24**, 0.50 g, 4.09 mmol) was dissolved in pyridine (4 mL) and cooled to 0 °C. Triflic anhydride (as 1M solution in DCM, 1.270 g, 4.50 mmol) was slowly added and the mixture was stirred for ten minutes at 0 °C. Then the reaction mixture was allowed to warm up to room temperature and stirred overnight. After the addition of Et₂O, the mixture was extracted with an aqueous solution of CuSO₄ (1M, three 10 mL-portions) and then washed with water (two 10 mL-portions). The organic phase was dried over Na₂SO₄ and evaporation of the solvent gave **30** as white crystals (0.863 g, 76% yield).

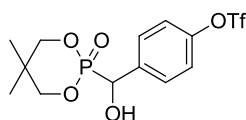
R_f (PE/EtOAc, 4:1) = 0.62.

M_p = 139 – 142 °C.

¹H-NMR (200 MHz, CDCl₃): δ_H = 10.05 (1H, s, CHO), 8.01 (2H, d, *J* = 8.6 Hz, H_{Ar}), 7.47 (2H, *J* = 8.7 Hz, H_{Ar}).

¹³C-NMR (50 MHz, CDCl₃): δ_C = 190.3 (d, CHO), 153.2 (C_{Ar}), 136.0 (C_{Ar}), 131.9 (C_{Ar}), 122.4 (C_{Ar}), 118.8 (q, ¹J_{CF} = 321 Hz, CF₃).

Analytical data were in accordance with literature values¹⁵⁴.

7.3.1.8. 4-((5,5-Dimethyl-2-oxido-1,3,2-dioxaphosphinan-2-yl)(hydroxy)methyl)-phenyl trifluoromethanesulfonate (31)

31
C₁₃H₁₆F₃O₇PS
404.30

Benzaldehyde **30** (0.817 g, 3.21 mmol) and 5,5-dimethyl-2-oxo-1,3,2-dioxaphosphorinane (**25**, 0.482 g, 3.21 mmol) were dissolved in anhydrous toluene (3.3 mL) and freshly distilled TEA (0.163 g, 1.61 mmol) was added. The resulting mixture was stirred overnight at room

temperature. The precipitated product was filtered off, washed with toluene and dried *in vacuo* at 30 °C. α -Hydroxyphosphonate **31** was obtained as white crystals (0.943 g, 73% yield).

R_f (DCM/MeOH, 20:1) = 0.26.

M_p = 125 – 129 °C.

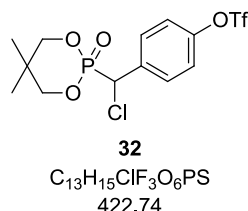
$^1\text{H-NMR}$ (200 MHz, DMSO): δ_H = 7.62 (2H, d, J = 7.1 Hz, H_{Ar}), 7.49 (2H, d, J = 7.5 Hz, H_{Ar}), 6.63 (1H, bs, OH), 5.36 (1H, d, 2J = 13.2 Hz, HO-CH), 4.54 – 4.32/4.08 – 3.84 (4H, 2m, 2xCH₂), 1.14/0.83 (6H, 2s, 2xMe).

$^{13}\text{C-NMR}$ (50 MHz, DMSO): δ_C = 148.5 (s, C_{Ar}), 139.7 (s, C_{Ar}), 129.3 (d, C_{Ar}), 121.0 (d, C_{Ar}), 118.3 (q, $^1J_{CF}$ = 320.9 Hz, C_{F_3}), 77.9/77.4 (2t, $^2J_{CP}$ = 7.1/7.0 Hz, O-CH₂), 69.1 (d, $^1J_{CP}$ = 156.4 Hz, HO-CH), 32.0 (s, $^3J_{CP}$ = 7.9 Hz, C_{Me_2}), 21.3/19.8 (2q, 2xMe).

IR (neat): ν = 1421, 1214, 1137, 1072, 1047, 1010, 990, 875, 605, 542.

HRMS (ESI): m/z [M+H]⁺ calcd. for C₁₃H₁₆F₃O₇PS: 405.0379; found: 405.0387.

7.3.1.9. 4-(Chloro(5,5-dimethyl-2-oxido-1,3,2-dioxaphosphinan-2-yl)methyl)phenyl trifluoromethanesulfonate (**32**)



α -Hydroxyphosphonate **31** (0.211 g, 0.52 mmol) was suspended in anhydrous chloroform (6 mL). Addition of freshly distilled thionyl chloride (0.62 g, 5.21 mmol) gave a clear solution that was stirred for three days at 60 °C. After hydrolysis with water, the phases were separated and the organic phase once again washed with water. It was dried over Na₂SO₄ and the solvent removed by rotary evaporation. The residue was digested in *n*-heptane to yield α -chlorophosphonate **32** as off-white crystals (0.228 g, 76% yield).

R_f (DCM/MeOH, 20:1) = 0.38.

M_p = 211 – 213 °C.

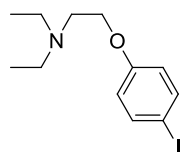
$^1\text{H-NMR}$ (200 MHz, CDCl₃): δ_H = 7.65 (2H, d, J = 8.7 Hz, H_{Ar}), 7.28 (2H, d, J = 8.5 Hz, H_{Ar}), 5.14 (1H, d, 2J = 14.5 Hz, Cl-CH), 4.29 – 4.09 (4H, 2m, 2xCH₂), 1.17/0.94 (6H, 2s, 2xMe).

^{13}C -NMR (50 MHz, CDCl_3): $\delta_{\text{C}} = 149.8$ (s, C_{Ar}), 134.5 (s, C_{Ar}), 130.9 (d, C_{Ar}), 121.8 (d, C_{Ar}), 118.8 (q, $^1J_{\text{CF}} = 323.8$ Hz, $\underline{\text{C}}\text{F}_3$), 78.6/78.5 (2t, $\text{O}-\underline{\text{C}}\text{H}_2$), 53.1 (d, $^1J_{\text{CP}} = 155.3$ Hz, $\text{Cl}-\underline{\text{C}}\text{H}$), 32.9 (s, $^3J_{\text{CP}} = 8.3$ Hz, $\underline{\text{C}}\text{Me}_2$), 21.8/21.0 (2q, 2xMe).

IR (neat): $\nu = 1429, 1262, 1208, 1137, 1050, 1002, 978, 864, 798, 768, 518$.

HRMS (ESI): m/z $[\text{M}+\text{H}]^+$ calcd. for $\text{C}_{13}\text{H}_{15}\text{ClF}_3\text{O}_6\text{PS}$: 423.0040; found: 423.0056.

7.3.1.10. *N,N*-Diethyl-2-(4-iodophenoxy)ethanamine (35)



35
 $\text{C}_{12}\text{H}_{18}\text{INO}$
319.18

Potassium hydroxide (1.285 g, 22.9 mmol) was added to a solution of 4-iodophenol (5.0 g, 22.7 mmol) in ethanol. After stirring for one hour at room temperature, the ethanol was evaporated to give the corresponding potassium phenolate as residue. In parallel, a solution of 2-chloro-*N,N*-diethylethanamine hydrochloride (3.993 g, 23.2 mmol) in water (8 mL) was cooled to 0 °C and an aqueous solution of sodium hydroxide (1.144 g, 28.6 mmol, dissolved in 3.5 mL water) was added slowly. The resulting mixture was saturated with NaCl and extracted with toluene. After drying over Na_2SO_4 , the combined toluene extracts were mixed with the previously prepared potassium phenolate and refluxed overnight. The reaction mixture was filtered through Celite and the resulting filtrate was washed with 4N NaOH and brine. Drying over Na_2SO_4 and solvent removal under reduced pressure afforded product **36** as yellow oil (5.054 g, 70% yield).

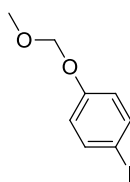
R_f (DCM/MeOH, 20:1) = 0.22.

^1H -NMR (400 MHz, CDCl_3): $\delta_{\text{H}} = 7.53$ (2H, d, $J = 8.9$ Hz, H_{Ar}), 6.67 (2H, d, $J = 9.0$ Hz, H_{Ar}), 3.99 (2H, t, $J = 6.3$ Hz, $\text{O}-\text{CH}_2$), 2.84 (2H, t, $J = 6.3$ Hz, $\text{N}-\underline{\text{C}}\text{H}_2-\text{CH}_2$), 2.62 (4H, q, $J = 7.1$ Hz, $\text{Me}-\text{CH}_2$), 1.05 (6H, t, $J = 7.2$ Hz, Me).

^{13}C -NMR (100 MHz, CDCl_3): $\delta_{\text{C}} = 158.9$ (s, C_{Ar}), 138.3 (d, C_{Ar}), 117.1 (d, C_{Ar}), 82.8 (s, C_{Ar}), 66.9 (t, $\text{O}-\underline{\text{C}}\text{H}_2$), 51.8 (t, $\text{N}-\underline{\text{C}}\text{H}_2-\text{CH}_2$), 48.0 (t, $\text{Me}-\underline{\text{C}}\text{H}_2$), 12.0 (q, Me).

IR (neat): $\nu = 1586, 1485, 1282, 1242, 1174, 1029, 819, 632$.

HRMS (ESI): m/z $[\text{M}+\text{H}]^+$ calcd. for $\text{C}_{12}\text{H}_{18}\text{INO}$: 320.0506; found: 320.0503.

7.3.1.11. 1-Iodo-4-(methoxymethoxy)benzene (37)¹⁵⁵

37
C₈H₉IO₂
264.06

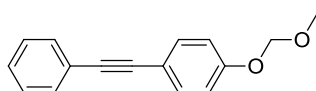
A suspension of sodium hydride (as 60% dispersion in mineral oil, 1.089 g, 45.4 mmol) in anhydrous THF (80 mL) was slowly added to a solution of 4-iodophenol (5.0 g, 22.7 mmol) in THF (50 mL). After one hour of stirring at room temperature, chloromethyl methyl ether (3.655 g, 45.4 mmol) was added and the resulting reaction mixture was stirred for two more hours at ambient temperature. After hydrolysis with water (10 mL), extraction with Et₂O (4 x 150 mL) was performed. The combined organic phases were consecutively washed with water (2 x 50 mL), brine (2 x 50 mL) and NaOH (5%, 2 x 50 mL). Removal of residual water with Na₂SO₄ and evaporation afforded the protected iodophenol **37** as yellow liquid (5.994 g, 100% yield).

R_f (PE/EtOAc, 10:1) = 0.47.

¹H-NMR (200 MHz, CDCl₃): δ_H = 7.56 (2H, d, *J* = 8.9 Hz, H_{Ar}), 6.81 (2H, d, *J* = 8.9 Hz, H_{Ar}), 5.14 (2H, s, CH₂), 3.46 (3H, s, Me).

¹³C-NMR (50 MHz, CDCl₃): δ_C = 157.2 (s, C_{Ar}), 138.4 (d, C_{Ar}), 118.7 (d, C_{Ar}), 94.5 (t, CH₂), 84.4 (s, C_{Ar}), 56.2 (q, Me).

Analytical data were in accordance with literature values¹⁵⁵.

7.3.1.12. 1-(Methoxymethoxy)-4-(phenylethynyl)benzene (38)¹¹⁴

38
C₁₆H₁₄O₂
238.28

Phenylacetylene (1.741 g, 17.0 mmol) and 1-iodo-4-(methoxymethoxy)benzene **37** (3.0 g, 11.4 mmol) were added to a suspension of copper(I) iodide (0.043 g, 0.23 mmol) and bis(triphenylphosphine)palladium(II) dichloride (0.080 g, 0.11 mmol) in Et₂NH (57 mL). The

resulting mixture was stirred at room temperature for 20 hours. Evaporation of the solvent under reduced pressure gave a residue, which was passed through a silica gel column with *n*-hexane/toluene (5:1) → toluene to obtain diarylacetylene **38** as light yellow oil (2.119 g, 78% yield).

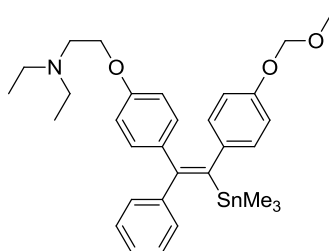
R_f (toluene) = 0.41.

$^1\text{H-NMR}$ (200 MHz, CDCl_3): δ_{H} = 7.58 – 7.44 (4H, m, H_{Ar}), 7.42 – 7.29 (3H, m, H_{Ar}), 7.04 (2H, d, J = 8.7 Hz, H_{Ar}), 5.21 (2H, s, CH_2), 3.50 (3H, s, Me).

$^{13}\text{C-NMR}$ (50 MHz, CDCl_3): δ_{C} = 157.4 (s, C_{Ar}), 133.1 (d, C_{Ar}), 131.6 (d, C_{Ar}), 128.4 (d, C_{Ar}), 128.1 (d, C_{Ar}), 123.6 (s, C_{Ar}), 116.7 (s, C_{Ar}), 116.3 (d, C_{Ar}), 94.4 (t, CH_2), 89.3 (q, $\text{C}_{\text{acetylenic}}$), 88.4 (q, $\text{C}_{\text{acetylenic}}$), 56.2 (q, Me).

IR (neat): ν = 2220 (alkyne triple bond), 1507, 1231, 1147, 1075, 992, 923, 831, 757, 691.

7.3.1.13. (*E*)-*N,N*-Diethyl-2-(4-(2-(4-(methoxymethoxy)phenyl)-1-phenyl-2-(trimethylstannyl)vinyl)phenoxy)ethanamine (**39**)⁶⁷



39

$\text{C}_{31}\text{H}_{41}\text{NO}_3\text{Sn}$
594.37

Small pieces of lithium (0.034 g, 4.9 mmol) were added to a 0.5 M solution of hexamethyldistannane in anhydrous THF (0.246 g, 0.75 mmol). Vigorous stirring at 0 °C for 15 hours gave a dark green solution. 1.1 mL of this solution were transferred into a Schlenk reaction vessel and volatiles were removed *in vacuo*. To the resulting trimethylstannyl lithium residue, diarylacetylene **38** (0.238 g, 1.0 mmol) and *n*-hexane (3.0 mL) were added and the mixture was then stirred for three hours at 0 °C. After the addition of zinc chloride (0.150 g, 1.1 mmol) as 1.1 M solution in THF, the reaction mixture was allowed to warm up to room temperature and stirring continued for 1.5 hours. Tris(dibenzylideneacetone)dipalladium-chloroform (0.052 g, 0.05 mmol), SPhos (0.082 g, 0.20 mmol) and aryl iodide **36** (0.335 g, 1.1 mmol) were added and stirring continued overnight. After the addition of water, the mixture was extracted with DCM and the

combined organic phases were washed with brine and dried over Na_2SO_4 . Evaporation of the solvent gave the crude product, which was purified by silica gel chromatography using DCM/MeOH (50:1 \rightarrow 10:1) to give **39** as a mixture of regioisomers (0.2931 g, 49% yield).

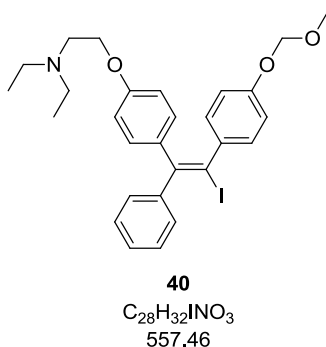
R_f (DCM/MeOH, 20:1) = 0.33/0.35.

GC-EI-MS: Major compound **39**: t_R = 20.71 min; m/z = 595.1 (M^+ , 0.6), 580.1 (2.7), 165.0 (0.9), 100.1 (70), 86.1 (100).

Minor compound, regioisomer **69**: t_R = 21.02 min; m/z = 595.1 (M^+ , 0.4), 580.1 (3.3), 165.0 (0.6), 100.1 (59), 86.1 (100).

HRMS (major compound **39**): m/z $[M+H]^+$ calcd. for $\text{C}_{31}\text{H}_{41}\text{NO}_3\text{Sn}$: 596.2187; found: 596.2210.

7.3.1.14. (*E*)-*N,N*-Diethyl-2-(4-(2-iodo-2-(4-(methoxymethoxy)phenyl)-1-phenyl-vinyl)phenoxy)ethanamine (**40**)



After the addition of iodine (0.043 g, 0.17 mmol) to a solution of vinyl stannane **38** (0.050 g, 0.08 mmol) in DCM (1.0 mL), the resulting mixture was stirred at ambient temperature. After two hours of stirring, saturated $\text{Na}_2\text{S}_2\text{O}_3$ solution (1.0 mL) was added and the mixture was extracted with DCM (3 x 10 mL). The combined organic phases were washed with brine (1 x 10 mL), dried over Na_2SO_4 and the solvent was removed by rotary evaporation. Purification of the crude product was performed by silica gel chromatography using chloroform/MeOH (30:1) to afford vinyl iodide **40** as brown oil (0.042 g, 91%).

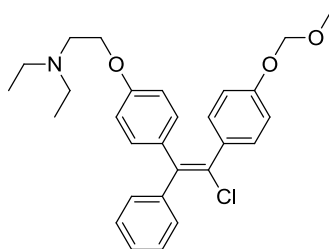
R_f (DCM/MeOH, 6:1) = 0.51/0.62.

GC-EI-MS: Major compound **40**: t_R = 22.16 min; m/z = 557.0 (M^+ , 0.3), 253.0 (0.2), 127.9 (1.2), 100.1 (22), 86.1 (100).

Minor compound, regioisomer of **40**: t_R = 22.41 min; m/z = 557.0 (M^+ , 0.2), 304.9 (0.4), 177.0 (1.3), 100.1 (14), 86.1 (100).

HRMS (major compound **40**): m/z $[M+H]^+$ calcd. for $C_{28}H_{32}NO_3$: 558.1500; found: 558.1512.

7.3.1.15. (*E*)-2-(4-(2-Chloro-2-(4-(methoxymethoxy)phenyl)-1-phenylvinyl)-phenoxy)-*N,N*-diethylethanamine (41**)**



41
 $C_{28}H_{32}ClNO_3$
466.01

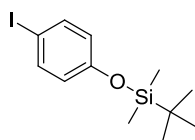
Copper chloride (0.050 g, 0.37 mmol) was added to a solution of vinyl stannane **39** (0.099 g, 0.17 mmol) in anhydrous THF (2.0 mL) at 0 °C. The resulting mixture was then allowed to warm up to room temperature and stirred overnight. It was diluted with EtOAc, filtrated through a short pad of silica gel and the filtrate was concentrated *in vacuo*. Purification was achieved by silica gel chromatography using DCM/MeOH (50:1 → 30:1) to afford compound **41** (0.053 g, 68% yield).

R_f (DCM/MeOH, 8:1) = 0.51/0.56.

GC-EI-MS: Major compound **41**: t_R = 20.51 min; m/z = 465.1 (M^+ , 0.8), 100.1 (11), 86.1 (100).

Minor compound, regioisomer of **41**: t_R = 20.08 min; m/z = 465.1 (M^+ , 0.2), 100.1 (11), 86.1 (100).

7.3.1.16. *tert*-Butyl(4-iodophenoxy)dimethylsilane (42**)¹⁵⁶**



42
 $C_{12}H_{19}IOSi$
334.27

After the addition of TEA (0.652 g, 6.44 mmol) to a solution of 4-iodophenol (**35**, 1.182 g, 5.37 mmol) and *tert*-butyldimethylsilyl chloride (0.971 g, 6.44 mmol) in DCM (2.5 mL), the resulting reaction mixture was stirred overnight at room temperature. It was poured into

water, extracted with EtOAc (3 x 5 mL) and the combined organic layers were washed with brine (2 x 5 mL). The solvent was removed by rotary evaporation to obtain the crude product, which was purified by silica gel chromatography using PE (100%) as mobile phase to afford compound **42** as colorless oil (1.559 g, 87%).

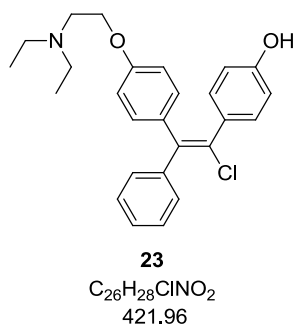
R_f (PE) = 0.43.

$^1\text{H-NMR}$ (400 MHz, CDCl_3): δ_{H} = 7.50 (2H, d, J = 8.5 Hz, H_{Ar}), 6.61 (2H, d, J = 8.5 Hz, H_{Ar}), 0.97 (9H, s, *t*-butyl), 0.18 (6H, s, Me).

$^{13}\text{C-NMR}$ (100 MHz, CDCl_3): δ_{C} = 155.8 (s, C_{Ar}), 138.4 (d, C_{Ar}), 122.7 (d, C_{Ar}), 83.9 (s, C_{Ar}), 25.8 (q, $\text{C}_{\text{t-butyl}}$), 18.4 (s), -4.3 (q, C_{Me}).

Analytical data were in accordance with literature values¹⁵⁶.

7.3.1.17. (*E*)-4-(1-chloro-2-(4-(2-(diethylamino)ethoxy)phenyl)-2-phenylvinyl)phenol (CM 2)



Conc. HCl (50 μl) was added to a solution of compound **41** (0.053 g, 0.11 mmol) in MeOH (3.0 mL) and the resulting mixture was stirred for one hour at 60 °C. The pH-value was adjusted to 7 - 8 by the addition of a saturated NaHCO_3 solution, followed by extraction with DCM (3 x 5 mL). The combined organic layers were dried over Na_2SO_4 and evaporated to afford compound **23** (0.043 g, 89% yield).

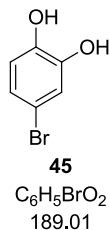
R_f (DCM/MeOH, 8:1) = 0.22/0.30.

GC-EI-MS: TMS-ether of major compound (**75**): t_{R} = 14.76 min; m/z = 493.4 (M^+ , 0.2), 478.5 (0.2), 100.1 (11), 86.1 (100).

TMS-ether of minor compound (**76**): t_{R} = 14.93 min; m/z = 493.3 (M^+ , 0.5), 252 (1), 100.1 (7), 86.1 (100).

7.3.2. 3,4-Di-hydroxy-di-hydroclomiphene

7.3.2.1. 4-Bromobenzene-1,2-diol (**45**)¹²⁸



A solution of catechol (12.0 g, 109.0 mmol) in MeCN (85 mL) was cooled to -30 °C. After the dropwise addition of tetrafluoroboric acid diethyl ether complex (19.415 g, 119.9 mmol), NBS (21.338 g, 119.9 mmol) was added in small portions. The reaction mixture was allowed to warm up to room temperature and stirred overnight. It was poured into water and extracted with Et₂O (3 x 60 mL). The combined organic layers were consecutively washed with an aqueous solution of NaHSO₃ (4%, 100 mL) and brine (100 mL), dried over Na₂SO₄ and evaporated. The crude product was purified by silica gel chromatography using PE/EtOAc (10:1 → 1:1) to afford compound **45** as white crystals (20.602 g, 100% yield).

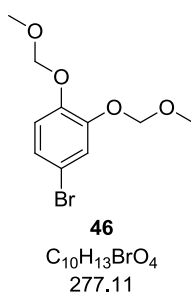
R_f (PE/EtOAc, 2:1) = 0.62.

M_p = 85 – 87 °C.

¹H-NMR (400 MHz, CDCl₃): δ_H = 7.01 (1H, d, *J* = 2.2 Hz, H_{Ar}), 6.92 (1H, dd, *J* = 2.2/8.5 Hz, H_{Ar}), 6.74 (1H, d, *J* = 8.5 Hz, H_{Ar}), 5.95 (1H, bs, OH), 5.79 (1H, bs, OH).

¹³C-NMR (100 MHz, CDCl₃): δ_C = 144.5 (s), 142.8 (s), 124.1 (d), 118.8 (d), 116.9 (d), 112.7 (s).

Analytical data were in accordance with literature values.¹²⁸

7.3.2.2. 4-Bromo-1,2-bis(methoxymethoxy)benzene (46)

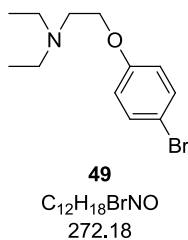
Sodium hydride (as 60% dispersion in mineral oil, 10.354 g, 431.6 mmol) was washed with *n*-hexane and suspended in anhydrous THF (600 mL). A solution of 4-bromocatechol (**45**, 20.401 g, 107.9 mmol) in THF (200 mL) was dropwise added and the reaction mixture was stirred at room temperature for one hour. Upon the addition of chloromethyl methyl ether (34.748 g, 431.6 mmol), the dark colored mixture turned yellow and was then stirred overnight. The reaction mixture was poured into water (200 mL) and extracted with Et₂O (3 x 300 mL). The combined organic layers were washed with water (200 mL) and brine (200 mL), dried over Na₂SO₄ and the solvent was removed *in vacuo*. Purification was performed by silica gel chromatography using PE/EtOAc (2% → 15% EtOAc) to obtain compound **46** as colorless oil (20.930 g, 70% yield).

R_f (PE/EtOAc, 3:1) = 0.52.

¹H-NMR (400 MHz, CDCl₃): δ_H = 7.16 (1H, d, *J* = 2.2 Hz, H_{Ar}), 6.92 (1H, dd, *J* = 2.2/8.6 Hz, H_{Ar}), 6.88 (1H, d, *J* = 8.6 Hz, H_{Ar}), 5.06/5.04 (4H, 2s, CH₂), 3.36/3.35 (6H, 2s, Me).

¹³C-NMR (100 MHz, CDCl₃): δ_C = 148.2 (s, C_{Ar}), 146.6 (s, C_{Ar}), 125.3 (d, C_{Ar}), 120.0 (d, C_{Ar}), 118.1 (d, C_{Ar}), 114.5 (s, C_{Ar}), 95.6 (2t), 56.4/56.2 (2q).

Analytical data were in accordance with literature values¹⁵⁷.

7.3.2.3. 2-(4-Bromophenoxy)-*N,N*-diethylethanamine (49)

Sodium hydride (as 60% dispersion in mineral oil, 4.539 g, 189.2 mmol) was washed with *n*-hexane and suspended in anhydrous DMF (100 mL). A mixture of 4-bromophenol (**47**, 16.370 g, 94.6 mmol) and 2-chloro-*N,N*-diethylethanamine hydrochloride (16.281 g, 94.6 mmol) was dissolved in DMF (100 mL) and the resulting solution was added in small portions to the previously prepared sodium hydride suspension. After the formation of gas had ceased, the reaction mixture was heated up and stirred at 90 °C overnight. Filtration through a pad of Celite and evaporation of the obtained filtrate gave a residue that was again dissolved in Et₂O (300 mL). This organic layer was then consecutively washed with aqueous NaOH (10%, 50 mL) and water (3 x 50 mL). Drying over Na₂SO₄ and removal of the solvent *in vacuo* afforded compound **49** as yellow oil (22.660 g, 88% yield).

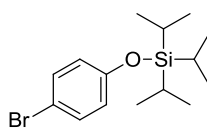
R_f (DCM/MeOH, 10:1) = 0.46.

¹H-NMR (400 MHz, CDCl₃): δ_H = 7.34 (2H, d, *J* = 8.8 Hz, H_{Ar}), 6.77 (2H, d, *J* = 8.9 Hz, H_{Ar}), 3.99 (2H, t, *J* = 6.3 Hz, O-CH₂), 2.84 (2H, t, *J* = 6.3 Hz, N-CH₂-CH₂), 2.62 (4H, q, *J* = 7.1 Hz, Me-CH₂), 1.05 (6H, t, *J* = 7.1 Hz, Me).

¹³C-NMR (100 MHz, CDCl₃): δ_C = 158.1 (s, C_{Ar}), 132.3 (d, C_{Ar}), 116.4 (d, C_{Ar}), 112.9 (s, C_{Ar}), 67.0 (t, O-CH₂), 51.8 (t, N-CH₂-CH₂), 48.0 (t, Me-CH₂), 12.0 (q, Me).

HRMS (ESI): *m/z* [M+H]⁺ calcd. for C₁₂H₁₈BrNO: 272.0645; found: 272.0636.

Analytical data were in accordance with literature values¹⁵⁸.

7.3.2.4. (4-Bromophenoxy)triisopropylsilane (57)**57**C₁₅H₂₅BrOSi
329.35

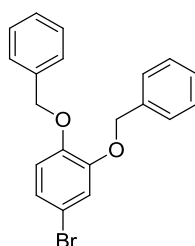
Triisopropylsilyl chloride (3.669 g, 19.0 mmol) was added to a solution of 4-bromophenol (**47**, 3.0 g, 17.3 mmol) in DMF (9 mL) and the resulting reaction mixture was stirred at room temperature for 8 hours. After quenching with saturated aqueous NH₄Cl solution (5 mL), the mixture was extracted with Et₂O (3 x 20 mL) and the combined organic layers were washed with brine (2 x 10 mL). Drying over Na₂SO₄ and removal of the solvent by rotary evaporation gave the protected bromophenol **57** as colorless liquid (5.698 g, 100% yield).

R_f (PE/EtOAc, 3:1) = 0.85.

¹H-NMR (400 MHz, CDCl₃): δ_H = 7.31 (2H, d, *J* = 8.8 Hz, H_{Ar}), 6.76 (2H, d, *J* = 8.8 Hz, H_{Ar}), 1.25 (3H, sept, *J* = 7.4 Hz, CH), 1.10/1.06 (18H, 2s, CH₃).

¹³C-NMR (100 MHz, CDCl₃): δ_C = 155.4 (s, C_{Ar}), 132.4 (d, C_{Ar}), 121.8 (d, C_{Ar}), 113.3 (s, C_{Ar}), 18.0 (q, CH₃), 12.7 (d, CH).

Analytical data were in accordance with literature values¹⁵⁹.

7.3.2.5. (((4-Bromo-1,2-phenylene)bis(oxy))bis(methylene))dibenzene (62)¹²⁸**62**C₂₀H₁₇BrO₂
369.25

To a solution of 4-bromocatechol (**45**, 2.858 g, 15.1 mmol) in acetone (75 mL), K₂CO₃ (7.758 g, 45.4 mmol) and benzyl bromide (6.269 g, 45.4 mmol) were added and the mixture was refluxed overnight. After filtration through a short pad of Celite, the filtrate was concentrated in vacuum to obtain a yellow oil. This residue was redissolved in Et₂O (100 mL)

and the so obtained organic layer was once washed with brine (20 mL), dried over Na₂SO₄ and evaporated again. Purification was achieved by silica gel chromatography using PE → PE/Et₂O (5%) to yield compound **62** as white solid (4.354 g, 78% yield).

R_f (PE/EE, 3:1) = 0.54.

M_p = 63 – 65 °C.

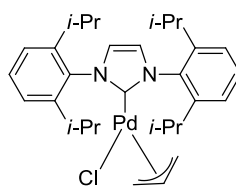
¹H-NMR (400 MHz, CDCl₃): δ_H = 7.48 – 7.31 (10H, m, H_{Ar}), 7.08 (1H, d, J = 2.2 Hz, H_{Ar}), 7.00 (1H, dd, J = 2.3/8.6 Hz, H_{Ar}), 6.80 (1H, d, J = 8.6 Hz, H_{Ar}), 5.13 (4H, 2s, CH₂).

¹³C-NMR (100 MHz, CDCl₃): δ_C = 150.0 (s, C_{Ar}), 148.3 (s, C_{Ar}), 137.0 (s, C_{Ar}), 136.7 (s, C_{Ar}), 128.7 (2d, C_{Ar}), 128.1 (2d, C_{Ar}), 127.5/127.2 (2d, C_{Ar}), 124.3 (d, C_{Ar}), 118.3 (d, C_{Ar}), 116.6 (d, C_{Ar}), 113.6 (s, C_{Ar}), 71.6/71.5 (2t, CH₂).

Analytical data were in accordance with literature values¹²⁸.

7.3.2.6. Allyl[1,3-bis(2,6-diisopropylphenyl)imidazol-2-ylidene]chloropalladium(II)

[(IPr)Pd(allyl)Cl] (**51**)¹⁶⁰



51

C₃₀H₄₂ClN₂Pd
572.54

A suspension of 1,3-bis(2,6-diisopropylphenyl)imidazolium chloride (IPr.HCl, 1.488 g, 3.50 mmol) in anhydrous THF (21 mL) was cooled to -40 °C and *n*-BuLi (1.6 M in hexanes, 2.3 mL, 3.68 mmol) was slowly added. The mixture was allowed to warm up to room temperature and after 45 minutes of stirring, (Pd(allyl)Cl)₂ (0.258 g, 0.70 mmol) was added and stirring continued for another three hours. After filtration of the reaction mixture, the resulting filtrate was concentrated in vacuum and the obtained residue was redissolved in anhydrous DCM. Filtration of this solution through a short pad of silica gel, followed by evaporation of the solvent gave a yellow residue that was purified by trituration with *n*-hexane to give (IPr)Pd(η^3 -allyl)Cl as white crystals (**51**, 0.669 g, 83% yield).

R_f (PE/EtOAc, 3:1) = 0.19.

¹H-NMR (400 MHz, CDCl₃): δ_H = 7.49 (2H, t, J = 7.4 Hz), 7.28 (4H, d, J = 3.7 Hz), 7.16 (2H, s), 4.82 (1H, m), 3.90 (1H, d, J = 6.7 Hz), 3.13 (2H, quin, J = 6.0 Hz), 3.05 (1H, d, J = 6.0 Hz), 2.86

(2H, quin, $J = 6.7$ Hz), 2.78 (1H, d, $J = 13.3$ Hz), 1.59 (1H, d, $J = 13.0$ Hz), 1.39 (6H, d, $J = 6.1$ Hz), 1.34 (6H, d, $J = 5.9$ Hz), 1.18 (6H, d, $J = 6.0$ Hz), 1.09 (6H, d, $J = 6.2$ Hz).

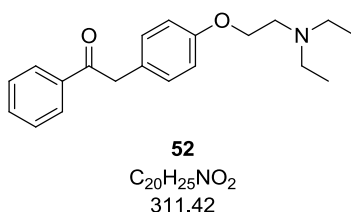
$^{13}\text{C-NMR}$ (100 MHz, CDCl_3): $\delta_{\text{C}} = 186.2, 146.3, 146.1, 135.9, 130.0, 124.3, 124.0, 123.9, 114.3, 72.6, 49.6, 28.7, 28.6, 26.7, 25.9, 23.1, 22.9$.

Analytical data were in accordance with literature values¹⁶¹.

7.3.2.7. General procedure for the preparation of deoxybenzoins **52**, **58** and **61**

A microwave vial is loaded in the glove box with (IPr)Pd(allyl)Cl (**51**, 2.0 mol%) and sodium *tert*-butoxide (3 equiv). A solution of freshly distilled acetophenone (2.5 equiv) and the appropriate aryl halogenide (1 equiv) in anhydrous THF (40 mL/g arylhalogenide) is also transferred into this reaction vial, before it gets subjected to microwave irradiation for one hour at 100 °C. After cooling down to room temperature, the reaction mixture is poured into saturated aqueous NH_4Cl solution (5 mL) and extracted with Et_2O (3 x 10 mL). The combined organic layers are washed with brine (10 mL), dried over Na_2SO_4 and the solvent is evaporated to afford the crude product.

7.3.2.7.1. 2-(4-(2-(Diethylamino)ethoxy)phenyl)-1-phenylethanone (**52**)



Bromide **49** (0.428 g, 1.58 mmol) was reacted with acetophenone according to the procedure described in 7.3.2.7. Purification of the crude product was performed by silica gel chromatography with DCM/MeOH (1% → 6% MeOH) to afford deoxybenzoin **52** as yellow crystals (0.473 g, 96% yield).

R_f (DCM/MeOH, 10:1) = 0.24.

$M_p = 68 - 69$ °C.

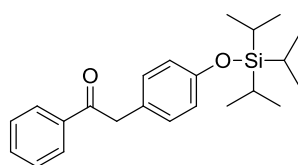
$^1\text{H-NMR}$ (400 MHz, CDCl_3): $\delta_{\text{H}} = 8.00$ (2H, d, $J = 7.3$ Hz, H_{Ar}), 7.58 – 7.52/7.48 – 7.42 (3H, 2m, H_{Ar}), 7.16 (2H, d, $J = 8.5$ Hz, H_{Ar}), 6.86 (2H, d, $J = 8.8$ Hz, H_{Ar}), 4.22 (2H, s, (CO)- CH_2), 4.04 (2H, t, $J = 6.3$ Hz, O- CH_2), 2.88 (2H, t, $J = 6.3$ Hz, N- CH_2 - CH_2), 2.65 (4H, q, $J = 7.1$ Hz, CH_3 - CH_2), 1.07 (6H, t, $J = 7.0$ Hz, CH_3).

$^{13}\text{C-NMR}$ (100 MHz, CDCl_3): δ_{C} = 198.1 (s, $\text{C}_{\text{carbonyl}}$), 157.9 (s, C_{Ar}), 136.7 (s, C_{Ar}), 133.2 (d, C_{Ar}), 130.6 (d, C_{Ar}), 128.7 (2d, C_{Ar}), 126.7 (s, C_{Ar}), 114.9 (d, C_{Ar}), 66.4 (t, O- CH_2), 51.8 (t, N- CH_2 - CH_2), 47.8 (t, CH_3 - CH_2), 44.8 (t, (CO)- CH_2), 11.8 (q, CH_3).

IR (neat): ν = 1690 (CO), 1512, 1336, 1237, 1218, 1202, 1177, 1034, 999, 795, 751, 689, 571.

HRMS (ESI): m/z [$\text{M}+\text{H}$] $^+$ calcd. for $\text{C}_{20}\text{H}_{25}\text{NO}_2$: 312.1958; found: 312.1956.

7.3.2.7.2. 1-Phenyl-2-(4-((triisopropylsilyloxy)phenyl)ethanone (58)



58

$\text{C}_{23}\text{H}_{32}\text{O}_2\text{Si}$
368.58

The reaction of aryl bromide **57** (0.450 g, 1.37 mmol) with acetophenone according to the procedure described under 7.3.2.7 gave deoxybenzoin **58**. Purification was achieved by silica gel chromatography using PE \rightarrow PE/benzene (35%) to afford the pure product as yellow oil (0.338 g, 67% yield).

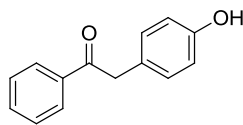
R_f (PE/EtOAc, 5:1) = 0.58.

$^1\text{H-NMR}$ (400 MHz, CDCl_3): δ_{H} = 7.89 (2H, d, J = 7.4 Hz, H_{Ar}), 7.40 – 7.29 (3H, m, H_{Ar}), 7.00 (2H, J = 8.2 Hz, H_{Ar}), 6.73 (2H, J = 8.3 Hz, H_{Ar}), 4.10 (2H, s, CH_2), 1.14 (3H, sept, J = 7.2 Hz, CH), 0.99/0.97 (18H, 2s, CH_3).

$^{13}\text{C-NMR}$ (100 MHz, CDCl_3): δ_{C} = 198.2 (s, $\text{C}_{\text{carbonyl}}$), 155.1 (s, C_{Ar}), 136.8 (s, C_{Ar}), 133.15 (d, C_{Ar}), 130.5 (d, C_{Ar}), 128.8 (d, C_{Ar}), 128.7 (d, C_{Ar}), 127.0 (s, C_{Ar}), 120.2 (d, C_{Ar}), 44.9 (t, CH_2), 18.0 (q, CH_3), 12.8 (d, CH).

IR (neat): ν = 1694 (CO), 1509, 1256, 903, 884, 757, 679, 660, 644.

HRMS (ESI): m/z [$\text{M}+\text{H}$] $^+$ calcd. for $\text{C}_{23}\text{H}_{32}\text{O}_2\text{Si}$: 369.2244; found: 369.2244.

7.3.2.7.3. 2-(4-Hydroxyphenyl)-1-phenylethanone (61)

61
C₁₄H₁₂O₂
212.24

The TBS-protected aryl iodide **59** (0.10 g, 0.30 mmol) was reacted with acetophenone according to the procedure described under 7.3.2.7. Additionally to the planned α -arylation also deprotection occurred, so that after purification by silica gel chromatography using PE \rightarrow PE/EtOAc (25%), the phenolic deoxybenzoin **61** was obtained (0.064 g, 65% yield).

R_f (PE/EtOAc, 5:1) = 0.15.

M_p = 134 – 136 °C.

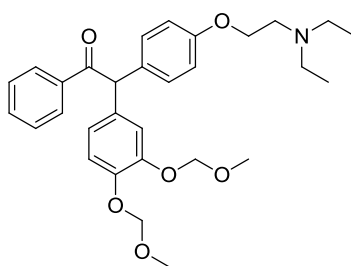
¹H-NMR (400 MHz, CDCl₃): δ_{H} = 8.01 (2H, d, J = 8.0 Hz, H_{Ar}), 7.56 (1H, m, H_{Ar}), 7.46 (2H, m, H_{Ar}), 7.11 (2H, d, J = 8.2 Hz, H_{Ar}), 6.77 (2H, d, J = 8.3 Hz, H_{Ar}), 5.25 (1H, bs, OH), 4.22 (2H, s, CH₂).

¹³C-NMR (100 MHz, CDCl₃): δ_{C} = 198.6 (s, C_{carbonyl}), 154.8 (s, C_{Ar}), 136.7 (s, C_{Ar}), 133.4 (d, C_{Ar}), 130.8 (d, C_{Ar}), 128.8 (2d, C_{Ar}), 126.5 (s, C_{Ar}), 115.8 (d, C_{Ar}), 44.7 (t, CH₂).

IR (neat): ν = 1682 (CO), 1515, 1448, 1334 (OH), 1218, 996, 797, 751, 689.

7.3.2.8. General procedure for the preparation of ketones 53 and 63

A microwave vial is loaded in the glove box with Pd₂(dba)₃.CHCl₃ (2 mol%), 1,1'-bis(di-*tert*-butylphosphino)ferrocene (2.5 mol%) and sodium *tert*-butoxide (3 equiv for the preparation of **53**/2 equiv for **63**). A solution of the appropriate deoxybenzoin (1 equiv) and bromide (1.5 equiv) in anhydrous THF (36 mL/g **52**, 46 mL/g **58**) is also transferred to this vial, before it gets subjected to microwave irradiation (temperature and time indications can be found in the corresponding substance sections 7.3.2.8.1 and 7.3.2.8.2). After the addition of water (5 mL), extraction with Et₂O (3 x 10 mL) is performed and the combined organic layers are washed with brine (10 mL) and dried over Na₂SO₄. Evaporation of the solvent gives the crude product.

7.3.2.8.1. 2-(3,4-Bis(methoxymethoxy)phenyl)-2-(4-(2-(diethylamino)ethoxy)phenyl)-1-phenylethanone (53)**53**C₃₀H₃₇NO₆
507.62

For the reaction of deoxybenzoin **52** (0.343 g, 1.10 mmol) with bromide **46** (0.449 g, 1.65 mmol), a microwave vial was loaded with the corresponding reagents following the above described procedure (see 7.3.2.8). Exposure to microwave irradiation was performed for one hour at 70 °C. NMR-analysis of a small sample showed 50% conversion, so that further portions of Pd-catalyst (0.023 g, 2 mol%) and ligand (0.013 g, 2.5 mol%) were added and microwave irradiation at 70 °C was continued for further 1.5 hours. The conversion was again checked and once again Pd-catalyst (0.023 g, 2 mol%) and ligand (0.013 g, 2.5 mol%) were added and the vial was one last time subjected to microwave irradiation at 70 °C for one hour. The crude product was obtained via the above described workup procedure (see 7.3.2.8) and purified by silica gel chromatography using DCM/MeOH (1% → 5% MeOH) to obtain ketone **53** as brown oil (0.441 g, 79% yield).

R_f (DCM/MeOH, 12:1) = 0.45.

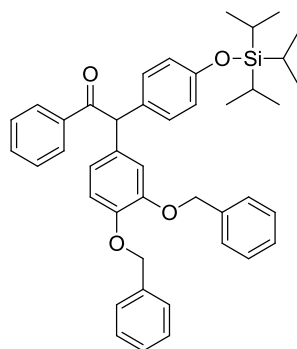
¹H-NMR (400 MHz, CD₂Cl₂): δ_H = 7.98 (2H, d, *J* = 7.5 Hz, H_{Ar}), 7.54 – 7.47/7.44 – 7.35 (3H, 2m, H_{Ar}), 7.16 (2H, d, *J* = 8.6 Hz, H_{Ar}), 7.07 – 7.00/6.90 – 6.78 (5H, 2m, H_{Ar}), 5.91 (1H, s, (CO)-CH), 5.14/5.12 (4H, 2s, O-CH₂-O), 3.98 (2H, t, *J* = 6.2 Hz, O-CH₂-CH₂), 3.45/3.44 (6H, 2s, O-CH₃), 2.80 (2H, t, *J* = 6.2 Hz, N-CH₂-CH₂), 2.57 (4H, q, *J* = 7.1 Hz, CH₃-CH₂), 1.01 (6H, t, *J* = 7.1 Hz, CH₂-CH₃).

¹³C-NMR (100 MHz, CD₂Cl₂): δ_C = 198.3 (s, C_{carbonyl}), 158.2 (s, C_{Ar}), 147.5 (s, C_{Ar}), 146.7 (s, C_{Ar}), 136.9 (s, C_{Ar}), 133.9 (s, C_{Ar}), 133.0 (d, C_{Ar}), 131.3 (s, C_{Ar}), 130.1 (d, C_{Ar}), 128.9 (d, C_{Ar}), 128.7 (d, C_{Ar}), 123.2 (d, C_{Ar}), 118.4 (d, C_{Ar}), 117.2 (d, C_{Ar}), 114.7 (d, C_{Ar}), 95.9/95.6 (2t, O-CH₂-O), 66.8 (t, O-CH₂-CH₂), 58.0 (d, (CO)-CH), 56.2/56.1 (2q, O-CH₃), 52.0 (t, N-CH₂-CH₂), 47.7 (t, CH₃-CH₂), 11.8 (CH₂-CH₃).

IR (neat): ν = 1685 (CO), 1597, 1508, 1248, 1151, 1072, 986, 693.

HRMS (ESI): m/z [M+H]⁺ calcd. for C₃₀H₃₇NO₆: 508.2694; found: 508.2701.

7.3.2.8.2. 2-(3,4-Bis(benzyloxy)phenyl)-1-phenyl-2-(4-((triisopropylsilyl)oxy)-phenyl)ethanone (**63**)



63

C₄₃H₄₈O₄Si
656.92

Starting from deoxybenzoin **58** (0.504 g, 1.37 mmol) and aryl bromide **62** (0.759 g, 2.06 mmol), ketone **63** was obtained by following procedure 7.3.2.8. The loaded reaction vial was exposed to microwave irradiation for one hour at 70 °C. NMR analysis of a small sample showed that there was still starting material present, so that more Pd-catalyst (0.028 g, 2 mol%) and ligand (0.016 g, 2.5 mol%) were added and irradiation was continued for 1.5 hours. Again a smaller amount of Pd-catalyst (0.014 g, 1 mol%) and ligand (0.008 g, 1 mol%) was added and the reaction mixture was subjected to irradiation for 20 more minutes, until the deoxybenzoin was fully converted. After reaction workup according to 7.3.2.8, the crude product was isolated and purification was achieved by silica gel chromatography using PE → PE/EtOAc (4%) to yield ketone **63** as colorless oil.

R_f (PE/EtOAc) = 0.46.

¹H-NMR (400 MHz, CDCl₃): δ_{H} = 7.95 (2H, d, J = 7.5 Hz, H_{Ar}), 7.53 – 7.27 (13H, m, H_{Ar}), 7.05 (2H, d, J = 8.4 Hz, H_{Ar}), 6.91 – 6.73 (5H, m, H_{Ar}), 5.85 (1H, s, (CO)-CH), 5.12/5.09 (4H, 2s, CH₂), 1.25 (3H, sept, J = 7.4 Hz, (CH₃)₂CH), 1.10/1.08 (18H, 2s, CH₃).

¹³C-NMR (100 MHz, CDCl₃): δ_{C} = 198.8 (s, C_{carbonyl}), 155.2 (s, C_{Ar}), 148.9 (s, C_{Ar}), 148.3 (s, C_{Ar}), 137.5 (s, C_{Ar}), 137.3 (s, C_{Ar}), 137.1 (s, C_{Ar}), 133.0 (d, C_{Ar}), 132.8 (s, C_{Ar}), 131.6 (s, C_{Ar}), 130.1 (d, C_{Ar}), 129.0 (d, C_{Ar}), 128.7 (d, C_{Ar}), 128.6 (d, C_{Ar}), 128.5 (d, C_{Ar}), 127.9/127.8 (2d, C_{Ar}), 127.6 (d,

C_{Ar} , 127.4 (d, C_{Ar}), 122.2 (d, C_{Ar}), 120.2 (d, C_{Ar}), 116.4 (d, C_{Ar}), 115.0 (d, C_{Ar}), 71.4 (2t, CH_2), 58.2 (d, (CO)- \underline{CH}), 18.0 (q, CH_3), 12.8 (d, $(CH_3)_2\underline{CH}$).

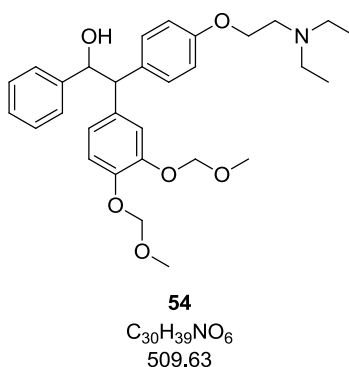
IR (neat): ν = 1685 (CO), 1605, 1506, 1262, 1002, 911, 883, 733, 688.

HRMS (ESI): m/z [$M-C_{20}H_{18}O_2+H$]⁺ calcd. for $C_{23}H_{30}O_2Si$: 367.2088; found: 367.2084.

7.3.2.9. General procedure for the preparation of alcohols **54** and **64**

$LiAlH_4$ (1 equiv) is added to a solution of the appropriate ketone in anhydrous THF (130 mL/g ketone). The resulting reaction mixture is stirred for one hour at room temperature, before it gets hydrolyzed with aqueous potassium sodium tartrate solution and stirred for another 30 minutes. The aqueous layer is extracted (using EtOAc for **54**/ Et_2O for **64**) and the combined organic layers are dried over Na_2SO_4 . Removal of the solvent by rotary evaporation gives the crude product as a 1:1-mixture of two diastereomers.

7.3.2.9.1. 2-(3,4-Bis(methoxymethoxy)phenyl)-2-(4-(2-(diethylamino)ethoxy)phenyl)-1-phenylethanol (**54**)



Starting from ketone **53** (0.023 g, 0.05 mmol) reduction according to the above described procedure (see 7.3.2.9) gave alcohol **54** as a 1:1-mixture of two diastereomers. Purification and separation of the two isomers was achieved by silica gel chromatography using DCM/MeOH (30:1) to obtain the two diastereomers as brown oils (0.016 g, 68% yield).

Diastereomer 1:

R_f = (DCM/MeOH, 6:1, +TEA) 0.39.

1H -NMR (400 MHz, CD_2Cl_2): δ_H = 7.25 – 6.97 (10H, m, H_{Ar}), 6.66 (2H, d, J = 8.5 Hz, H_{Ar}), 5.26 (1H, d, J = 9.1 Hz, HO- \underline{CH}), 5.14 (4H, 2s, O- \underline{CH}_2 -O), 4.10 (1H, d, J = 9.1 Hz, HO-CH- \underline{CH}), 3.91

(2H, t, $J = 5.4$ Hz, O-CH₂-CH₂), 3.47/3.46 (6H, 2s, O-CH₃), 2.77 (2H, t, $J = 5.4$ Hz, N-CH₂-CH₂), 2.57 (4H, q, $J = 5.5$ Hz, N-CH₂-CH₃), 1.00 (6H, t, $J = 7.0$ Hz, CH₂-CH₃).

¹³C-NMR (100 MHz, CD₂Cl₂): $\delta_C = 162.0$ (s, C_{Ar}), 147.6 (s, C_{Ar}), 146.4 (s, C_{Ar}), 142.7 (s, C_{Ar}), 134.2 (s, C_{Ar}), 129.4 (d, C_{Ar}), 128.0 (d, C_{Ar}), 127.5 (d, C_{Ar}), 127.1 (d, C_{Ar}), 125.8 (s, C_{Ar}), 122.4 (d, C_{Ar}), 118.0 (d, C_{Ar}), 117.5 (d, C_{Ar}), 114.2 (d, C_{Ar}), 95.8/95.7 (2t, O-CH₂-O), 76.9 (d, HO-CH), 66.6 (t, O-CH₂-CH₂), 58.9 (d, HO-CH-CH), 56.2/56.1 (q, O-CH₃), 51.9 (t, N-CH₂-CH₂), 47.7 (t, CH₃-CH₂), 11.8 (q, CH₂-CH₃).

IR (neat): $\nu = 1508, 1245$ (OH), 1152, 1071, 992, 702, 632.

HRMS (ESI): m/z [M+H]⁺ calcd. for C₃₀H₃₉NO₆: 510.2850; found: 510.2864.

Diastereomer 2:

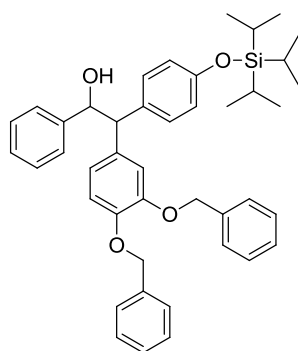
R_f = (DCM/MeOH, 6:1, +TEA) 0.25.

¹H-NMR (400 MHz, CD₂Cl₂): $\delta_H = 7.29$ (2H, d, $J = 8.6$ Hz, H_{Ar}), 7.26 – 7.15 (5H, m, H_{Ar}), 6.89 – 6.82 (4H, m, H_{Ar}), 6.72 (1H, dd, $J = 1.7/8.4$ Hz, H_{Ar}), 5.25 (1H, d, $J = 9.0$ Hz, HO-CH), 5.05/4.99 (4H, 2s, O-CH₂-O), 4.10 (1H, d, $J = 9.0$ Hz, HO-CH-CH), 3.98 (2H, t, $J = 6.2$ Hz, O-CH₂-CH₂), 3.40/3.39 (6H, 2s, O-CH₃), 2.80 (2H, t, $J = 6.2$ Hz, N-CH₂-CH₂), 2.58 (4H, q, $J = 7.1$ Hz, N-CH₂-CH₃), 1.01 (6H, t, $J = 7.1$ Hz, CH₂-CH₃).

¹³C-NMR (100 MHz, CD₂Cl₂): $\delta_C = 158.0$ (s, C_{Ar}), 154.7 (s, C_{Ar}), 153.9 (s, C_{Ar}), 142.8 (s, C_{Ar}), 136.7 (s, C_{Ar}), 133.3 (s, C_{Ar}), 129.8 (d, C_{Ar}), 128.1 (d, C_{Ar}), 127.5 (d, C_{Ar}), 127.1 (d, C_{Ar}), 122.4 (d, C_{Ar}), 117.8 (d, C_{Ar}), 117.0 (d, C_{Ar}), 114.7 (d, C_{Ar}), 95.8/95.7 (2t, O-CH₂-O), 76.9 (d, HO-CH), 66.8 (t, O-CH₂-CH₂), 58.8 (d, HO-CH-CH), 56.1 (q, O-CH₃), 52.0 (t, N-CH₂-CH₂), 47.8 (t, CH₃-CH₂), 11.8 (q, CH₂-CH₃).

IR (neat): $\nu = 1509, 1247$ (OH), 1154, 1073, 998, 701, 631.

HRMS (ESI): m/z [M+H]⁺ calcd. for C₃₀H₃₉NO₆: 510.2850; found: 510.2869.

7.3.2.9.2. 2-(3,4-Bis(benzyloxy)phenyl)-1-phenyl-2-(4-((triisopropylsilyl)oxy)phenyl)-ethanol (64)**64**

C₄₃H₅₀O₄Si
658.94

Ketone **63** (0.068 g, 0.10 mmol) was subjected to LiAlH₄-reduction according to procedure 7.3.2.9 to obtain the crude compound **64**, which was purified by silica gel chromatography using PE/EtOAc (5% → 40% EtOAc) to obtain the pure alcohol as mixture of two diastereomers (0.053 g, 78% yield).

R_f (PE/EtOAc, 5:1) = 0.33/0.22.

¹H-NMR (400 MHz, CDCl₃): δ_H = 7.48 – 7.24/7.23 – 7.04/6.98 – 6.77/6.73 – 6.53 (4H, 4m, H_{Ar}), 5.17/5.16 (2H, 2d, HO-CH), 5.14/5.13 (4H, 2s, CH₂), 5.05/4.96 (4H, 2s, CH₂), 4.04/4.03 (2H, 2d, *J* = 8.2/8.3 Hz, HO-CH-CH), 2.06 (2H, bs, OH), 1.30 – 1.15 (6H, m, (CH₃)₃-CH), 1.11/1.09/1.06/1.04 (36H, 4s, CH₃).

¹³C-NMR (100 MHz, CDCl₃): δ_C = 155.1/154.6 (2s, C_{Ar}), 148.4/148.2 (2s, C_{Ar}), 147.6 (2s, C_{Ar}), 142.4 (2s, C_{Ar}), 137.5 (2s, C_{Ar}), 135.2 (2s, C_{Ar}), 134.3/134.2 (2s, C_{Ar}), 132.9 (2s, C_{Ar}), 130.0 (2d, C_{Ar}), 129.5 (2d, C_{Ar}), 128.6 (2d, C_{Ar}), 128.5 (2d, C_{Ar}), 128.1/128.0 (2d, C_{Ar}), 128.9 (4d, C_{Ar}), 127.6 (2d, C_{Ar}), 127.5/127.4 (2d, C_{Ar}), 127.0 (2d, C_{Ar}), 122.0/121.7 (2d, C_{Ar}), 120.3/119.7 (2d, C_{Ar}), 116.4/116.2 (2d, C_{Ar}), 115.2/114.8 (2d, C_{Ar}), 77.2 (2d, HO-CH), 71.4 (2t, CH₂), 59.3/59.0 (2d, HO-CH-CH), 18.1/18.0 (2q, CH₃), 12.8/12.7 (2d, (CH₃)₂-CH).

IR (neat): ν = 1606, 1507, 1454, 1261 (OH), 1014, 911, 696, 634.

HRMS (ESI): *m/z* [M-H₂O+H]⁺ calcd. for C₄₃H₄₈O₃Si: 641.3445; found: 641.3488.

7.4. Metabolic model reactions

7.4.1. Chemical oxidation of clomiphene

Table 10 and Table 11 summarize all experiments that were conducted for the simulation of clomiphene's metabolism via biomimetic model systems. Whereas Table 10 focuses on the application of common chemical oxidants, Table 11 shows all applied Fenton-based systems. If not stated otherwise, the listed oxidants and additives were added to a solution of clomiphene citrate (0.015 g, 0.025 mmol) in the respective solvent and stirred at the indicated temperature for a period of one to three days. The conversion of the substrate was checked periodically by TLC. In cases where no conversion was detected, the temperature was raised from room temperature to 80 °C. The mixtures were treated with aqueous ammonia solution (25%) to adjust their pH-value to 7 – 8, followed by extraction with EtOAc. The combined EtOAc-layers were dried over Na₂SO₄ and evaporated under reduced pressure to give the corresponding product(s) as residue, which was subjected to GC-MS and LC-MS analysis.

Table 10 Chemical oxidation of clomiphene. ^aAq. H₂O₂/*t*-BuOOH solution (30%/70%) was added dropwise to the substrate solution over a period of 15 minutes. ^bAddition of CF₃COOH was followed by addition of oxidant.

entry	oxidant	additives	solvent	T [°C]
1 ^a	H ₂ O ₂ (6 equiv)	-	H ₂ O (1.0 mL)	r.t./80 °C
2 ^a	<i>t</i> -BuOOH (6 equiv)	-	H ₂ O (1.0 mL)	r.t./80 °C
3 ^b	H ₂ O ₂ (0.2 equiv)	CF ₃ COOH (3 equiv)	DCM (2.5 mL)	r.t.
4 ^b	<i>m</i> -CPBA (0.2 equiv)	CF ₃ COOH (3 equiv)	DCM (2.5 mL)	r.t.

Table 11 Oxidation of clomiphene via Fenton systems. ^aAq. H₂O₂/t-BuOOH solution (30%/70%) was added dropwise to a solution of all other compounds over a period of 15 minutes. ^bSubstrate solution was heated up to 80 °C, followed by addition of aq. Fe-salt solution (0.5 M) and H₂O₂ (50%). ^cApplication of anhydrous FeSO₄. ^dCombination of FeCl₃ (10mM in MeCN), EDTA (10mM in MeCN), clomiphene citrate (10 mM in MeCN), ascorbic acid (1M in H₂O) and H₂O₂ (50%). ^epH-value of a solution containing all compounds was set to 3 using H₂SO₄, followed by the addition of H₂O₂. ^fInverse addition of aq. solution of FeSO₄ (0.05 M) to solution of other compounds.

entry	Fe(II) salt	oxidant	additives	solvent	T [°C]
5 ^a	FeCl ₂ x 4H ₂ O (2 equiv)	H ₂ O ₂ (4 equiv)	-	H ₂ O (1 mL)	r.t./80
6 ^a	FeSO ₄ x 7H ₂ O (2 equiv)	H ₂ O ₂ (4 equiv)	-	H ₂ O (1 mL)	r.t./80
7 ^a	FeCl ₂ x 4H ₂ O (2 equiv)	t-BuOOH (4 equiv)	-	H ₂ O (1 mL)	r.t./80
8 ^b	FeSO ₄ x 7H ₂ O (1 equiv)	H ₂ O ₂ (2 equiv)	-	H ₂ O (1 mL)	80
9 ^b	FeCl ₂ x 4H ₂ O (1 equiv)	H ₂ O ₂ (2 equiv)	-	H ₂ O (1 mL)	80
10 ^c	FeSO ₄ (2 equiv)	H ₂ O ₂ (2 equiv)	-	DCM (4 mL)	r.t.
11	FeCl ₂ x 4H ₂ O (5 equiv)	H ₂ O ₂ (5 equiv)	EDTA (5 equiv)	H ₂ O (0.5 mL)	80
12	FeCl ₂ x 4H ₂ O (1 equiv)	H ₂ O ₂ (2 equiv)	EDTA (1 equiv)	H ₂ O (0.5 mL)	80
13 ^d	FeCl ₃ (1 equiv)	H ₂ O ₂ (10 equiv)	EDTA (1 equiv), L-(+)-ascorbic acid (5 equiv)	H ₂ O (1.5 mL)/MeCN	r.t.
14 ^a	FeSO ₄ x 7H ₂ O (1 equiv)	H ₂ O ₂ (2 equiv)	CuSO ₄ (3 equiv) H ₂ SO ₄ (5 equiv)	H ₂ O (0.5 mL)	80
15 ^e	FeCl ₃ (1 equiv)	H ₂ O ₂ (10 equiv)	TMPD (1 equiv) H ₂ SO ₄	H ₂ O (2.5 mL)	80
16 ^f	FeSO ₄ x 7H ₂ O (1 equiv)	K ₂ S ₂ O ₈ (2 equiv)	CuSO ₄ (3 equiv), H ₂ SO ₄ (5 equiv)	H ₂ O (2.5 mL)	80

LC-MS (ESI) (Method B):

CM 4 (clomiphene-*N*-oxide): $t_R = 7.1/7.3$ min; m/z [M+H]⁺ = 422.

CM 5 (deschloro-hydroxy-clomiphene): $t_R = 9.4$ min; m/z [M+H]⁺ = 388.

CM 6/7 (hydroxy-clomiphene): $t_R = 5.6/6.1/6.4/6.7$ min; m/z [M+H]⁺ = 422.

7.4.2. Incubation of clomiphene with human liver microsomes

7.4.2.1. Experiments for the optimization of incubation parameters

All test reactions for the optimization of incubation parameters were carried out in 1 mL-scale. Each incubation mixture contained purified water (713 µl), potassium phosphate buffer (0.5 M, pH 7.4, 200 µl), NADPH regenerating system solution A (BD Biosciences, 50 µl), NADPH regenerating system solution B (BD Biosciences, 10 µl) and substrate solution in

DMSO (2 μl). The concentration of the substrate solution was adapted to the required final concentration of clomiphenone in the incubation sample. After five minutes of preincubation at 37 °C in a water bath, the reactions were initiated by the addition of liver microsomes (25 μl for a final concentration of 0.5 mg/mL; 12.5 μl for a final concentration of 0.25 mg/mL). The reaction mixtures were incubated for the required periods of time and monitoring of the reaction progress was accomplished by sample-taking at regular intervals. For this purpose, the required amount (depending on the respective substrate concentration; absolute amount of substrate in the sample should be around 3 μg) was withdrawn from the incubation solution and added to 100 μl MeCN to stop the reaction. After centrifugation of the sample for three minutes (10 000 x g), the supernatant was withdrawn from the protein pellet and added to an aqueous carbonate buffer solution (20%, pH 9, 2 mL). The resulting solution was then extracted with MTBE (3 x 5 mL) and the combined organic phases were subjected to solvent removal *in vacuo*. After drying over P_2O_5 for 20 minutes, the residues were redissolved and analyzed via GC-MS or LC-MS. Blank samples without clomiphenone citrate for comparison were prepared and treated in the same way.

7.4.2.2. Identification of the unknown clomiphenone metabolites

To produce the unknown clomiphenone metabolites in amounts sufficient for characterization, the optimized HLM-incubation was scaled up to a final volume of 5 mL and four of these 5 mL-scale experiments were conducted in parallel. Each incubation mixture contained purified water (3565 μl), potassium phosphate buffer (0.5 M, pH 7.4, 1000 μl), *NADPH regenerating system solution A* (BD Biosciences, 250 μl), *NADPH regenerating system solution B* (BD Biosciences, 50 μl) and clomiphenone citrate (10 μl of a stock solution in DMSO with $c = 50.3$ mg/mL; final concentration in incubation mixture: 167 μM). After preincubation for five minutes at 37 °C in a water bath, the reaction was initiated by the addition of liver microsomes (125 μl). According to the optimized protocol, incubation was performed for 23 hours at 37 °C. The reaction was stopped by the addition of MeCN (5 mL) and the falcon tube was then subjected to centrifugation for three minutes (10 000 x g). The supernatants of all four experiments were combined and the protein pellets were rinsed with MeCN to detach residues. After the addition of an aqueous potassium phosphate buffer solution (0.5 M, pH 7.4), extraction with MTBE was performed. By the addition of an

aqueous carbonate buffer solution (20%, pH 9) the pH-value of the aqueous layer was raised and extraction with MTBE was conducted again. The combined organic layers were dried over Na_2SO_4 and the solvent was removed *in vacuo* to afford the enzyme extract as solid residue.

The separation of the enzyme extract and characterization of the unknown metabolites was accomplished by LC-SPE-NMR/MS. For this purpose the microsomal extract was dissolved in a MeOH/ H_2O -mixture (4:1) at 50 °C and afterwards filtered through a syringe filter. Concentration under reduced pressure gave a residue that was redissolved in MeOH/ H_2O (4:1) to give a completely clear solution (475 μl) that was used as injection solution.

8. APPENDICES

8.1. LIST OF ABBREVIATIONS

AAF	adverse analytical finding
ADAMS	Anti-Doping Administration & Management System
ATF	atypical finding
Ac	acetyl
AcOH	acetic acid
aq.	aqueous
Ar	aryl, aromatic
BINAP	2,2'-bis(diphenylphosphino)-1,1'-binaphthyl
Bn	benzyl
Bu	butyl
<i>n</i>-Bu	<i>n</i> -butyl
<i>t</i>-Bu	<i>t</i> -butyl
<i>t</i>-BuBrettPhos	2-(di- <i>tert</i> -butylphosphino)-2'-4'-6'-triisopropyl-3,6-dimethoxy-1,1'-biphenyl
<i>n</i>-BuLi	<i>n</i> -butyllithium
<i>t</i>-BuLi	<i>t</i> -butyllithium
c	concentration
calcd.	calculated
cat.	catalyst
conc.	concentrated
COSY	correlated spectroscopy
Cy	cyclohexyl
Da	dalton or unified atomic mass unit
DBU	1,8-diazabicyclo[5.4.0]undec-7-ene
dba	dibenzylideneacetone
DCC	<i>N,N'</i> -dicyclohexylcarbodiimide
DCE	1,2-dichloroethane
DCM	dichloromethane
DEAD	diethyl azodicarboxylate
DET	diethyl tartrate
DIPEA	<i>N,N</i> -diisopropylethylamine
DMAP	4-(dimethylamino)pyridine
DME	ethylene glycol dimethyl ether
DMF	<i>N,N</i> -dimethylformamide
DMSO	dimethylsulfoxide
DtBPF	1,1'-bis(di- <i>tert</i> -butylphosphino)ferrocene
EDTA	ethylenediaminetetraacetic acid
<i>ee</i>	enantiomeric excess
EI	electron ionization
EPO	erythropoietin
equiv	equivalent
ESI	electrospray ionization

Et	ethyl
<i>et al.</i>	latin: "et alii", meaning "and others"
Et₂O	diethyl ether
EtOAc	ethyl acetate
eV	electron Volt
EWG	electron-withdrawing group
GC	gas chromatography
HATU	<i>O</i> -(7-azabenzotriazol-1-yl)-1,1,3,3-tetramethyluronium hexafluorophosphate
HBTU	<i>O</i> -(benzotriazol-1-yl)-1,1,3,3-tetramethyluronium hexafluorophosphate
HDMA	1-((dimethylamino)(morpholino)methylene)-1 <i>H</i> -[1,2,3]-triazolo[4,5- <i>b</i>]pyridinium hexafluorophosphate 3-oxide
HDMB	1-((dimethylamino)(morpholino)methylene)-1 <i>H</i> -benzotriazolium hexafluorophosphate 3-oxide
HLM	human liver microsome
HMPA	hexamethylsilylphosphoramidate
HOAt	1-hydroxy-7-azabenzotriazole
HOBt	1-hydroxy-1 <i>H</i> -benzotriazole
HRMS	high resolution mass spectrometry
HPLC	high performance liquid chromatography
HWE	Horner-Wadsworth-Emmons
Hz	Hertz
IPr	1,3-bis(2,6-diisopropylphenyl)imidazolium
IR	infrared
<i>J</i>	coupling constant
<i>k</i>	rate constant
KHMDS	potassium hexamethylsilylazide
LC	liquid chromatography
LDA	lithium diisopropylamide
LHMDS	lithium hexamethylsilylazide
LiN	lithium naphthalenide
M	molar
<i>m</i>	meta
<i>m</i>-CPBA	<i>m</i> -chloroperbenzoic acid
Me	methyl
MeCN	acetonitrile
MeOH	methanol
min	minute
MOM	methoxy-methyl
Mp	melting point
MS	mass spectrometry
MSTFA	<i>N</i> -Methyl- <i>N</i> -(trimethylsilyl)trifluoroacetamide
MTBE	methyl <i>tert</i> -butyl ether
MTPE	α -methoxy- α -trifluoromethylphenylacetic acid
MW	microwave
<i>m/z</i>	mass-to-charge ratio
N	normal

NADA	National Anti-Doping Agency
NADPH	nicotinamide adenine dinucleotide phosphate
NaHMDS	sodium hexamethylsilylazide
NBS	<i>N</i> -bromosuccinimide
NCS	<i>N</i> -chlorosuccinimide
NHC	<i>N</i> -heterocyclic carbene
NMM	<i>N</i> -methylmorpholine
NMO	<i>N</i> -methylmorpholine- <i>N</i> -oxide
NMR	nuclear magnetic resonance
no conv.	no conversion
<i>o</i>	<i>ortho</i>
<i>p</i>	<i>para</i>
PCC	pyridinium chlorochromate
PE	petroleum ether
PG	protecting group
Ph	phenyl
ppm	parts per million
<i>i</i>-Pr	isopropyl
R^(1,2,...n)	any substituent
R_f	ratio of fronts (TLC)
r.t.	room temperature
SARM	selective androgen receptor modulator
SAE	Sharpless asymmetric epoxidation
sat.	saturated
SERM	selective estrogen receptor modulator
SIM	selective ion monitoring
SPE	solid phase extraction
SPhos	2-dicyclohexylphosphino-2',6'-dimethoxybiphenyl
SRM	selective reaction monitoring
TATU	<i>O</i> -(7-azabenzotriazol-1-yl)-1,1,3,3-tetramethyluronium tetrafluoroborate
TBTU	<i>O</i> -benzotriazol-1-yl-1,1,3,3-tetramethyluronium tetrafluoroborate
TBS	<i>tert</i> -butyldimethylsilyl
TEA	triethylamine
TEMPO	2,2,6,6-tetramethylpiperidinyloxy
Tf	trifluoromethanesulfonate
THF	tetrahydrofuran
TIC	total ion current
TIPS	triisopropylsilyl
TLC	thin layer chromatography
TMS	trimethylsilyl
TPAP	tetrapropylammonium perruthenate
TPE	triphenylethylene
<i>p</i>-TsOH	<i>para</i> -toluenesulfonic acid
UV/VIS	ultraviolet/visible
WADA	World Anti-Doping Agency
X	any halide

8.2. SELECTED SPECTRA

8.2.1. *rac*-2,3-Dihydroxy-2-methyl-*N*-(4-nitro-3-(trifluoromethyl)phenyl)-propanamide (*rac*-8, AM 1)

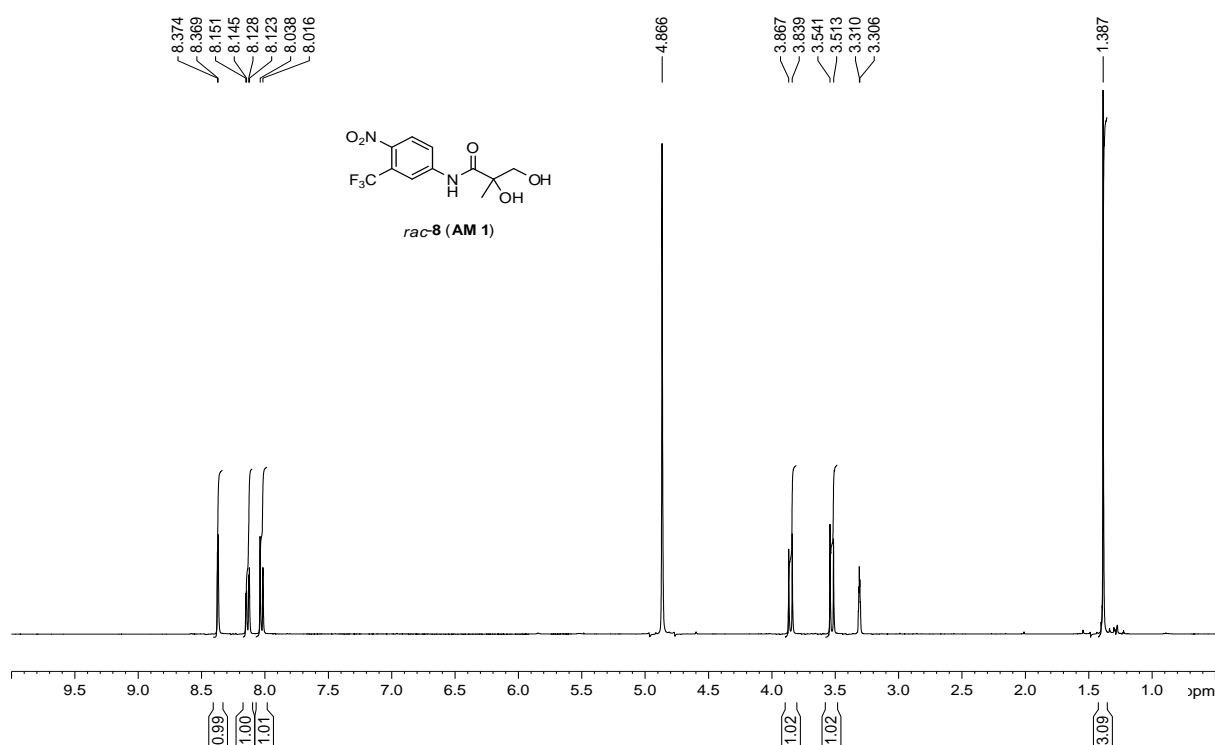


Figure 95 ¹H-NMR spectrum of compound *rac*-8 (AM 1).

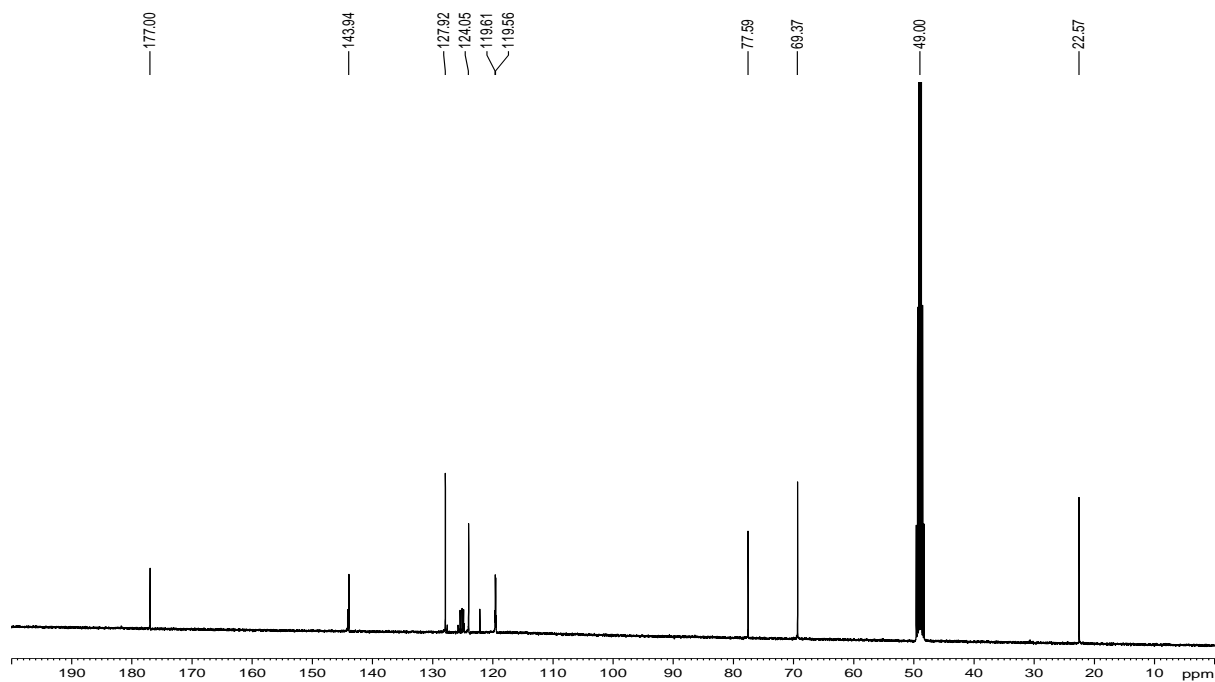


Figure 96 ¹³C-NMR spectrum of compound *rac*-8 (AM 1).

8.2.1.1. Comparison of synthetic AM 1 with excretion sample

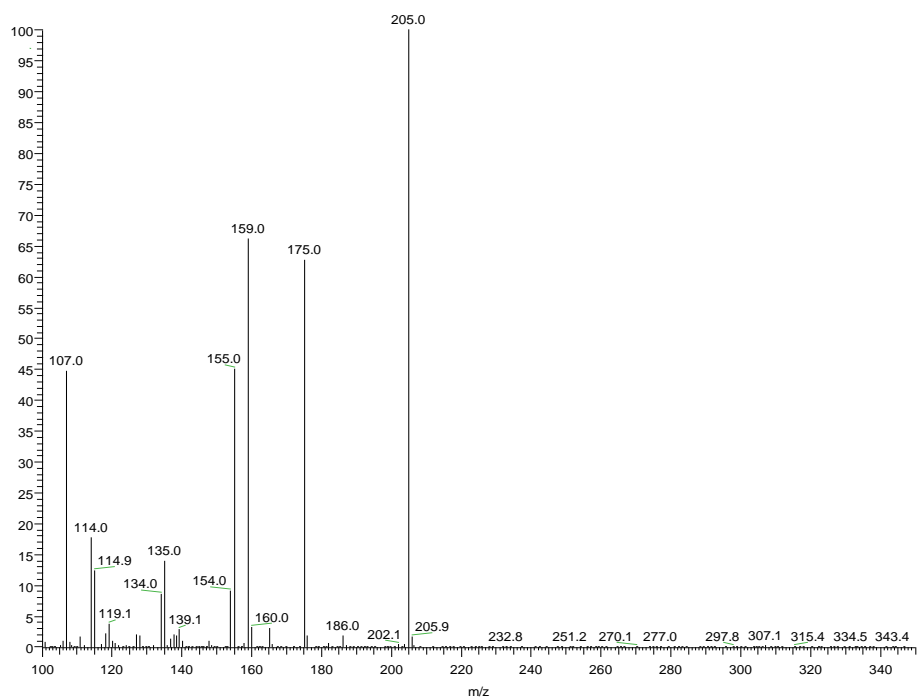


Figure 97 Product ion scan of synthetic AM 1 performed on precursor ion m/z 307.

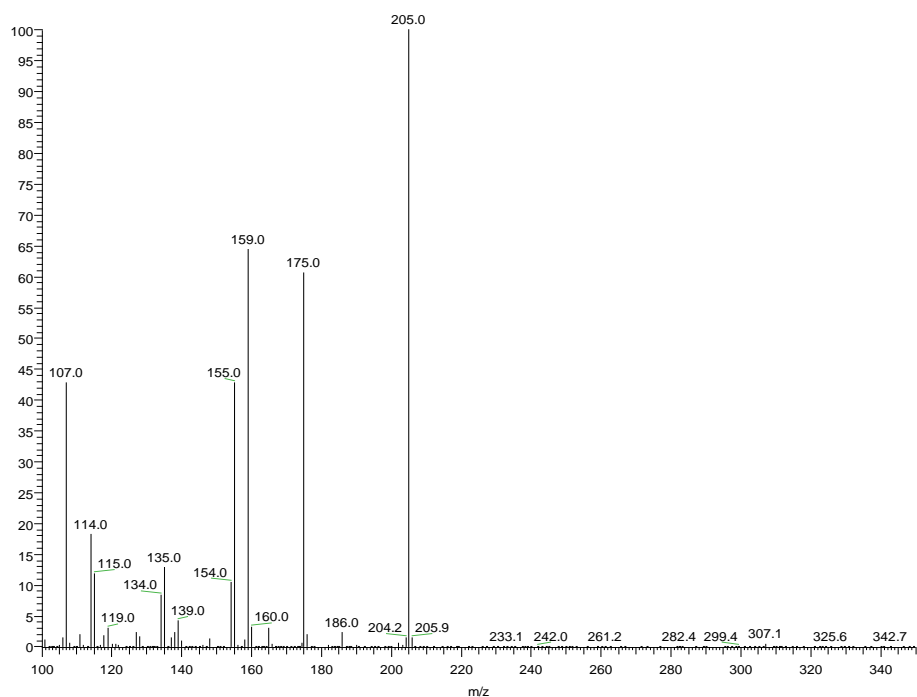


Figure 98 Product ion scan of urinary AM 1 performed on precursor ion m/z 307.

8.2.2. *rac*-*N*-(4-Cyano-3-(trifluoromethyl)phenyl)-2,3-dihydroxy-2-methylpropanamide (*rac*-13, OM 1)

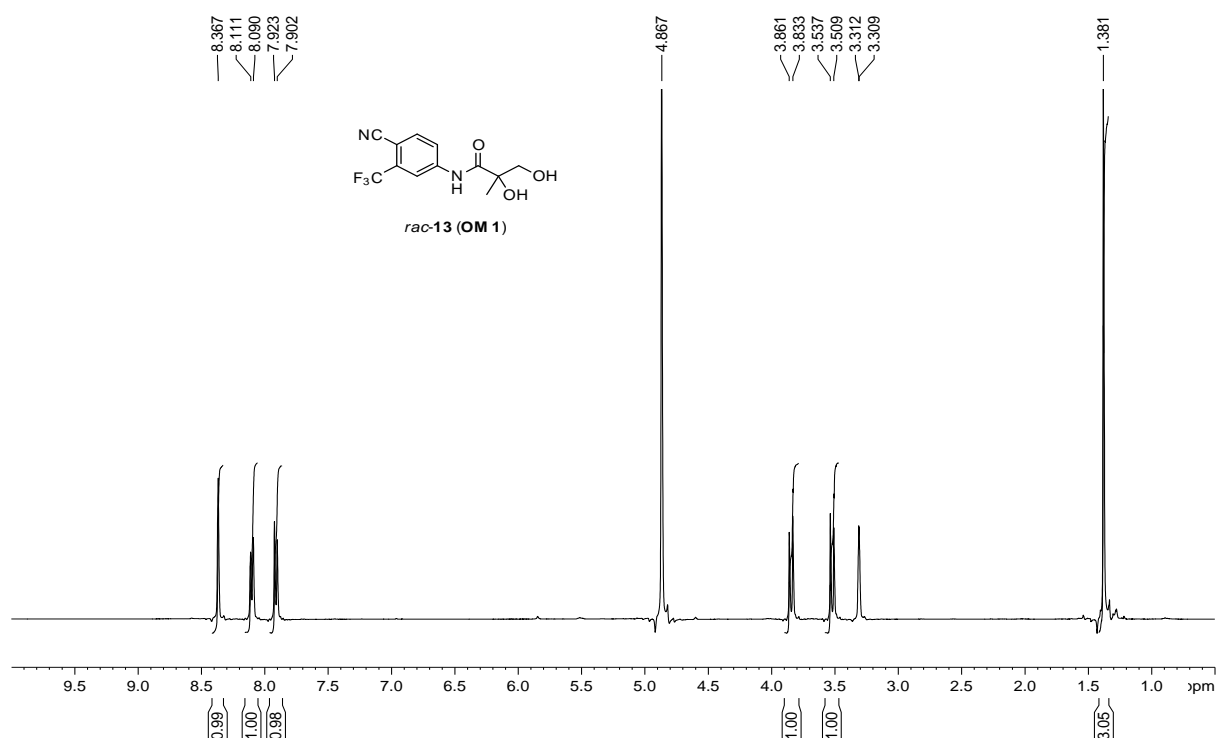


Figure 99 ¹H-NMR spectrum of compound *rac*-13 (OM 1).

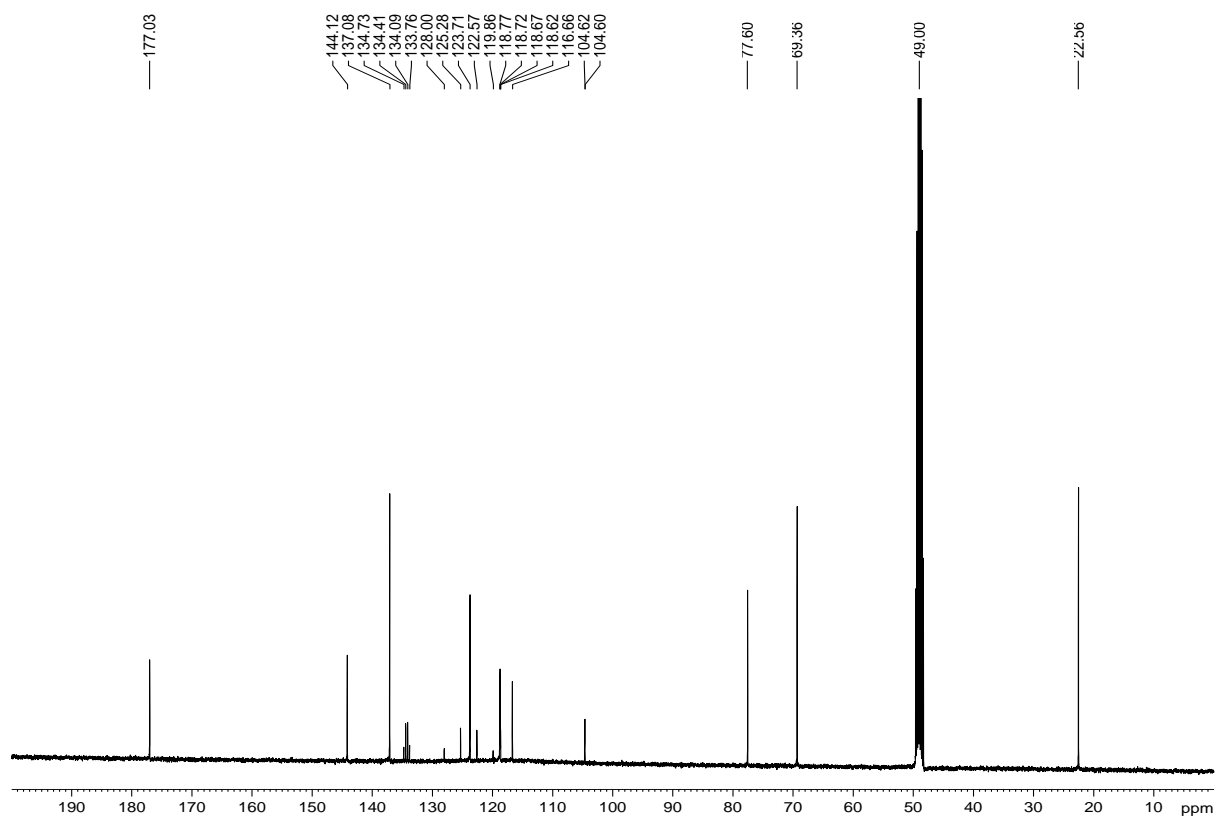


Figure 100 ¹³C-NMR spectrum of compound *rac*-13 (OM 1).

8.2.2.1. Comparison of synthetic OM 1 with excretion sample

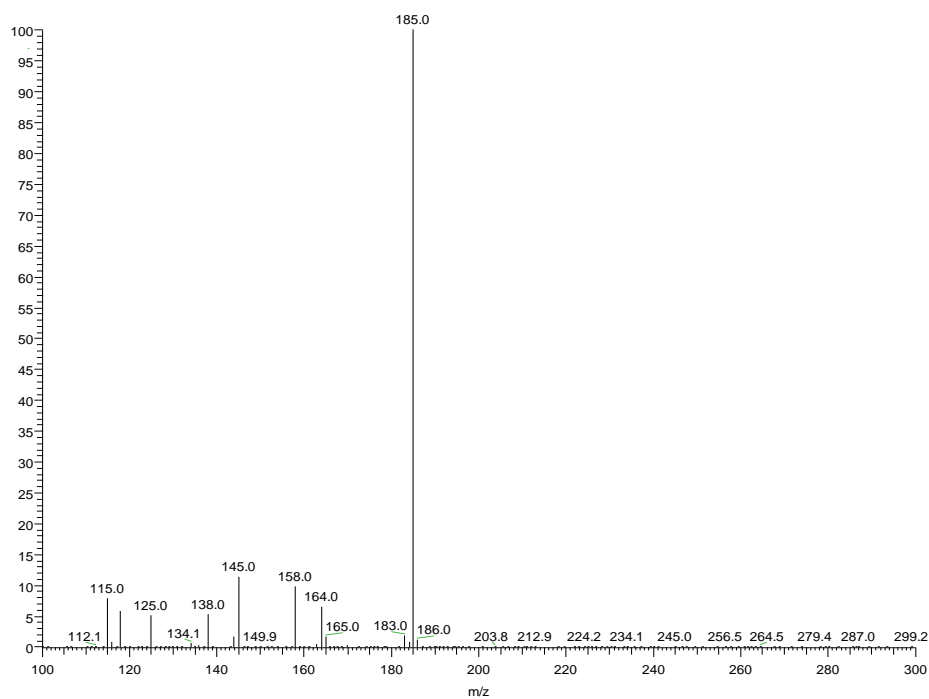


Figure 101 Product ion scan of synthetic **OM 1** performed on precursor ion 287.

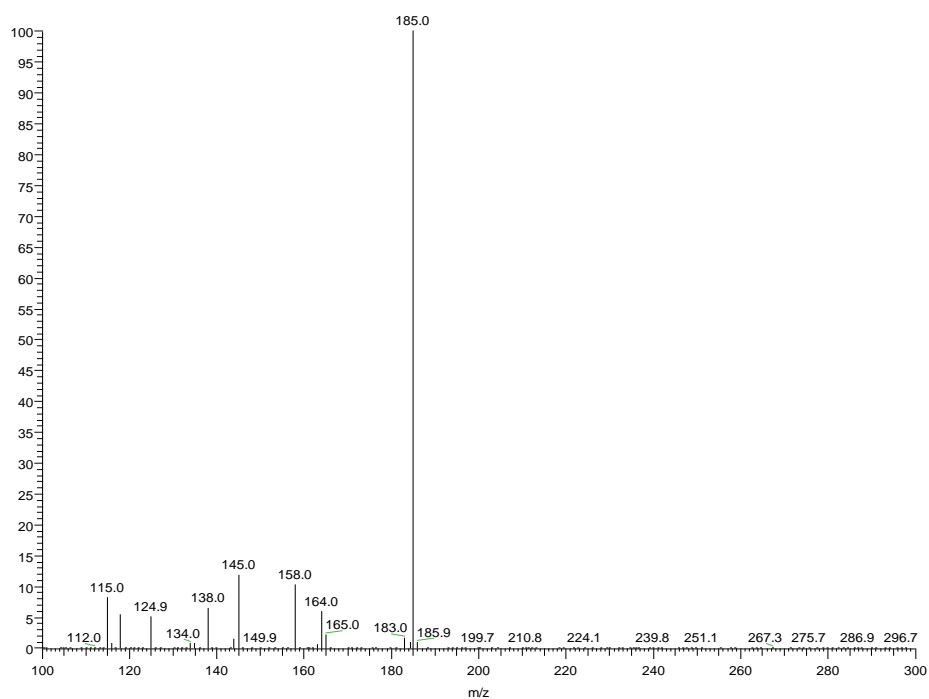


Figure 102 Product ion scan of urinary **OM 1** performed on precursor ion 287.

8.2.3. (2S)-2-Hydroxy-2-methyl-3-((4-nitro-3-(trifluoromethyl)phenyl)amino)-3-oxopropyl 3,3,3-trifluoro-2-methoxy-2-phenylpropanoate (16)

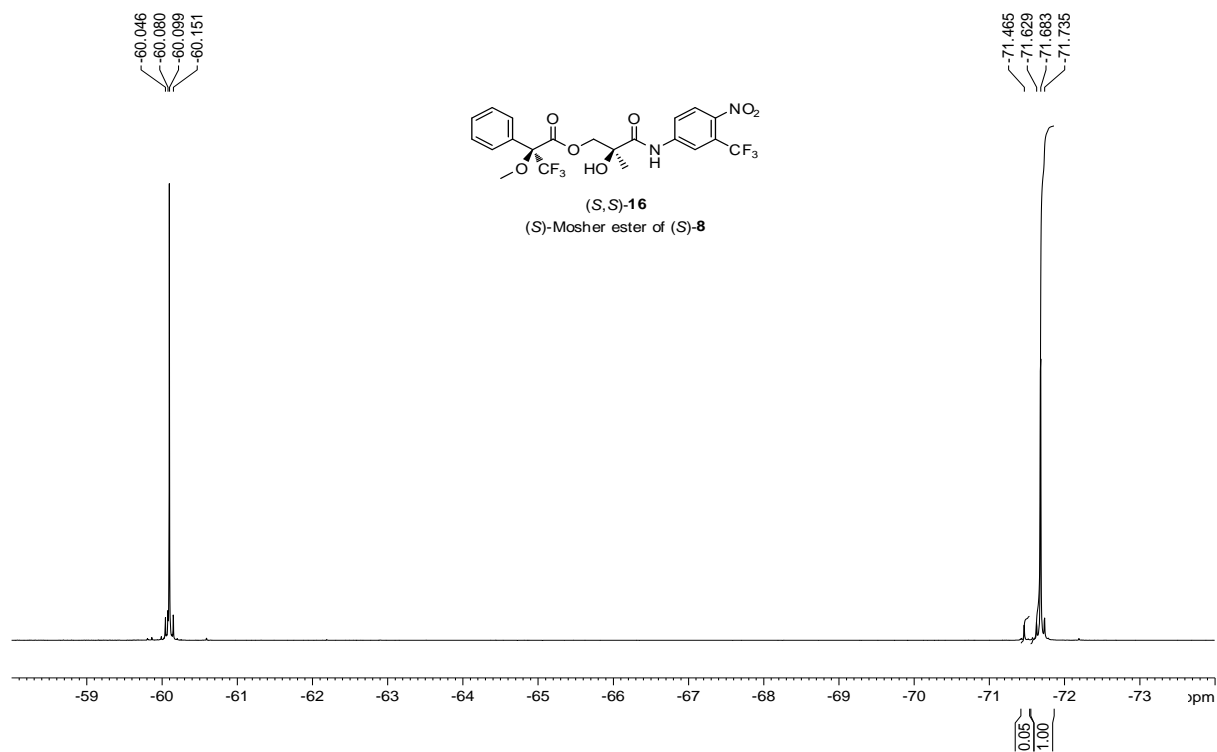


Figure 103 ^{19}F -NMR spectrum of compound (S,S)-16.

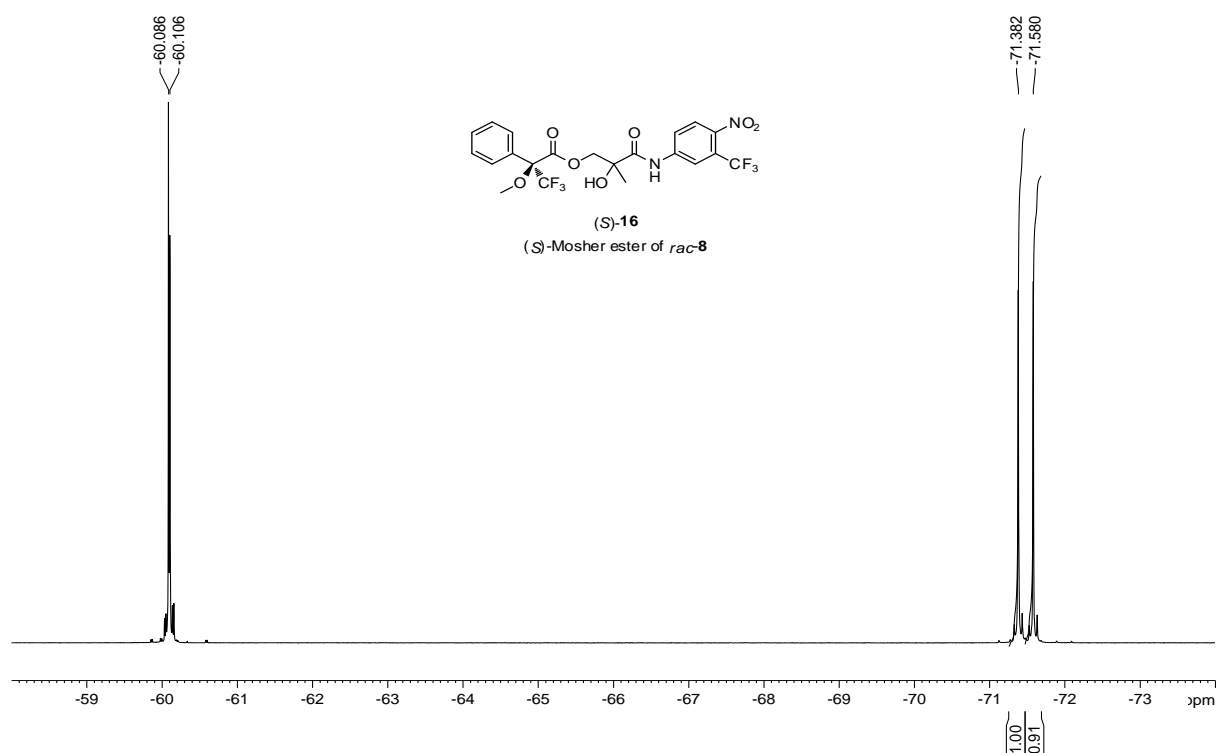


Figure 104 ^{19}F -NMR spectrum of compound (S)-16.

8.2.4. (2S)-3-((4-Cyano-3-(trifluoromethyl)phenyl)amino)-2-hydroxy-2-methyl-3-oxopropyl 3,3,3-trifluoro-2-methoxy-2-phenylpropanoate (17)

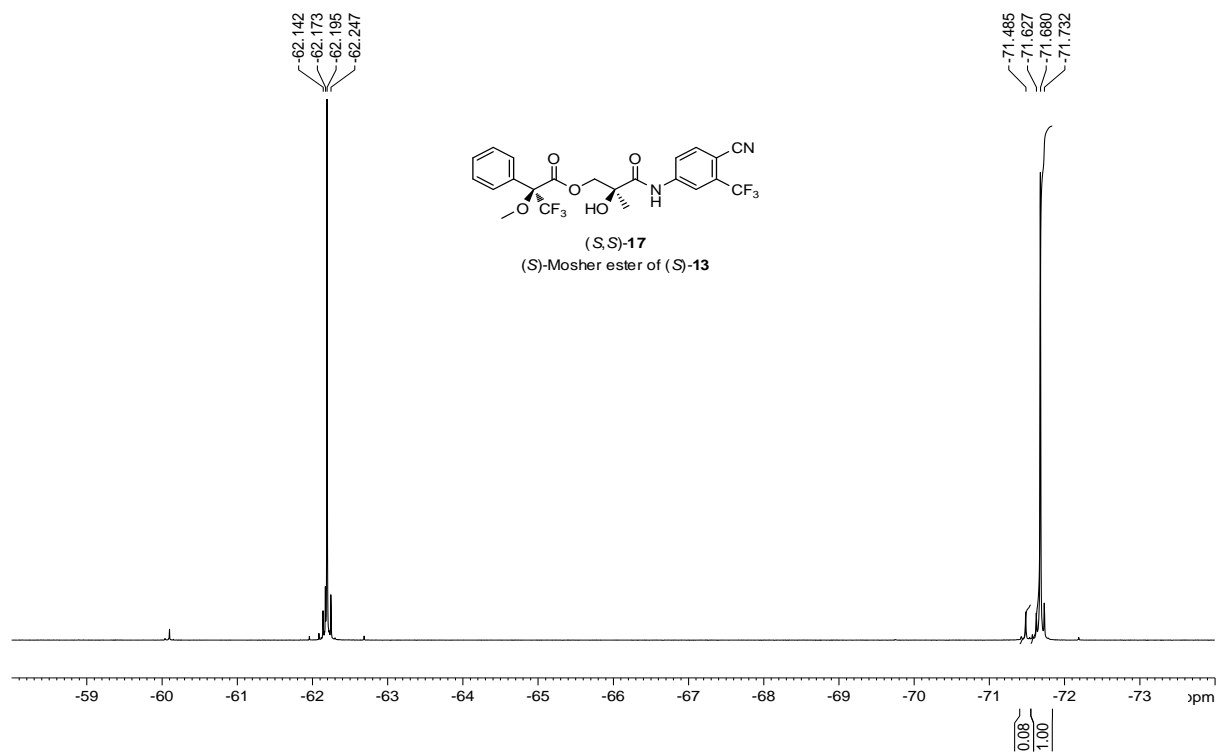


Figure 105 ^{19}F -NMR spectrum of compound (S,S)-17.

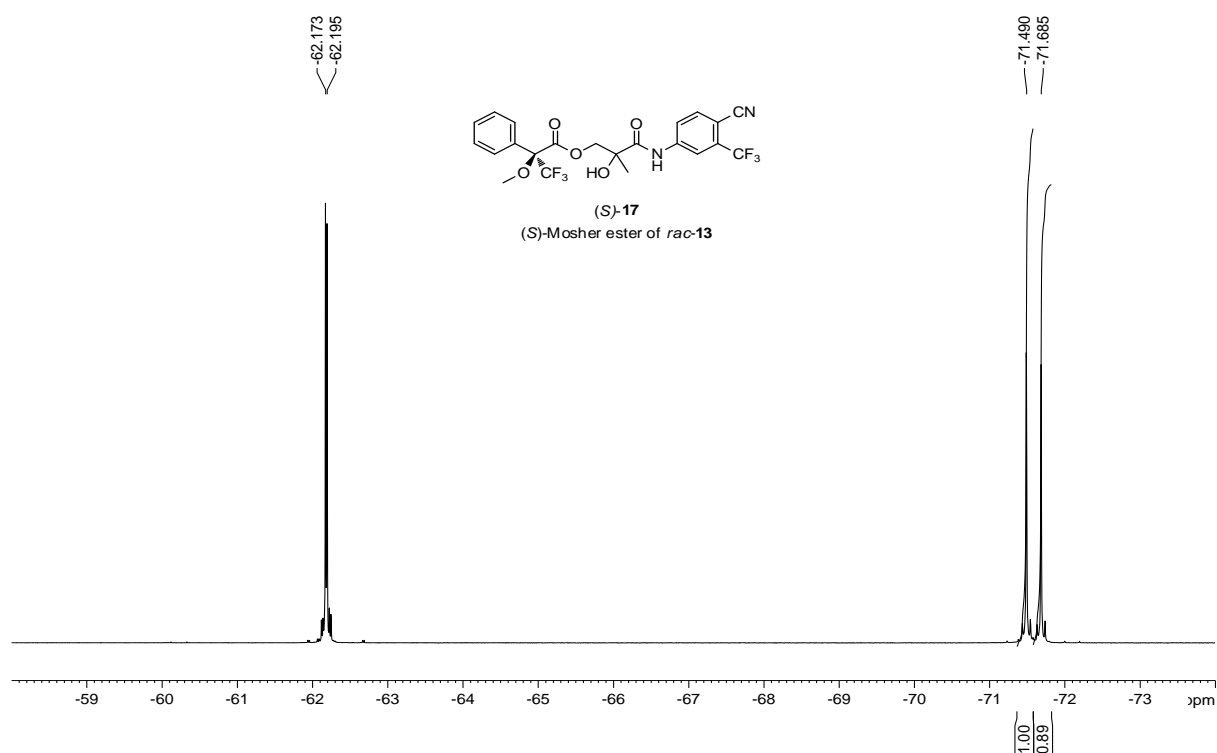


Figure 106 ^{19}F -NMR spectrum of compound (S)-17.

8.2.5. (*E*)-4-(1-chloro-2-(4-(2-(diethylamino)ethoxy)phenyl)-2-phenylvinyl)-phenol (CM 2)

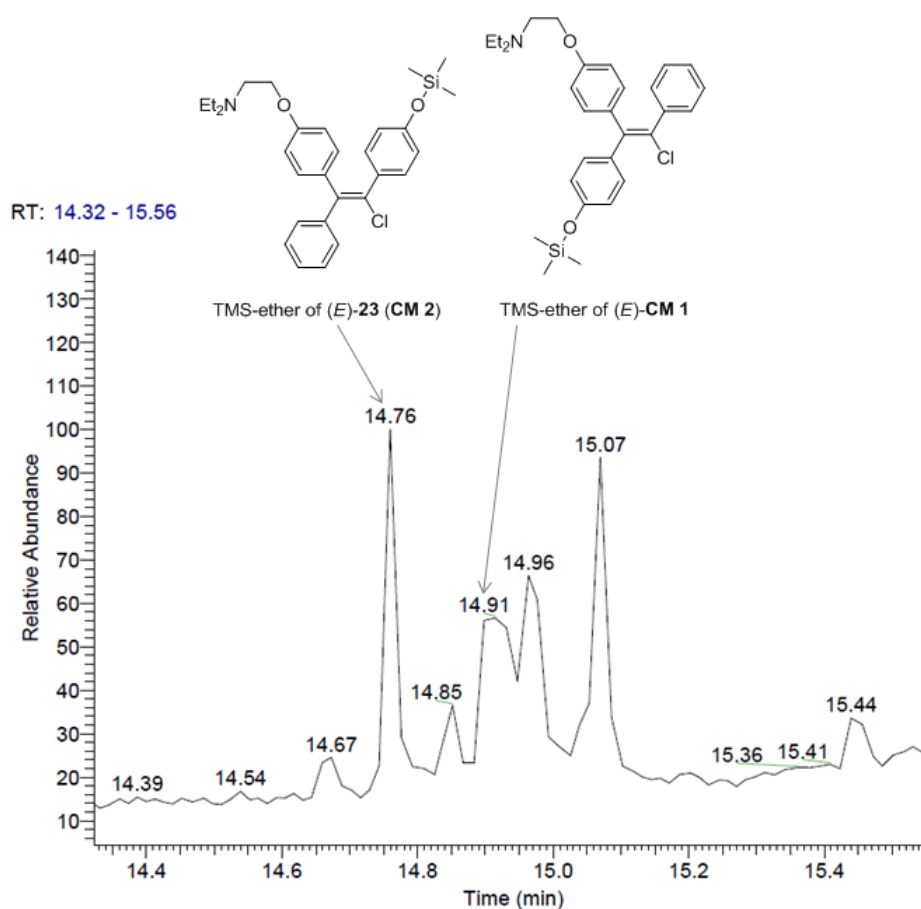


Figure 107 TIC of product mixture containing CM 2 obtained via Negishi approach.

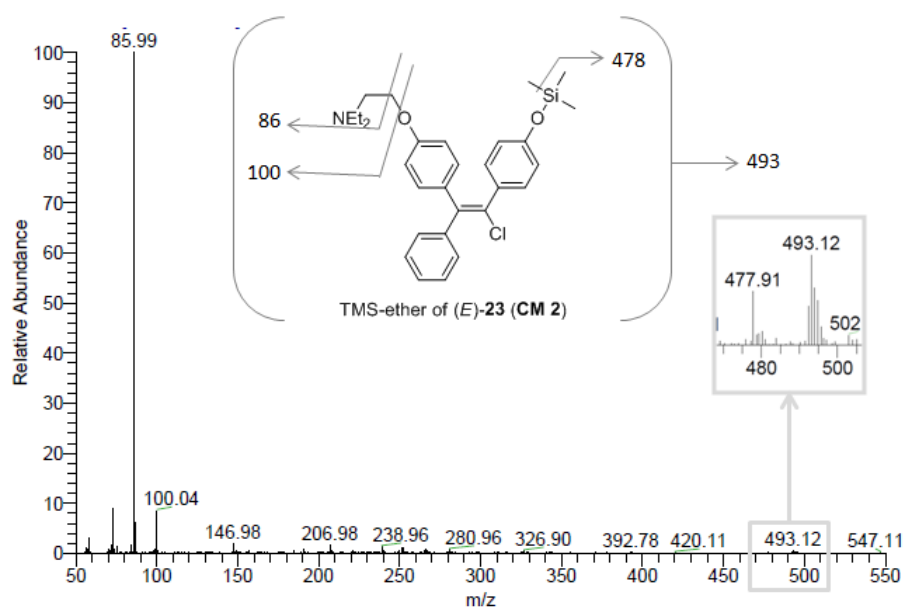


Figure 108 Mass spectrum of (*E*)-4'-hydroxyclo MPHENE (CM 2).

8.2.6. 2-(3,4-Bis(methoxymethoxy)phenyl)-2-(4-(2-(diethylamino)ethoxy)-phenyl)-1-phenylethanone (53)

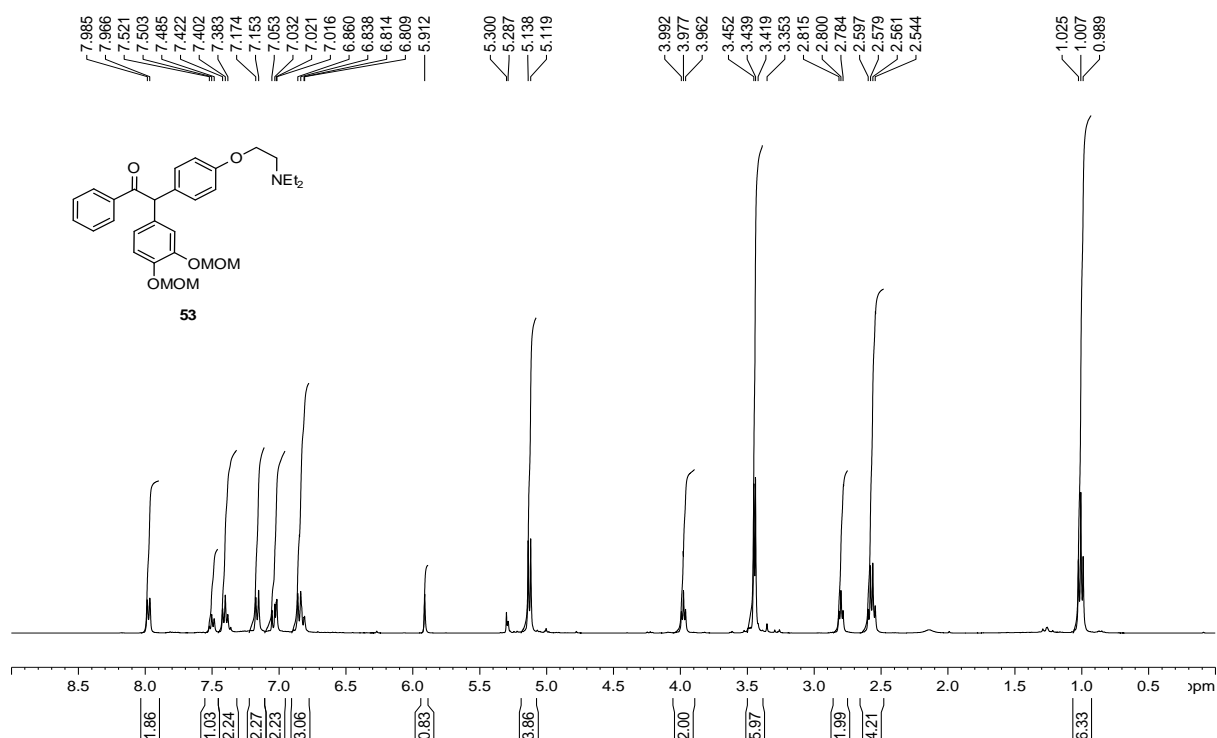


Figure 109 ¹H-NMR spectrum of compound 53.

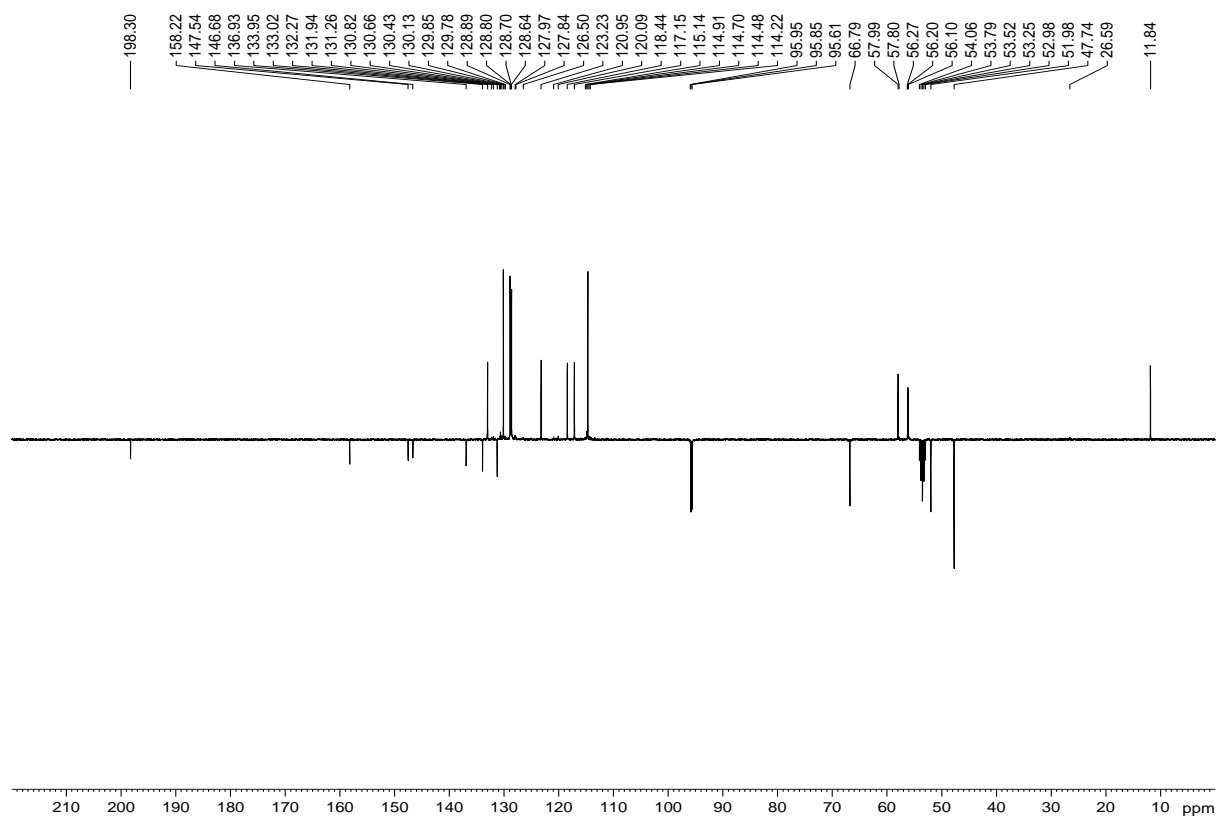


Figure 110 ¹³C-NMR spectrum of compound 53.

8.2.7. 2-(3,4-Bis(benzyloxy)phenyl)-1-phenyl-2-(4-((triisopropylsilyl)oxy)-phenyl)ethanone (63)

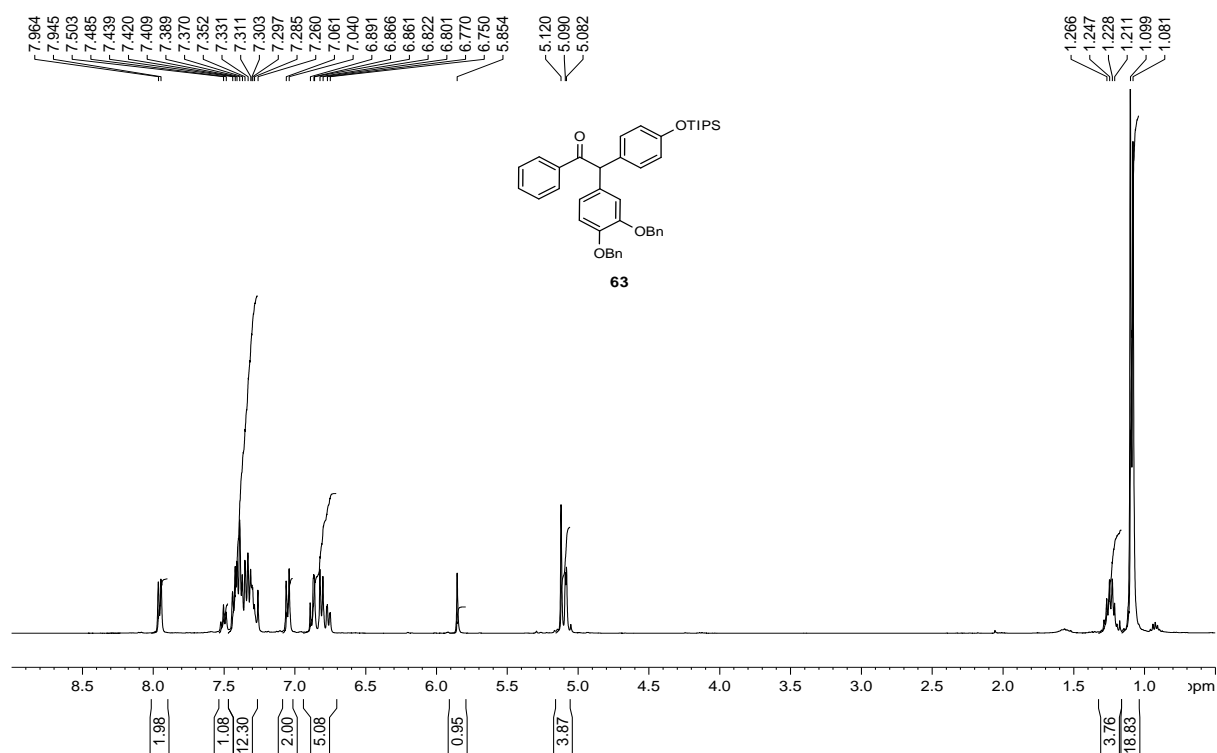


Figure 111 ¹H-NMR spectrum of compound 63.

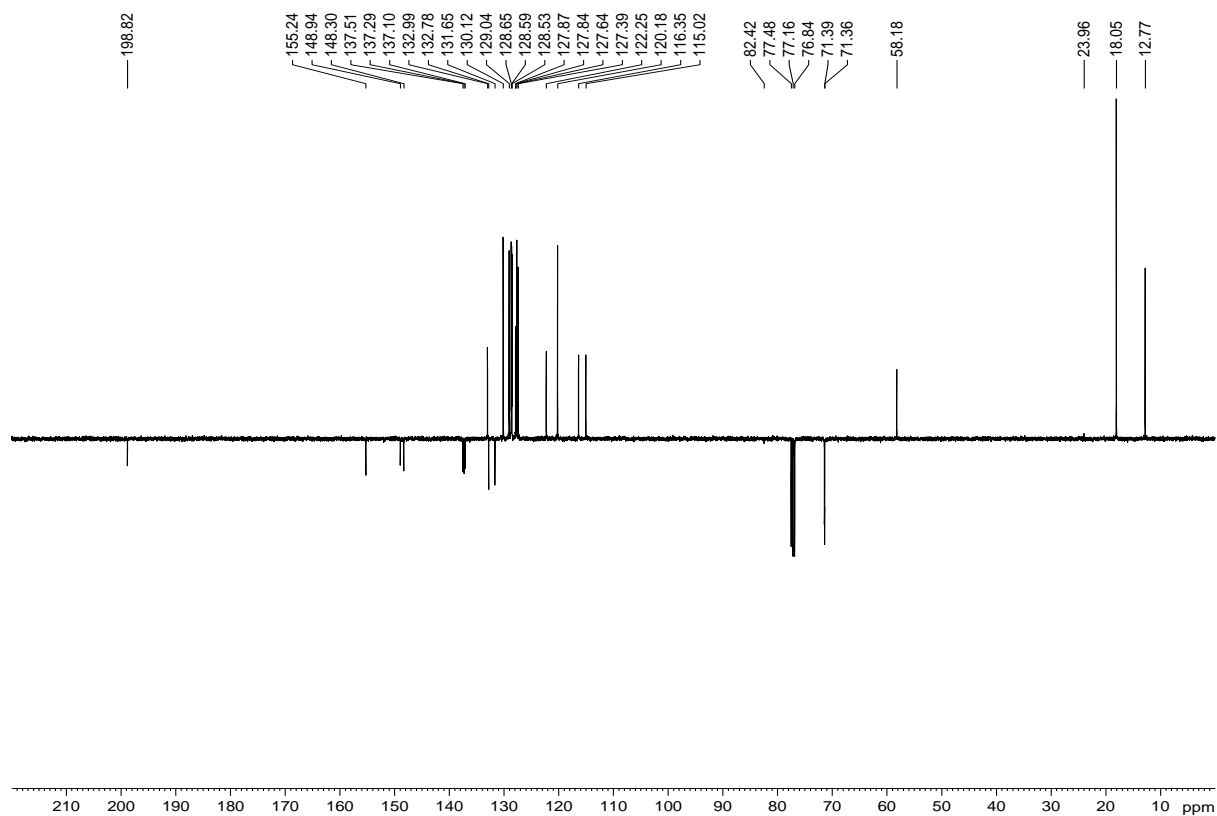


Figure 112 ¹³C-NMR spectrum of compound 63.

8.2.8. 4-Hydroxyclo MPHene (CM 1)

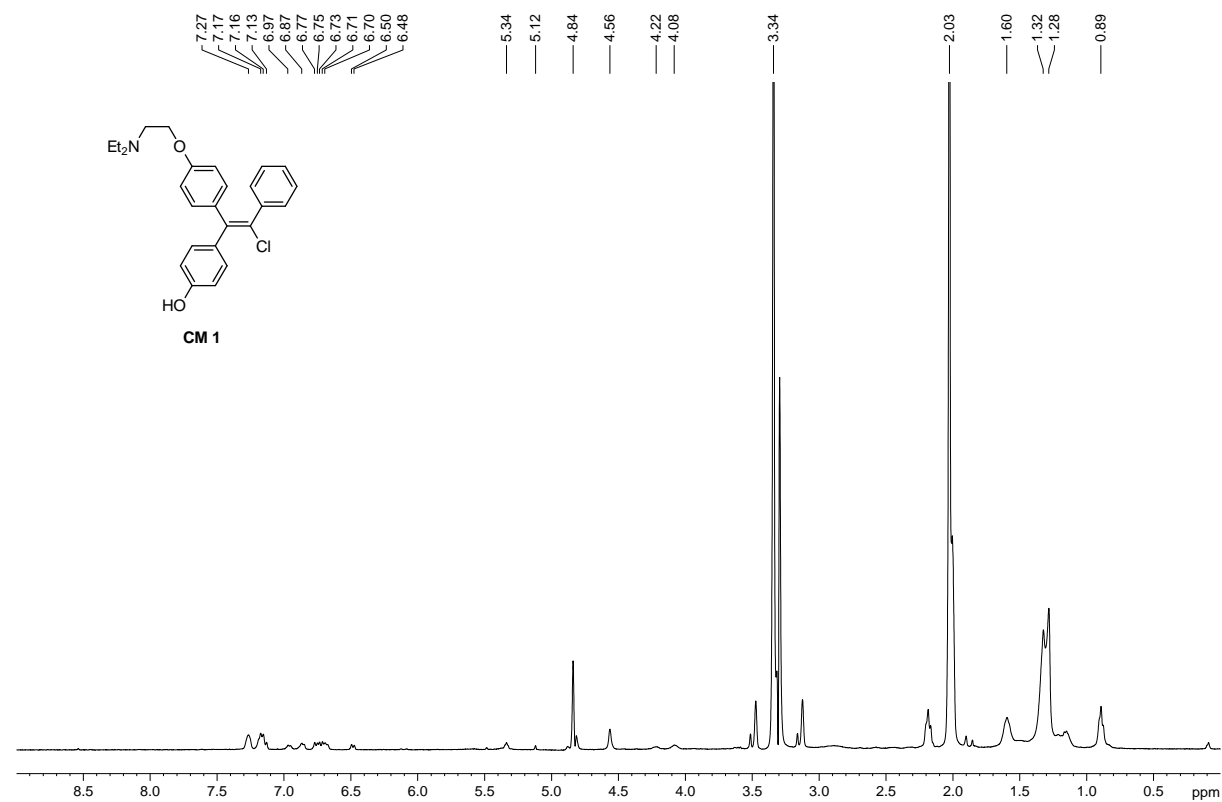


Figure 113 ¹H-NMR spectrum of compound **CM 1** isolated from HLM incubation (0 – 9.0 ppm).

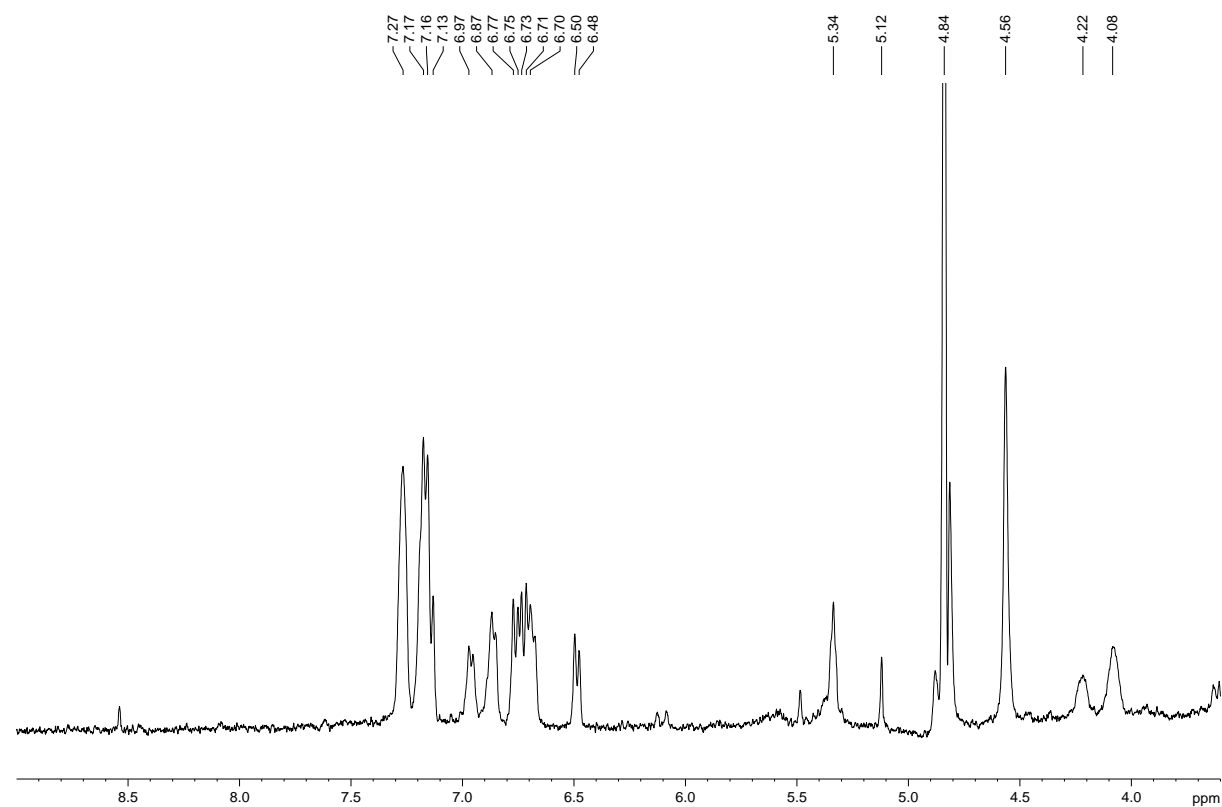


Figure 114 ¹H-NMR spectrum of compound **CM 1** isolated from HLM incubation (3.6 – 9.0 ppm).

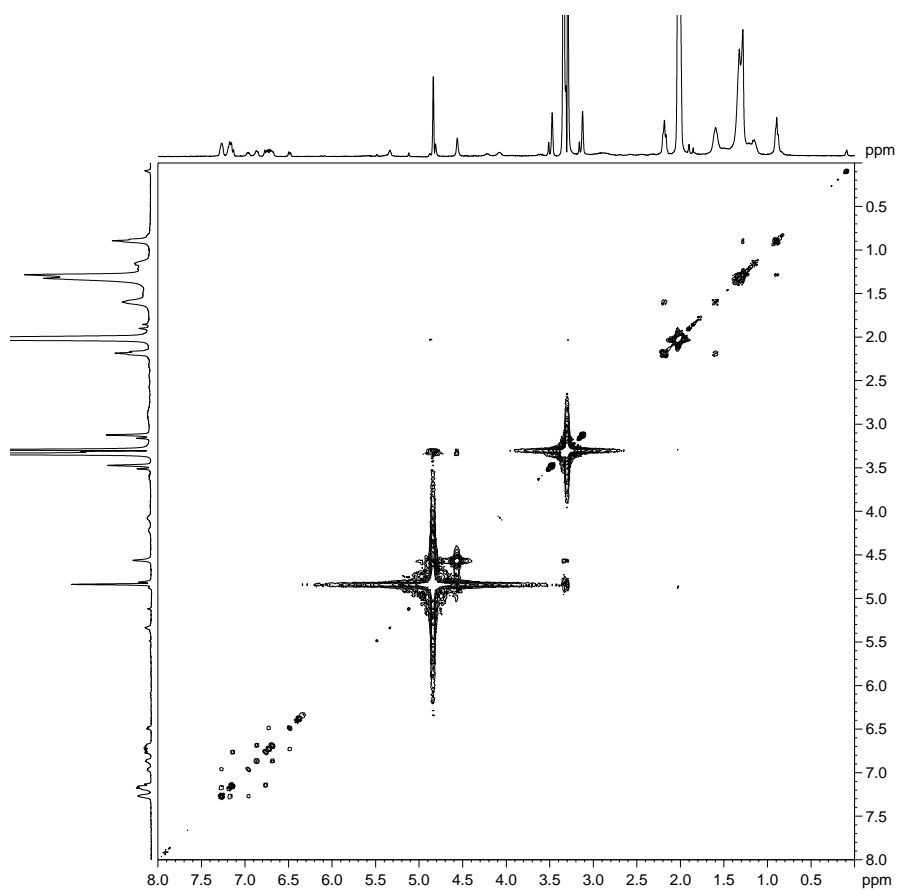


Figure 115 $^1\text{H},^1\text{H}$ -COSY spectrum of compound **CM 1** isolated from HLM incubation.

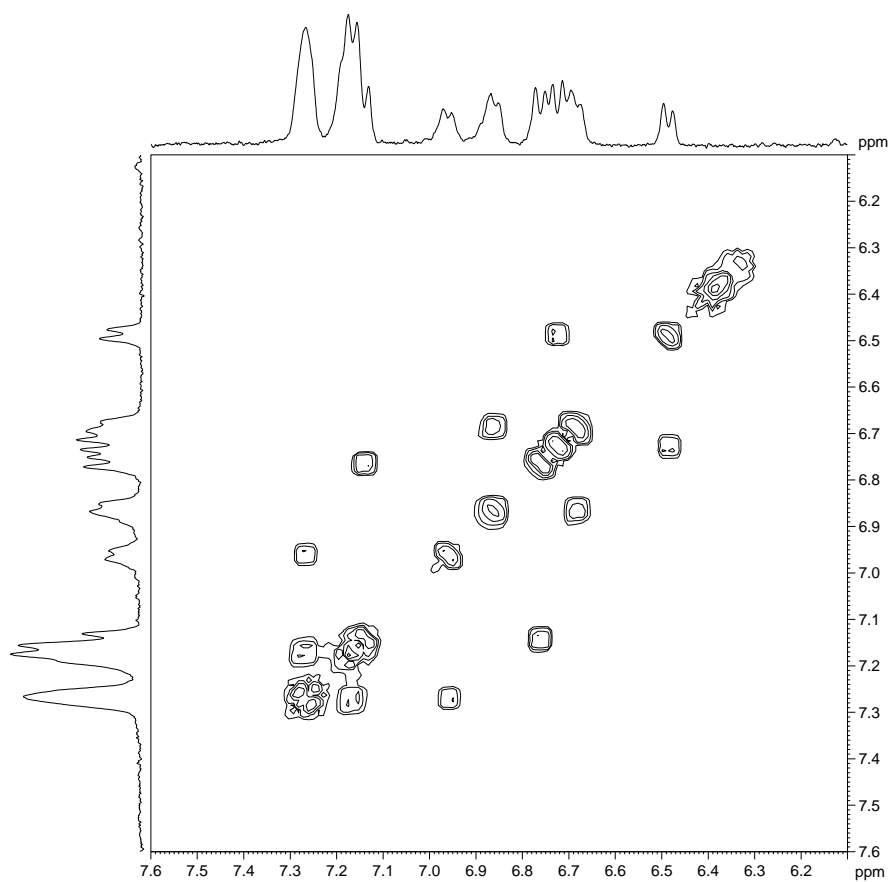


Figure 116 Aromatic region of $^1\text{H},^1\text{H}$ -COSY spectrum of compound **CM 1** isolated from HLM incubation.

9. REFERENCES

- [1] World Anti-Doping Agency 2013, *World Anti-Doping Code*. http://www.wada-ama.org/Documents/World_Anti-Doping_Program/WADP-The-Code/Code_Review/Code_Review_2015/Code_Final_Draft/WADC-2015-final-draft-EN.pdf. Accessed: 24.02.2014.
- [2] Todd, T. J. *Sport. Hist.* **1987**, *14*, 87.
- [3] Schänzer, W. In *25 Jahre Trainerausbildung. Die Trainerakademie Köln.*; Kozel J., Ed.; Sport und Buch Strauss: Köln, 1999; 59.
- [4] Masse, R.; Ayotte, C. *J. Chromatogr. Biomed. Appl.* **1989**, *497*, 17.
- [5] Lasne, F.; de Ceaurriz, J. *Nature* **2000**, *405*, 635.
- [6] Holdhaus, H.; Schober, P.H. *Doping. Wirkung, Nebenwirkung, Kontrolle, Alternativen zum Doping*; Verlagshaus der Ärzte: Wien 2009; 22.
- [7] Institute for Sports Medicine and Science Austria. <http://imsb.at/en>. Accessed: 24.02.2014.
- [8] The International Olympic Committee. <http://www.olympic.org/ioc>. Accessed: 24.02.2014.
- [9] World Anti-Doping Agency. <http://www.wada-ama.org/>. Accessed: 24.02.2014.
- [10] Nationale Anti-Doping Agentur Austria. <http://www.nada.at/en>. Accessed: 24.02.2014.
- [11] World Anti-Doping Agency 2013, *2012 Anti-Doping Testing Figures Report*. <http://www.wada-ama.org/Documents/Resourcen/Testing-Figures/WADA-2012-Anti-Doping-Testing-Figures-Report-EN.pdf>. Accessed: 05.03.2014.
- [12] World Anti-Doping Agency 2013, *The 2014 Prohibited List International Standard*. http://www.wada-ama.org/Documents/World_Anti-Doping_Program/WADP-Prohibited-list/2014/WADA-prohibited-list-2014-EN.pdf. Accessed: 05.03.2014.
- [13] Donike, M.; Bärwald, K. R.; Klostermann, K.; Schänzer, W.; Zimmermann, J. In *Sport: Leistung und Gesundheit*; Heck, H.; Hollman, W.; Liesen, H.; Rost, R., Eds.; Deutscher Ärzte Verlag: Köln, 1983; 293.
- [14] Piper, T.; Emery, C.; Saugy, M. *Anal. Bioanal. Chem.* **2011**, *401*, 433.
- [15] Reichel, C. *Anal. Bioanal. Chem.* **2011**, *401*, 463.
- [16] World Anti-Doping Agency 2013, *Athlete biological passport. Operating guidelines and compilation of required elements*. http://wada-ama.org/Documents/Science_Medicine/Athlete_Biological_Passport/WADA-ABP-Operating-Guidelines_v4.0-EN.pdf. Accessed 05.03.2014.
- [17] (a) Schänzer, W. *Chem. unserer Zeit* **1997**, *31*, 218. (b) Trout, G. J.; Kazlauskas, R.; *J. Chem. Soc. Rev.* **2004**, *33*, 1.
- [18] Thevis, M.; Thomas, A.; Schänzer, W. *Anal. Bioanal. Chem.* **2011**, *401*, 405.
- [19] (a) Swiss Laboratory for Doping Analyses. http://www.doping.chuv.ch/en/lad_home/lad-prestations-laboratoire/lad-prestations-laboratoire-liste-methodes.htm. Accessed 05.03.2014. (b) Doping Prevention-Technische Universität München. <http://www.doping-prevention.sp.tum.de/control-system-analytics/testing-procedures.html>. Accessed 05.03.2014.
- [20] Gillotin, F.; Chiap, P.; Frédérick, M.; Van Heugen, J. C.; Francotte, P.; Lebrun, P.; Pirotte, B.; de Tullio, P. *Drug Metab. Dispos.* **2010**, *38*, 232.
- [21] Watanabe, N.; Niki, E. *Proc. Jpn. Acad., Ser. B* **1978**, *54*, 194.
- [22] (a) Exarchou, V.; Krucker, M.; van Beek, T. A.; Vervoort, J.; Gerothanassis, I. P.; Albert, K. *Magn. Reson. Chem.* **2005**, *43*, 681. (b) Ceccarelli, S. M.; Schlotterbeck, G.; Boissin, P.; Binder, M.; Buettelmann, B.; Hanlon, S.; Jaeschke, G.; Kolczewski, S.; Kupfer, E.; Peters, J. U.; Porter, R. H. P.; Prinssen, E. P.; Rueher, M.; Ruf, I.; Spooren, W.; Stämpfli, A.; Vieira, E. *Chem. Med. Chem.* **2008**, *3*, 136. (c) Sturm, S.; Seger, C. *J. Chromatogr. A* **2012**, *1259*, 50.

- [23] (a) Seger, C.; Godejohann, M.; Tseng, L. H.; Spraul, M.; Girtler, A.; Sturm, S.; Stuppner, H. *Anal. Chem.* **2005**, *77*, 878. (b) Yang, Z. J. *Pharm. Biomed. Anal.* **2006**, *40*, 516. (c) Tatsis, E. C.; Boeren, S.; Exarchou, V.; Troganis, A. N.; Vervoort, J.; Gerothanassis, I. P. *Phytochemistry* **2007**, *68*, 383. (d) van der Hooft, J. J. J.; Mihaleva, V.; de Vos, R. C. H.; Bino, R. J.; Vervoort, J. *Magn. Reson. Chem.* **2011**, *49*, 55. (e) Liu, H.; Zheng, A.; Liu, H.; Yu, H.; Wu, X.; Xiao, C.; Dai, H.; Hao, F.; Zhang, L.; Wang, Y.; Tang, H. *J. Agric. Food Chem.* **2012**, *60*, 129.
- [24] Miner, J. N.; Chang, W.; Chapman M. S.; Finn, P. D.; Hong, M. H.; Lopez, F. J.; Marschke, K. B.; Rosen, J.; Schrader, W.; Turner, R.; van Oeveren, A.; Viveros, H.; Zhi, L.; Negro-Vilar, A. *Endocrinology* **2007**, *148*, 363.
- [25] Chen, J.; Hwang, D. J.; Bohl, C. E.; Miller, D. D.; Dalton, J. T. *J. Pharmacol. Exp. Ther.* **2005**, *312*, 546.
- [26] (a) Chen, J.; Kim, J.; Dalton, J. T. *Mol. Interv.* **2005**, 173. (b) Gao, W.; Dalton, J. T. *Mol. Interv.* **2007**, *7*, 10. (c) Mohler, M. L.; Nair, V. A.; Hwang, D. J.; Rakov, I. M.; Patil, R.; Miller, D. D. *Exp. Opin. Ther. Patents* **2005**, *15*, 1565.
- [27] Kearbey, J. D.; Wu, D.; Gao, W.; Miller, D. D.; Dalton, J. T. *Xenobiotica* **2004**, *34*, 273.
- [28] GTx. <http://www.gtxinc.com/Pipeline/Overview.aspx?Sid=1>. Accessed: 18.12.2013.
- [29] Nique, F.; Hebbe, S.; Peixoto, C.; Annoot, D.; Lefrancois, J.; Duval, E.; Michoux, L.; Triballeau, N.; Lemoullec, J.; Mollat, P.; Thauvin, M.; Prangé, T.; Minet, D.; Clément-Lacroix, P.; Robin-Jagerschmidt, C.; Fleury, D.; Guédin, D.; Deprez, P. *J. Med. Chem.* **2012**, *55*, 8225.
- [30] (a) Piu, F.; Gardell, L. R.; Son, T.; Schlienger, N.; Lund, B. W.; Schiffer, H. H.; Vanover, K. E.; Davis, R. E.; Olsson, R.; Bradley, S. R. *J. Steroid Biochem. Mol. Bio.* **2008**, *109*, 129. (b) Dayger, C.; Villasana, L.; Pfankuch, T.; Davis, M.; Raber, J. *Brain Res.* **2011**, *1381*, 134.
- [31] Thevis, M.; Geyer, H.; Kamber, M.; Schänzer, W. *Drug Test. Analysis* **2009**, *1*, 387.
- [32] (a) Kohler, M.; Thomas, A.; Geyer, H.; Petrou, M.; Schänzer, W.; Thevis, M. *Drug Test Analysis* **2010**, *2*, 533. (b) Thevis, M.; Geyer, H.; Thomas, A.; Schänzer, W. *Drug Test. Analysis* **2011**, *3*, 331.
- [33] Grata, E.; Perrenoud, L.; Saugy, M.; Baume, N. *Forensic Sci. Int.* **2011**, *213*, 104.
- [34] The Guardian. <http://www.theguardian.com/sport/2013/jun/07/vaconsoleil-nikita-novikov-doping>. Accessed: 06.02.2014.
- [35] (a) Gao, W.; Wu, Z.; Bohl, C. E.; Yang, J.; Miller, D. D.; Dalton, J. T. *Drug Metab. Dispos.* **2006**, *34*, 243. (b) Kuurane, T.; Leinonen, A.; Schänzer, W.; Kamber, M.; Kostianen, R.; Thevis, M. *Drug Metab. Dispos.* **2008**, *36*, 571.
- [36] (a) Perera, M. A.; Yin, D.; Wu, D.; Chan, K. K.; Miller, D. D.; Dalton, J. *Drug Metab. Dispos.* **2006**, *34*, 1713. (b) Kearbey, J. D.; Wu, D.; Gao, W.; Miller, D. D.; Dalton, J. T. *Xenobiotica* **2004**, *34*, 273.
- [37] Thevis, M.; Thomas, A.; Fußhöller, G.; Beuck, S.; Geyer, H.; Schänzer, W. *Rapid Commun. Mass Spectrom.* **2010**, *24*, 2245.
- [38] (a) Thevis, M.; Gerace, E.; Thomas, A.; Beuck, S.; Geyer, H.; Schloerer, N.; Kearbey, J. D.; Dalton, J. T.; Schänzer, W. *Drug Test. Analysis* **2010**, *2*, 589. (b) Thevis, M.; Thomas, A.; Möller, I.; Geyer, H.; Dalton, J. T.; Schänzer, W. *Rapid Commun. Mass Spectrom.* **2011**, *25*, 2187.
- [39] Tucker, H.; Crook, J. W.; Chesterson, G. J. *J. Med. Chem.* **1988**, *31*, 954-959.
- [40] Tucker, H.; Chesterson G. J. *J. Med. Chem.* **1988**, *31*, 885-887.
- [41] (a) Jew, S. S.; Terashima, S.; Koga, K. *Tetrahedron* **1979**, *35*, 2337. (b) Jew, S. S.; Terashima, S.; Koga, K. *Tetrahedron* **1979**, *35*, 2345.
- [42] Kirkovsky, L.; Mukherjee, A.; Yin, D.; Dalton, J. T.; Miller, D. D. *J. Med. Chem.* **2000**, *43*, 581.
- [43] Marhefka, C. A.; Gao, W.; Chung, K.; Kim, J.; He, Y.; Yin, D.; Bohl, C.; Dalton, J. T.; Miller, D. D. *J. Med. Chem.* **2004**, *47*, 993.
- [44] Thijs, L.; Keltjens, R.; Ettema, G. J. B. US Patent 0073742, 2003.
- [45] Thevis, M.; Lohmann, W.; Schrader, Y.; Kohler, M.; Bornatsch, W.; Karst, U.; Schänzer, W. *Eur. J. Mass Spectrom.* **2008**, *14*, 163.

- [46] (a) Riggs, B. L.; Hartmann, L. C. *N. Engl. J. Med.* **2003**, *348*, 618. (b) Maximov, P. Y.; Lee, T. M.; Jordan, V. C. *Curr. Clin. Pharmacol.* **2013**, *8*, 135.
- [47] Murphy, L. C.; Sutherland, R. L. *J. Clin. Endocrinol. Metab.* **1983**, *57*, 373.
- [48] (a) Huppert, L. C. *Fertil. Steril.* **1979**, *31*, 1. (b) Adashi, E. Y. *Fertil. Steril.* **1984**, *42*, 331.
- [49] Plouffe, L.; Siddhanti, S. *Ann. N. Y. Acad. Sci.* **2001**, *949*, 251.
- [50] (a) Handelsblatt. <http://www.handelsblatt.com/archiv/hormonmittel-tamoxifen-nolvadex-gefunden-aegypten-gohar-war-gedopt/2223868.html>. Accessed: 13.02.2014. (b) Neue Zürcher Zeitung. <http://www.nzz.ch/aktuell/startseite/article9B0RN-1.347584>. Accessed: 13.02.2014.
- [51] (a) Ruenitz, P. *Drug. Metab. Dispos.* **1981**, *9*, 456. (b) Ruenitz, P.; Baggeley, J.; Mokler, C. *Biochem. Pharmacol.* **1983**, *32*, 2941. (c) Ruenitz, P.; Arrendale, R.; George, G.; Thompson, C.; Mokler, C.; Nanavati, N. *Cancer Res.* **1987**, *1*, 4015. (d) Ruenitz, P.; Arrendale, R.; Schmidt, W.; Thompson, C.; Nanavati, N. *J. Med. Chem.* **1989**, *32*, 192.
- [52] Geyer, H.; Mareck-Engelke, U.; Opfermann, G.; Schänzer, W.; Sigmund, G. In *Recent advances in doping analysis (9)*; Sport und Buch Strauß: Köln 2001; 53.
- [53] (a) Schänzer, W.; Geyer, H.; Gotzmann, A.; Mareck, U. In *Recent advances in doping analysis (15)*; Sportverlag Strauß: Köln 2007; 113. (b) Oueslati, F.; Maatki, M.; Osman, Z.; Loueslati, H. In *Proceedings of the Manfred Donike Workshop 26th*, Cologne Workshop on Dope Analysis 2008.
- [54] Mazzarino, M.; Fiacco, I.; De la Torre, X.; Botre, F. *Eur. J. Mass Spectrom.* **2008**, *14*, 171.
- [55] Lu, J.; He, G.; Wang, X.; Xu, Y.; Wu, Y.; Dong, Y.; He, Z.; Liu, X.; Bo, T.; Ouyang, G. *J. Chromatogr. A* **2012**, *1243*, 23.
- [56] (a) Mazzarino, M.; Biava, M. *Anal. Bioanal. Chem.* **2013**, *405*, 5467. (b) Lu, J.; He, G.; Wang, X.; Xu, Y.; Wu, Y.; Shen, L.; Yan, K.; He, Z. *Anal. Methods* **2013**, *5*, 6677.
- [57] Ruenitz, P.; Arrendale, R.; Schmidt, W.; Thompson, C.; Nanavati, N. *J. Med. Chem.* **1989**, *32*, 192.
- [58] (a) Foster, A. B.; Jarman, M.; Leung, O.; McCague, R.; Leclercq, G.; Devleeschouwer, N. *J. Med. Chem.* **1985**, *28*, 1491. (b) Hardcastle, I. R.; Horton, N. M.; Osborne, M. R.; Hewer, A.; Jarman, M.; Phillips, D. H. *Chem. Res. Toxicol.* **1998**, *11*, 369.
- [59] Olier-Reuchet, C.; Aitken, D. J.; Bucourt, R.; Husson, H. *Tetrahedron Lett.* **1995**, *45*, 8221.
- [60] (a) Yao, D.; Zhang, F.; Yu, L.; Yang, Y.; van Breemen, R. B.; Bolton, J. L. *Chem. Res. Toxicol.* **2001**, *14*, 1643. (b) Zheng, L.; Wei, Q.; Zhou, B.; Yang, L.; Liu, Z. L. *Anti-cancer drugs* **2007**, *18*, 1039.
- [61] Gauthier, S.; Mailhot, J.; Labrie, F. *J. Org. Chem.* **1996**, *61*, 3890.
- [62] (a) Detsi, A.; Koufaki, M.; Calogeropoulou, T. *J. Org. Chem.* **2002**, *67*, 4608. (b) Yu, D. D.; Forman, B. M. *J. Org. Chem.* **2003**, *68*, 9489. (c) Fauq, A. H.; Maharvi, G. M.; Sinha, D. *Bioorg. Med. Chem. Lett.* **2010**, *20*, 3036. (d) Lv, W.; Liu, J.; Lu, D.; Flockhart, D. A.; Cushman, M. *J. Med. Chem.* **2013**, *56*, 4611.
- [63] Castellnou, D.; Pericás, M. A.; Riera, A.; Rodríguez, I.; Solá, L. *Adv. Synth. Catal.* **2003**, *345*, 1305.
- [64] Vitoriano, B. C.; Carvalho, L. C. R.; Estevao, M. S.; Sekera, M. H.; Marques, M. M. B. *Synlett* **2010**, *5*, 753.
- [65] Al-Hassan, M. I.; Miller, R. B. *J. Org. Chem.* **1985**, *50*, 2121.
- [66] Zhou, C.; Larock, R. C. *J. Org. Chem.* **2005**, *70*, 3765.
- [67] Tsuji, H.; Ueda, Y.; Ilies, L.; Nakamura, E. *J. Am. Chem. Soc.* **2010**, *132*, 11854.
- [68] Hofbauer, K. *Dissertation* 2008, Institut für Angewandte Synthesechemie, TU Wien.
- [69] Grill, J. M.; Ogle, J. W.; Miller, S. A. *J. Org. Chem.* **2006**, *71*, 9291.
- [70] Valeur, E.; Bradley, M. *Chem. Soc. Rev.* **2009**, *38*, 606.
- [71] Vaughan, J.; Osato, R. L. *J. Am. Chem. Soc.* **1951**, 5553.
- [72] Anderson, G. W.; Zimmerman, J. E.; Callahan, F. M. *J. Am. Chem. Soc.* **1967**, *89*, 5012.
- [73] More, S. S.; Vince, R. *J. Med. Chem.* **2008**, *51*, 4581.

- [74] Inanaga, J.; Hirata, K.; Saeki, H.; Katsuki, T.; Yamaguchi, M. *Bull. Chem. Soc. Jpn.* **1979**, *52*, 1989.
- [75] (a) Carpino, L. A. *J. Am. Chem. Soc.* **1993**, *115*, 4398. (b) Carpino, L. A.; Elfaham, A.; Albericio, F. *Tetrahedron Lett.* **1994**, *35*, 2279.
- [76] (a) Ekegren, J. K.; Gising, J.; Wallberg, H.; Larhed, M.; Samuelsson, B.; Hallberg, A. *Org. Biomol. Chem.* **2006**, *4*, 3040. (b) Wangsell, F.; Nordeman, P.; Sävmarker, J.; Emanuelsson, R.; Jansson, K.; Lindberg, J.; Rosenquist, A.; Samuelsson, B., Larhed, M. *Bioorg. Med. Chem.* **2011**, *19*, 145.
- [77] Sasaki, K.; Crich, D. *Org. Lett.* **2011**, *13*, 2256.
- [78] Willwacher, J.; Rakshit, S.; Glorius, F. *Org. Biomol. Chem.* **2011**, *9*, 4736.
- [79] (a) Sugiyama, S.; Ohigashi, S.; Sawa, R.; Hayashi, H. *Bull. Chem. Soc. Jpn.* **1989**, *62*, 3202. (b) Liu, Y.; Liu, Q.; Zhang, Z. *J. Mol. Catal. A: Chem.* **2008**, *296*, 42.
- [80] Jiang, J.; Xiu, Z.; Hua, R. *Synth. Commun.* **2008**, *38*, 232.
- [81] Katsuki, T.; Sharpless, K. B. *J. Am. Chem. Soc.* **1980**, *102* (18), 5974.
- [82] Hanson, R. M.; Sharpless, K. B. *J. Org. Chem.* **1986**, *51*, 1922.
- [83] Martin, V. S.; Woodard, S. S.; Katsuki, T.; Yamada, Y.; Ikeda, M.; Sharpless, K. B. *J. Am. Chem. Soc.* **1981**, *103*, 6237.
- [84] Gao, Y.; Hanson, R. M.; Klunder, J. M.; Soo, Y. K.; Hiroko, M.; Sharpless, K. B. *J. Am. Chem. Soc.* **1987**, *109*, 5765.
- [85] Finn, M. G.; Sharpless, K. B. *J. Am. Chem. Soc.* **1991**, *113*, 113.
- [86] *Organic Chemistry*; Clayden, J.; Greeves, N.; Warren, S., Eds.; Oxford University Press: New York, 2012; 1120.
- [87] Dale, J. A.; Dull, D. L.; Mosher, H. S. *J. Org. Chem.* **1969**, *34* (9), 2543.
- [88] Neises, B.; Steglich, W. *Angew. Chem. Int. Ed.* **1978**, *17* (7), 522.
- [89] Millar, J. G.; Oehlschlager, A. C.; Wong, J. W. *J. Org. Chem.* **1983**, *48*, 4404.
- [90] De Nooy, A. E. J.; Besemer, A. C.; Van Bekkum, H. *Synthesis* **1996**, *10*, 1153.
- [91] Hunsen, M. *Synthesis* **2005**, *15*, 2487.
- [92] Schmidt, A. C.; Stark, C. B. W. *Org. Lett.* **2011**, *13* (16), 4164.
- [93] Djerassi, C.; Engle, R. R. *J. Am. Chem. Soc.* **1953**, *75*, 3838.
- [94] Lee, D. G.; Van den Engh, M. In *Oxidation in Organic Chemistry*; Trahanovsky, W. S., Ed.; Academic Press: New York, 1973; Part B, Chapter 4.
- [95] World Anti-Doping Agency 2010, *Technical Document – TD2010IDCR*. http://www.wada-ama.org/Documents/World_Anti-Doping_Program/WADP-IS-Laboratories/Technical_Documents/WADA_TD2010IDCRv1.0_Identification%20Criteria%20for%20Qualitative%20Assays_May%2008%202010_EN.doc.pdf. Accessed: 21.04.2014.
- [96] Bogdanovic, B.; Fürstner, A. *Angew. Chem.* **1996**, *108*, 2582.
- [97] McMurry, J. E. *Chem. Rev.* **1989**, *89*, 1513.
- [98] McMurry, J. E.; Krepski, L. R. *J. Org. Chem.* **1976**, *41*, 3929.
- [99] Schragl, K. M. *Diplomarbeit* 2010, Institut für Angewandte Synthesechemie, TU Wien.
- [100] Johnson, D. W.; Phillipou, G.; Seaborn, C. J. *Aust. J. Chem.* **1980**, *33*, 461.
- [101] Patai, S.; Bergmann, F. *J. Am. Chem. Soc.* **1950**, *72*, 1034.
- [102] (a) Nagano, T. *J. Org. Chem.* **1957**, *22*, 817. (b) Hirakawa, K.; Ogiue, E.; Motoyoshiya, J.; Kakurai, T. *J. Org. Chem.* **1986**, *51*, 1083.
- [103] Mellegaard-Waetzig, S. R.; Wang, C.; Tunge, J. A. *Tetrahedron* **2006**, *62*, 7191.

- [104] (a) Ayrey, G.; Barnard, D.; Woodbridge, D. T. *J. Chem. Soc.* **1962**, 338. (b) Kamigata, N.; Satoh, T.; Yoshida, M. *Bull. Chem. Soc. Jpn.* **1988**, *61*, 449.
- [105] Wadsworth, W. S.; Emmons, W. D. *J. Am. Chem. Soc.* **1961**, *83*, 1733.
- [106] (a) Horner, L.; Hoffmann, H. M. R.; Wippel, H. G. *Ber.* **1958**, *91*, 61. (b) Horner, L.; Hoffmann, H. M. R.; Wippel, H. G.; Klahre, G. *Ber.* **1959**, *92*, 2499.
- [107] Bisceglia, J. Á.; Orelli, L. R. *Curr. Org. Chem.* **2012**, *16*, 2206.
- [108] Still, W. C.; Gennari, C. *Tetrahedron Lett.* **1983**, *24* (41), 4405.
- [109] (a) Ando, K. *J. Org. Chem.* **1997**, *62*, 1934. (b) Ando, K. *J. Org. Chem.* **1998**, *63*, 8411. (c) Ando, K. *J. Org. Chem.* **1999**, *64*, 8406. (d) Ando, K.; Oishi, T.; Hirama, M.; Ibuka, T. *J. Org. Chem.* **2000**, *65*, 4745.
- [110] (a) Crenshaw, M. D.; Zimmer, H. *J. Org. Chem.* **1983**, *48*, 2782. (b) Tsai, H. J. *Tetrahedron Lett.* **1996**, *37*, 629. (c) Petrova, J.; Coutrot, P.; Drefux, M.; Savignac, P. *Synthesis* **1975**, 658. (d) Sano, S.; Takehisa, T.; Ogawa, S.; Yokohama, K.; Nagao, Y. *Chem. Pharm. Bull.* **2002**, *50* (9), 1300. (e) Rossi, D.; Baraglia, A. C.; Serra, M.; Azzolina, O.; Collina, S. *Molecules* **2010**, *15*, 5928.
- [111] Muthiah, C.; Kumar, K. P.; Kumaraswamy, S.; Kumara Swamy, K. C. *Tetrahedron* **1998**, *54*, 14315.
- [112] (a) Pudovik, A. N.; Konovalova, I. V. *Synthesis* **1979**, 81. (b) Kumaraswamy, S.; Senthamizh Selvi, R.; Kumara Swamy, K. C. *Synthesis* **1997**, 207.
- [113] *Reaktionsmechanismen*; Brückner, R., Ed.; Springer-Verlag Berlin: Heidelberg, 2007; 469.
- [114] Yoneda, E.; Sugioka, T.; Hirao, K.; Zhang, S.; Takahashi, S. *J. Chem. Soc., Perkin Trans. 1* **1998**, 477.
- [115] Nakamura, E.; Miyachi, Y.; Koga, N.; Morokuma, K. *J. Am. Chem. Soc.* **1992**, *114*, 6686.
- [116] Wells, W. L.; Brown, T. L. *J. Organometal. Chem.* **1968**, *11*, 271.
- [117] Simpkins, S. M. E.; Kariuki, B. M.; Aricó, C. S.; Cox, L. R. *Org. Lett.* **2003**, *5* (21), 3971.
- [118] (a) Heckmann, J. *Ann.* **1883**, *220*, 128. (b) Bunnett, J. F.; Zahler, R. E. *Chem. Rev.* **1951**, *49*, 273. (c) Paradisi, C. In *Comprehensive Organic Synthesis*; Trost, B. M.; Fleming, I.; Semmelhack, M. F., Eds.; Pergamon Press: New York, 1991; Vol. 4, Chapter 2.1. (d) Kessar, S. V. In *Comprehensive Organic Synthesis*; Trost, B. M.; Fleming, I.; Semmelhack, M. F., Eds.; Pergamon Press: New York, 1991; Vol. 4, Chapter 2.3.
- [119] Kim, J. K.; Bunnett, J. F. *J. Am. Chem. Soc.* **1970**, *92*, 7463.
- [120] Rossi, R. A. *Acc. Chem. Res.* **1982**, *15*, 164.
- [121] (a) Rossi, R. A.; Bunnett, J. F. *J. Org. Chem.* **1973**, *38*, 3020. (b) Semmelhack, M. F.; Barger, T. *J. Am. Chem. Soc.* **1980**, *102*, 7765.
- [122] (a) Beugelmans, R.; Boudet, B.; Quintero, L. *Tetrahedron Lett.* **1980**, *21*, 1943. (b) Durandetti, M.; Nédélec, J.-Y.; Périchon, J. *J. Org. Chem.* **1996**, *61*, 1748. (c) Kang, S.-K.; Ryu, H.-C.; Hong, Y.-T. *J. Chem. Soc., Perkin Trans. 1* **2000**, 3350. (d) Barton, D. H. R.; Donnelly, D. M. X.; Finet, J.-P.; Guiry, P. J. *J. Chem. Soc., Perkin Trans. 1* **1992**, 1365. (e) Pinhey, J. T. *Pure Appl. Chem.* **1996**, *68*, 819. (f) Mino, T.; Matsuda, T.; Maruhashi, K.; Yamashita, M. *Organometallics* **1997**, *16*, 3241. (g) Ryan, J. H.; Stang, P. J. *Tetrahedron Lett.* **1997**, *38*, 5061.
- [123] (a) Palucki, M.; Buchwald, S. L. *J. Am. Chem. Soc.* **1997**, *119*, 11108. (b) Hamann, B. C.; Hartwig, J. F. *J. Am. Chem. Soc.* **1997**, *119*, 12382. (c) Satoh, T.; Kawamura, Y.; Miura, M.; Nomura, M. *Angew. Chem., Int. Ed. Engl.* **1997**, *36*, 1740. (d) Satoh, T.; Inoh, J.-I.; Kawamura, Y.; Kawamura, Y.; Miura, M.; Nomura, M. *Bull. Chem. Soc. Jpn.* **1998**, *71*, 2239.
- [124] Ahman, J.; Wolfe, J. P.; Troutman, M. V.; Palucki, M.; Buchwald, S. L. *J. Am. Chem. Soc.* **1998**, *31*, 805.
- [125] Viciu, M. S.; Germaneau, R. F.; Nolan, S. P. *Org. Lett.* **2002**, *4* (23), 4053.
- [126] Fox, J. M.; Huang, X.; Chieffi, A.; Buchwald, S. L. *J. Am. Chem. Soc.* **2000**, *122*, 1360.
- [127] Churrua, F.; San Martin, R.; Carril, M.; Tellitu, I.; Domínguez, E. *Tetrahedron*, **2004**, *60*, 2393.
- [128] Quideau, S.; Lebon, M.; Lamidey, A.-M. *Org. Lett.* **2002**, *4* (22), 3975.

- [129] Rao, D. V.; Stuber, F. E.; Ulrich, H. *J. Org. Chem.* **1979**, *44*, 456.
- [130] Ho, P.-T.; Davies, N. *J. Org. Chem.* **1984**, *49*, 3027.
- [131] Manna, S.; Falck, J. R.; Mioskowski, C. *Synth. Commun.* **1985**, *15* (8), 663.
- [132] *Reagents for Organic Synthesis*; Fieser, M., Fieser, L. F., Eds.; Wiley-Interscience: New York, 1974; Vol. 4, 551.
- [133] (a) Pan, J.; Wang, X.; Zhang, Y.; Buchwald, S. L. *Org. Lett.* **2011**, *13* (18), 4974. (b) Shen, X.; Hyde, A. M.; Buchwald, S. L. *J. Am. Chem. Soc.* **2010**, *132*, 14076. (c) Shirakawa, E.; Imazaki, Y.; Hayashi, T. *Chem. Commun.* **2009**, 5088.
- [134] Comins, D. L.; Dehghani, A. *Tetrahedron Lett.* **1992**, *33*, 6299.
- [135] Lohmann, W.; Karst, U. *Anal. Bioanal. Chem.* **2008**, 391, 79.
- [136] Fenton, H. J. H. *J. Chem. Soc.* **1894**, 65, 899.
- [137] (a) Hage, J. P.; Llobet, A.; Sawyer, D. T. *Bioorg. Med. Chem.* **1995**, *3* (10), 1383. (b) Goldstein, S.; Meyerstein, D.; Czapski, G. *Free Radical Biol. Med.* **1993**, *15*, 435.
- [138] Jefcoate, C. R. E.; Smith, L. J. R.; Norman, R. O. C. *J. Chem. Soc. B*, **1969**, 1013.
- [139] Ito, S.; Mitarai, A.; Hikino, K.; Hiramata, M.; Sasaki, K. *J. Org. Chem.* **1992**, *57*, 6937.
- [140] Walling, C.; Camaioni, D. M.; Kim, S. S. *Journal of the American Chemical Society* **1978**, *100* (15), 4814.
- [141] Van der Steen, J.; Timmer, E. C.; Westra, J. G.; Benckhuysen, C. *J. Am. Chem. Soc.* **1973**, *95* (22), 7535.
- [142] Zbaida, S.; Kariv, R.; Fischer, P.; Silman-Greenspan, J.; Tashma, Z. *Eur. J. Biochem.* **1986**, *154*, 603.
- [143] (a) Tamagaki, S.; Sasaki, M.; Tagaki, W. *Bull. Chem. Soc. Jpn.* **1989**, *62*, 153. (b) Jurva, U.; Wikström, H. V.; Bruins, A. P. *Rapid Commun. Mass Spectrom.* **2002**, *16*, 1934.
- [144] Johansson, T.; Weidolf, L.; Jurva, U. *Rapid Commun. Mass Spectrom.* **2007**, *21*, 2323.
- [145] Treiber, A. *J. Org. Chem.* **2002**, *67*, 7261.
- [146] Sepuri, A.; Maravajhala, V. *Appl. Biochem. Biotechnol.* **2010**, *160*, 1699.
- [147] For recent examples see: (a) De Brabanter, N.; Esposito, S.; Geldof, L.; Lootens, L.; Meuleman, P.; Leroux-Roels, G.; Deventer, K.; Van Eenoo, P. *Forensic Toxicol.* **2013**, *31* (2), 212. (b) Uutela, P.; Monto, M.; Iso-Mustajärvi, I.; Madetoja, M.; Yliperttula, M.; Ketola, R. A. *Eur. J. Pharm. Sci.* **2014**, *53*, 86. (c) Szultka, M.; Krzeminski, R.; Jackowski, M.; Buszewski, B. *Chromatographia* **2014**, DOI 10.1007/s10337-014-2648-2.
- [148] Khmel'nitsky, Y. L.; Mozhaev, V. V.; Cotterill, I. C.; Michels, P. C.; Boudjabi, S.; Khlebnikov, V.; Madhava Reddy, M.; Wagner, G. S.; Hansen, H. C. *Eur. J. Pharm. Sci.* **2013**, *64*, 121.
- [149] Jafarpour, L.; Stevens, E. D.; Nolan, S. P. *J. Organomet. Chem.* **2000**, *606*, 49.
- [150] Gottlieb, H. E.; Kotlyar, V.; Nudelman, A. *J. Org. Chem.* **1997**, *62*, 7512.
- [151] Shao, H.; Zhu, Q.; Goodman, M. *J. Org. Chem.* **1995**, *60*, 790.
- [152] Meegan, M. J.; Hughes, R. B.; Lloyd, D. G.; Williams, D. C.; Zisterer, D.M. *J. Med. Chem.* **2001**, *44*, 1072.
- [153] Fauq, A. H.; Ziani-Cherif, C.; Richelson, E. *Tetrahedron: Asymmetry* **1998**, *9*, 2333.
- [154] Seganish, W. M.; DeShong, P. *J. Org. Chem.* **2004**, *69* (4), 1137.
- [155] Flaherty, D. P.; Dong, Y.; Vennerstrom, J. L. *Tetrahedron Lett.* **2009**, *50*, 6228.
- [156] Ogawa, T.; Ohta, K.; Iijima, T.; Suzuki, T.; Ohta, S.; Endo, Y. *Bioorg. Med. Chem.* **2009**, *17* (3), 1109.
- [157] Steinke, N.; Jahr, M.; Lehmann, M.; Baro, A.; Frey, W.; Tussetschläger, S.; Sauer, S.; Laschat, S. *J. Mater. Chem.* **2009**, *19*, 645.
- [158] Han, Y. T.; Choi, G.; Son, D.; Kim, N.; Yun, H.; Lee, S.; Chang, D. J.; Hong, H.; Kim, H.; Ha, H.; Kim, Y.; Park, H.; Lee, J.; Suh, Y. *J. Med. Chem.* **2012**, *55*, 9120.
- [159] Hart, M. E.; Suchland, K. L.; Miyakawa, M.; Bunzow, J. R.; Grandy, D. K.; Scanlan, T. S. *J. Med. Chem.* **2006**, *49* (3), 1101.

- [160] Marion, N.; Navarro, O.; Mei, J.; Stevens, E. D.; Scott, N. M.; Nolan, S. P. *J. Am. Chem. Soc.* **2006**, *128*, 4101.
- [161] Viciu, M. S.; Navarro, O.; Germaneau, R. F.; Kelly III, R. A.; Sommer, W.; Marion, N.; Stevens, E. D.; Cavallo, L.; Nolan, S. P. *Organometallics* **2004**, *23*, 1629.

10. CURRICULUM VITAE

Katharina Schragl

Personal Data:

Date of Birth: 29th October 1985
Birth Place: Scheibbs (Austria)
Nationality: Austrian



Education:

- 07/'14 **Ph.D viva, Institute of Applied Synthetic Chemistry, Vienna University of Technology**
- 04/'10 – to date **Ph.D Research – Institute of Applied Synthetic Chemistry, Vienna University of Technology**
Ph.D degree under the supervision of Professor Peter Gärtner (in cooperation with Dr. Günter Gmeiner at the Doping Control Laboratory Seibersdorf) on “Structural elucidation and Synthesis of Doping-Relevant SARM- and SERM-Metabolites”.
- 03/'10 **Diploma examination** with distinction (MSc equivalent)
Diploma thesis on “Synthesis and Analytics of 4'-Hydroxycyclomiphene as Reference Substance for Doping Control” under the supervision of Professor Peter Gärtner.
- 10/'04 – 03/'10 **Studies of Technical Chemistry, Vienna University of Technology**
Specialization: Technical Synthesis, Organic Chemistry.
- 09/'00 – 06/'04 **Bundesoberstufenrealgymnasium Scheibbs**
Grammar school with A-level with distinction.

Professional Experience & Internships:

- 04/'10 – 04/'14 **University Assistant** at the *Institute of Applied Synthetic Chemistry/Vienna University of Technology*.
- 05/'08 – 02/'10 **Student Assistent/Tutor** at the *Institute of Applied Synthetic Chemistry/Vienna University of Technology*.
- 07/'09 **Supervision of chemistry summer workshops for adolescents** in the course of a program for scientific promotion of young people, held by *fForte-WIT-Women in Technology*.
- 07/'08 – 08/'08 **Baxter Innovations GmbH**, 1221 Vienna – Internship at the Research & Development BioScience Headquarter/Orth a. d. Donau, Department Cell Culture Fermentation.
- 09/'07 **OMV Refining & Marketing GmbH**, 2320 Schwechat – Internship at the Department for Technical Quality Control at the Refinery in Schwechat.
- 07/'06 **OMV Refining & Marketing GmbH**, 1223 Vienna – Internship at the Competence Center
10/'05 – 01/'06 Lubricants.
09/'05
- 07/'03 **Wittur GmbH**, 3270 Scheibbs – Internship at the Department for Logistics.
-

Further academic commitment:

'11/'12 Participation in **TUtheTOP 2011/12** (High Potential Program of the *Vienna University of Technology*).

Publications:

Schragl, K. M.; Forsdahl, G.; Gmeiner, G.; Enev, V. S.; Gaertner, P. **Novel pathway for the synthesis of arylpropionamide-derived selective androgen receptor (SARM) metabolites of andarine and ostarine.** *Tetrahedron Lett.* **2013**, *54* (18), 2239 – 2242.

Oral Presentations:

Schragl, K. M. **Novel pathway for the synthesis of arylpropionamide-derived selective androgen receptor (SARM) metabolites of andarine and ostarine**, 15. *Österreichische Chemietage 2013*, Graz, Austria.

Poster Presentations:

Schragl, K. M.; Forsdahl, G.; Gmeiner, G.; Enev, V. S.; Gaertner, P. **Synthesis of Doping-Relevant Arylpropionamide-Derived SARM metabolites**, 20th International Conference on Organic Synthesis (ICOS) **2014**, Budapest, Hungary.

Schragl, K. M.; Forsdahl, G.; Gmeiner, G.; Enev, V. S.; Gaertner, P. **Mimicry of Drug Metabolism and Synthesis of Relevant Metabolites of the Doping Substance Clomiphene**, 14. *Österreichische Chemietage 2011*, Linz, Austria.
